SYNTHESIS, ELECTRODYNAMICS AND BIOSENSOR APPLICATIONS OF NOVEL SULPHONATED POLYANILINE NANOCOMPOSITES.

IMMACULATE NYAMBURA MICHIRA

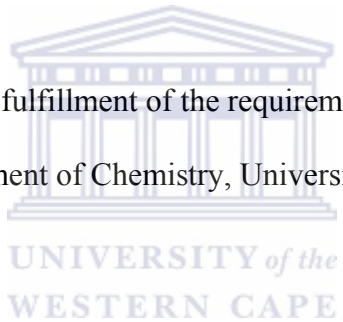

A thesis submitted in partial fulfillment of the requirements for the degree of Doctor Philosophiae in Department of Chemistry, University of the Western Cape.

Supervisors: Prof. Emmanuel Iwuoha

Dr. Priscilla Baker

May 13, 2007

Keywords

Sulphonated polyaniline nanocomposites

Anthracene sulphonic acid

Horseradish peroxidase

Cytochrome P_{450} 3A4

Erythromycin

Diazinon

N-demethylation

Cyclic Voltammetry

Biosensor

Abstract

The overall aim of the thesis was to prepare nanostructured more processable heteronuclear sulphonated polyaniline nanocomposites with electroconductive properties suitable for applications in biosensors. The sulphonated self-assembled polyaniline and derivatised polyaniline nanocomposites (SPAHs) were prepared by chemical oxidative polymerization or electrochemical deposition. The SPAHs prepared include those of polyaniline (PANi), poly-*o*-methoxyaniline (POMA) and poly-2,5 dimethoxyaniline (PDMA). Two types of sulphonic acids of heteronuclear aromatic hydrocarbons were used in the production of sulphonated SPAH composites. These were anthracene sulphonic acid (ASA) and naphthalene sulphonic acids (NSA) which played both doping and surfactant roles.

The electrodynamics of the SPAH was interrogated through various electrochemical techniques. Cyclic (CV) and square wave (SQW) voltammetric studies revealed that both the chemically synthesized and electrodeposited SPAHs were conductive and electroactive and marked by the presence of either two or three prominent formed redox couples. The redox couples that occurred at formal potentials ($E^{0'}$) of ca. 200 mV was attributed to the polyleucoemeraldine/polyemeraldine salt (PLE/PES) and that at 600 mV was assigned to the polyemeraldine/polypernigraniline (PES/PPN) transitions. In addition, another redox couple that occurred at ca. 400 mV indicated the existence of entrapped dimers and/or oligomers within the polymer matrix. Additional peaks observed in the CVs of derivatised polyanilines were associated with the formation of dopant/ polymer hybrids.

UV-Vis and FTIR studies were used as spectroscopic signatures for conductivity. The existence of polaron bands at ca. 420 and ca. 800 nm for most SPAHs and the presence of an 'electronic–like' band in the FTIR of most SPAH suggested that they were conductive. Using the classical Ohms relation, the conductivities of the various SPAHs were estimated to be between 0.27-7.8 $x10^{-3}$ S/cm and (0.085-3.47) x 10^{-2} S/cm for the chemically and electrodeposited SPAH, respectively and were several orders of

magnitude higher than those of undoped PANi. The sulphonated polyanilines were also electroactive and conductive even at neutral pH which indicated successful grafting of the sulphonic groups into the polymer matrix. Scanning electron microscopy (SEM) images revealed an influence of the initial heat pre-treatment and monomer:dopant ratio on the morphological characteristics of the resultant SPAH. A 0.5:1 monomer to dopant ratio produced SPAH with suitable characteristics.

Biosensors containing SPAH were interrogated by cyclic and/or differential pulse (DPV) voltammetry in a phosphate buffer medium. PANi and POMA/ASA-doped biosensor gave rise to sensors for hydrogen peroxide with sensitivities of 205.4 and 167.4 μA /cm^2/ mM respectively. The PANi biosensor obeyed typical Michaelis-Menten kinetics with an estimated apparent Michaelis–Menten constant ($K'M_{app}$) of 0.4 mM and a limit of detection (LOD) of 2.0 x 10^{-6} M. Inhibition of horseradish peroxidase (HRP) by exposure to diazinon in concentration range of 0.88 – 4 μM attained 41% and 81% inhibition for the PANi and POMA biosensors, respectively. The sensor for diazinon detection had an LOD value of 0.21 and 0.71 μM for PANi and POMA, respectively. Similarly the PANi/ASA system was used for the encapsulation of CYP 3A4 biosensor for erythromycin detection. The resultant data was modelled to the Michaelis-Menten model and yielded an apparent $K'M_{app}$ for erythromycin of 0.8 ± 0.1 μmol L^{-1} and an upper linear range limit of 1.3 μM (r^2 = 0.971). The sensitivity of the biosensor for erythromycin was 1.57 x 10^{-3} μA cm^{-2} $(\mu M)^{-1}$ and the LOD was estimated to be 7.58 x 10^{-2} μM.

Declaration

I declare that this piece of work entitled: ***Synthesis, Electrodynamics and Biosensor Applications of Novel Sulphonated Polyaniline Nanocomposites*** is my own work, that it has not been submitted before for any degree or examination in any other university, and all sources I have used or quoted have been acknowledged as complete references.

Michira Immaculate Nyambura May 13, 2007

Signature……

Supervisors: Prof. Emmanuel Iwuoha

Signature……

Dr. Priscilla Baker

Signature……

Acknowledgements

I would like to thank the most High Almighty Father, for His unconditional Love and renewed strength for each day, which enabled me to complete this thesis.

Many thanks go to my family: my husband Mr. Eric Michira for his love and support at all times. Thanks too to my children, Brenda, Joy, Bryan, Tracy, and Daisy, for persevering during the period I was away. I thank you all very much for your love and encouragement.

To my supervisors, Professor Emmanuel Iwuoha and Dr. Priscilla Baker: thank you very much for your excellent supervision, friendship and encouragement when things became difficult for me.

I also thank Professor G. Kamau of the University of Nairobi for encouraging me to further my education. It was through your linkage and professional advice that I was motivated to further my studies. Thank you very much Professor.

A lot of thanks also go to all colleagues of the Sensor Research Laboratory and the Chemistry Department at large, for all their support during my stay at UWC.

Great thanks to Dr. Mantoa Sekota of the University of Lesotho for the support in the synthesis of some of the dopants used in this work. Thanks too to Dr. Miranda of the University of Cape Town and Dr. Gerald Malgas of Physics Department, UWC, for advice on SEM analysis.

Finally, I sincerely thank the National Research Foundation (NRF) of South Africa for awarding me a PhD bursary. To all of you: may the Almighty God, the Creator of heaven and earth, and all that dwell in them, bless you all.

Table of contents

List of Figures and Tables

List of Publications

Immaculate N. Michira, M. Klink, R. O. Akinyeye, V. Somerset, M. Sekota, A. Al-Ahmed, P. G. L Baker, Emmanuel I. Iwuoha. (**2007**). Anthracene Sulfonic Acid-Doped Polyanilines: Electrodynamics and Application as Amperometric Peroxide Biosensor. *Book chapter: Recent Advances in Conducting Polymers (In Press).*

Michira I. N, Klink M., Akinyeye R., Somerset V., Sekota M., Al-Ahmed A., Baker P. and Iwuoha E. (**2006**). Synthesis, Characterization of Novel Polyaniline Nanomaterials and Application in Amperometric Biosensors. Paper presented at the 9th Annual UNESCO/IUPAC Conference on Macromolecules: Polymers for Advanced Applications, Stellenbosch University, 20 – 23 November 2006, Stellenbosch, South Africa. *Macromolecular Symposia, 2006 (In Press).*

Michira I. N., Akinyeye R. A., Al-Ahmed A., Sekota M., Baker P., Iwuoha E. I (**2007**). Electrokinetics of Anthracene Sulphonic acid-doped Polyaniline Biosensor for Diazinon. Manuscript ready for submission in Sensors and Actuators B. Chemical.

Richard Akinyeye, **Immaculate Michira**, Mantoa Sekota, Amir Al-Ahmed, Priscillar Baker, Emmanuel Iwuoha (**2006**). Electrochemical Interrogation and Sensor Applications of Nanostructured Polypyrroles. *Electroanalysis* 18, 24:2441-2450.

Richard Odunayo Akinyeye, **Immaculate Michira**, Mantoa Sekota, Amir Al-Ahmed, Duarte Tito, Priscilla Gloria Lorraine Baker, Christopher Michael Ashton Brett, Maher Kalaji, Emmanuel Iwuoha (**2007**). Electrochemical Synthesis and Characterization of 1,2-Naphthaquinone-4-Sulfonic acid Doped Polypyrrole. *Electroanalysis*, 19, No.2-3, 303-309.

Chapter 1

Introduction

1 Thesis overview

This chapter gives an overview of the peculiarity of conducting polymers compared to other polymers with respect to doping. The scope of applicability, methods of synthesis and the rationale behind the choice of organic conducting spectroscopical and electrochemical characterizations is discussed. Nanostructurization procedures and the problems associated with large scale application of conducting polymers are looked into. The statement of purpose of this project and the research objectives are presented. The chapter closes with a general outline of the thesis layout.

1.1 Introduction

Polyaniline belongs to the conducting polymer group (Maceij et al., 2003: 403-407) of which other members include polypyrrole, polythiophene and polyphenylene. The peculiarity of these polymers is that they are characterized by alternating single and double bonds and therefore can be reversibly oxidized or reduced (Iwuoha and Smyth: 1996: 297-328). Interaction between these conjugated systems with charge transfer species or dopants leads to the introduction of charge carriers within the polymer backbone with an insulator to conductor transition effect (Pud et al., 2003: 1701-1753). Doping, whether n-, p- or protonic-doping converts the supposedly insulators into intrinsic conductors with conductivity characteristics near the metal domain.

The inherent conductivity characteristics, coupled with good environmental stability, facile synthetic process and a high applicability potential has led polyaniline to be the

most widely studied conducting polymer in the last decade (Varela et al., 2001: 321-327). Its scope of applications ranges from energy storage, electrochromic devices, chemical sensors, biosensors as well to a series of other electrochemical devices (Malinauskas et al., 2005: R51-R62).

It is well known that both polyaniline (PANi) and derivatised PANi (e.g. poly-*o*-methoxyaniline, POMA, and poly-2,5-dimethoxyaniline, PDMA) can be produced through the chemical or electrosynthetic polymerisation processes (Iwuoha et al., 1997: 749-761, Grennan et al., 2006: 1591-1600). Of the two, the chemical approach is simple, inexpensive and the more preferred route for bulk production (Njuguna and Pielichowski, 2004). Though the electrochemical approach is expensive since it involves use of power and therefore uneconomical for large scale technological applications, it is the approach the choice for the production of thin films for use in small geometric systems such as sensors, micro-electronics, optical devices and batteries (Malinauskas et al., 2005: R51-R62). This is because electrosynthetic route allows for easy control of the polymer properties such as thickness and minimizes tendencies towards by-products formation.

Chemical synthesis entails the oxidative polymerisation of the requisite monomeric materials in acidic media in the presence of strong oxidants. Ammonium persulfate (APS) ($NH_4S_2O_8$), potassium persulfate ($K_2S_2O_8$) or dichromate (K_2CrO_7), ferric ions or hydrogen peroxide (H_2O_2) are some of the most commonly used oxidants. The oxidation of the monomeric species leads to the formation of chemically active cationic radicals. These cationic radicals may then react with more monomer molecules in solution culminating into the formation of oligomers or insoluble polymers (Malinauskas et al., 2005: R51-R62). During the chemical synthesis, polymerisation occurs in the bulk and the resultant polymers precipitate as insoluble solids. On the contrary, electrosynthetic procedures utilize potential in place of chemical oxidants. The potential of the working electrode is scanned oxidatively and then reductively. Scanning the potential of the electrode oxidatively raises the electrode Fermi level. At a suitable positive potential, the electrode Fermi level interacts with the monomer frontier molecular orbitals. The flow of electrons from the monomers' highest occupied molecular orbital (HOMO) to the lowest

unoccupied electrode molecular orbital (LUMO) constitutes oxidation and yields highly reactive nitrenium cations. Dimerization or deprotonation of these cationic radicals may give rise to various products depending on the electrosynthetic conditions (Palys et al., 2000: 108:111-119).

Recently, nanostructurization of conducting polymers and their composites emerged as a new field of research and development. The aim is to produce new smart materials for use in modern and future technologies (Malinauskas et al., 2005: R51-R62). Nanostructured conducting polymers are known to exhibit different properties compared to those of their corresponding macroscopic materials. With grain sizes in the order of a billionth of a meter, nanomaterials exhibit excellent mechanical, catalytic, magnetic and optical properties. Their scope of applications extend across a variety of fields including; chemistry, physics, electronics, optics, material science and biomedical sciences (Delvaux et al., 2000: 275-280). Of the several methods adopted to synthesize nanosized PANi, the template and the templateless procedures are the most common. The template synthesis involves the polymerization of monomeric species within the nanoscopic void spaces of the template. Anodic alumina, polycarbonate track-etched membranes and mesoporous alummosilicate have been used (Wei et al., 2002: 917-921). However, the use of templates for nanostructurization often requires a rather tedious post synthesis processing in order to remove the template. This has a limiting effect as to the number of materials suitable as templates given the fact that the template must have a dissolving solvent. Also the need for a 'molecular anchor' to prevent the collapse of nanostructures upon formation poses a major challenge (Wei et al., 2002: 917-921). Electrosynthetic template–assisted nanostructures can be obtained by electropolymerisation of the relevant monomers within the channels, cavities, holes or related nanosized structural units previously created on the electrode surface.

The templateless process on the other hand, involves the use of structure modulating aids such as surfactants for molding the organic conducting polymers to desirable shapes and sizes. Surfactant based nanostructurization relies on the fact that surfactants in solution exist in micellic formats availing nanoscopic void spaces in between the micelle units

utilizable for polymerisation (Wei et al., 2002: 917-921, Delvaux et al., 2000: 275-280). The fact that surfactants are also dopants eliminates the need for post synthetic template dissolution. This way monomeric species diffuse into the surfactants' nanoscopic spaces with polymerisation occurring at the micelle/solution interface to produce a kind of self-assembled structures. Protonic acid dopants such as sodium dodecyl benzene sulfonic acid (DBSA), camphor sulfonic acid (CSA) and maleic acid (MA) have been used as 'soft inbuilt templates' towards polymer nanostructurization. In one such study, it was established that the monomer to dopant ratio, reaction temperature amongst others were critical towards determining the nanoparticle size (Zhang and Wan, 2005: 24-31).

Spectroscopical techniques are highly valuable in the determination of the conducting state of organic polymers. The basis of spectroscopical characterisation is that doping creates structural and electronic modifications in the polymer backbone (Fernandes et al., 2005: 279-284). It has been established that doping modulates the vibration spectra of most organic polymers resulting in the emergence of new bands in their vibrational spectra (e.g. FTIR). The new bands are due to the displacement of the position of the double bonds as some of the benzoid structures converts to quinoid ones due to doping (Fernandes et al., 2005: 279-284). Emergence of these new bands therefore is proof of successful doping. Furthermore, conducting polymers are made of a continuous valence and conduction band constituting the band gap. Under normal circumstances, electronic transitions in the band gap are energetically prohibited. Doping, however, introduces new electronic energy levels within the polymer sub-gap energies. Consequently more energetically favourable intra-gap transitions can take place. The introduction of charge carriers within the polymer back bone results in conductivity enhancement often with an insulator to conductor transition effect. Depending on the doping level two (bipolaron) to three (polaron) transitions can take place within the band gap. These transitions correspond to the appearance of new bands in the polymer electronic spectra and are indicators that the polymer is conducting (Wei et al., 2002: 917-921).

The electrochemical characterization of polyanilines is based on the fact that polyanilines are electroactive. Organic molecules with extended π-systems are characterized by

accessible frontier molecular orbitals with measurable redox potentials (activity). Therefore, potentiodynamic (e.g. cyclic voltammetry, CV) and pulse techniques (e.g. square wave voltammetry, SQW and differential pulse voltammetry, DPV) are often used to measure their electrochemical behaviour and redox kinetics. It is now well known that all polyanilines generally have one basic structure consisting of alternating reduced and oxidized repeated units (Fig 1.1) (MacDiarmid, 2001: 2581-2590).

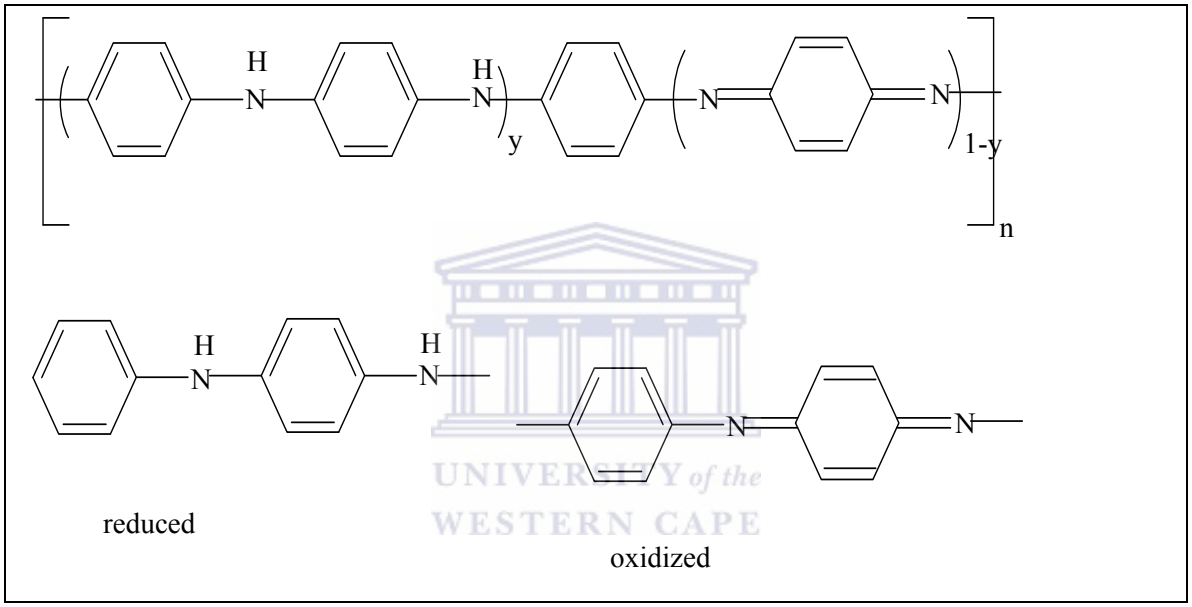

Figure 1.1: Basic structure of polyaniline consisting of alternating reduced and oxidized repeated units.

Also, although in principle polyaniline can exist in a continuum of oxidation states between y = 0 and y = 1, there are generally three allowed oxidation states. These oxidation states are the fully reduced leucoemeraldine (y = 1), the half oxidized emeraldine form (y = 0.5) and the fully oxidized pernigraniline form (y = 0) (MacDiarmid, 2001: 2581-2590; Wei et al., 2005: 19-26). Protonation of the emeraldine base (EB) form of PANi, or the oxidation of the leucoemeraldine (LE) form leads to the production of a polysemiquinone radical cation (the ES form of PANi). The ES PANi form consists of a half-filled broad polaron energy band and is the only conductive form of PANi.

It has also been shown that polyanilines are able to reversibly bind many small anions during their oxidation from the polyleucoemeraldine (PLE) to the polyemeraldine salt (PES) form and to expel them out during the reduction cycle (Malinauskas 1999: 75-83). When doped with large sized anions or polyanions, however, conducting polymers cannot expel these anions into solution. This then forms the basis of fabrication of new versatile composite materials often with desirable catalytic or electrocatalytic properties. Electrocatalysis and heterogeneous catalysis at conducting polymer electrodes doped with various anions is the basis of chemical sensors and actuators. Polyaniline based sensors and actuators for carbon monoxide, aliphatic alcohols amongst others have been reported (Dixit et al., 2005: 90-93, Segal et al., 2005: 140-150).

Of great interest, however, is the role played by organic conducting polymers in the fabrication of biosensors. A biosensor is an electroanalytical device capable of providing specific quantitative or semi-quantitative analytical information by employing a biological recognition element in direct or spatial contact with a transducing element (Thévenot at el., 2001: 121-131). Biosensors combine the exquisite selectivity of biology with the processing power of modern microelectronics and optoelectronics to offer powerful new analytical tools with major applications in medicine, environmental diagnostics and the food processing industries (Chaplin, 2004). Modification of electrodes with multi-layered polymeric materials is a popular procedure towards the fabrication of high performance reagentless sensors (Bartlett and Cooper, 1996: 233-269). Use of organic conducting polymers for electrode modification allows for the tailoring of the electrode surface towards detection of a specific analyte besides overcoming overpotential problems related to the analyte detection. When used in biosensors, organic conducting polymers provide a suitable micro-environment for the biocatalyst immobilization. They also localize the biocatalyst close to the electrochemical interface thus minimizing interferences which may lead to undesirable side reactions or large background currents. Furthermore, since conducting polymers are characterized by a distributed array of catalytic sites, they are able to mimic natural redox polymers and can bind productively with the biocatalyst culminating in electron exchange thereby

providing a link between the electronic and biological worlds (Bartlett and Cooper, 1996: 233-269).

This thesis, therefore, envisaged the fabrication of reagentless biosensors for hydrogen peroxide, erythromycin and diazinon based on the encapsulation of test enzymes on to the conducting anthracene sulfonic acid (ASA) and naphthalene sulfonic (NSA) doped sulphonated polyanilines (SPAH). Horseradish peroxidase (HRP) and cytochrome P_{450} 3A4 (CYP 3A4) were used as the test enzymes.

Horseradish peroxidase (HRP) enzyme (EC.1.11.1.7) belongs to the group of oxido-reductase enzymes. Oxidoreductases are known to catalyze the exchange of electrons or redox equivalents between donor and acceptor molecules, in reactions involving electron transfer, proton abstraction, hydrogen extraction, hydride transfer, oxygen insertion, or other key steps and have been extensively employed in the fabrication of biosensors (Feng, 2005). Horseradish peroxidase (HRP) is a heme-containing glycoprotein with an Fe^{3+} prosthetic group bound to four nitrogen ligands that form part of the four pyrrole rings of the protopophyrin IX (Fig. 1.2). Closely lying to the heme-protopophyrin is the proximal and distal histidines which together with an argenine residue define the specificity of the enzyme's active site to bind only the relevant molecules such as peroxides.

The detection of peroxides is of interest because peroxides are environmental hazards. Commonly used in household bleaching, in deodorants, teeth whiteners, disinfectants and in sewerage treatment, hydrogen peroxide is a corrosive, mutagenic chemical that can cause serious skin burns and eye damage. Apart from the pollution effects, the detection of peroxides is of interest in biosensor fabrication because it is often a product of most biological reactions and, therefore, forms the basis of most electroanalytical biosensor systems.

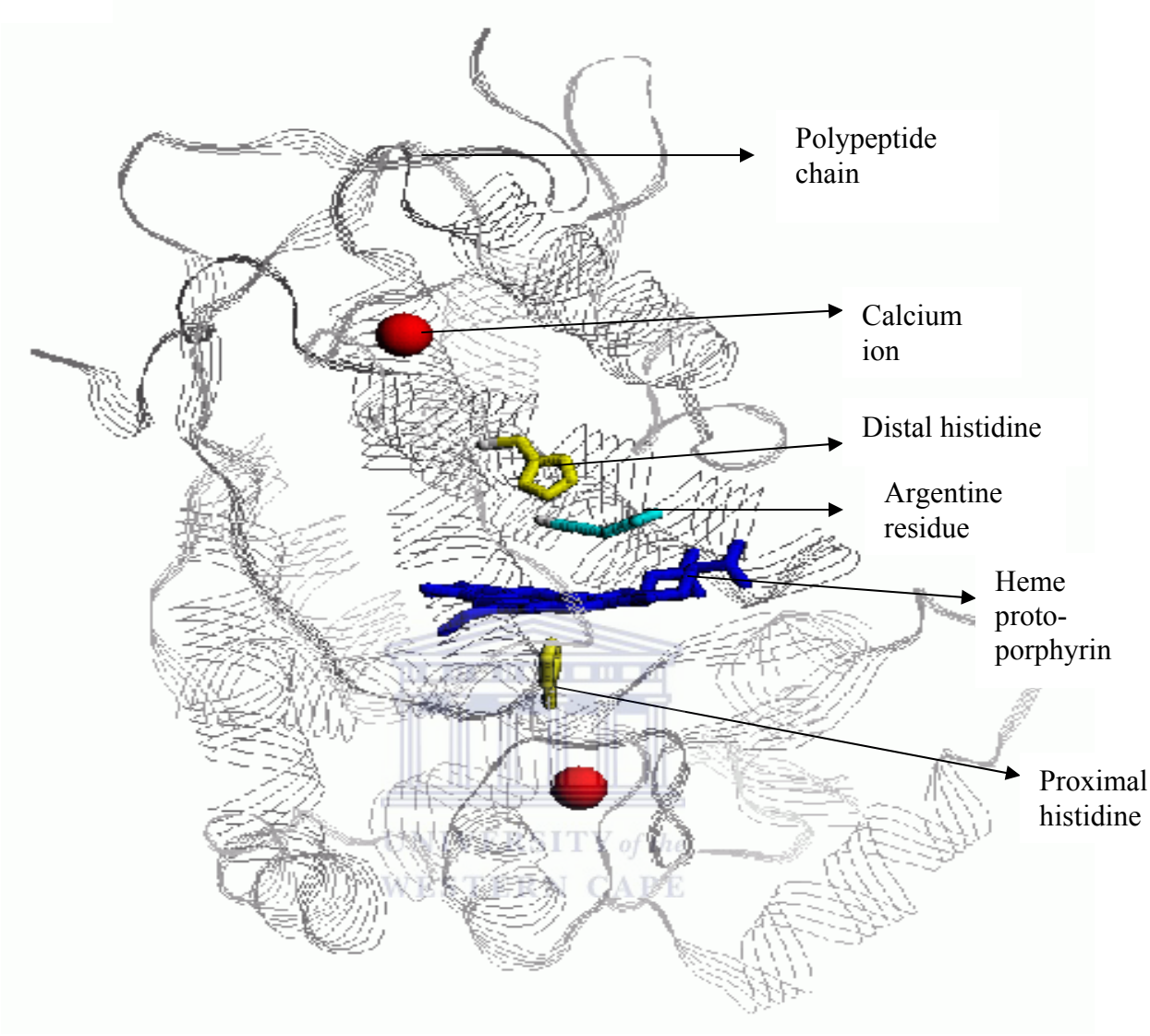

Figure 1.2: A diagram representing the structure of a horseradish peroxidase enzyme showing the polypeptide chains, the heme protopophyrin (type- I) covalently bound to an Fe^{3+} prosthetic group and the morphology of the active site.

***Source*:** http://www.unige.ch/LaBPV/Publications/silaghi/Dumistrecu.html

Also of great concern is the rate at which pesticide residues are accumulating in our environment. The rapidly growing population has placed an increasing high demand on the agricultural sector to increase crop production. To this effect use of pesticides has seen the agricultural crop production rise dramatically. However, the use of pesticides calls for great care and control. Pesticides can be carcinogenic, citogenic and can lead to adverse effects on the immunological, respiratory and nerve impulse transmission

mechanism. There is need for rapid, accurate, out-of-lab pesticide residue analysis to keep pesticide residue levels in the environment controlled. The current HPLC and GC-MS chromatographic techniques, though highly sensitive and expensive, often require a detailed sample preparation. Biosensor technology could provide a rapid sensing alternative, in a cheap, portable, less complicated format. It is now known that horseradish peroxidase can be inhibited by organic-sulfur containing compounds such as organophosphate pesticides (OPs) thus forming the basis for the fabrication of diazinon biosensors (Adeyoju et al. 1995: 57-64).

Diazinon ($C_{12}H_{21}N_2O_3PS$) is a non-systemic organophosphate insecticide and acaricide whose IUPAC name is O, O-diethyl O-(2-Isopropyl-6-methyl pyrimidin-4-yl) phosphorothioate. Commonly sold under the names: basudin, dazzle, knox out, spectracide etc, it may also be present in a variety of formulations such as pyrethrins, lindane and disulfoton (Extonet, 1996). Diazinon finds use in the household, agricultural and veterinary sectors for control of sucking and chewing insects and mites in a range of situations. Like other pesticides, use of diazinon above the allowed limits is detrimental to health. Its poisoning occurs due to its ability to irreversibly modify the catalytic serine residue in acetylcholine esterases, which subsequently inhibits the hydrolysis of acetylcholine, the across-synaptic impulse transmitter causing nervous impulse communication breakdown (Vakurov et al., 2004:1118-1125). However, diazinon detection by use of the acetylcholine esterase enzyme inhibition is expensive owing to the high cost of the enzyme. Construction of alternate biosensors based on the inhibition of a cheaper more tolerable enzyme to pH changes, like HRP would be appropriate.

Cytochrome P_{450} 3A4 (EC 1.14.14.1), (Fig. 1.3), a member of the cytochrome P_{450} mixed-function oxidase system, is arguably the most important enzyme involved in the metabolism of xenobiotics in the body.

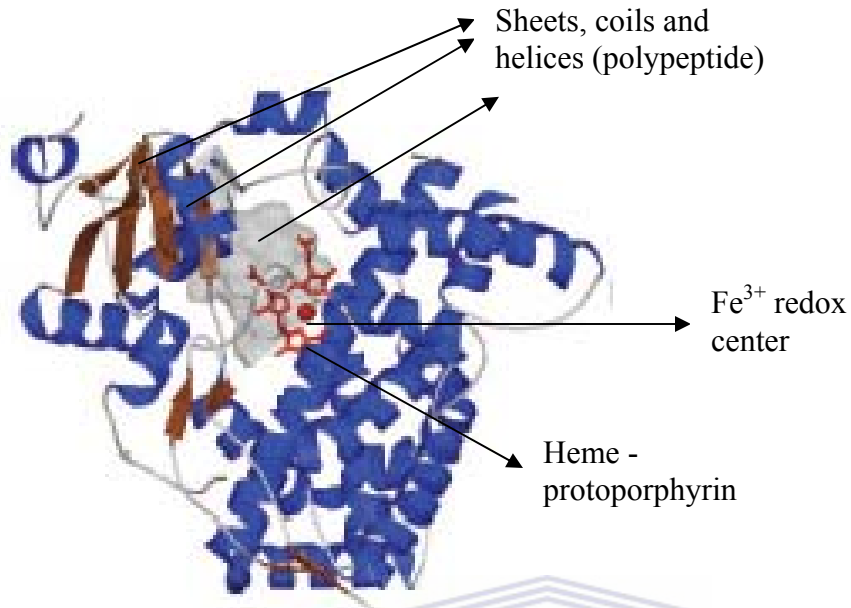

Figure 1.3: Structure of the Human Microsomal cytochrome P450 3A4 as determined by X-ray crystallography. Center the Fe^{3+} redox centre bound in a protopophyrin type IX.

Source: Yano et al., (2004: 38091-38094).

Located mainly in the liver and to a lesser extent in the intestinal tracts these enzymes are actively involved in the phase I bio-transformation of xenobiotics involving the attachment/modification of a functional group in the parent drug resulting in loss of its pharmacological activity (Shiba et al., 2003: 1817-1826). With the onset of 'polypharmacy' (the simultaneous prescription of more than one drug to treat one or more conditions in a single patient) drug - to- drug interactions have been cited as one of the major causes of hospitalization / death (Walsky and Obach, 2004: No.6). Besides, such interactions can increase/lower the efficacy of the other drugs calling for dosage adjustment. It has been shown that CYP 3A4 catalyses the N-demethylation of erythromycin (Wang et al., 1997). Erythromycin is a macrolide antibiotic, which has antimicrobial properties and is therefore used to treat various conditions including respiratory tract infections. It has been found that the simultaneous administration of erythromycin with other drugs such as theophylline can lead to fatal drug-to-drug

interactions (www.medicinenet.com/erythromycin/article.htm). A prerequisite towards the development of bioprobes for in vivo drug level testing especially those prone to antagonism would be to develop simple biosensors for the same. In view of this the project undertakes to develop a simple biosensor for erythromycin based on the electromediation power of polyaniline -based polymers.

1.2 Statement of the problem

Despite the enormous application potential of PANi, its large scale processability is encumbered by its insolubility in common organic solvents. PANi dissolves only in toxic N-methyl pyrrolidone (NMP) and in strong acids and thus does not render itself to large scale production (Troitsky et al., 2002). Also the fact that PANi decomposes before melting means it cannot be processed by the melt- processing technique. To circumvent this problem several strategies toward more soluble PANi have been adopted. Functionalization of the PANi backbone with more polar molecules (Chandrakanthi and Careem, 2002: 51-56), co-polymerization of the aniline monomers in the presence of polymeric host stabilizers (Mirmohseni and Wallace, 2003: 3523-3528), preparation of PANi blends/composites with other polymers with desirable characteristics have led to more soluble PANi (Pud et al., 2003: 1701-1753). Also, incorporation of surfactant dopants within the PANi matrix promotes solubility besides enhancing the conductivity and the morphology of the resultant PANi (Wei et al., 2002: 917-921). Despite the above efforts, the processability of PANi is still an issue of concern and a lot of research towards producing more proccessable PANi is still on going. In this thesis a dual approach towards improving PANi processability was adopted. New polyaniline materials were prepared based on the polymerization of both functionalized and non-functionalised anilines in the presence of stabilizing surfactant dopants to improve PANi processability and widen the scope of applicability.

The determination of H_2O_2, diazinon and erythromycin has important environmental, industrial and clinical implications respectively. The current assay techniques based for these analytes based on volumetric, colorimetric, chemiluminescence and

chromatographic analysis are complex, and take long periods of analysis. This thesis was aimed at producing faster operational devices with reasonable sensitivities.

1.3 Objectives of the Thesis

The ultimate aim of the thesis was to synthesize sulphonated polyanilines (SPAH), evaluate their electrodynamics and explore their possible application for sensor technology as effective electron transfer mediators. Sulphonated polyanilines prepared included those of polyaniline (PANi), poly-*o*-methoxyaniline (POMA) or poly-2,5-dimethoxyaniline (PDMA). Preparation of the polyaniline and functionalized polyaniline was carried out in the presence of sulphonated polynuclear aromatic hydrocarbons (anthracene sulfonic acid (ASA) and naphthalene sulfonic acids (NSA)) which played both surfactant and dopant roles. The resultant nanostructured composites doped with stabilizing protonic acids are expected to make stable biosensors even at neutral pH.

1.3.1 Specific Objectives

1) To prepare novel sulphonated polynuclear aromatic hydrocarbons, SPAH-doped polyaniline (PANi), poly-*o*-methoxyaniline (POMA) and poly-2,5-dimethoxyaniline (PDMA) by chemical and electrosynthetic procedures in the presence of anthracene sulfonic acid or naphthalene sulfonic acid.

2) To probe the redox properties of the SPAH- polyaniline materials by cyclic voltammetry (CV), Osteryoung square wave voltammetry (SQW) and differential pulse voltammetry (DPV).

3) To perform spectroscopic (UV-Vis, FTIR) and microscopic (SEM) characterization of the polymers to determine their conductivity and morphological properties.

4) To study the behaviour of the SPAH- polyanilines under simulated physiological conditions (i.e. phosphate buffer medium) in order to assess their suitability as electrode modifying matrices for biosensors.

5) To construct biosensors for various analytes (H_2O_2, erythromycin, diazinon) by the modification of the SPAH-polyanilines with HRP and/or CYP 3A4 enzymes.

6) To model biosensor reactivities to the electrochemical the Michaelis-Menten kinetics.

1.4 Thesis Layout

Chapter 2 reviews on the literature related to conducting polymers with respect to their synthesis, characterization procedures and application for electromediation roles in biosensors. It outlines the major procedures that have been employed towards overcoming polyaniline inprocessability problems some of which include the derivatization of aniline and nanostructurization. A literature search into the major synthetic routes for preparation of doped polyanilines and the properties of the resultant composites together with the various nanoparticle characterization procedures is discussed. The chapter also highlights some of the works in which conducting polymers and the biomolecules used in this work have been used for biosensor construction.

In Chapter 3, all the procedures that were employed for the synthesis and characterization of novel sulphonated polyanilines (SPAH) and their applications in biosensor construction are summarized. Firstly, the procedures followed towards the production of the novel sulphonated polynuclear aromatic hydrocarbon, anthracene sulfonic acid, and those governing its characterization are presented. A summary of the preparation procedures employed for the production of the novel sulphonated polyaniline materials namely: anthracene and naphthalene sulphonic acid doped –polyanilines then follows. The chapter also includes the spectroscopic and electrochemical procedures for the characterization and/or deposition of the SPAH together with those employed for the

immobilization of the biomolecules during the construction of amperometric biosensors for the detection of the various analytes.

Chapter 4 presents the characterization results of the chemically synthesized sulphonated polyanilines and the anthracene sulfonic acid dopant using FTIR and cyclic voltammetry. Using UV-Vis spectroscopy, the most suitable monomer: dopant ratio for the composite preparation was determined as scanning electron microscopy results of the various SPAH is given. This is followed by a critical analysis of the resultant voltammograms and the extraction of suitable data which is then used for the estimated for important kinetic parameters describing the electrochemical behaviour of the sulphonated polyanilines. The chapter also estimates the conductances of the sulphonated polyanilines by use of the classical Ohms relationship based on the voltammetric data. Finally, a conclusion highlighting the major properties of the novel sulphonated polyanilines as electromediators is given.

The results for the electrochemical preparation SPAH including a study of the electrodeposition mechanisms are discussed in Chapter 5. The electrochemical behaviour of the resultant SPAH was then studied in both acidic and neutral media. The electrodynamics of the SPAH was investigated through the calculation of the necessary kinetic parameters such as the diffusion coefficients (D_e, cm^2/s), the heterogeneous rate constant (k^0, cm/s) and the surface concentration mol cm^{-2}). The conductivity of the SPAH was also evaluated through the classical Ohm relationship.

Chapter 6 presents some of the applications of the resultant electroconductive SPAH as effective electromediators in biosensors. Sensors based on either NSA and/or ASA doped SPAH utilizing either the HRP or CYP 3A4 enzymes are discussed. The enzymatic reactivities are finally fitted into the Michaelis-Menten enzyme kinetics model.

Finally, Chapter 7 summarizes the major results for the synthesis, characterization and application of the sulphonated polyanilines. The chapter also draws conclusions from the various results and this forms a basis for suggested recommendations that follow.

Chapter 2

Literature review

2 Conducting polymers

Conducting polymers are polymers that consist of conjugated π-systems (Iwuoha and Smyth, 1996: 297-328). They are characterized by alternating single and double bonds with continuous mobile π electrons forming a valence band (VB) and conduction band (CB). The distinction between these polymers and others is that although they are insulators, doping converts them into intrinsic conductors sometimes with near metal conductivity characteristics. Owing to this behaviour, they are known by several names including; intrinsic conducting polymers (ICPs), synthetic metals and organic conducting polymers.

The increased conductivity of these conducting polymers emanate from the fact that they can interact with charge transfer species or dopants thus undergoing oxidation or reduction depending on the dopant type (Iwuoha and Smyth, 1996: 297-328). This way, charge carriers-electrons or holes- are introduced into the polymer backbone with an effect of converting the supposedly insulators into conductors. Among the conducting polymers (CPs), polyaniline (PANi), polypyrrole and polythiophene (Fig. 2.1) and their derivatives are the most considered due to a good combination of properties such as; good electrical conductivity, facile synthetic processes, environmental stability and good optical and electrochromic properties (Zhang, 2005: 1373-1379).

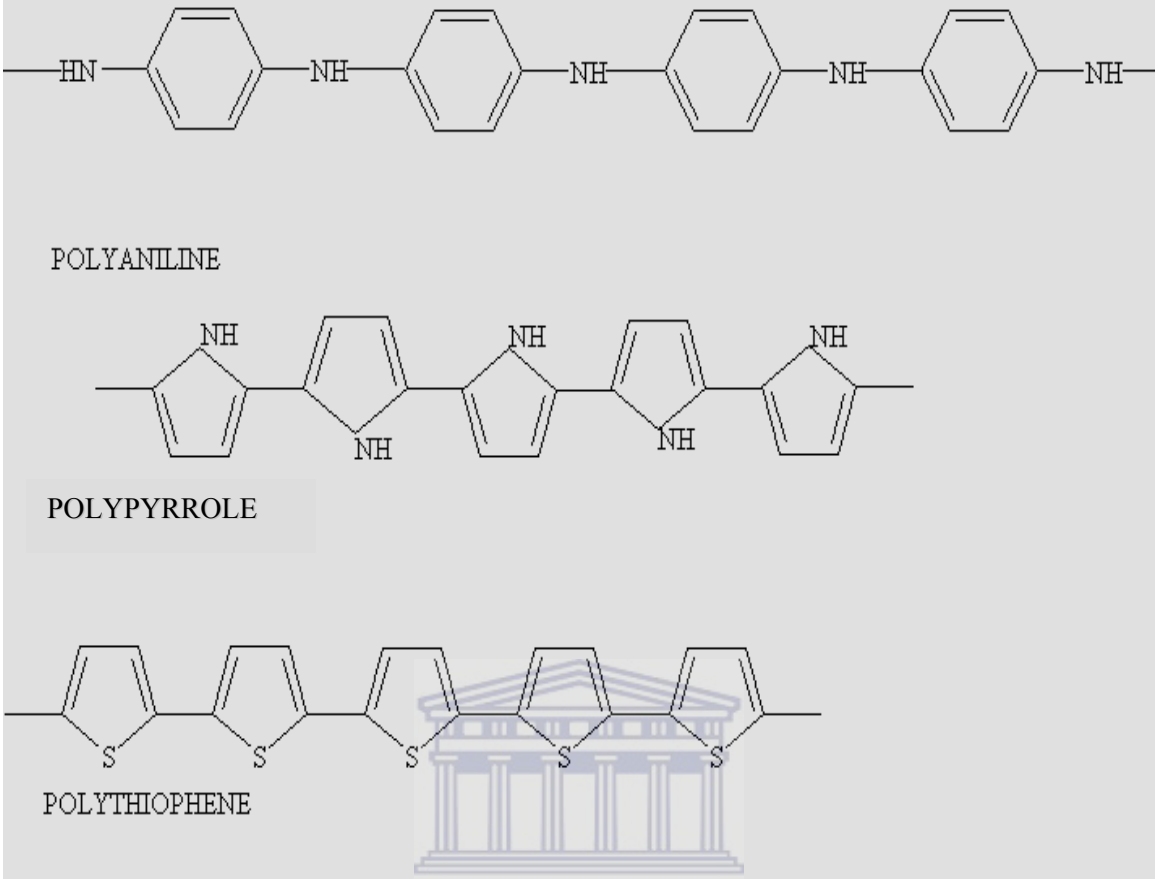

Figure 2.1: Examples of the most studied conjugated polymers.

2.3 The concept of doping

Doping refers to the controlled addition of non-stoichiometric quantities of chemical species resulting in dramatic changes in the polymer electronic, magnetic, optical and structural properties (MacDiarmid, 2001: 269-279). In the undoped state, conjugated polymers are either electrical insulators or semi-conductors. A pure semi-conductor is basically neutral, containing no free electrons in its conduction band. The accidental doping of polyacetylene in 1976 by Shirakawa was the hallmark and a turning point for the conducting polymers (Shaw and Marrin, 2002: 446). Previously regarded as plastics, the discovery that these polymers' conductivity could easily be manipulated through doping opened a new dimension in research. The development of the field of conducting polymers has continued to accelerate at an unexpected rate and a variety of polymers and

their derivatives have been discovered (MacDiarmid, 2001: 269-279). Basically it is now known that conductive polymers can undergo mainly oxidative (p-doping) or reductive (n-doping). Oxidative doping refers to the partial oxidation of the organic polymer π-backbone through the interaction between the polymer and the p-type dopant. In this type of interaction the flow of electrons from the valence band (VB) to the acceptor dopant introduces delocalized holes within the polymer backbone resulting in enhanced conductivity (Gavryshin and Žukauskas, 2002). On the contrary, during reductive doping (n-type), there is a partial introduction of mobile electrons into the π system. Figure 2.2 attempts to illustrate the concept of n- and p- doping.

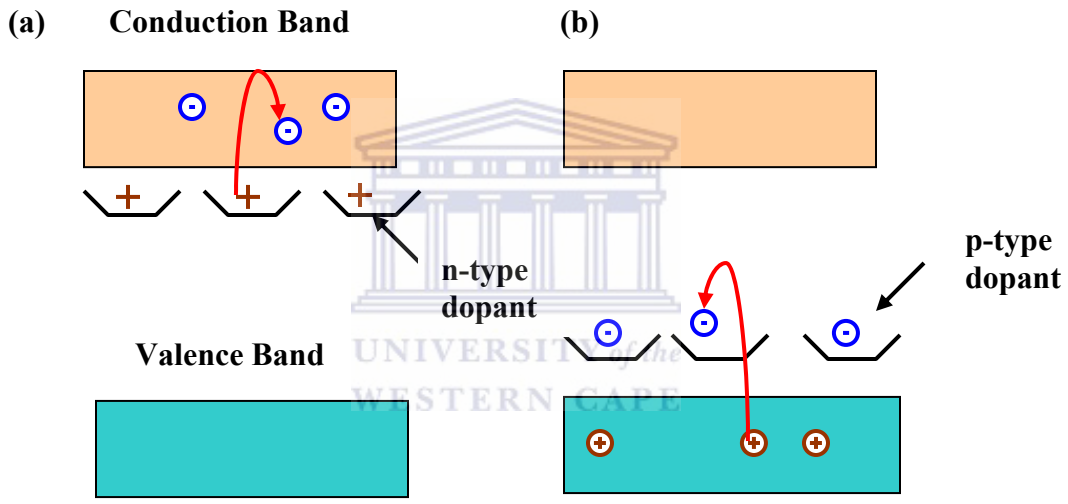

Figure 2.2: An illustration of n and p- doping processes respectively.

The first diagram (a) shows electrons flowing from a donor (n-type) dopant to the conduction band (CB). The second diagram (b) shows the acceptor dopant (p-type) receiving electrons from the valence band (CB) leaving positive charges or holes in the polymer backbone.

Either way, redox doping introduces charge carriers (electrons and holes) into the polymer backbone thus converting it into an intrinsic conductor. Intrinsically conducting polymers are thus organic conducting polymers that possess the electrical, electronic,

magnetic and optical properties of a metal while at the same time maintaining the mechanical and processibility properties of the polymer (MacDiarmid, 2001: 2581-2590).

Polyaniline is a special kind of conducting polymer because besides redox doping it also undergoes protonic doping. Protonic doping differs from redox doping in that in the former case the number of electrons associated with polymer backbone does not change during the doping process but instead a re-arrangement of the polymer energy levels occurs (MacDiarmid, 2001: 269-279). Protonic doping in polyaniline has been achieved through the protonation of the imine nitrogens of the polyleucoemeraldine (PLE) form of PANi using strong acids (Pud at al., 2003: 1701-1753). This leads to the production of a highly conductive, delocalized, stable polysemiquinone radical cation-the PANi polyemeraldine salt form (PES) (MacDiarmid, 2001: 269-279; Lindfors and Ivaska, 2002: 65-74). During doping/undoping processes dopant counterions stabilize the doped state.

2.4 Oxidation states of doped polyaniline

Polyaniline belongs to a special class of electronic/conducting polymers which are characterized by alternating reduced and oxidized repeated units. Although in principle the average oxidation state of the polyanilines can be varied between y = 0 to y =1, there are only three polyaniline allowed oxidation states (MarcDiamid, 2001: 269-279; Lindfors et al., 2002: 65-74). The allowed oxidation states of the polyanilines are; the fully reduced polyleucoemeraldine (PLE), the half-oxidized polyemeraldine (PEM), and the fully-oxidized polypernigraniline (PPN) forms (Fig. 2.3). In addition the protonation of the polyemeraldine form of PANi or the chemical oxidation of the fully reduced polyleucoemeraldine form leads to the formation of the polyemeraldine salt of PANi which is the most conductive form of PANi (MacDiarmid, 2001: 269-279; Lindfors et al., 2002: 65-74; Hino et al., 2006: 1327-1332).

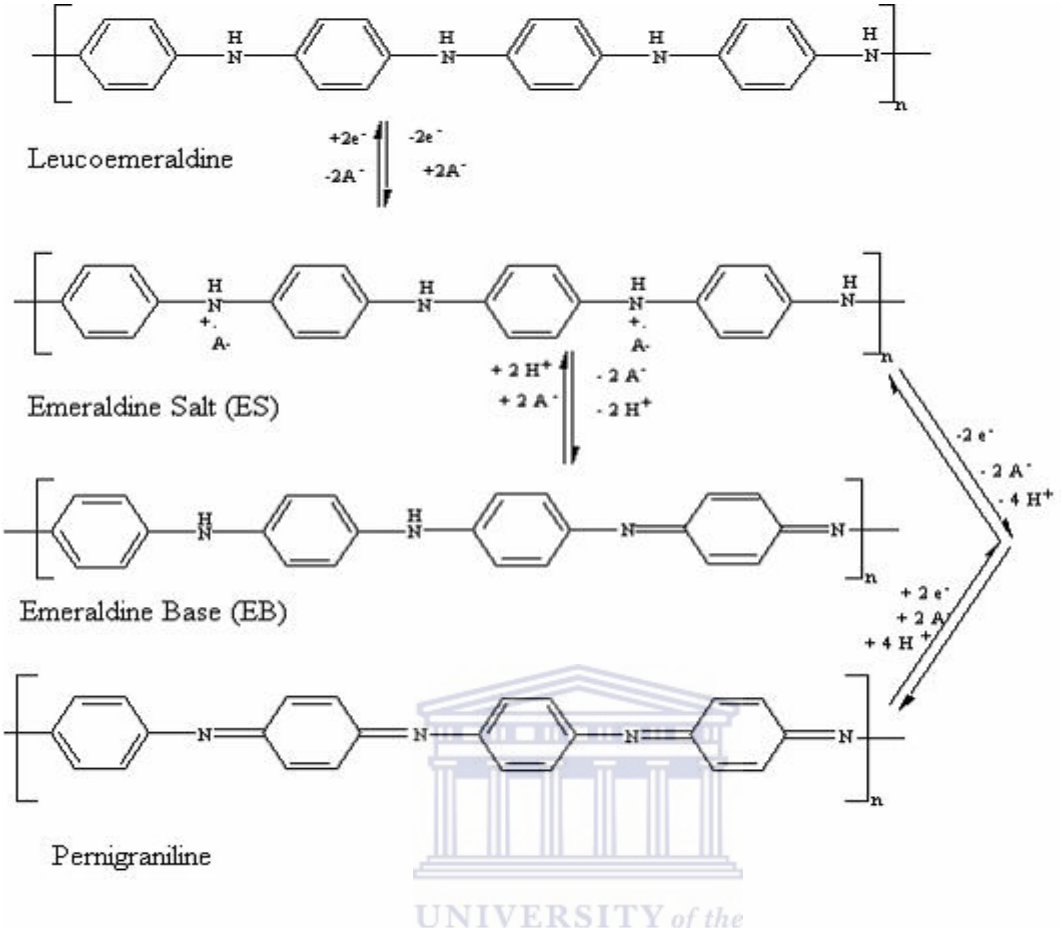

Figure 2.3: Oxidation/Reduction processes of polyaniline.

Source: Lindfors et al., 2002: 65-74

2.5 Synthesis of polyanilines

Basically, PANi and derivatised PANi such as poly-*o*-methoxyaniline (POMA) and poly-2,5-dimethoxyaniline (PDMA) can be produced through chemical or electrosynthetic routes (Iwuoha et al., 1997: 749-761, Grennan et al., 2006: 1591-1600. The chemical synthesis entails the oxidative polymerisation of the requisite monomers in an acidic media using strong oxidants such as ammonium persulfate (APS), potassium persulfate or dichromate, ferric ions or hydrogen peroxide in presence or absence of templates. These oxidants are able to oxidize the monomers leading to chemically active cationic radicals of the respective monomers. The cationic radicals formed react with more monomer molecules yielding oligomers or insoluble polymers (Malinauskas, 2001: 3957-3972).

During the chemical synthesis, polymerisation occurs in the bulk and the resultant polymers precipitate as insoluble solids.

The electrosynthetic procedures, utilize potential in place of a chemical oxidant. The potential of the working electrode is scanned oxidatively and then reductively. Scanning the potential of the electrode oxidatively lowers the electrode Fermi level. At a sufficiently positive potential, the electrode Fermi level can interact with the frontier molecular orbitals of the requisite monomers. The flow of electrons from the monomers' highest occupied molecular orbital (HOMO) to the lowest unoccupied electrode molecular orbital (LUMO) constitutes oxidation and yields highly reactive nitrenium cations. Dimerization or deprotonation of these cationic radicals may give rise to various products depending on the electrosynthetic conditions. 4-Aminodiphenylamine, p-benzoquinone, and benzidine are possible products (Palys et al., 108:111-119). It is now well known that the electrodeposition process is usually a two stage process. The initial rate determining step involves the nucleation of the polymer on the bare parts of the electrode - the polymer adsorbing covalently to the electrode. This chemisorption process is possible because although inert, the platinum metal has a face-centered cubic system implying that the atoms on the surface have unsatisfied valences. Also, the rather deceptive smooth, shiny platinum electrode surface is often rather rugged, further increasing the area for nucleation. The chemisorption step results in a reaction pathway with lowered activation energy and the autocatalytic effect leads to rapid polymer growth and deposition.

It is generally agreed that the mechanism for the chemical/electrosynthetic oxidative polymerisation of the aniline/aniline related monomers is similar (Bejan and Duca, 1998: 745-756). A scheme (Fig. 2.4) for the oxidative polymerisation of aniline as proposed by

Bejan and Duca, (1998: 745-756) and Wei et al. (1990: 758-764) is presented below.

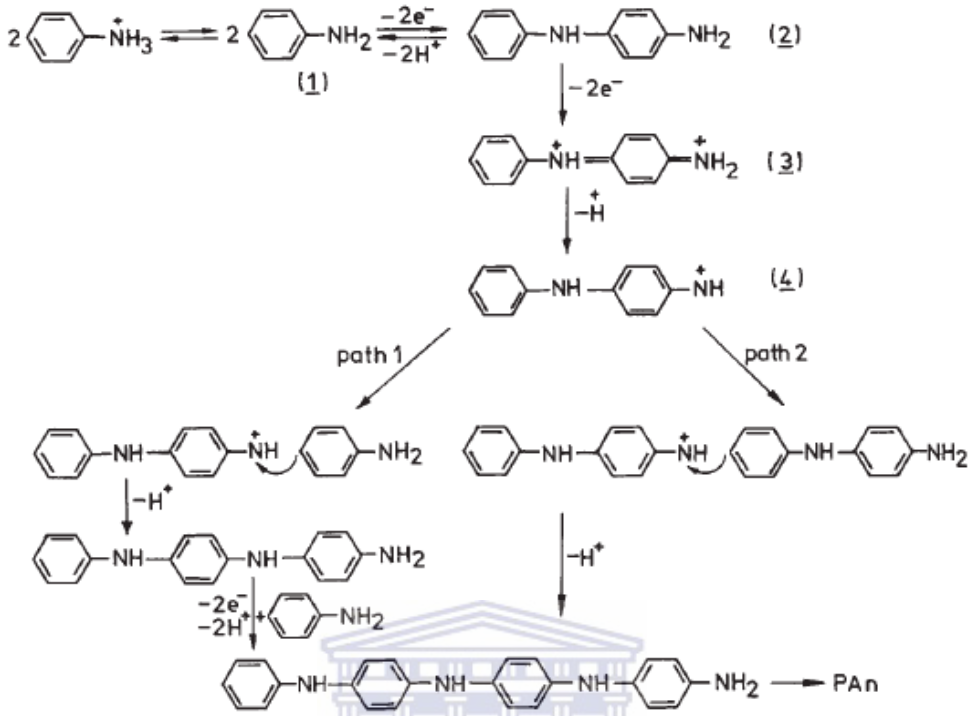

Figure 2.4: Oxidative polymerisation of aniline.

Source: Bejan and Duca, (1998:745-756) and Wei et al., (1990: 758-764)

Figure 2.4 shows that the oxidation of aniline (or *o*-methoxy-aniline, 2,5-dimethoxyaniline) in an acidic medium propagates through a chain of steps beginning with the abstraction of an electron from the bonding π-orbital of the monomer yielding highly reactive radical cations. These cations then rapidly undergo de-protonation and electron loss with 'head to tail' coupling to form dimers. In the anodic oxidative process, the dimmer formation is the rate determining step. In the chain propagation step, dimer/dimer or dimer/monomer cation 'head to tail' coupling, amidst deprotonation or de-electronation leads to elongation of the polymer chain and the consequential deposition of the polymer in solution for chemical synthesis or on the electrode for electrosynthetic route.

2.5.1 Chemical synthesis of polyaniline

2.5.1.1 Oxidants

The majority of reported works on the chemical synthesis of PANi are based on use of ammonium persulphate oxidant (Kim et al., 2007: 205-210; Oh and Im, 2002: 273-277; Long et al., 2003: 208-213; Stejskal et al., 2006: 8253-8262). However, the chemical synthesis of PANi using other oxidants has been reported as well. The oxidation of aniline using hydrogen peroxide as oxidant yielded PANi that was electroactive and exhibited redox behaviour similar to that of conventionally synthesized polyaniline (Michaelson and McEnvoy, 1994: 79-80). Elsewhere, the oxidation of aniline using chloroaurate acid, $HAuCl_4$, as an oxidizing agent produced polyaniline that was decorated with gold nanoparticles emanating from the reduction of the chloroaurate acid oxidant (Kaushik et al., 2005: 232-235). In another instance, the chemical synthesis of conductive polyaniline was conducted by use of benzoyl peroxide as oxidant. The resultant polymers were conductive electroactive and thermally stable (Karaşkila et al., 2002: 1349-1359). A variety of very many other oxidants for PANi synthesis have been reported (Erdem et al., 2004: 785-791). However, over the years the use of ammonium persulphate (APS) as oxidant for synthesis of polyanilines has persistently prevailed. This is probably because APS is relatively cheap and does not pose environmental problems as use of some oxidants such as hydrogen peroxide or benzoyl peroxide would.

2.5.1.2 Polymerisation medium

It is generally accepted that conductive polyanilines are prepared in acidic media (Pud et al., 2003: 1701-1753). Protonic mineral acids, aliphatic and bulky aromatic protonic acids have been employed to produce conductive PANi (Lindfors and Ivaska, 2002: 65-74; Prokeš and Stejskal, 2004: 187-195; Bańka and Łużny, 1999: 715-716). However, also the chemical synthesis of biocompatible PANi prepared in phosphate buffer has been reported. Even so the pH of the phosphate buffer was maintained at a very low range of between $1.7 \leq pH \leq 2.2$. The growth rate and characteristics of the phosphate doped PANi were similar to those of H_2SO_4 - PANi (Sandra et al., 2004: 2033-2041; Sandra et

al., 2003: 28-33). Elsewhere, the chemical synthesis of polyaniline at an organic/aqueous phase interface has been reported by use of ammonium persulphate as oxidant (Siwei et al., 2006: 7680-7683; Xinyu et al., 2004: 23-29). However, in all the procedures employed by the different authors, the aqueous phase consisted of aniline monomers dissolved in a strong protonic acid which further emphasizes the importance of the presence of protons towards the production of conductive PANi.

2.5.1.3 Ease of synthesis

Unfortunately, despite the fact that the chemical synthetic route for the production of PANi is facile and suitable for large scale production, the resultant PANi is usually an intractable powder with limited commercial applications due to inprocessibility. Also in general, the use of protonic acids makes the process environmentally unfriendly due to the high acid concentrations required (Rumbau et al., 2007: 1412-1421). Use of acids demands further purification steps which may make the process rather cumbersome. Many approaches have been proposed towards improvement of this process. In other situations, the total diversification of the process has been reported. Biocatalytically, plasma membrane, vacuum vapour deposition, sonochemically produced PANi has been reported (Hu et al., 2005: 239-248; Sivakumar and Gedankan, 2005: 301-306; Zaharis et al., 2006: 341-345). Hu et al., (2005: 239-248) for instance reported on the biomimetic Hb-catalyzed production of PANi. In this work, hemoglobin was used to catalyze the polymerization of hemoglobin in the presence of sodium dodecylsulphate (SDS) thus providing an alternative route for PANi production. The reaction was initiated by the addition of H_2O_2 and the PANi-produced through this method was found to be electroactive and conductive exhibiting electrochemical and spectroscopic behaviour similar to those of doped PANi produced from the tradition methods. This biocatalytic PANi production method was thought to be superior over the traditional methods because it was environmentally benign, gave rise to high yield and offered a high degree of control over the reaction kinetics. Elsewhere, horseradish peroxidase (HRP), soyabean peroxidase, biluribin oxidase enzymes have been reported to produce conductive polyaniline in some cases even soluble in water (Hu et al., 2005: 239-248; Jin et al.,

2001: 237-242; Aizawa et al., 1990: 301-309). However, despite the advantages of the biocatalytic PANi production, the method may not be suitable for bulk production given the fact that enzymes are extremely expensive. Also these reactions are initiated by the addition of H_2O_2 which itself is a pollutant. The use of enzymes or other biomolecules will implicate stringent control of reaction conditions since biomolecules are easily de-natured if exposed to harsh conditions.

The sonochemical production of conductive polyaniline has been reported (Jing et al., 2007: 75-80; Sivakumar and Gedankan, 2005: 301-306). In general the sonochemical polyaniline production process is similar to the conventional methods save for slower addition of the initiator and the use of ultrasonic irradiation. Jing et al., (2007: 75-80), compared the properties of polyaniline produced through the traditional magnetic stirring methods with that produced by use of ultrasonication. The authors claimed that the ultrasonicated PANi was more soluble to the extent that its dispersion in distilled water either in the doped or undoped forms could be used for UV-Vis analysis. This was impossible for magnetically prepared PANi. Ultrasonically prepared PANi takes a shorter time to form because the polymerization rate of aniline is higher compared to the conventional methods that involve magnetic stirring (Sivakumar and Gedanken, 2005: 301-306). Despite these positive properties of the ultrasonic PANi preparation, the use of ultrasonic baths may make the large scale PANi production economically unviable. It has also been reported that preparation of PANi through ultrasound method converts water to hydrogen peroxide (Sivakumar and Gedanken, 2005: 301-306) which may lead to pollution and may also lead to over-oxidation of PANi due to excess presence of oxidant.

Elsewhere, the hot wire vapour deposition of polyaniline has been reported (Zaharis et al., 2006: 341-345; Urdal et al., 1989: 451-456). According to the authors, hot wire or vacuum deposition methods are faster one step processes producing cleaner PANi films since the hazardous solvents utilized for PANi dissolution in the convectional methods are not used. These methods allow for the use of insoluble PANi thus eliminating inprocessibility problems. Vacuum deposition, therefore, has potential as a technique for the growth of highly uniform, ultrathin polymeric films for applications such as

integrated circuits where 'wet' processing techniques are incompatible with device fabrication (Plank et al., 1997: 1-9). However, although the vapour deposition techniques are faster and produce pure polyaniline films (suitable for commercial applications especially in optoelectronic devices), it has been said that the PANi films produced are mostly in the polyleucoemeraldine form. This has been verified by the absence of the band (IR, 1160) for the polymeraldine salt PANi which may indicate that vacuum deposited PANi is much less conductive compared to convectional PANi. While the vapor deposition method is excellent for production of ultrathin films some times as thin as 1000 Aº (Cornelison et al., 1995: 87-94) there is a likelihood for an increased cost of production, given the high temperatures required and the need for pressure resistant equipment.

The production of PANi through plasma methods has also been reported (Cruz et al., 1997: 213-218; Mathai et al., 2003: 2253-2257). According to the latter author, plasma methods are excellent for producing high quality ultrathin films. Plasma method films are pin-hole free, chemically inert, uniformly thick, and thermally stable unlike those from conventional methods (Mathai et al., 2003: 2253-2257). Cruz et al. (1997: 213-218) prepared undoped and iodine doped ultrathin PANi films in the range of 2.1-10.63 µm depending on the reaction time using the RF plasma polymerization methods. The resultant solution were contamination free since no solvents were used but exhibited low conductivity values of 10^{-10} -10^{-12} undoped PANi; 10^{-4}-10^{-11} iodine doped PANi. Since the conventional methods produce powdered PANi, the plasma methods and the vapour/vacuum techniques can be considered suitable for ultra-thin film production. However, the PANi film produced from the two methods is less conductive than conventional PANi (Mathai et al., 2003: 2253-2257). Furthermore, the use of sophisticated equipment in the plasma methods is likely to make bulk PANi production through this method expensive.

Therefore, despite the fact that PANi produced from these new methods may be much purer and the methodologies allow for easy control of the reaction kinetics, the traditional methods for PANi synthesis still remain the most economical and suitable for large scale

production. New approaches, therefore, are now focused on the *improvement* of the *traditional methods* with the aim of tailoring the properties of the PANi product as need demands. The major goals of these improvements are to: improve PANi processability, improve PANi stability, improve PANi biocompatibility and conductivity amongst others.

2.6 Improvement of the chemical method to enhance processability

A major drawback of the traditional chemical synthetic production of PANi is that the resultant product is insoluble in common solvents, decomposes before melting and therefore does not lender itself for large scale production. Polyaniline inprocessability has been addressed through two methods. Firstly, solubilization has been achieved through co-polymerization of the requisite monomers with molecules of polymers that can induce solubilisation. Secondly, a nanostructurization approach to produce more dispersible PANi has been used.

2.6.1 Solubilization approaches.

2.6.1.1 Use of bulky molecules such as surfactants

One of the ways towards the production of more processable PANi has been achieved through the preparation of PANi colloids in the nano/micro ranges or by the use of reactive/non reactive surfactants (Kohut-Svelko et al., 2005: 107-114). Surfactant bearing sulphonic groups can act as both stabilizers and dopants thus influence the resultant PANi properties in terms of conductivity, stability, and solubility. PANi prepared in the presence of sodium dodecyl benzene sulphonic acid (SDBS), camphorsuphonic acid, sulphosalicylic (Erdem et al., 2004: 785-791) and in dinonylnaphthalene sulphonic acid – DNNSA-(Kohut-Svelko et al., 2005: 107-114) was reported to have improved solubilities. The improvement of solubility with use of these molecules was attributed to the introduction of polar and non-polar moieties with the polymer matrix which promoted solvent compatibility with improved organic solubility. On working with different

surfactants, Erdem et al., (2004: 785-791) concluded that the organic solubilization ability of a surfactant increased with its chain length.

Elsewhere, the addition of ammonium persulphate (APS) solution to a mixture of aniline, toluene and (sodium dodecyl benzene sulphonic acid) SDBS at 0 ºC under a nitrogen atmosphere produced toluene soluble PANi (Kim et al., 2007: 205-210). A novel polyaniline-maleic acid-dodecyl hydrogensulfate salt chemically synthesize was found to be soluble in common polar organic solvents such as DMSO, NMP and DMF with a maximum solubility of 6 % w/v. The improved solubility of the PANi complex was associated to the long and non polar chain dopant present in polyaniline that created space for penetration of solvent molecules thus improving solubility (Palaniappan and Amarnath., 2006: 1741-1748). Elsewhere, acrylic acid doped PANi exhibited greater solubility in m-cresol and NMP compared to that doped with HCl (Athawale et al., 2002: 106-110). A camphor-sulfonic acid –PANi complex displayed improved organic solubility. The complex was found to dissolve in chloroform and m-cresol (Santos et al., 69: 141-142). The preparation of DBSA doped in a reversed micellar system of dodecylbenzene sulfonic acid (DBSA)-(2,2,4-trimethylpentane)-(isooctane)-water has been reported (Han et al., 2005: 179-187). The PANi made in this way exhibited improved solubility in common organic solvents the order been $CHCl_3$ >DMSO >THF > DMF. The solubilities of PANi-HCl was correspondingly lower than that of PANi-DBSA in all cases (Han et al., 2005:179-187). Even with the use of surfactants, complete solubility has not yet been realized. In most cases PANi is doped with specific acids such as dodecylbenzene sulfonic acid or camphor sulfonic acid and, the resulting salts are partially soluble in solvents such as NMP or *m*-cresol and the search for new technologies to obtain 'ideal' PANi in terms of processability is still ongoing (Falcou et al., 2005: 115-122).

2.6.1.2 Derivatisation of PANi

There have been several reports on the synthesis and properties of alkyl, alkoxy ring substituted polyanilines (Nateghi et al., 2005: 11476-11483; Komsiyska et al., 2005: 88-95; Norris et al., 2000: 3237-3243). Polymerisation of other functionalized anilines such as ortho alkyl (Falcou et al., 2005: 115-122), sulphonated (Yue et al., 1991: 765-768; Tang et al., 1998: 43-48), and *N*-alkyl anilines (Wei et al., 2005: 19-26) have been reported. These studies have shown that the resultant substituted PANi complexes have improved solubilities in common solvents such as $CHCl_3$, THF, and DMF etc. Similarly, sulphonated or carboxylated ring substituted PANi has been found to be water soluble (Norris et al., 2000: 3237:3243; Gök et al., 2004: 41-48). The aniongenic functional groups in the sulfonated polymer interact positively with charged nitrogen ions in the PANi chain with new effects such as improved solubility (Varela et al., 2001: 321-327).

Falcou et al., (2005: 115-122) prepared *o* and *N* -polyanilines using methane sulphonic acid in a hexane, THF and water mixture and found out that the resultant polymers were more soluble in THF and NMP but showed relatively low conductivities in the range 10^{-9} in their emeraldine base forms and between 10^{-4} -10^{-6} in their emeraldine salt forms. It has been said that, such substituents cause steric hindrance that lead to the twisting of the polyaniline chain out of planarity with serious conductivity effects (Norris et al., 2000: 3237-3243). Some of the substituted polyanilines which have created a lot of interest include poly-*o*-methoxyaniline and poly-2, 5-dimethoxyaniline whose structure is shown in Figure 2.5.

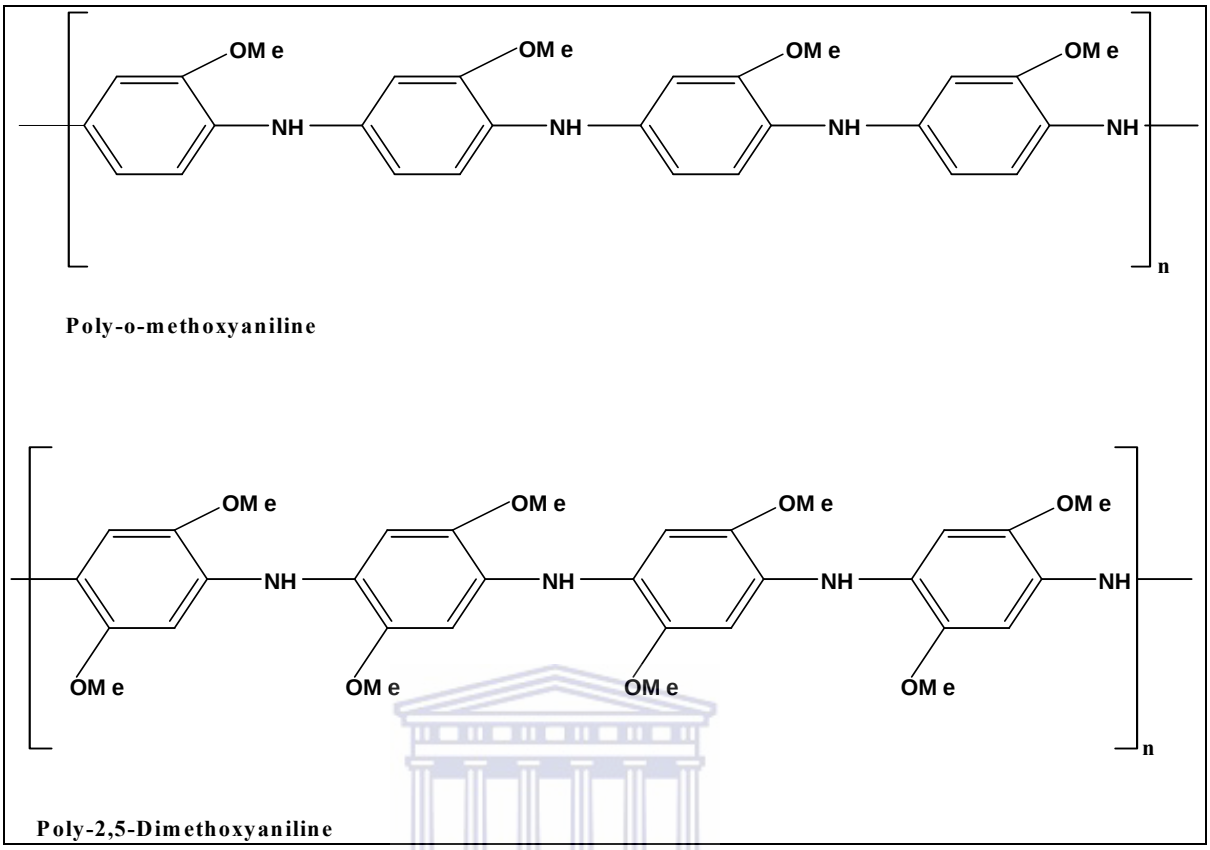

Figure 2.5: Examples of some of the derivatised polyanilines: poly-o-methoxy aniline and poly-2,5 – dimethoxyaniline. OMe = OCH_3.

These PANi derivatives have been found to exhibit improved organic solubilities compared to native PANi (Nateghi et al., 2005: 11476-11483). Research has also been carried out on other substituted polyanilines with different electron donor groups such as $-CH_3$, $-OCH_3$ and $-OC_2H_5$ (Komsiyska et al., 2005: 88-95). Poly(*o*-methoxyaniline) (POMA) and poly(2,5-dimethoxyaniline) (PDMA) have been reported to be more soluble in common organic solvents with conductivies similar to PANi and show different electrochromic behavior than PANi (Huang et al., 2003: 88-95). Therefore derivatisation in itself is not adequate towards solving PANi inprocessability problems since it compromises the conductivities of the resultant polymers and also the steric and /or inductive effects could make functionalised monomers difficult to polymerise (Falcou et al., 2005: 115-122; Babero et al., 2004: 3671-3686).

2.6.1.3 Preparation PANi composites/blends with other copolymers

Another route towards more processable PANi has been through composite or blend formation. Preparation of polyaniline composites/blends with suitable polymers has been achieved through the in-situ or ex-situ polymerisation processes (Mirmohseni and Wallace 2003: 3523-3528). In the in-situ polymerisation process, the polymerisation of the monomer (aniline) is carried out in the presence of a polymeric host stabilizer. For instance, the polymerisation of aniline monomers in the presence of water soluble polymeric stabilizers such as polyvinyl pyrrolidone (PVP), polyvinyl alcohol (PVA), polystyrene sulfonic (PSSA), and polyacrylic acid (PAA) has been found to produce water soluble polyaniline composites/ blends (Cho et al., 2004: 15-18). The improved water solubility after co-polymerisation is associated with the formation of hydrogen bonding linkages between PANi and the co-polymer thereby enhancing PANi solvation.

2.6.1.4 Counter-ion induction techniques

Counter-ion induced processability method involves the post-synthetic protonic doping of chemically synthesized undoped PANi with suitable functionalized protonic acid dopants. It is therefore a type of secondary doping phenomenon attributable to the expanded coil conformation adopted by doped PANi in a suitable solvent (Pud et al., 2003: 1701-1753). The protonic acids are found to induce the solubility of doped PANi in polar or weakly polar solvents. However, since the counter-ion method is a post-synthetic process, this would unnecessarily increase the time required for PANi production.

2.6.1.5 Shortcomings of the solubilisation approach

Despite the above efforts to improve the solubility of chemically synthesized PANi, solubility is still an issue of concern. First, complete solubilisation of PANi in cheap ordinary organic solvents such as hexane, methanol etc. has not yet been achieved. Furthermore, even with the use of polar solvents, sometimes only partial solubility has been achieved. Second, the introduction of bulky substituents into the PANi backbone

has been found to hamper other desirable PANi properties such as conductivity due to increased steric hindrance. For these reasons, a *combinational approach* is now found more favourable towards more processable PANi. In such approaches, the chemical synthesis of PANi/or PANi derivatives is carried out in the presence of nanostructuring aids which at the same time may have solubilizing properties.

2.7 Nanostructurization approaches

The prefix "nano" is used to represent materials with grain sizes in the order of a billionth of a meter. A composite refers to a material that is made up of two or more constituents which exhibit different physical/chemical properties and which remain separate/distinct within the finished structure. Polyaniline nanocomposites have been prepared for various reasons which include: improving dispersibility (processability) to improve conductivity, to create new smart materials for future technological use. This has been achieved because polyaniline nanocomposites have increased stability and a high surface to volume ratio.

2.7.1 Processability

Since the intractability, i.e., infusibility and insolubility, is the major factor hampering its large scale applications, dispersing of the polymer in common solvents is regarded as one of the most effective approaches to address this problem from both a scientific and technological point of view (Zhang and Wang, 2006: 9-19; Wessling, 1998: 143-154). Accordingly, synthesis of nano-structured PANi, on one hand, is the key step in preparing highly dispersed blends of PANi with other processable polymers, and thus to improve the processability of PANi (Zhang and Wang, 2006: 9-19). On the other hand, nanostructurization will produce new smart materials for new applications (Malinauskas et al., 2005: R51-R62). The fabrication of more dispersible nanosized PANi has been reported by many works (Zhang and Wang, 2006: 9-19; Kohut-Svelko et al., 2005: 107-114; Han et al., 2005: 179-187; Tran and Kaner, 2006: 3915-3917).

Accordingly, nanostructurization of PANi has mainly been achieved through two processes; the template and the template-free processes. Nanostructurization through the template synthesis method involves the placement of suitable nano-pored templates in the polymerisation bath. Polymer deposition within the nano-pores moulds them into nano-shapes. Figure 2.6 displays the structures of two of the most commonly used membranes for the template assisted nanostructurization.

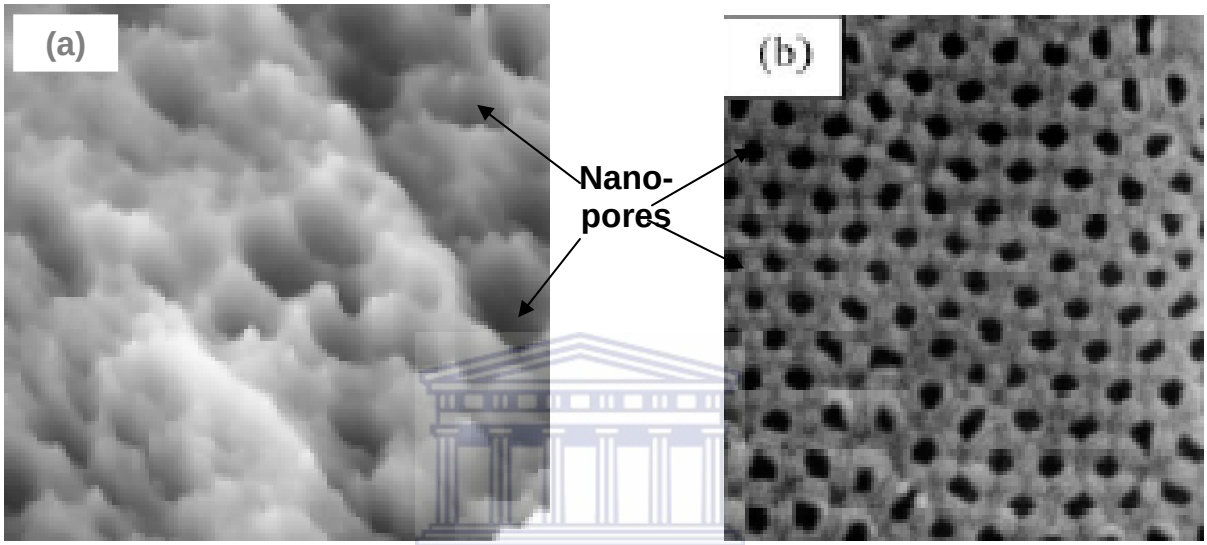

Figure 2.6: A poly-carbonate track-etched membrane (PCM) (a) and an anodic alumina membrane (ALM) (b) showing uniformly sized nano-pores within which polymer deposition takes place.

Source: Yang et al., (2005: 65-68).

Using the template synthesis in anodic alumina pores (ALM), Yang et al., (2005: 65-68) prepared nanosized polyaniline particles which took the rod like shape. The dispersible rods were found to exhibit uniform diameters. PANi and poly-*o*-methoxyaniline (POMA) nanotubes in polycarbonate membranes (PCM) were prepared through the chemical in-situ deposition method (Maceij et al., 2003: 403-407; Palys and Celuch, 2006: 4115-4124). The authors discovered that although the resultant materials were in the nano-range and therefore more dispersible, the mechanisms of formation of the resultant nanotubular structures were different. The PANi nanotube formation began in the polymerisation bath before deposition into the membrane pores. For POMA the process began by the adsorption of *o*-methoxyaniline monomers onto the membranes followed by polymerisation.

Although the template synthesis has been used greatly to obtain dispersible nanosized PANi and that it yields uniformly sized nanostructures (which might be an added advantage), several limitations have been associated with this process. Firstly, the template synthesis demands the post- synthetic removal of template, and secondly: it demands the use of a 'molecular anchor' to maintain the nanostructures shapes which in itself is a challenge and thirdly: the need for the post synthesis template dissolution is limiting in itself because only those templates with a corresponding dissolving solvent can be used (Wei et al., 2002: 917-921; Long et al., 2003:208-213).

Therefore, new approaches towards PANi dispersibility through nanostructurization are now focused on use of 'inbuilt templates' or 'soft templates' (Wei et al., 2002: 917-921; Zhang and Wang, 2006: 9-19). The method entails the synthesis of PANi/PANi derivatives in the presence of structure-directing materials such as surfactants, nucleic acids, polyelectrolytes, and sulphonated porphyrins amongst others (Zhang and Wang, 2006: 9-19). Naphthalene sulfonic acid (Wei et al., 2002: 917-921), camphor sulphonic acid (Zhang and Wan, 2005: 24-31), dodecyl benzene sulphonic acid (Han et al., 2002: 53-60) are some of the complex acids with bulky side groups that have been used for the production of one dimensional dispersible PANi. Surfactant molecules in solution exist in micellic form leaving nanoscopic spaces available for monomer polymerization (Fig. 2.7).

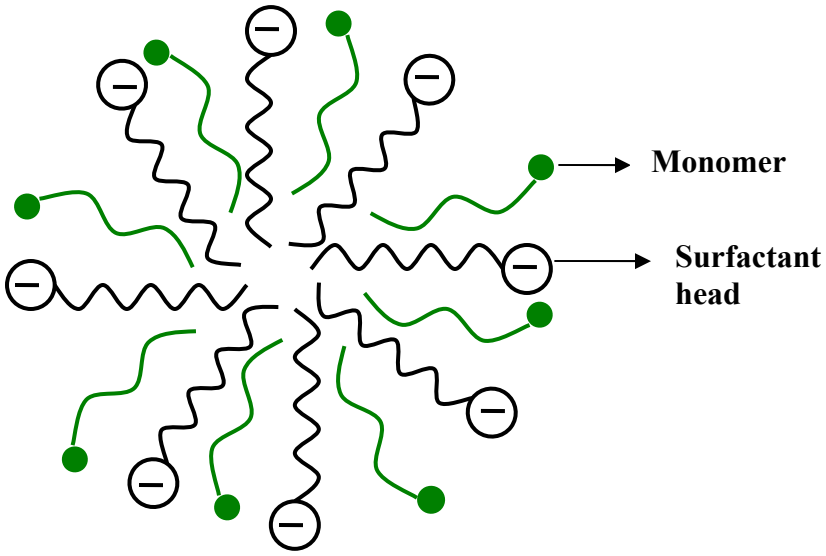

Figure 2.7: A schematic diagram showing the micelle-monomer orientation adopted by an anionic-surfactant in a polar solvent during template-free polymerization process.

This way surfactants act as soft templates for nanostructurization. Several advantages accompany the use of the 'soft template' method to improve processibility. Nanostructurization of PANi leads to increased surface area which boosts its stability and conductivity. Also, through the 'soft template method', several one dimensional structures taking various forms depending on the nature of template can be obtained. That is, besides processability improvement, conductivity and morphology are also improved. Oh and Im, (2002: 273-277) prepared nanoparticles of electroconductive polymers such as PANi in sodium dodecyl sulphate and (SDS) micellar solutions to improve processability. The resultant nanoparticles exhibited sizes and shapes similar to those of the SDS micelles and were dispersible and showed enhanced conductivity. Elsewhere, the chemical oxidative polymerisation of aniline was performed in a micellar solution of DBSA to obtain nanoparticles with enhanced thermal stability and processibility (Han et al., 2002: 53-60). The average size of the PANi particles was between 20-30 nm meaning they could easily be dispersed. Dispersible chiral camphor-sulphonic acid-doped polyaniline nanotubes with external diameters of between 80-200 nm have been prepared. Polyaniline-polyvinylsulfonic acid nanotubular/rod were prepared in the presence of β-NSA. The formation of the nanostructures were attributed to the self-assembling of the β-

NSA molecules and/or aniline salts into nanostructural template acting complex. The resultant nanostructures exhibited diameters between 60-80 nm and were soluble in water due to the presence of PVA (Zhang and Wan, 2002: 83-89).

By variation of the polymerisation bath additives, PANi – composites tailored to suit various applications have been produced. Compared to other methods, the template free method is simple, cheap and is very desirable for the improvement of PANi dispersibility and gives room for the improvement of other properties as well. Although the control of the diameters of the nanostructures is not easily achieved through this method, it is an avenue for the fabrication of many new smart materials (composites) achieved by just varying the contents of the polymerisation bath.

2.8 Electrosynthesis of polyanilines

Besides the chemical synthetic route, conducting polymers has been prepared through electrosynthetic routes (Crutz et al., 1997: 213-218, Palaniappan et al., 2006: 1741-1748). Three electrosynthetic approaches have generally been used namely: potentiostatic, galvanostatic and potentiodynamic techniques. The potenstiostatic technique involves the electrodeposition of the polymer on the electrode by the application of constant potential. In galvanostatic methods the polymerisation is achieved by application of a constant current. The cyclic voltammetric technique on the other hand involves sweeping the potential of the electrode to and fro between predetermined potential limits, upon which electrodeposition takes place on the surface of the electrode.

The potentiostatic deposition of optically active polyaniline salts of camphor sulphonic acid have been reported (Innis et al., 1998: 6521-6528). The chiral PANi-HCSA composites were co-doped with polystyrene sulphonic acid and exhibited great water solubility. The potentiostatically deposited films displayed two redox couples at 0.155 V and 0.515 in HCl, the couples being associated with the oxidation states of polyaniline (Innis et al., 1998: 6521-6528). Elsewhere, polyaniline-polycarbonate composites were potentiostatically deposited by first dipping the electrode in polycarbonate solution (1 %

$CHCl_3$) followed by the electrodeposition of polyaniline on to the electrode by the application of a constant potential for 12 h. The casting solution consisted of 0.1 M aniline and 0.1 M HCl (Anand et al., 1998:993-1018).The potentiostatic deposition of poly-*o*-methoxyaniline doped with camphorsulphonic acid was carried out on a Pt or ITO electrodes by a applying a constant potential of +0.8 V or 1.1 V respectively. The resultant films were green in nature and chronoamperograms revealed that the electrodeposition process was two phased involving the nucleation and the polymer growth stages (Norris et al., 2000: 3237-3243).

The galvanostatic electrodeposition of polyaniline has been reported (Genies and Tsintavis, 1995: 109-128; Anand et al., 1998: 993-1018). Elsewhere, poly-*N*-methylaniline (PNMA) was electrodeposited through potentiostatic and galvanostatic methods (Sivakumar and Saraswathi, 2003: 381-390). According to these authors, potenstiostatic deposition of PNMA could be effected with potentials as low as 0.55 V. However, the resultant polymer dissolved in the electrolytic solution to give a blue coloration which indicated that there was a high tendency to form oligomers. On application of an optimal current density of 2 mA cm^{-2} galvanostatically deposited PNMA was a greenish black uniform film with good adhesion which led the authors to conclude that galvanostatic technique was superior to the potentiostatic one. In another instance, tungsten trioxide based polyaniline films were prepared by the galvanostatic polymerization of aniline in an aqueous HCl solution containing suspended tungsten trioxide particles with the application of a current density of 1 mA cm^{-2}. Free standing films were obtained (Anand et al., 1998: 993-1018). Recently, polyaniline formation through pulse potentiostatic methods (PPM) and pulse galvanostatic methods (PGM) has been reported (Tang et al., 2000: 32-35). But the majority of the works report the electrodeposition of polyanilines using cyclic voltammetry. It has been said that CV produces stable thin homogeneous compact films unlike in the case of both potentiostatic and galvanostatic electrodeposition (Komsiyska et al., 2005: 88-95; Iwuoha et al., 1997: 749-761). The electrodeposition of PANi and *N*-alkyl PANi on glassy carbon or quartz glass tin oxide (TO) coated electrodes using, HCl, $HClO_4$ or DBSA solutions have been reported (Lindfors and Ivaska, 2002: 65-74). According to the authors, the initial

polymerisation rate for the aniline monomers was slower than that of the *N*-alkyl monomers but the situation changed beyond 50 cycles. Elsewhere, a layer of polyaniline was cast on a platinum electrode by the potentiodynamic mode to form a solution containing 0.2 M aniline in 1 M HCl between -200 and +1100 potential limits for 10 cycles (Mathebe et al., 2004: 115-120). In this report, an initial oxidation of polyaniline occurred at +900 mV followed by the formation of three well formed redox couples characteristic of polyaniline.

2.8.1 Various electrodeposition goals

Like in the case of chemically synthesized polyanilines, electrodeposition of polyanilines has been made for various reasons. Similar to the chemical synthesis, the electrochemical synthesis has been structured around issues such as processibility, stability, biocompatibility and the creation of novel smart materials for future technological use. Through the inclusion of specific additives in the polymerisation bath, polyaniline polymers with desirable characteristics have been produced. In view of these new modes of electrosynthetic procedure for polyaniline such as enzymatic and vapour deposition techniques have been used (Rumbau et al. 2007:1412-1421; Nekrasov et al., 421:133-137). However, just like in the case of chemical synthesis such techniques are bound to be highly expensive and may lead to adverse environmental effects (e.g where enzymes are used) due to use of H_2O_2 to initiate the reaction.

Österholm et al., (1993: 1034-1039) synthesized polyaniline in a DBSA micellar medium. The resultant polymer was found to exhibit high molecular weight, high conductivities and was soluble in some common organic solvents. Elsewhere, DBSA-doped PANi, besides maintaining electroactivity even at neutral medium, exhibited high conductivities of 0.004 S/cm at pH 7.0 (Choi et al., 1999: 253-256). The synthesis of a PANi-CSA (camphor sulphonic acid) film cast from a 1 M CSA solution containing 0.5 M aniline with potential cycling between -0.1→0.8 V has been reported (Santos et al., 1995: 141-142). The exhibited redox waves were similar to those of PANi-HCl and was quite soluble in various organic solvents such as m-cresol and chloroform with

conductivity values of 1 S/cm. Elsewhere, POMA (poly-*o*-methoxyaniline) was cast on a Pt electrode either potentiostatically and/or potentiodynamically from a 1 M camphor sulphonic acid solution containing 0.2 M *o*-methoxyaniline or aniline (Norris et al., 2000: 3237-3243). The potentiostatic oxidation was achieved by application of a constant potential of 0.8 V. Cyclic voltammetry was performed by sweeping of potential between -0.2 and 1.0 V for 50 cycles. Results showed that the resultant films were soluble in NMP, DMF, MeOH and DMSO. The authors contributed such improved organic solubility to the presence of methoxy groups that decreased the stiffness of the polyaniline chains due to the polar moieties introduced by the sulphonic acid.

Akin to the chemical synthesis, nanostructurization of conducting polymers in the electrosynthetic process has been done to improve dispersibility, conductivity and form new materials through both the template and template free processes. The template-based nanostructurization has been carried out within the holes, cavities or channels pre-created on the electrode surface (Yang et al., 2005: 65-68) or by use of special membranes. PANi-nano/microstructures were prepared through the electropolymerisation of aniline in a metallic layer pre-deposited on one side of a polycarbonate track-etched membrane (Devaulx et al., 2000: 295-280; Palys and Celuch, 2006: 4115-4124). The method allowed for easy control of the tubules sizes through the variation of monomer/concentration and reaction times. Elsewhere, polyaniline nanoparticles were electrodeposited on high pyrolytic graphite electrodes (HOPG) by use of the pulse potentiostatic method. The potential was stepped from -0.2 → +0.9 V. Formation of nanoparticles were verified through CV and SEM (Barriós et al., 2006: 128-135).

Biocompatible polyaniline composites of PANi-polyitaconic acid a hydrogel-like composite with promising uses like in drug delivery have been prepared. The resultant materials exhibited redox characteristics similar to those of PANi-HCl. Itaconic acid is a biomolecule derived form the carbohydrate fermentation by primitive yeasts and has characteristics similar to those of acrylic and metacrylic and thus can form an avenue for production of biocompatible PANi. The electrodeposition or incorporation of metal-containing particles to conducting polymers like PANi has been done to improve their

applicability in biosensors, for electrocatalysis, magnetic shielding and corrosion protection etc. (Sofiane et al., 2006: 62-67). The incorporation of liquid mercury into PANi to form PANi-Hg composite electrodes has been reported. The electrodes were used for the polarographic detection of heavy metals such as lead in tap water. Elsewhere, the conductivity of PANi-montomorrilonite clay composites were found to exhibit conductivities in the range of 10^{-1} -10^{-4} S/cm (Nascimental et al., 2006: 6131-6139). Elsewhere, PANi-CNT (carbon nanotube composites) nanocables with improved stability and conductivity have been synthesized (Sathiyaranayanan et al., 2007: in press). The ongoing discussion attempts to highlight the versatility of the electrosynthetic procedure as an avenue for the generation of smart materials. Through the process, composites of PANi with new or improved characteristics can easily be made.

2.8.2 Factors affecting the electrodeposition processes

A study was conducted to investigate the effect of anions on the electrodeposition of polyaniline. The various effects were marked with peak shifting, decrease in polymerisation current as well as in the degradability of the polymer. Of all the anions studied, the PANi-SO_4^{2-} system showed the highest degree of degradation followed by PANi-Cl. Little or no degradation was observed in PANi doped with surfactant anions even at pH 4.0. The presence of surfactant ions stabilized the PANi and the stabilization trend was found to follow $DS^- > DBS^- > TS^-$ where the anions originated form sodium dodecyl sulphate, sodium dodecyl benzene sulphonate, toluene sulphonated surfactants respectively (Rahmanifar et al., 2006: 3463-3468). The authors associated the observed trend to the different surfactant head group charges, distance of anion from PANi positive sites and to the shielding effect of anions on the PANi positive sites. The rate of polymerization may also be affected by the nature of substituents and the position of substituents on the ring. Roković et al., (2006: 6045-6050), on studying the effect of different substituents on the polymerization rate, suggested that substitution in the ortho position leads to longer polymerisation rate and decreased molar mass. Anions present in the polymerization bath may affect the monomer oxidation potential and the mechanisms of nucleation because different anions are adsorbed differently at the electrode. A

comparison between the Cl^-, $HClO_4^-$, HSO_4^- revealed that the rate of electropolymerisation was higher in the Cl^- than in the presence of either the $HClO_4^-$ or HSO_4^-. To justify this trend, the authors argued that the formation of ion pairs between the anilium cations and/or positive charges in the polymer backbone controlled the polymerisation rate. Faster polymerisation rate was observed in the Cl^- system because the latter formed stronger ion pairs.

2.8.3 Synthesis, properties and electrochemical characterisation of sulphonated polyanilines

Of particular interest to biosensor technology are sulphonated polyanilines, because they exhibit extraordinary stability at neutral medium allowing them for use in electromediation purposes in biosensors. There are two types of sulphonated polyanilines: firstly, polyanilines with sulphonic group on the ring (SPANi) and secondly those formed through the incorporation of aliphatic or heteronuclear sulphonated hydrocarbons (SPAH).

Sulphonated polyanilines (SPANi) refers to polyanilines that bear aniongenic functional groups such as –COOH, -OH and $-SO_3H$ directly or spacer bound to the aromatic ring (Màrquez et al., 2007). They can be produced through two methods, firstly: the grafting of sulphonic groups into the polyaniline backbone (self-doped PANi) and secondly by doping polyaniline with sulphonic group containing compounds. Self-doped PANi has been prepared through the traditional chemical and electrochemical methods by use of fuming sulphuric acid or the direct electropolymerisation of metanilic acid (aminobenzenesulphonic acid), or the direct sulphonation of the emeraldine salts with chlorosulphonic acid (Benard and Hugot, 2006: 728-735). Elsewhere, sulphonated PANi was produced by the refluxing of aniline with 4-bromobutylchloride followed by debromination using Na_2SO_3 to yield N-(4-sulphonic butyl) aniline. This SPANi displayed electrochemical properties similar to that of HCl-doped PANi with the monomer oxidation beginning at 900 mV and the redox couples appearing at 280, 600, 780 mV (Zheng et al., 2006: 2328-2333).

Alternatively, sulphonated polyaniline (SPAH) may be achieved by the preparation of PANi-complexes with sulphonated aliphatic or heteronuclear aromatic hydrocarbons such as camphor-sulphonic acid and naphthalene sulphonic acids or with sulphonated polyelectrolytes (Wei et al., 2002: 917-921; Zhang and Wan, 2005:24-31; Chen et al., 2006: 489-494).

According to Benard and Hugot (2006: 728-735), a comparison between the properties of HCl-doped PANi and self-doped PANi (SPANi) revealed that the latter exhibited lower conductivity despite its higher ability to prevent corrosion. However, the authors revealed that the conductivity of SPANi was pH independent unlike that of PANi-HCl. Therefore sulphonated polyaniline is advantageous over the other forms of polyaniline because its pH-independence means it can perform perfectly even under neutral pH. Other properties that make the SPANi stand out include: its high aqueous solubility, good electrochemical activity both at alkaline and neutral media, pH independent conductivity, and ability to be n-doped (some) which makes them particularly suitable for biosensor applications (Màrquez et al., 2007). However, the low conductivities of SPANi sometimes as low as 10^{-5} S/cm may hinder their application in such fields (Carlos et al., 2007: 2978-2986).

Elsewhere, the effect of pH on PANi doped with different anions including Cl^-, methane sulphonic acid (MSA), benzene sulphonic acid (BSA) and DBSA was studied (Lindfors and Ivaska, 2002: 43-52). In this study PANi-Cl exhibited the polyleucoemeraldine/polyemeraldine couple at a formal potential $E^{0'}$ = 120 mV; redox couple due to polymer degradation at $E^{0'}$ = 521 mV and the polyemeraldine to polypernigraniline transition couple at > 600 mV. Similar trends were observed for the PANi doped with the various sulphonic anions but with a greater increase in the peak to peak separation. On performing the potentiometric study of the resultant PANi, it was found that PANi-DBSA was completely insensitive to any pH changes implying it was very difficult to deprotonate. The presence of the bulky DBS- anion was thought to be responsible for the stability of PANi-DBS given that its bulkiness could not allow it to diffuse out of the polymer sites. It means therefore, aliphatic sulphonated hydrocarbons

can stabilize PANi and allow it to remain electroactive at neutral pH-a necessity for biosensor applications.

It is also now known that sulphonated heteronuclear aromatic hydrocarbon or sulphonated polyelectrolyte doped polyanilines (SPAH) are somehow much more superior to SPANi because besides having similar properties, they also exhibit high conductivities. Chen et al., (2006: 489-494) reported on the preparation of sulphonated polyaniline using sulphonated polyelectrolytes such as Nafion, polyvinyl sulphonic acid and polystyrene sulphonic acid. The resultant PANi-polyelectrolyte modified electrodes were conductive at pH 7.2 showing well formed peaks, although the electrochemical behaviour of Nafion-doped PANi was somehow hampered. For the unmodified PANi electrode however, at this pH only one oxidation and vaguely defined reduction peaks were seen indicating the polyaniline was unstable. Loss of the PANi stability for undoped PANi was associated with rapid deprotonation of the immine nitrogen sites (Chen et al., 2006: 489-494). The sulphonated PANi, however, still displayed redox couples at 200, 400, and 600 mV as expected for other doped polyanilines.

The preparation of SPAH by use of aliphatic sulphonated hydrocarbons such as sodium dodecyl sulphate (SDS) and sodium dodecyl benzene sulphonic acid has been reported (Cai et al., 1997: 209-212). The SPAH was prepared in a solution of 0.5 M aniline and 0.5 M H_2SO_4 by potential cycling between -200 → 750 mV versus a SCE electrode at a scan rate of 50 mV/s in the presence of 10^{-4} M SDS and SDBS. The resultant SPAH displayed improved conductivity characteristics. In particular the SPAH derived from SDBS showed good stability, electroactivity and an enhanced conductivity of 65 S/cm which was five times greater than that of native PANi. Elsewhere, SPAH was produced by preparing polyaniline in the presence of various surfactants: SDS, DBSA and their salts. The presence of surfactants improved the colloidal solubility of conducting polymers in organic solvents thus improving processability; however, there was no significant effect of the presence of a surfactant on the conductivity of PANi. However the authors noted that when large surfactant counter-ions constituted a part of the polymer, such materials might be less prone towards deprotonation and their electrical

stability at thermal ageing might be thus improved (Stejskal et al., 2003: 1353-1358). The results reported in this study show that the polymerization of aniline in the presence of anionic surfactants such as SDS and SDBS leads to the deposition of films having improved characteristics. The PANi DS^- film revealed a good resistance against the electrochemical degradation. This may allow a suitable modulation of the electrical properties of polymer films for use in novel applications. Shilpa et al., (2001: 401-403) demonstrated the stabilizing effect of NSA on the resultant PANi. In this study, SO_4^{2-}, p-TSA (toluene sulphonic acid) doped polyaniline were subjected to a pH of 2 for 24 h. Cyclic voltammograms taken after this time showed that only the PANi-NSA film displayed all the three redox couples expected for doped PANi highlighting the superior NSA stabilizing effect. The formation of polyaniline-camphor sulfonic acid composite on a Pt electrode via electrochemical polymerization of aniline in camphor sulphonic acid medium has been reported (Zhang and Dong 2004: 189-194). The PANi-CSA formed good electrocatalytic surfaces for the oxidation of ascorbic acid at pH 7.0 in phosphate buffer. The PANi-CSA film extended electroactivity to beyond pH 9.0 highlighting the stabilizing effect of the sulphonic groups. Elsewhere, Lukachova et al., (2003: 59-63) and co- workers mixed CSA with regular chemically synthesized PANi and dissolved them in chloroform. The PANi-CSA composite exhibited a fully reversible potentiometric response of 90 mV pH^{-1} in a wide pH range of between 3 – 9. It has been said that the redox activity of polyaniline extends up to a pH of 4 beyond which applicability of PANi is unreliable (Lukachova et al., 2003: 59-63; Kocherginsky and Wang, 2006: 1384-1393). The latter authors explained that for PANi-HCl, dopant anions can be released from the polymeric network during the oxidation/deprotonation processes leading to sluggish activity of PANi-HCl material beyond pH 4. However, for PANi doped with large anions such as CSA^- , the resultant polymer is stable since the large dopants cannot diffuse out of the of the polymer matrix. This fact was demonstrated by the fact that the PANi-CSA films prepared using $K_3Fe(CN)_6$ oxidant did not show any depressed electroactivity even at neutral pH (Kocherginsky and Wang, 2006: 1384-1393).

The ongoing discussion illustrates the superiority of sulphonated heteronuclear aromatic hydrocarbon-doped polyaniline over PANi doped with simple anions such as Cl^- , SO_4^{2-}

etc. PANi-doped with bulky sulphonic acids is electroactive even at neutral pH a characteristic which is very favourable for biosensor applications since enzymes operate best around their physiological pH usually around pH 7.0.

2.9 UV-Vis spectroscopy

UV-Vis spectroscopic characterization of conducting polymers relies on the fact doping modulates their structural and electronic properties with the emergence of new bands in their electronic spectra (Fernandes et al., 2005: 279-284). The overlapping of the p_z orbitals in the organic conducting polymers creates a continuous valence and conduction band separated by a band gap. Due to the large size of the band gap in conducting polymers, intra-gap transitions are not energetically viable. The absence of charge carriers in the undoped polymers therefore, means they are non conductive. A UV-Vis spectrum of undoped PANi (PANi-EB) consists of two characteristic bands: at ca. 320 nm assigned to the π- π* transition of the benzoid rings and ca. 600 nm related to the π-π* quinonoid rings (Zhang et al., 2005: 1373-1379; Cho et al., 2004: 15-18; Wei et al., 1989: 495-499, Norris et al., 2000: 3237-3243). However, in presence of dopants, new electronic energy levels are introduced within the polymer sub-gap energies (Fernandes et al, 2005:279-284) due to more energetically favourable intra-gap transitions. This corresponds to the appearance of polaronic (three transitions) and bipolaronic bands in their spectra and the consequential introduction of charge carriers - electrons or holes - within the polymer chain. Emergence of these new bands can thus be taken as spectroscopic signatures for conductivity (MacDiarmid 2001: 269-279).

In general the UV-Vis spectra of doped polyanilines have the same basic structure. Apart from the benzoid π- π* transition occurring at ca. 320 nm in most polyaniline-based polymers, doped PANi is characterized by the appearance of new bands at ca. 420 and >700 nm depending on the polymer and dopant type. The band at ca. 420 nm is generally assigned to an intermediate state formed during the oxidation of the polyleucoemeraldine salt of PANi and involves three sub-band gap transitions (Benard et al., 2005: 1615-1623). It is due to the charged para-coupled phenyl structures

corresponding to phenyl excitons or polarons (Malinauskas, 1998: 31-36). The band at > 700nm is also normally assigned to the polaronic charge carriers or to defects in the polymer chain (Guerra et al., 2002: 134-139). It is now well known that doped PANi can be converted in to its emeraldine base form (undoped) PANi through dissolving it in aqueous ammonium solution (dedoping). Also, the appearance of the quinonoid π-π^* transition band at ca. 600 in the spectra of doped polyanilines is indicative of incomplete doping (Geng et al., 1999: 5723-5727).

The characterization of phosphonic acid doped PANi dispersed in different solvents gave rise to closely related peaks (Geng et al., 1999: 5723-5727). While PANi dispersed in *N*-Methylpyrrolidone (NMP) and in ethanol/chloroform of acetonitrile displayed three peaks at 325, 430 nm in their spectra, the third peak for NMP occurred at 620 nm compared to between 750-800 nm for the other solvents. This variation in results were attributed to the basic nature of NMP that hindered the complete conversion of the phosphonic acid doped PANi into emeraldine salt form (Geng et al., 1999: 5723-5727). A comparison was made between the UV-Vis spectral properties of camphor sulphonic acid (CSA) PANi and POMA electrodeposited on ITO (indium tungsten oxide) electrodes. The peaks recorded were in close agreement being: 350, 420, 790 nm PANi; 350, 425, 785 nm POMA basically proving that the two polyanilines have a similar basic structure. However, in PANi -CSA the third peak at 790 nm occurred as a free carrier tail extending in to the infra-red region of the spectra an indication that the CSA doped PANi was in an 'expanded coil' conformation (Norris et al., 2000:3237-3243) and was therefore more conductive.

In another instance, CSA doped poly-2,5-dimethoxyaniline (PDMA) electrodeposited on an ITO electrode exhibited peaks at slightly different wavelength compared to those of PANi and POMA above. The bands occurred at 375, 460 and 770 nm (Huang et al., 2002: 155-163). Elsewhere, PANi doped with different NSA protonic acids displayed peaks at 320 nm, 400-430 nm and > 700nm. The occurrence of the polaron bands at > 700 nm was found to be dependent on dopant type. Also a shift in the position of the polaron bands from lower to higher wavelength occurred as the monomer concentration

was increased (Zhang et al., 2005: 1373-1379). Santos et al. (1995:141-142) compared the UV-Vis characteristics of PANi-HCl to those of PANi-CSA. In both cases a free carrier tail was observed from ca. 1000 nm but the PANi-HCl one was less intense. The authors observed that the interactions between a solvent with a composite also influence the properties of the composite.

Wei et al. (1989: 495-499) studied the effect of substitution on the position of the π- π* in unsubstituted and substituted PANi. A hyposchromic shift (a shift of the band to lower wavelengths) of the π- π* band in the substituted PANi was observed and related to a decrease in the degree of conjugation with substitution (i.e an increase in the band gap). According to the writers, this hyposchromic effect could be associated with lowered conductivities as is observed for substituted polyanilines. Elsewhere a hyposchromic shift was seen for PANi doped with polystyrene sulfonic acid (PSSA) compared to that doped with CSA. In another instance, $HClO_4^-$ doped POMA exhibited well defined peaks at 320, 420 and 700 nm. The peak at 420 nm was assigned to a radical cation intermediate and the rather broad band at 700 nm was assigned to the electron transfer from the valence band to the polaronic/bipolaronic states (Viva et al., 1999: 180-189). Elsewhere according to Palys et al. (2000: 111-119), the UV-Vis spectra of $HClO_4^-$ doped PDMA displayed peaks at 365, 465-500, 800 nm compared well to those of HCl –doped PDMA which occurred at 350, 420 and > 800nm. The differences were attributed to dopant type. Hino et al. (2006: 1327-1332), characterized PANi-HCl, PANi-SDS and PANi-PVA/SDS composites using UV-Vis spectroscopy. Nearly similar bands were obtained for all the systems. The band at 320 nm was attributed to the π- π* system, that at 420 to the protonation of the PANi backbone, and that at 800 nm to the polaron band of the emeraldine salt of PANi. In addition, bands at 540 and 640 nm normally associated with the insulating pernigraniline/emeraldine forms of PANi were absent.

The UV-Vis of PANi/DBSA gave rise to band at 350, 420 and 785 nm which were assigned to the π- π* system of the benzoid ring and to the localized polaron bands respectively (Moulton et al., 2004:402-406). According to the authors, the overlapping of the π- π* at 350 nm with that 420 nm to form a flat and/or distorted single peak indicated

a high level of doping. Elsewhere, Jiang et al. (1997: 125-126), on working on different camphor sulphonic acid –doped (CSA) polyaniline systems demonstrated the correlation between band intensities and conductivity. For all the three systems, poly(*o*-toluidine), poly(*o*-chloroaniline) poly(*o*-anisidine), the UV-Vis bands occurred at 325, 435, 800-850 nm. The intensities of the polaron band at 435 indicated the doping levels and the broadness of the band at 800 nm related to the distribution of conjugation length. The existence of a free carrier tail was indicative of a more conductive system (Jiang et al., 1997: 125-126). The ongoing discussion indicated that sulphonated heteronuclear aromatic hydrocarbon-doped PANi (SPAH) such as PANi-NSA or PANi-CSA is highly conductive with tendency to form intense polaron bands and a free carrier tail.

2.10 FTIR spectroscopy

Similar to the UV-Vis case, the interaction between an organic conducting polymer and dopants brings about structural and electronic modifications in their polymer backbone. This modification manifests itself in the appearance of new bands in their vibrational spectra (FTIR) observed due to the displacement of the position of the double bonds leading to the formation of quinoid structures upon doping (Fernandes et al., 2005: 279-284). It has been argued that the resultant dopant modification are independent on the dopant used and can serve as spectroscopic signatures for successful doping (Fernandes et al., 2005: 279-284). For instance the FTIR spectra of PANi doped with α-NSA, β-NSA and 1,5-NDBSA was similar to that of HCl-doped PANi (Zhang et al., 2005: 1373-1379). However, it is unanimously agreed that doping brings about the displacement of the quinonoid and benzoid bands (Cataldo and Maltese, 2002:1791-1803). This bond displacement and the presence of vibrational bands due to the respective dopants can be useful indicators for successful doping. The occurrence of an electronic like band at ca. 1100 is taken as evidence for the existence of polarons in the polymer structure. It serves as an indication that the polymer is in the most conductive emeraldine salt form (ES) (Patil et al., 2004: 57-63). The ratio of the intensities of the quinonoid and benzoid bands (I_Q/I_B) is an indicator as to the degree to which the polymer exists in the ES- form.

The FTIR characterisation of PANi-DBSA nanoparticles prepared in a reversed micelle process has been reported (Han et al., 2005: 179-187). In this work, the benzonoid and quinonoid peaks of the undoped PANi were observed at 1504 and 1590 cm^{-1} respectively. The absorption peaks of PANi-DBSA quionoid and benzonoid structures were observed at 1559 and 1489 cm^{-1} respectively indicating a shift to lower frequencies with respect to those of EB-PANi. The shift was associated to electronic differences in the polymer caused by the electron withdrawing tendency of the $–SO_3H$. In the PANi-DBSA spectrum bands at 1033, 2922, 1007 cm^{-1} were assigned to the S=O stretching vibrations, $-CH_2$ and >CH stretching vibrations of the benzoid rings in DBSA. Elsewhere, PANi prepared in a DBSA micellar system exhibited the bands for the C=C benzoid and quinoid ring stretches at 1460, 1570 cm^{-1} respectively (Han et al., 2002: 53-60). These bands were found to occur at lower frequencies compared to those of undoped PANi which was indicative of successful doping. The band at 1293 cm^{-1} was assigned to the C-N stretching mode while that at 1242 cm^{-1} was an 'electronic–like' band associated with the emeraldine salt form of PANi (PANi-ES). The bands at 1120 and that at 2800-3000 cm^{-1} were due to the in plane bending vibration of C-H and the aliphatic C-H stretching modes respectively (Han et al., 2002: 53-60).

Elsewhere, the FTIR responses of potentiostatically electrodeposited polyaniline in the presence of absence of naphthalene-1,5-disulphonic acid and catechol-3,5-disulphonic acid was recorded (Murugesan et al., 2003: 731-739). In general, the FTIR of prepared in H_2SO_4 showed all the principle characteristic bands associated with PANi. In the presence of naphthalene-1,5-disulphonic acid (NDSA) however, the intensities of all the bands for PANi-SO_4^{2-} increased and at the same time the band due to the C=C benzoid stretch is more intense than that due to the C=C quinoid stretch. According to the authors the observation indicates that in the presence of NDSA the existence of the polymer in benzoid moieties is more favourable and this has a stabilizing effect. The authors claimed that such effects were responsible for the disappearance of the hydroquinone peak in the PANi/H_2SO_4/NDSA cyclic voltammogram. Such results were not observed for catechol-3,5-disulphonic acid which was easily hydrolyzed.

It has been observed that FTIR responses for both doped and undoped PANi is similar save for the slight low frequency shift of especially the quinoid and the benzoid bands and the appearance of bands due to dopants. For example, the FTIR characteristics of PANi doped with H_2SO_4, camphor sulphonic acid (CSA) and sulphosalicylic acid (SSA) were compared (Rao et al., 2002: 311-316). According to the authors, the undoped PANi (PANi-EB) displayed bands at 1574, 1489, 1371, 1296, 1234, 1135 and 797 cm^{-1}. Similar bands were observed for all doped PANi with only a slight shift to lower frequency. For the doped PANi, the authors assigned the bands at 1293 and 1230 cm^{-1} to the N-H bending and C-N stretching modes respectively. The band at ca. 1480 cm^{-1} was due to the C-N stretching modes due to the quinoid ring and is evidence that the PANi-salts are protonated. Besides the N-H stretching bands between 3230-3450 cm^{-1}, a band at 570 cm^{-1} represented the degenerate bending mode of $–SO_3$ group and indicated successful doping. In addition, a ketonic-like band at ca. 1720 cm^{-1} was observed for PANi-CSA and PANi-SSA and is due to the C=O stretching vibrations.

It has been observed that the FTIR spectrum of unsubstituted and substituted PANi has basically the same structure, difference been slight band shifts. Widera et al. (1998: 265-272) employing IR, studied the effect of anions (Cl^-, ClO_4^-) on the properties of the resultant (poly-*o*-methoxyaniline) POMA. The authors found out that apart from the appearance of extra peaks due to different dopants, the principle IR bands for both POMA-HCl and POMA- ClO_4^- were very similar. In both cases, Evan holes were observed at 1660, 1375, 880 cm^{-1} and were absent at 1180 cm^{-1}. According to the authors, the trend was characteristic of 1,2,4- aromatic ring substitution. The single N-H POMA-Cl peak compared to the broad corresponding peak for POMA- ClO_4^- indicated the higher conducting nature of the latter composite. Elsewhere, Patil et al. (1999: 31-36) galvanostatically deposited POMA exhibited bands close to those reported for PANi indicating the presence of a similar basic structure. The band were: N-H 3437; 1579/1490 cm^{-1} due to the C=C stretching vibrations of the quinoid and benzoid ring respectively; 500-1200 cm^{-1} C-H in - plane and out -of -plane vibrations of the aromatic rings; 1206, 1117, 1014, 803 cm^{-1} bands indicating 1-4 substitution in the benzene ring.

The properties of galvanostatically electrodeposited poly-2,5-dimethoxyaniline (PDMA) on Low Carbon Steel (LCS) was studied using FTIR (Patil et al., 2004: 57-63). The trend was similar to that reported for PANi and POMA. The bands were (cm^{-1}), N-H (3440); C=C stret. quinoid (1587); C=C stret. benzoid (1484); C-N (1271); 1115, 1001, 791 bands indicating 1-4 substitution in the benzoid ring. According to the authors the ratio of the intensities of the quinoid: benzoid bands (I_Q / I_B) was greater than 1 which indicated overoxidation and a decreased conductivity.

Huang et al. (2003: 1765-1774) compared the properties of chemically prepared PANi, PDMA and their copolymer using FTIR spectroscopy. The characteristic bands for the PANi, PDMA and PANi/PDMA copolymer were similar save for the wide variations in intensity of the quinoid and benzoid band observed at ca. 1600 and 1500 cm^{-1} respectively for all the polymers. According to the authors, the (I_Q / I_B) ratio was very informative on levels of oxidation of the copolymer. An I_Q / I_B >1 which was achieved as the DMA content was increased meant a higher degree of immine conjugation with implications of overoxidation. It means the conductivity of the copolymer decreased with increase with the DMA content and the vice versa which was reasonable because the -OCH_3 substituents in DMA make the immine units oxidize preferentially. Bands between 860-870 cm^{-1} were assigned to 1, 2, 4 ring-substitution and were due to C-H out-of-plane vibrations of the aromatic ring. The C-N bands were observed at 1210, 1300 cm^{-1} and that at 1140 cm^{-1} was indicative of the copolymer oxidative level. The ratio of intensities of the I_{1140} / I_{1210} bands showed a similar trend to that of the I_Q / I_B and was a measure of the oxidation level of the polymer (Huang et al., 2003: 1765-1773).

2.11 Scanning Electron Microscopy

Different PANi morphologies have been reported. Granulated (Goel et al., 2007: 71-76), nanotubular, grain-like, spherical, (Wei et al., 2002: 917-921), nanofibrillar (Huang, 2006: 3915-3917), rodular (Jayanty et al., 2003: 7265-7270) amongst others. According to Wei et al. (2002: 917-921), the resultant morphology is dependent on the synthesis conditions. The variation of the monomer: dopant ratio, synthesis temperature, type of

templating molecule, synthesis methodology etc. play a key role towards the determination of the final PANi morphology. By varying the monomer: dopant ratio, Wei et al. (2002: 917-921) could manipulate the sizes of the resultant nanoparticles. Huang et al. (2006: 3915-3917), predominantly produced the nanofibrillar PANi through the interfacial polymerisation process. By varying the synthesis temperature, Zhang and Wan (2002:750-755) could manipulate the morphologies of the resultant PANi. At a synthesis temperature of about 15 º C, the resultant tubes were thick, short and about 180 nm wide and 0.6 μm in length with intermingled granular structures. However, at 0-5 º C, the tubular structures were 140 nm wide and 3 μm long. The recent interest in nanotubular or nanofibrillar PANi emanates from the fact that these one dimensional structures are a kind of desirable wire-like material with metal-like and controllable conductivity (Wei et al., 2002: 917-921). It has been shown that aliphatic and heteronuclear aromatic sulphonated acids such as DBSA, NSA, CSA can be utilized reliably to obtain this one dimensional structures (Zhang and Wan, 2002: 750-755; Wei et al., 2002: 917-921; Huang and Wan, 1998: 255-259; Zhang et al., 2005: 1373-1379). Similar morphologies have been reported for POMA and PDMA (Widera et al., 2001: 4125-4131; Storrier et al., 1994: 179-186).

2.12 Reported Kinetic parameters on polyaniline systems

The utility of an organic conducting polymer is measured in terms of the rate of electron hopping along the polymer units as well as the rate at which electron transfer occurs across the interface. The calculation of diffusion coefficient (D_e, cm^2/s) and the standard rate constants k^0 (cm/s) can serve as a useful tool for prediction of polymer value especially for sensor applications. An electrosynthetic PANi film doped with polyvinyl sulfonate (PVS), exhibited a diffusion coefficient value of 6.46×10^{-8} cm^2/s (Iwuoha et al., 1997: 749-761). Elsewhere, polystyrene sulfonic acid doped PANi, PSSA, exhibited a D_e value of 8.68×10^{-9} cm/s. The lower D_e value of the PANi/PSSA film as compared to that of PANi/ PVS was attributed to different electrodeposition conditions, film homogeneity as well as dopant size (Mathebe et al., 2004: 115-120). Elsewhere, the Langmuir-Schaeffer equation was used to estimate the D_e value of a glass substrate

deposited POMA layer. Diffusion coefficient values of 2.6 x 10^{-7} and 1.9 x 10^{-8} cm^2/s were estimated for the nucleation and diffusional controlled growth processes respectively (Raposo and Oliveira, 2002: 6866-6874). Nanocomposites of multi-walled carbon nanotubes (MWNTs) embedded in POMA synthesized through the oxidative polymerisation process exhibited D_e values in the range of 1.78 - 0.75 x 10^{-8} cm^2/s in different supporting electrolytes. Thus in general, the observed D_e and k^0 are a function of the polymer preparation conditions as well as the exact nature of the polymer. It is expected that substituted polyanilines should exhibit lower D_e and k^0 than the parent polyaniline, as long as the polymers are synthesized under the same conditions. The argument is based on the fact that the presence of substituents in the polyaniline chain causes steric hindrance with consequences of increased interchain distance and a lowered frequency of electron hopping along the polymer chain (Delvaux et al., 2000: 275-280).

2.13 HRP / PANi biosensors

Several HRP-based enzyme electrodes for the detection of a myriad of analytes including various peroxides, oxidizable drugs, inhibitors such as ethylenethiourea has been reported (Erdem et al., 2000: 349-354; Xu et al., 2004: 533-537; Adeyoju et al., 1995: 57-64). Depending on the mode of enzyme immobilization, several generations of HRP-enzyme electrodes have been reported. A direct electron transfer between the HRP enzyme immobilized with the help of a polyethylene glycol membrane on a pyrolytic graphite electrode was reported by Xu et al.(2004: 533-537). The biosensor for H_2O_2 showed good electrocatalytic response to the reduction of H_2O_2 with a calibration range between 2.0 x 10^{-6} and 6.0 x 10^{-4} M. Elsewhere, Adeyoju et al. (1994: 177-179) demonstrated a direct electron transfer between HRP and the platinum electrode. This amperometric biosensor for butanone peroxide and hydroxylamine determination was constructed by the entrapment of the HRP enzyme within a poly (ester-sulfonic acid) Eastman AQ-55D polymer matrix as a binder. The biosensor was reported to exhibit high catalytic activity in various organic solvents in the range of 0.9 - 1.1 μA $mmol^{-1}$. However, this mediatorless biosensor fabrication process has been reported to be quite unreliable given the lack of reproducibility and diminished responses owing to ineffective electron relays.

Direct electron transfer between the electrode and the prosthetic group of catalytically active protein-enzymes possessing a considerably greater molar mass is prevented by exceedingly large electron hopping distances, by improper orientation of the adsorbed enzyme, or by adsorptive denaturization (Guo and Guadalupe, 1997: 1437-1438). Furthermore the use of membranes for enzyme entrapment could create a new additional diffusional barrier to the sensing scheme which could have direct impact on sensor sensitivity (Bartlett and Whitaker, 1988: 3: 359-379). Salomi et al. (2007: 1825-1829) has reported on the use of phenazine group dyes such as safranine O and neutral Red as electron transfer mediators in the construction of a H_2O_2 biosensor based on HRP. Although this biosensor allowed for the detection of hydrogen peroxide well below -200 mV, which is appropriate to exclude interferences, the lack of properly formed peaks in the cyclic voltammograms of the HRP/safranine/glassy carbon or HRP/Neutral Red/glassy carbon electrodes indicate the instability of the system. This was reflected in the poorly formed biosensor responses and very high background currents. Elsewhere, a HRP-based biosensor for H_2O_2 peroxide using anthraquinone sulphonic acid as a redox mediator has been reported (Mogharrab and Hedayatolla, 2005: 466-471). There was a first order relation between the current response and the concentration of H_2O_2 when it was kept below 2.0 mM and detection was done at -450 mV which was appropriate to ensure no interferences could be detected. However, above this concentration, the current response decrease was associated with deactivation of the HRP enzyme into inactive oxyperoxidase form. Furthermore, other shortcomings have been associated with the use of small molecules as electron transfer (ET) mediators. Such molecules may leach into solution causing sample contamination, and may affect the long-term sensor stability (Mogharrab and Hedayatolla, 2005: 466-471). A solution to this problem has been to covalently attach the biomolecule to the mediator but this also may lead to decreased enzyme activity since some enzymatic functional groups will be used for bonding.

Recently the use of organic conducting polymers as immobilization matrices has become very popular (Gerald et al., 2002: 345-359) due to several factors. The simultaneous polymer deposition with the enzyme entrapment makes the biosensor fabrication process very easy. Conducting polymers can provide direct electrical communication between the

enzyme redox centre and the electrode surface thus fulfilling the role played by the physiological electron mediators. They achieve these by delocalizing redox charges over a series of conducting polymer groups thereby acting as self-contained electron transfer mediators (Grennan et al., 2006: 1591-1600). Organic conducting polymers also offer a measurable degree of flexibility in their chemical structure which can be modified as need be to accommodate different biomolecule types (Malhotra et al., 2006: 59-74). This way they permit the localization of biologically active molecules on electrodes of any size and geometry and are particularly appropriate for the application of multi-analyte micro-amperometric sensors.

Organic conducting polymers also provide a suitable micro-environment for the biocatalyst immobilization. They also localize the biocatalyst close to the electrochemical interface thus evading interferences which may lead to undesirable side reactions or large background currents. Furthermore, since conducting polymers are characterized by a distributed array of catalytic sites, they are able to mimic natural redox polymers and can bind productively with the biocatalyst culminating in electron exchange thereby providing a link between the electronic and biological worlds (Bartlett and Cooper, 1996: 233-269). This way they are able to enhance speed, sensitivity, and to enhance or create detection signals where previously none was detected (Bartlett and Cooper, 1996: 233-269).

Of the conducting polymers, polyaniline has been most utilized. It exhibits good conductivity, is easily prepared and has well defined redox chemistry. Most PANi utilized in biosensor fabrication is the sulphonated type (SPAH). Unlike PANi-doped with inorganic acids, SPAH is stable and electroactive even at neutral pH. An amperometric peroxide based biosensor for H_2O_2 was electrochemically prepared by immobilization of a horseradish peroxidase enzyme (HRP) onto a PANi-PVS film. The biosensor was stable in both aqueous and organic media with an operational potential of -100 mV versus Ag/AgCl when operated at an optimal pH of 6.88. Different apparent Michaelis-Menten (K'_m) values were reported for the biosensor in the various media with

a best performance of 3461 pmol cm^2s^{-1} being attained in phosphate buffer (Iwuoha et al., 1997: 749-761).

Elsewhere, an in-situ polymerisation process was used to prepare a PANi-PSSA (polystyrene sulfonic acid) electrode. The presence of redox peaks at formal potentials ($E^{0'}$, mV), 200, 500, 800 indicated the film was electroactive as the shifting of one of the peaks indicated the presence of a diffusion controlled process. The authors proposed this movement of electrons to have occurred along the benzene units in the polymer chain. The cathodic polarization of the PANi-PSSA-Pt electrode at -500 mV followed by an anodic polarization at +650 mV electrostatically doped the HRP enzyme unto the electrode. The performance of the resultant biosensor was evaluated using small amounts of 0.01 M H_2O_2. The sensor exhibited a linear response in the range 2.5 x 10^{-4} - 5 x 10^{-3} M. The sensitivity of the sensor was found to be 2.88 x 10^{-2} μA mm^{-1} cm^{-2}. This low sensitivity was associated with a low protein concentration in the immobilization process (Mathebe et al., 2004: 115-120).

Alternatively, an increase in the enzyme electrostatic doping time may ensure better sensitivities. However, in studying the optimization of biosensor parameters in terms of enzyme loading and film thickness, Grennan et al. (2006: 1591-1600) have stated that a protein concentration of 1 mg/mL is quite high and infact yielded low catalytic responses compared to lower enzyme concentrations. According to the latter authors, a protein concentration of 0.6 mg/mL was optimal. However, given there are many factors that may affect enzyme loading including type of protein, purity of protein, nature of binding between the protein and the mediator, experimental conditions in general etc. it is difficult to generalize on a single optimal enzyme loading. Again working on PANi-PVS films, Grennan et al. (2006: 1591-1600) studied the effect of polymer thickness on sensor performance and concluded that a higher polymer thickness led to higher background currents which might affect sensor performance since it would be difficult to measure the contribution due to the analyte.

Various biosensor works have reported the use of polymer thicknesses electrodeposited through use of 10 voltammetric cycles (Mathebe et al., 2004: 115-120; Iwuoha et al., 1997: 749-761; Grennan et al., 2006: 1591-1600). The reported sensors were high performing with good sensitivities. Another approach would be to optimize the best scan rate producing the most reversible redox responses. Reversibility would mean fast electron exchange between the polymer/enzyme and polymer/electrode which would boost sensor performance.

Elsewhere, an amperometric biosensor for H_2O_2 utilizing DBSA or PVS doped nanoPANi has been reported (Morrin et al., 2005: 423-430). In this biosensor format, the superiority of nanoPANi was first prepared chemically using APS as the oxidant with the monomer: dopant: oxidant ratio being 1: 1: 1. The final product after purification using the dialysis method was dispersed in Millipore water and potential cycling between -500 to +1100 mV potential limits at 100 mV/s. This electrodeposited nanoPANi displayed the usual PANi redox couples at ca. 100, 350 and 650 mV similarly assigned as for other previously reported PANi. The resultant nanoPANi modified glassy carbon electrodes were electrostatically doped with 0.1 or 0.66 mg/mL HRP (optimal, dependent on polymer) before being used for the detection of hydrogen peroxide. According to the authors, nanoPANi allowed uniform absorption of protein with improved biosensor performances. The PANi-DBSA sensor was found to be better performing with a signal-to-noise ratio (S/N) of 61 ± 3 compared to that of PANi- PVS which was 17 ± 14. The response times for the PANi-DBSA and PANi-PVS sensors were 0.62 ± 0.04 s and 9.46 ± 4.12 s respectively. Despite the higher performance of the nanoPANi sensors, this sensor fabrication may be quite tedious and expensive given it involves a kind of double polymerisation. Alternative pathways to this preformed polymer casting method would be to drop coat the GC electrode with the nanoPANi dispersion in the presence or absence of crosslinkers.

The fabrication of a poly-5-methoxy aniline /HRP indium tin oxide (ITO) electrode for the detection of H_2O_2 has been reported (Ngamna et al., 2005: 185-188). In this biosensor format, the soluble poly-5-methoxyaniline (PMAS), was mixed with poly (L-Lysine),

(PLL) to render the material insoluble, a prerequisite for aqueous biosensors. An optimal mixture of the PMAS/ PLL and /or bovine serum albumin (BSA)/HRP were drop coated onto the ITO coated mylar. Biosensor measurements were conducted at a pH of 6.4 with the dynamic linear range being 0.01 - 0.1 mM and a sensitivity of. 24.91 $\mu A/cm^2/mM$ (r^2=0.9966).The sensor response times were obtained at a constant applied potential of -100 mV versus Ag/AgCl under hydrodynamic conditions in phosphate buffer saline conditions (PBS). Accordingly therefore, the fabrication of biosensors through the drop-coating technique or preformed polymer solutions can yield high performing sensors just like in other in-situ deposition processes.

2.13.1 Other biosensors based on PANi

Killard et al. (2000: 81-84) developed an antibody-based biosensor for environmental analysis. In this biosensor format the antibody was electrostatically doped onto a sulphonated PANi film (PANi-PVS) prepared through the cyclic voltammetric electrostatic doping techniques. This therefore means the electrostatic doping of biomolecules onto conducting polymers is a viable method for protein immobilization irrespective of the type, size and shape. According to the authors, the resultant 'molecular wiring' due to the use of the PANi-PVS film was crucial in avoiding some burdensome procedures normally conducted in non-mediated immunoanalysis in order to exclude non-specific responses from the system.

The versatility of sulphonated polyanilines in sensor technology has been exploited for other purposes. Sulphonated polyaniline (SPAH) prepared through the stabilization of PANi by use of Nafion, PVS and PSS has been reported and consequently used for the detection of ammonium ions (Chen et al., 2006: 489-494). Best sensor sensitivities towards ammonium ions were recorded for PANi-PSS and PANi-PVS which were 7.96 ± 0.34 and 7.16 ± 0.1 $\mu Amm^{-1}cm^{-2}$ respectively measurements being taken at pH 7.0. The other advantage of using polyaniline for biosensor fabrication is that it can host any protein of any size and /or geometry leading to the detection of a variety of analytes.

Biosensors based on PANi composites such as PANi-metal (e.g. gold) nanoparticle, PANi-carbon nanotubes (CNTs), PANi- Prussian blue etc. have been reported (Ma et al., 2005: 1-6; Zou et al., 2007: 2669-2674). In addition, several protein materials that have been employed include glucose oxidase, uricase, etc (Li et al., 1996: 137-145; Kan et al., 2004: 1635-1640; Xiu et al., 2004: 137-141).

A PANi-glucose oxidase (GOx) biosensor has been fabricated through physical adsorption and electrochemical techniques (Li et al., 1996: 137-145). The physical adsorption technique involved the standing of polyaniline modified working electrode into a buffer/glucose oxidase (containing 1.5 μmol dm^{-3} GO_x) solution for 20 min. The electrochemical doping procedure was carried out by reducing the working electrode at -200 mV for 15 min followed by oxidation in the presence of GO_x. According to the authors, only partial doping was achieved in the case of physical adsorption resulting in lower catalytic currents compared to those reported for electrochemical doping highlighting the superiority of the electrostatic protein doping process over the adsorption process. Furthermore, since in physical adsorption process the enzyme is attached to the polymer through weak forces, there is a danger of enzyme leaching into the solution with an overall sensor instability. The best sensor responses through the electrochemical process were obtained at a H_2O_2 concentration range of between 1.0×10^{-4} - 2.0×10^{-3} mol dm^{-3} at pH 5.6.

Elsewhere, the versatility of polyaniline to immobilize different biomolecules has been utilized in the fabrication of macro- and microsensor arrays for the estimation of glucose, urea and tri-glycerides (Sangodkar et al., 1996: 779-783). In this biosensor array, both the PANi and the enzymes were electrochemically deposited on closely spaced interdigitated microelectrodes and the directing of different enzymes to the designated electrodes was achieved through careful control of potential. This biosensor array enabled the detection of glucose, urea, and triolein. The sensitivities realized for the first two analytes were 0.027 and 0.15 /mM which were far high compared to those of the corresponding macrosensors.

2.13.2 Biosensors based on HRP inhibition

An amperometric sol-gel-based enzyme inhibition electrode for the detection of low levels of cyanide was constructed by immobilizing horseradish peroxidase (HRP) and an osmium redox polymer ($[Os(bpy)_2(PVP)_{10}Cl]Cl$ as mediator (Park et al., 1997: 1120-1123). A comparison of the bioelectrocatalytic reduction wave in the presence of hydrogen peroxide alone and hydrogen peroxide/cyanide containing compound) was used to determine levels of cyanide in solution. The concentration range of linear response, apparent inhibition constant (*K*), and detection limit were 0.004-0.04 mM, 0.0637 mM, and 0.5 μM, respectively. Sodium azide, potassium thiocyanide and thiourea were used.

Elsewhere, an amperometric biosensor for the determination of sulfides was constructed based on the inhibition of HRP. The HRP was encapsulated on a thiolato self - assembled monolayer and cross-linked to the electrode using gluteraldehyde. The sensor exhibited a linear range of 0.5-12.7 μM and a detection limit of 0.3 μM (Yang et al., 2004: 162-168).

The ability of hydroxylamine to inhibit the proper functioning of the HRP enzyme was utilized in the construction of a biosensor for hydroxylamine itself. The sensor was constructed by the immobilization of HRP onto a poly (ester-sulfonic acid) Eastmann AQ-55D modified platinum electrode. Levels of butanone peroxide, a HRP, substrate were also quantified. The catalytic activity and the degree of inhibition of the sensor depended on type of solvent (Adeyoju et al., 1994: 177-179).

So far, the detection of organophosphate pesticides has been carried through the inhibition reactivities of acetylcholine esterase enzyme (Vakurov et al., 2004: 1118-1125). However, the method is expensive due to the high cost of the enzyme and its substrates such as acetyl choline or thiocholine compared to the cost of HRP and H_2O_2. Also, since HRP has a higher pH tolerance, it is possible that OP biosensors based on HRP inhibition are likely to be more stable especially in situations where pH is likely to change like in industrial effluent. Since it has been shown that horseradish peroxidase can be inhibited by organic sulfur-containing compounds (Adeyoju et al., 1995: 57-64), it means biosensors for the detection of OPs can be constructed based on HRP inhibition.

The measurement of the enzyme activity before and after exposure to the organophosphate inhibitors can lead to the quantification of OP levels in solution.

2.14 Biosensors based on cytochrome P450 enzymes

The CYP P_{450} isoforms are ubiquitous heme-thiolato monooxygenase enzymes of microbial, mitochondrial or microsomal origin (Iwuoha and Smyth, 2003: 237-244). As in the horseradish peroxidase case, they contain an Fe^{3+} redox centre bound to a heme-protopophyrin type IX. In mammals, they are primarily localized in the liver tissue endoplasmic reticulum where they catalyze the oxidative conversion of drugs and other xenobiotics to more soluble and water extractable metabolites through hydroxylation, N-dealkylation reactions, N-deacylation reactions etc. (Iwuoha and Smyth, 2003: 237-244). This enzyme family is involved in the biotransformation of drugs, the bioconversion of xenobiotics, the metabolism of chemical carcinogens, the biosynthesis of physiologically important compounds such as steroids, fatty acids, eicosanoids, fat-soluble vitamins, bile acids, the conversion of alkanes and terpenes, and aromatic compounds as well as the degradation of herbicides and insecticides (Bernhardt, 2006:128-145).

There are more than 1000 known isoforms of P_{450} enzymes with 50 of these already identified in man but the most commonly encountered are the cytochrome P_{450} camphor (CYP P450 $_{cam}$, or CYP101), CYP 2D6, CYP 3A4 amongst others. It is now known that cytochromes are capable of metabolizing over 1,000,000 chemicals involving about 60 distinct classes of biotransformation reactions (Shumyantseva et al., 2006: 1353-1357). The presence of various important substrates for P450 enzymes shows the possibility of utilizing the interaction between these enzymes and some specific substances for biodevice applications (Paternolli et al., 2004: 11706-11712). Under normal physiological conditions, electrons required for the monooxygenation reactions of CYP 450 enzymes are supplied by small molecules such as NADP in a detailed electron transport chain mechanism.

2.14.1 Catalytic cycle of P450 enzymes

In general all the cytochrome P_{450} enzymes have the same basic catalytic cycle. At the resting state, the ferric P_{450} enzymes consist of an Fe^{3+} prosthetic group bound to four nitrogen ligands of a heme–protoporphyrin type IX.

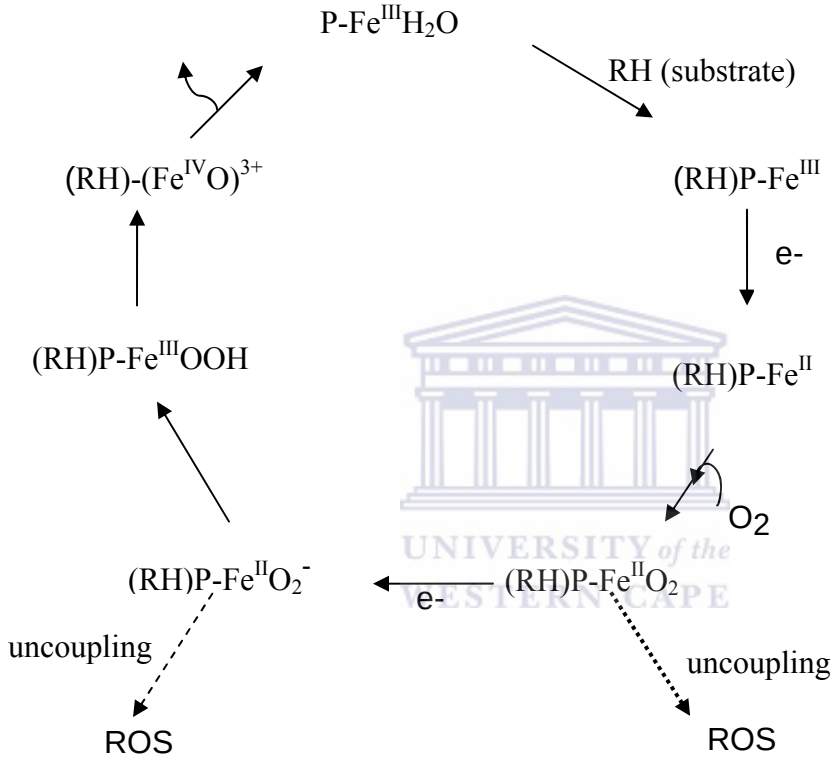

Figure 2.8: A scheme showing the catalytic hydroxylation of CYP substrates with a general formula RH.

Source: Bistolas et al. (2005: 2408-2423)

An axial thiolato cystein ligand occupies the fifth coordination site. At the resting state the polarity of the enzyme is maintained by a H_2O ligand that occupies the sixth coordination site (Fig. 2.8). The cycle begins when a substrate molecule (represented as RH) binds at the sixth coordination site. Substrate binding decreases the enzyme polarity with a positive potential shift of the redox potential to lower values. The transfer of a first

electron is then thermodynamically feasible leading to the reduction of the ferric enzyme into a ferrous-enzyme complex, (RH)P-Fe^{II}. The consequential binding of molecular oxygen converts the ferrous –enzyme complex into a ferrous di-oxygen complex (RH)P-$Fe^{II}O_2$ which rapidly accepts a second electron from the donor molecule at the same time abstracting a proton from the solvent forming a hydroperoxo intermediate (RH)P-Fe^{III}OOH. This is followed by the cleavage of the O-O bond with release of a water molecule and the formation of a highly active iron-oxoferryl intermediate (RH)-$(Fe^{IV}O)^{3+}$. This iron-oxo-ferryl intermediate may react in a concerted reaction with the substrate (RH) leading to the insertion of an oxygen atom into the substrate (RH) to form a conjugate group at the same time regenerating the free enzyme. The conjugated substrate is now pharmacologically inactive and more eliminable. In the absence of a suitable substrate, some reduced P450 enzymes very efficiently produce reactive oxygen species (ROS) by autoxidation. This can take place either in vitro or in vivo and in mammals can lead to apoptosis or cell death (Bernhardt, 2006: 128-145).

The CYP_{450} N-demethylation of substrates is similar to the hydroxylation cycle above. However, slight variations in mechanisms do occur (Fig. 2.9). N-demethylation of CYP has been explained through the HAT (H-atom transfer) and the SET (single-electron transfer) mechanisms (Meunier et al., 2004: 3947-3980). However, both mechanisms terminate in the formation of a carbinolamine intermediate (Meunier et al., 2004: 3947-3980; Guengerich et al., 1996: 27321-27329). During N-demethylation, the formation of hydroxyperoxo intermediate (RH)P-Fe^{III}OOH is followed by the release of a water molecule to form a iron oxoferryl radical (Fe IV-O$^{\cdot}$). This unstable oxyferryl radical abstracts a proton from the substrate ($R_1R_2NCH_2R$) to form a one-electron reduced ferryl species (FeIV-OH) and a substrate radical cation ($R_1R_2NC^{\cdot}HR$). The process is followed by an oxygen rebound to form a carbinolamine ($R_1R_2NCH(OH)R$) terminating in the demethylation of the substrate and regeneration of the free enzyme with the release of an aldehyde molecule(R-CHO) (Meunier et al., 2004: 3947-3980).

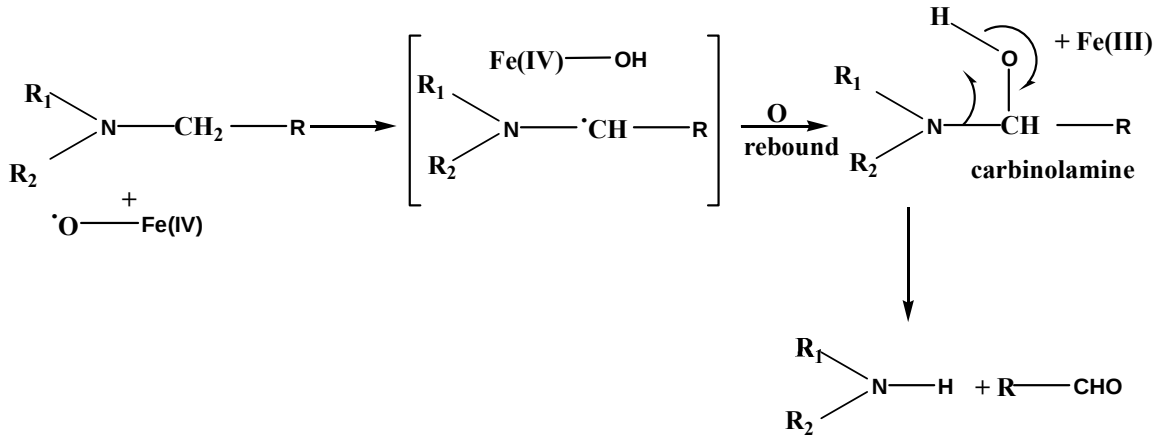

Fig. 2.9: Steps to the catalytic N-demethylation of tertiary amine CYP 450 substrates after the formation of the hydroxoperoxo intermediate (RH)P-Fe^{III}OOH.

(Source: Meunier et al., 2004: 3947-3980)

2.14.2 Application of CYP 450 enzymes in biosensors

Since the first demonstration by Clark and Lyons that enzymes could be integrated into an electrode to form a biosensor, the development of such electrochemical devices has made considerable progress (Shumyantseva et al., 2001: 185-190). Given the wide scope of substances they can metabolize, P450 enzymes can be used for the practical applications in environmental monitoring or in drug or biologically active compounds monitoring. The construction of CYP 450 based electrochemical biosensors is of great medical, pharmacological and toxicological importance. In CYP 450 biosensors, the need for cofactors is replaced by a supply of electrons from the electrode. Electrical communication between the electrode and the enzyme's heme prosthetic group is achieved through mediated or non-mediated procedures. According to Fleming et al. (2003: 4082-4088), the initial problem of slow electron transfer between the CYP proteins and the electrode has been overcome by use of an electron shuttle or mediator. Several immobilization techniques in use for P450 include; sol-gel matrices (Hara, 2000: 103-109), alternating cationic and anionic polymers (Shiba et al., 2003: 1817-1826), and

use of entrapping synthetic lipid materials such as didodecyldimethylammonium bromide DDAB (Iwuoha and Smyth, 2003: 237-244) have been reported.

2.14.2.1 Cytochrome P450 cam

Cytochrome P450 $_{cam}$ or CYP 101 is one of the P450 enzymes that has generated a lot of interest in the field of biocatalysis and bioelectrochemistry (Wong et al., 1995: 4818-4822; Reipa et al., 1997: 13554-13558; Zhang et al., 1997: 1769-1774). It is mainly found in the bacterium *pseudomonas putida* PpG786 when it is cultured with camphor and catalyses the regio- and stereospecific hydroxylation of camphor to 5-exo-hydroxycamphor (Iwuoha and Smyth, 2003: 237-244; Shumyantseva et al., 2005: 1051-1063). Wong et al., (1995: 4818-4822) has studied electrochemical response of mediated and non-mediated putidaredoxin in order to verify the importance of mediation in the CYP 101 electrochemistry. In this experiment, a single compartment three electrode cell was used carrying a 1 mm gold disc electrode, a Ag/AgCl reference electrode and a platinum counter electrode. At the unmodified gold electrode, which was previously cleaned with chromic-sulfuric acid, polished in alumina slurries and then sonicated in a suitable solvent, only a cathodic peak which deteriorated with subsequent scanning was observed at 500 μM putidaredoxin concentration. However, the same electrode when modified with mercaptoethylamine displayed a pair of redox peaks from as low as 100 μM putaredoxin concentration. The redox activity was maintained even after several cycles. This then may highlight the importance of mediation for the proper function of the P450s in biosensors.

Elsewhere, the use of antimony-doped tin–oxide (ITO) coated glass slides as a source of electrons for the reduction of the intermediate redox protein (putidaredoxin, Pdx) of $P450_{cam}$ 101, without the presence of any redox mediators has been reported (Reipa et al., 1997: 13554-13558). The electrodes were first sonicated in 1 M NaOH followed by multiple rinsing in distilled water. A Ag/AgCl (3 M KCl) and a platinum counter electrode was used. According to the authors, the choice of the antimony-doped tin oxide was due to its rather flat band potential ensuring excess positive charge in the potential

range of interest (-0.5 to -0.9 V). The putidaredoxin reduction response was stable up to 60 h. The heterogeneous electron transfer rate constant obtain for the electron transfer between the electrode/putidaredoxin was 1.1 x 10^{-4} cm/s and was one order of magnitude lower than that on a modified gold electrode indicating the superiority of mediated electrodes over unmediated ones in CYP P450 biosensor construction. A shift of the Soret band from 392 to 408 nm after adding camphor was evidence of the electron transfer from reduced putidaredoxin to camphor bound CYP101. It has been shown that the direct immobilization of P450 enzymes on the electrode can lead to unfavorable orientations of the proteins at the electrode hence lowering the probability an electron transfer between the enzyme and the electrode (Shumyantseva et al., 2005: 1051-1063). Furthermore, such direct immobilization on metal electrodes could lead to protein denaturization.

Zhang et al. (1997: 1769-1774) has recently used biomembrane-like environments to house biological proteins such as enzymes, myoglobin, haemoglobin, ferridoxins etc. in order to facilitate electron exchange with underlying electrodes. In this respect, didodecylmethylammonium bromide (DDAB) and dimyristoyl-L-α-phosphaditylcholine (DMPC) have been found to form stable lamellar liquid-crystal at 25 ºC which can host the enzyme. In one such instance, 15 µl of a mixture of either DDAB or DMPC vesicles with $P450_{cam}$ were dropped onto a pyrolytic graphite electrode and the resultant voltammograms recorded in phosphate buffer in an oxygen free environment displayed a reversible couple whose peak currents increased with scan rate characteristic of a thin film. On bare pyrolytic graphite electrodes, the CVs obtained showed diminished peaks indicating the role played by the lipid vesicles in enhancing electrical communication between the enzyme redox center and the electrode.

Elsewhere, cytochrome $P450_{cam}$ bioelectrodes suitable for applications in organic phases were prepared from genetically engineered CYP101 and DDAB vesicular dispersions. The biosensor reactivities as characterized through cyclic and square wave voltammetry showed a direct reversible electrochemistry between the heme iron atom and the glassy carbon (GC) electrode, the couple exhibiting a formal potential of -380 mV versus

Ag/AgCl reference electrode. In this study it was found out that upon substrate binding, the formal potential shifted anodically thus decreasing the potential necessary to initiate the monooxygenation reaction of the cytochrome $P450_{cam}$ (Iwuoha and Smyth, 2003: 237-244). Earlier, Iwuoha et al. (1998: 1101-1110) prepared a biosensor for camphor by using glutaraldehyde in the presence of bovine serum albumin to cross-link the cytochrome $P450_{cam}$ /DDAB vesicular system mixture on a GC electrode. Cyclic voltammograms under degassed systems exhibited reversible electrochemistry due to the direct electron exchange between the heme prosthetic group and the GC electrode.

In another instance, use of small bi- or multifunctional promoter molecules of the type X-Y which can bind both to the electrode and to the enzyme in order to avoid irreversible conformational changes due to direct immobilization has been reported (Shumyantseva et al., 2005: 1051-1063). Such promoter molecules included 4,4' dipyridyl, 4,4' dithiodipyridyl and alkanethiols. Recently, the entrapment of oxygenases into conducting polymers such as polyaniline, polypyrrole, polythiophene etc. has generated more interest (Gerard et al., 2002: 345-359). Cytochrome $P450_{cam}$ was potentiostatically immobilized on a polypyrrole modified tin oxide-indium electrode (ITO) by application of a constant potential of 3 V for I h in the presence of the enzyme in solution (Cosnier: 1999: 443-456). The increase in catalytic current was found to be proportional to the concentration of substrate (camphor) in solution. Given the many advantages associated with biomolecule immobilization in conducting polymer films, this technique is bound to be the most facile and versatile for the immobilization of the P450s.

2.14.2.2 CYP 2D6

Another type of cytochrome P450 enzymes that plays a great role in drug metabolism is the CYP 2D6 form. It has been said that CYP 2D6 metabolizes over 25 % of most drugs commonly used (Slanar et al., 2006). It is known to partly or wholly metabolize a variety of substances mainly the tricyclic psychotics that contains an N protonable atom (Gillman, psychotropic research). This range of substances includes the antihistamines, antidepressants, steroids, arachidonic acid and various others (Kirchheiner et al., 2007:

489-494). A major class of antidepressants metabolized by this enzyme includes the selective serotonin reuptake inhibitors (SSRIs) like fluoxetine, paroxetine, setraline, debrosoquine etc. (Ducharme et al., 1996: 113-128; Carrilo et al., 1996: 183-190; Dalen et al., 1999: 697-706). It has been shown that CYP 2D6 catalyzes the *o*-demethylation of dextromethorphan (DM) to dextrophan (DX), the hydroxylation of debrisoquine to 4-hydroxydebrisoquine and the N-demethylation of fluoxetine to *nor*-fluoxetine amongst others (Ducharme et al., 1996: 113-128; Dalen et al., 1999: 697-706; Iwuoha et al., 2004: 929-941).

There are more than 50 different allelic variants of CYP 2D6 and a great inter-individual variability in drug biotransformation owing to the great genetic polymorphism of these enzymes thus demarcating between high and poor metabolisers (Iwuoha et al., 2004: 929-941; Dalen et al., 1999: 697-706). The latter author used HPLC technique to analyze levels of debrisoquine and 4-hydroxydebrosequine in urine. The debrisoquine / 4-hydroxydebrosequine ratio was used to categorize various subjects as either extensive or poor metabolisers. The wide variety of substances catalysed by this enzyme implies its high applicability in especially clinical drug monitoring. The preparation of bioprobes is necessary in order to monitor drug-to-drug interactions. Romach et al. (2000: 43-45) has shown that the co-administration of codeine and fluoxetine can lead to a lowering of the former in the bloodstream. Codeine is a commonly used oral opioid analgesic. The simultaneous administration of codeine and fluoxetine would lower codeine levels in the body and may lead to uses of higher dosage of codeine if symptoms are not relieved. This could be lethal because codeine is metabolized to a more potent drug -morphine. The conversion of codeine to morphine is catalysed by CYP 2D6 enzyme.

Cytochrome P450 bioprobes can also be used for routine analysis for the evaluation of how best a subject can metabolize a drug. Sproule et al. (1997: 102-106) studied the ability of 40 male subjects to metabolize setraline, an antidepressant. By measuring levels of setraline before, during and after administration, the urinary ratio of the *o*-demethylated metabolites to parent drugs the subjects phenotype status could be determined. The knowledge of the phenotype status of a subject is useful in determining

the dose of that particular drug to be administered to the patient. Previously, drug bioprobes have been based on spectroscopical measurements involving the shifting of the Soret bands upon substrate binding (Bistolas et al., 2004: 810-816; Honeychurch et al., 1999: 351-353). Under such circumstances the oxidation of the substrate relies on the biological electron delivery to initiate the CYP 2D6 cycle. During drug biotransformation in the CYP 2D6 cycle, the transfer of reduction equivalents delivered by NADPH: P450 reductase which contains two flavoproteins FAD and FMN occurs. In the construction of cytochrome 2D6 based biosensors, the reducing equivalents are supplied by the application of a negative potential via the electrode.

It has been shown that biological electron delivery can be replaced by supply of the reduction equivalents from the electrode (Iwuoha et al., 2004: 929-941; Brahim et al., 2003: 123-137; Shumyantseva et al., 2005: 1051-1063; Bistolas et al., 2004: 810-816). However, the construction of drug bioprobes based on the P450 enzymes based on electrochemical techniques is bound to be much faster and relatively cheaper compared to the spectroscopic techniques and therefore more favourable. The need for biological electron delivery systems and the detailed sample preparation and incubation times make the spectroscopic methods slower. Iwuoha et al. (2004: 929-941) demonstrated the ability of a polyaniline (PANi) modified glassy carbon electrode (GC) electrostatically doped with CYP 2D6 enzyme to catalyse the oxidation of fluoxetine. In this preparation the PANi film was cast potentiostatically on the GC electrode from a 1.0 M aniline/2M HCl solution using a Ag/AgCl reference and a platinum mesh counter electrode. Electrostatic doping of the enzyme on the PANi film was achieved by applying a positive potential on a previously cathodically polarized GC/PANi electrode in the presence of 14.4 μM/L enzyme solution. In this biosensor format it was found that upon substrate addition, positive potential shift from -113 to + 87 mV was indicative of that the catalytic reduction process was coupled to the electrode transfer reaction. An increase of the peak current with increase of substrate (fluoxetine) concentration was observed but reached a plateau at 700 μM indicative of substrate limited kinetics. The sensor exhibited a Michaelis- Menten constant K'_m value of 3.7 ± 0.1 μM/L of fluoxetine. The maximum current density (I_{max}) of 4.76 ± 0.03 x 10^3 μA/cm^{-2} for the bioelectrode. The sensitivity of

the sensor was found to be 1008.7 μA/cm^{-2}/μM and a limit of detection (LOD) of 1 x 10^{-3} μM.

Elsewhere, the use of a similar PANi/GCE/CYP 2D6 system was used to demonstrate the importance of oxygen during a monooxygenation reaction for flouxetine (Brahim et al., 2003:123-137). Under aerobic conditions, clear visible cathodic peaks were observed but the reverse was true for the anaerobic conditions suggesting the importance of oxygen in the fluoxetine monooxygenation reaction. No redox peaks were observed under anaerobic conditions.

2.14.2.3 CYP 3A enzymes

Among the various CYP gene families, CYP 3A4 subfamily accounts for the majority of the P450 enzymes present in the adult human liver and intestines (Dorne et al., 2003: 201-224). There are other allelic forms of the CYP 3A subfamily like: CYP 3A4, CYP 3A5 and CYP 3A7 which have a closely related homologous sequence but differ in substrate specificity and expression and therefore may metabolize drugs through different pathways. Among the various alleles, the CYP 3A4 type is arguably the most abundant and therefore the most important in drug metabolism. Over 30-40 % of all the total CYPs in the human liver is composed of CYP 3A4 and it is known to metabolize fully or in part 40-50 % of all the drugs used in humans (Thummel and Wilkinson, 1998: 389-430). In additional CYP 3A4 metabolizes a variety of other substances including pesticides, steroids and hormones (Dorne et al., 2003: 201-224). They are known to exhibit great substrate specificity and can metabolize an extremely large number of structurally divergent chemicals via different metabolic pathways often in a regio- and stereoselective fashion (Thummel and Wilkinson, 1998: 389-430). It has been shown that CYP 3A4 is almost the sole metabolizer of drugs such as budesonide (>90%), midazolam (>80%), licodaine (>80%) and triazolam (>70%). In addition, this enzyme catalyses the N-demethylation of erythromycin so efficiently that erythromycin has been used as a probe substrate for CYP 3A4 metabolism (Kenworthy et al., 1999: 716-727). It has been shown that CYP 3A4 substrates may also act as inhibitors (Kato et al., 2001: 505-513;

Kenworthy et al., 1999: 716-727). As to whether a substance will act as a substrate or inhibitor is dependent on the concentration used. Erythromycin is both a substrate and inhibitor.

Previously, various bioanalytical techniques have been employed for drug analysis. HPLC-UV, HPLC-MS, fluorescence techniques have been used (Shou et al., 1994: 6450-6455; Walsky et al., 2004: 647-660; Boopathy and Karnes, 2002: 1-6). Shou et al. (1994: 6450-6455) have studied the CYP 3A4 catalyzed metabolism of phenanthrene and the influence of 7,8 –benzoflavone on this metabolism using HPLC techniques. Sample preparations involved the incubation of the enzyme and substrate in phosphate buffer before addition of NADPH to initiate the process. The overall reaction time took over 30 minutes and necessitated termination by addition of dichloromethane. The residue obtained after solvent evaporation was dissolved in methanol in the presence of metabolite standards before spiking on to the HPLC column. Despite the high precision of these methods, the need for incubation may be time-consuming, not to mention the long procedures involved in the whole process. Furthermore, since the reaction has to be terminated by the addition of organic solvents it means the enzyme/substrate mixture is not re-usable and can thus not be used for batch analysis. Elsewhere, use of fluorogenic compounds to study the inhibition mechanisms of the P450s has been reported. In one such instance, 3-[2-(*N*,*N*-diethyl-*N*-*N*-Methyl-ammonium)ethyl]-7-methoxy-4-methylcoumarin has been used (Chauret et al., 2001: 1196-1200). While fluorescence techniques are fast, sensitive and homogeneous, they are prone to interferences and limited only to fluorogenic materials.

In view of the existence of genetic polymorphism among the CYP enzymes and therefore the existence of individualized drug metabolizing abilities, the fabrication of CYP probes for various substrates is vital towards understanding the mechanisms involved. Drug-to-drug interactions for instance are a major issue of concern. They are responsible for a large part of hospitalization or even death (Lazarou, 1998: 1200-1205) and results from the co-administration of two or more antagonizing drugs. The inhibition action of one drug on the enzyme may cause the accumulation of the other drug to toxic levels in the

body. The majority of drug-to-drug interactions are based on the inhibition of the CYP 450 enzymes and such probes will through light into such interactions. Several drugs in common use such as erythromycin, clarithromycin, itraconazole, paroxetine, nefazodone, diltiazem amongst can increase exposure to other drugs through inhibition (Walsky et al., 2004: 647-660). The latter author employed the HPLC-MS technique to study the metabolism of various drugs based on several P450 enzymes. According to the authors, the HPLC-MS technique afforded highly selective assays with low limits of quantification than either the fluorescence or the ultraviolet techniques thus allowing for the reduction of concentration of microsomes used for the incubation, with the benefits of reducing non specific substrate binding and obtaining more accurate kinetic parameters. However, even with this technique, there was need for isolation and purification of some of the substrates such as felodipine. Also, the termination of the incubation procedure by use of acidic solutions could mean the system can only be used for a single substrate concentration and for each analyte concentration the whole incubation process would be repeated which is time consuming.

Based on the HPLC-MS technique, the kinetic parameters (Michaelis-Menten constant, K_m) related to the conversion of felodipine by CYP 3A4 were (μM); 2.81 ± 0.61 for the pooled liver microsomes and 0.938 ± 0.137 for the CYP 3A4 racemate mixture. Similarly, the results for the hydroxylation of midazolam based on the same enzyme the K_m estimates were: 2.27 ± 0.18 μM and 0.622 ± 0.025 μM for the pooled liver microsomes and racemate CYP 3A4 respectively.

Elsewhere, Wang et al., (1997: 502-507), studied the hydroxylation of 6β-testosterone and the N-demethylation of erythromycin based on the CYP 3A4 enzymes from different sources. Human liver microsomes from two different subjects were used and the incubation method was employed. The resultant supernant solution after quenching the incubation product with a mixture of $ZnSO_4/Ba(OH)_2$ was centrifuged in the presence of Nash reagent and absorbance monitored at 405 nm using a UV-spectrophotometer. The apparent K_m obtained for the two substrates using the two forms of human liver microsomes were in the range 53-128 μM for testosterone and 44-78 μM for *N*-

demethylation of erythromycin. Similarly the maximum reaction velocity (V_m) recorded for the two substrates were; 2-20 nmol/min/mg for testosterone and 0.22–2 nmol/min/mg for erythromycin. At the substrate concentrations studied i.e. 10-100 μM no significant inhibition between the substrates was observed.

Recently, biosensors are replacing the long incubation procedures by the detection of the CYP 3A4 analytes at the electrode with the reducing equivalents been provided by application of negative potential. Elimination of incubation processes means biosensors are a faster means of detection. Furthermore, careful control of potential can eliminate interferences not to mention that biosensors require minimal sample preparations. Other benefits of using biosensors include possible elucidation of the mechanisms involved an ability to perform batch analysis. Shiba et al. (2003: 1817-1826) have demonstrated the use of the redox properties of human CYP3A4 to directly monitor electron transfer to the heme, protein thus consequently developing biosensors for verapamil, midazolam, progesterone and quinidine. In this biosensor format, an alternating layer of poly-dimethyldiallylammonium chloride (PDDA)/ CYP 3A4 was adsorbed on the gold working electrodes. Quartz crystal microbalance (QCM) techniques were used to monitor film growth based on changes in resonance frequency. Cyclic and square wave voltametric techniques were employed for electrochemical measurements.

Results showed that in anaerobic buffer, no observable peaks were observed in the CVs of the CYP 3A4/gold electrode. However, well defined redox couples appeared on the CV of the CYP 3A4/PDDA/gold electrode after 50-60 min of equilibration. These results could be interpreted to mean there was no electrical communication between the bare gold electrode and the enzyme. The presence of PDDA placed the enzyme close to the electrode allowing effective electrical relays. The formal potential for the CYP 3A4 Fe^{III}/Fe^{II} was 98 ± 5 mV versus NHE with a peak separation of 98 mV. For the redox couple, peak current I_p increased proportionally to the scan rate and a maximum reduction charge for the CYP Fe^{III}/Fe^{II} conversion was 1.9 μC/cm^2. On addition of substrates in the presence to the MPS/PDDA/CYP3A4 system a substrate concentration dependent current was observed in the presence of oxygen but none was observed under

anaerobic conditions. The dynamic linear range for the verapamil biosensor had an upper value of 2.85 mM. The sensitivity realized was of 1.46 x 10^3 μA/M. Amperometric studies with the other substrates showed similar concentration dependent currents with reaction responses obeying typical Michaelis-Menten kinetics, (K'_m apparent) values being; 547 ± 57 μM for midazolam; 271 ± 71 μM for progesterone; 1082 ± 353 μM for quinidine. The analysis of various metabolites for the sensing systems generated through electrolysis at -500 mV, showed the presence of the expected metabolites showing biosensors are as effective as other incubation techniques even if the natural redox polymers are replaced. The concentrations of the metabolites increased with electrolysis time.

2.15 Substrates

2.15.1 Hydrogen peroxide

The detection of peroxides is of interest because peroxides are environmental hazards. Commonly used in household bleaching, in deodorants, teeth whiteners, disinfectants and in lotions, hydrogen peroxide is a corrosive, mutagenic chemical that can cause serious skin burns, eye damage and is extremely destructive to tissue of the bodily mucous membranes (MSDS, 2000). It is also utilized in several industrial processes particularly in the food and textile industries due its high oxidant power, and for effluent treatment where it acts as a sterilizing, cleaning and oxidizing agent (Fernandes et al., 2005: 3441-3445). Apart from the pollution effects, the detection of peroxides is of interest in biosensor fabrication because it is often a product of most biological reactions and given its electroactive nature forms the basis of most electroanalytical biosensor systems (Song et al., 2006: 1001-1006). Based on the electroactivity of hydrogen peroxide, the determination of glucose, galactose, aspartame, cholesterol and fatty acids, choline, acetylcholine, water and others physiological substances has been carried out (Fernandes et al., 2005: 3441-3445). The determination of hydrogen peroxide and organic peroxides in clinical samples and the environment is rapidly gaining practical importance. Measurement of lipid peroxides in food products and biological tissues is necessary in establishing a relationship between diseases such as breast cancer and the level and type

of fat in the diet (Adhikari and Majumdar, 2004: 699-766). It is necessary to monitor the level of organic peroxides released in the environment from many industrial processes, and that produced during ozonation of drinking water and ozonation reactions in air (Adhikari and Majumdar, 2004: 699-766).

2.15.1.1 Diazinon

Among the pesticides, organophosphate pesticides (OPs) are popular due to their high toxicity to incests, limited persistence in the environment and the lack of bioconcentration (Vakurov et al., 2004: 1118-1125). Diazinon ($C_{12}H_{21}N_2O_3PS$) is a non-systemic organophosphate insecticide and acaricide whose IUPAC name is O,O-dimethyl O-(2-Isopropyl-6-methyl pyrimidin-4-yl) phosphorothioate (Fig. 2.10). It finds use in the household, agricultural and veterinary sectors to control sucking and chewing insects and mites in a range of situations. It is through these modes of usage, and during its manufacturing process that diazinon infiltrates to the humans and environment often with adverse effects. The mode of action of the OPs depends on their ability to irreversibly modify the catalytic serine residue in acetylcholine esterases (AChE), which subsequently inhibits the hydrolysis of acetylcholine, the across-synaptic impulse transmitter causing nervous impulse communication breakdown (Vakurov et al., 2004: 1118-1125).

Though classified as a class II poison with the recommended daily exposure guidelines of 0.002 mg/kg/day for mammals, both dermal and oral exposure incidences of diazinon poisoning have been reported in the manufacturing and the application sectors (Gandhi and Snedeker, 1999: 1-27). Also, diazinon is highly toxic to birds (LD_{50} = 2.75 - 40.8 mg/Kg), fish (LD_{50} = 2.6 - 3.2 mg/Kg) and is very highly toxic to bees (extonet: html). Given that the common chromatographic techniques for OP analysis are expensive and require detailed sample preparations, it is hoped that the construction of diazinon amperometric biosensors based on the inhibition of HRP may provide an alternative to quantification of diazinon.

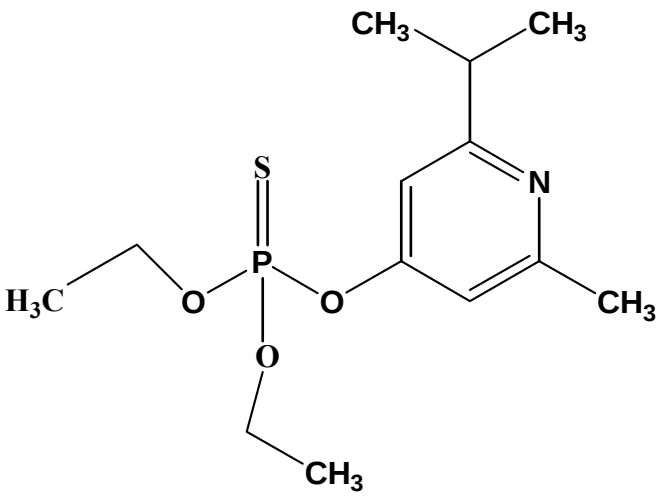

Figure 2.9: Chemical structure of Diazinon.

2.15.2 Erythromycin

Erythromycin (Fig. 2.11) is a macrolide antibiotic, which has antimicrobial spectrum similar to that of penicillin (Faulkner et al., 2005: 997-1004).

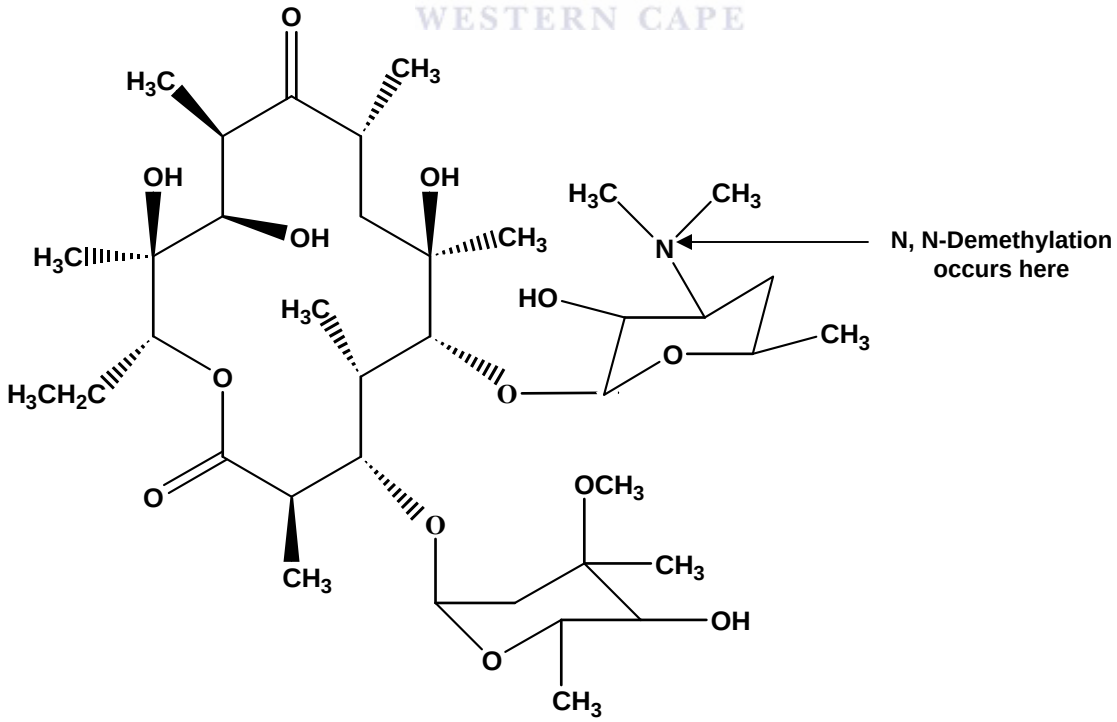

Figure 2.10: Chemical structure of Erythromycin .

It is used to treat various conditions including respiratory tract infections. It has been found that the simultaneous administration of erythromycin with other drugs such as verapamil and diltiazem can lead to fatal drug-to-drug interactions (Walsky and Obach, 2004: 647-660). It has been shown that CYP 3A4 catalyses the *N*-demethylation of erythromycin. Erythromycin is so efficiently metabolized by the CYP 3A4 that it is used as an in vivo probe to determine CYP 3A4 activity. It is now known that erythromycin is a substrate/inhibitor of CYP 3A4 depending on the concentration used.

2.16 Enzyme Kinetics

Apart from allosteric enzymes that show cooperative substrate binding, the rate of catalysis, v, for most enzymes varies with the concentration of the substrate [S] in a hyperbolic manner (Fig. 2.12) (Stryer, 2000: 104-128). The effect of substrate concentration on the initial rate of an enzyme-catalysed reaction is a central concept in enzyme kinetics and the Michaelis-Menten kinetics model is designed to explain this relationship.

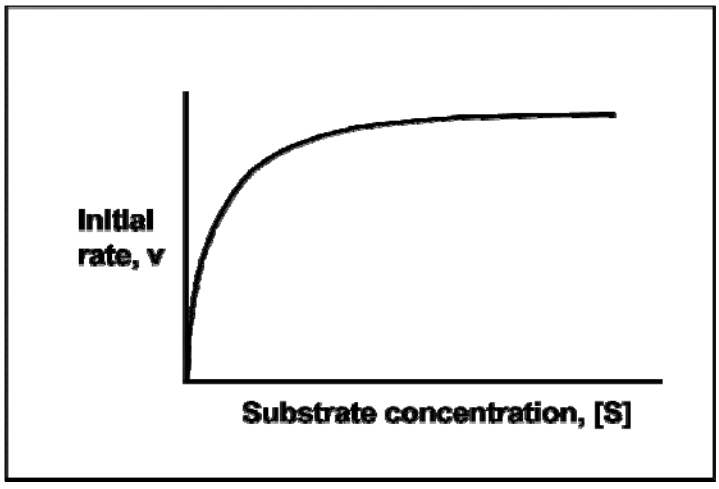

Figure 2.11: A plot of the reaction velocity V, as function of substrate concentration an enzymatic reaction following a typical Michaelis-Menten case.

The Michaelis-Menten kinetics model postulates that enzymatic reactions proceed through the formation of a transition complex intermediate ES;

$$E + S \underset{k_2}{\overset{k_1}{\rightleftharpoons}} ES \xrightarrow{k_3} E + P$$

with the rate of the formation of the transition complex ES being k_1. Once formed, the ES complex may either convert to a product P at a rate constant of k_3 or decompose at a rate constant k_2 to the free enzyme E and substrate S. The Michaelis-Menten model assumes that only a negligible amount of enzyme-substrate complex reverts back to reactants. According to this model the hyperbolic relations governing the rate of catalysis and the substrate concentrations is then governed by the equation:

$$v = V_{max} [S] / K_m + [S] \qquad (2.1)$$

where v is the initial rate, V_{max} is the maximum rate of catalysis, K_m is the apparent Michaelis-Menten constant and [S] is the substrate concentration. The Michaelis-Menten constant refers to the substrate concentration at which the enzymatic reaction occurs at half the maximum velocity ($V_{max}/2$). K_m is a measure of the affinity that an enzyme has for the substrate and hence can be used as indicator of the stability of the enzyme-substrate complex. According to this model then: at low substrate concentration, <<[S], the availability of substrate becomes the limiting factor. At low substrate concentration [S], the relationship between the rate of reaction and the concentration of substrate is linear - it is this portion of the Michaelis-Menten curve that is useful for bioanalytical purposes. This linear portion of Michaelis-Menten curves is referred to as the dynamic linear range in biosensors. At a K_m equivalent substrate concentration, 50% of the enzyme active sites are bound and the rate of enzyme catalysis starts to drop. At high substrate concentration, the theoretical supposition is that all the enzyme active sites are substrate bound and therefore the rate of enzymatic reaction is independent of substrate concentration. A leveling of the reaction rate/substrate concentration curves occurs and the Michaelis-Menten curve then reaches a plateau. In reality, the true V_{max} are never

realized. Instead the apparent values of these parameters V_{max} and K_m are estimated from the hyperbolic curves.

In amperometric biosensors, the rate of catalysis is measured in terms of the catalytic current. The maximum rate of catalysis is represented as I_{max}, and the apparent K'_m values are obtained from the plots of substrate concentration, [S], versus the catalytic current.

2.16.1 Biosensors based on enzyme inhibition

Enzymatic inhibition refers to the blockage of the enzyme catalytic sites either reversibly or irriversibly with the reduction of enzyme activity. In biosensors, the development of inhibition-based biosensing schemes relies on the quantitative measurement of the enzyme activity before and after exposure to the target analyte (Amine et al., 2006: 1405-1423). The presence of inhibitors blocks some of the enzyme's active centers leading to a decreased signal. This signal de-attenuation is directly proportional to the concentration of the inhibitor in the solution (Ciucu et al., 2003: 303-310).

Enzymatic inhibition can be classified into competitive and non-competitive inhibition (Stryer, 2000: 104-128). In reality competitive and non-competitive can be distinguished by construction of Lineweaver-Burk plots (double reciprocal plot obtained by reciprocating the Michaelis-Menten equation). For a competitive inhibition, the intercept of the plot of reciprocal of reaction velocity $1/V$ versus $1/[S]$ is the same in the presence or absence of inhibitor. Increase of substrate concentration can be used to overcome this inhibition type.

In non competitive inhibition, the y- intercept of the Lineweaver-Burk plots increases in the presence of an inhibitor. However, maximum reaction velocity (V_{max}) and K_m are unaffected by the presence of inhibitor. Competitive inhibition cannot be removed by increase in substrate concentration.

2.17 Summary

Conducting polymers including sulphonated polyanilines (SPAH) can be prepared either through the chemical or the electrosynthetic routes. The chemical route is preferred for bulk production since it is cheap but the electrosynthetic route is used when purity is required. A major problem encountered with conducting polymers especially those prepared chemically is intractability and insolubility in common organic solvents thus limiting their scope of applications. New methods of synthesis including enzymatic synthesis, plasma, vapour deposition etc. have been tried out but do not offer permanent solutions to the intractability problems given that they are much more expensive and may even lead to environmental pollution, especially where additives such as H_2O_2 are needed to initiate the process. The new approach has been to improve the traditional chemical synthetic methods with the aim of improving the properties of the resultant materials. In one such approach, nanostructurization has been considered an attractive alternative.

Nano-polymers are more processable in that they are more dispersible and sometimes more soluble. They exhibit enhanced morphology often with improved conductivity. Nanostructurization has been achieved through the use of aids such as 'hard' and 'soft' templates. Soft templates which essentially involve the use of molecules such as surfactants are more appropriate since the bother of post-template dissolution is eliminated. Furthermore surfactants bearing sulphonic groups, like those employed in this work, have an added advantage of producing polymers that are less pH sensitive. These polymers like SPAH and SPANi are stable around neutral pH and are thus excellent for biosensor applications given enzymes operate best around their physiological pH and within a narrow PH range. Furthermore the SPAH type polymers have conductivities similar to that of PANi doped with simple mineral acids and by varying reaction conditionalities can be shaped into desired morphologies, e.g. tubular, granular, rod-like, micellic etc.

Spectroscopic techniques have been verified to provide evidence for conductivity and doping state of the polymers, while electrochemical techniques, such as square wave voltammetry, can verify electroactivity. It has been shown that direct electrical

communication between various PANi polymers including SPAH and various biomolecules is possible. The choice of HRP for detection of hydrogen peroxide was based on the fact that the latter is one of its substrates. Although previous pesticide studies are based on the inhibition action of OPs on acetylcholine esterase, the fact that HRP is inhibited by organic sulphur-containing compounds including OPs, forms the basis of the alternative method of analysis. Applicability of the latter method is bound to be much cheaper given HRP is cheap, robust and more resistant to pH related denaturing. Among the CYP P450 enzymes, it has been shown CYP 3A4 is the most important in drug biotransformation. It has also been shown that due to the existence of genetic polymorphism drug biotransformation vary across individuals. Since previous drug analysis methods involve long incubation and detection processes, the detection of drugs (erythromycin in this case) on SPAH modified electrodes may provide a rapid alternative. If successful, such biosensor formats will be useful for study of drug-to-drug interactions and other processes related to the CYP 3A4 drug biotransformation mechanisms.

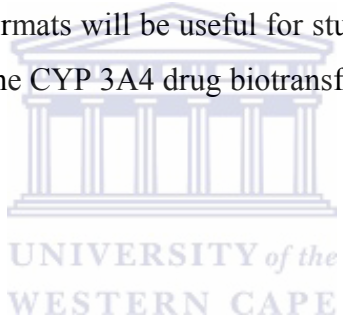

Chapter 3

Experimental

3 Chapter Overview

This chapter presents the principles of the electrochemical techniques utilized in the preparation and characterization of the sulphonated polyanilines (SPAH). The SPAH prepared were those doped with the sulphonated heteronuclear aromatic hydrocarbons, anthracene sulphonic and naphthalene sulphonic acid. Both chemical and electrochemical methods were utilized. Firstly, the preparation and the characterization of the anthracene sulphonic acid dopant is presented. The chemical and electrochemical oxidative procedures for the preparation of the polymer ASA and NSA composites and the standard characterization procedures (UV-Vis, FTIR and SEM) are also discussed. Finally a description of the final immobilization procedures for the biomolecular recognition systems, and the applications of the resultant biosensors to the detection of various analytes are discussed.

3.1 Principles of the electrochemical techniques used.

The major technique used for the preparation and/or characterization of the SPAH were electrochemical in nature. Cyclic (CV), square wave (SQW) and differential pulse (DPV) voltammetric techniques were utilized. The application of each of these techniques and their choice for the preparation of SPAH was governed by the existing theories of electrode processes. The ability to utilize these techniques for the electrodeposition and characterization of SPAH was based on the fact that these organic molecules have accessible frontier molecular orbitals with well defined formal potentials.

3.2 Principles governing electrode processes

An electrode process is a heterogeneous reaction occurring at the electrode-electrolyte interface. The rate of electrode process is dependent upon the mass transfer rate at which the analytes are brought to the electrode surface, the electrodynamics of electron transfer across the interface, chemical reactions preceding or following electron transfers as well as various other surface reactions. In general, the net rate of a heterogeneous electrode process can be presented by the equation;

$$\text{Rate (mol s}^{-1}\text{cm}^{-2}) = \quad i / n F A \qquad (3.1)$$

where F and A are the Faraday constant (C mol^{-1}) and the area of the electrode respectively. The observed current (i) is a function of all the electrode processes and is limited by the more sluggish reactions (rate determining step) (Monk, 2001: 17-24). In particular, the mass transfer issue is a function of three components namely: migration, diffusion and convectional effects. The mass transfer of the analyte species to an electrode is governed by the Nernst-Planck equation (Bard and Faulkner, 2001: 23-35)

$$J_i(x) = - D_i \frac{\partial C_i(x)}{\partial x} - \frac{z_i F}{RT} D_i C_i \frac{\partial \phi(x)}{\partial x} + C_i \upsilon(x) \qquad (3.2)$$

where $J_i(x)$ is the flux of species i (mol s^{-1} cm^{-2}) at distance x from the surface, D_i is the diffusion coefficient (cm^2/s), $\partial C_i(x)/\partial x$ represents the concentration gradient at a distance x, and $\partial \Phi(x)/\partial x$ is the potential gradient. The parameters z_i and C_i are the charge and the concentration (mol cm^{-3}) respectively where υ is the velocity (cm/s) in which a volume element in solution moves in the direction along the distance (x).

In general, the three terms at the right hand side of the equation represent the three components of mass transfer.

In practice, the electrode reactions can be tailored to simplify the complications related to mass transfer. For organic conducting polymers for instance, keeping the monomer concentration very low compared to the concentration of the supporting electrolyte nullifies the migration effect (Brett and Brett, 2005: 137-142). Also, carrying out the electrodeposition/electrochemical characterisation under quiescent (unstirred) conditions eliminates the conventional contribution (Brett and Brett, 2005: 83-96; Monk, 2001: 17-24). This way the Nernst-Planck equation collapses to only the diffusion term (first term). Under the circumstances, the rate at which flux is transported to the electrode surface becomes the rate determining step and its movement is governed by Fick's laws of diffusion so long as the working electrode (WE), is kept at right-angles to the incoming flux. Other factors that might affect the overall observed current such as the IR drop are minimized by placing the reference electrode at close proximity to the working electrode and through use of IR compensation modes in the instruments.

In order to simplify the electrode processes during the preparation of SPAH, quiescent (unstirred) conditions were adopted and it was always ensured that the WE was always in a vertical position.

3.3 Cyclic Voltammetry

Cyclic voltammetry represents the most versatile and useful technique for performing electrochemical measurements. In cyclic voltammetry the execution signal is a linear potential scan with a triangular waveform that sweeps the potential of the working electrode back and forth between two designated values called switch potentials. The triangle returns at the same speed and permits the display of a complete voltammogram with oxidative and reductive waveforms one above the other as shown in Figure 3.1.

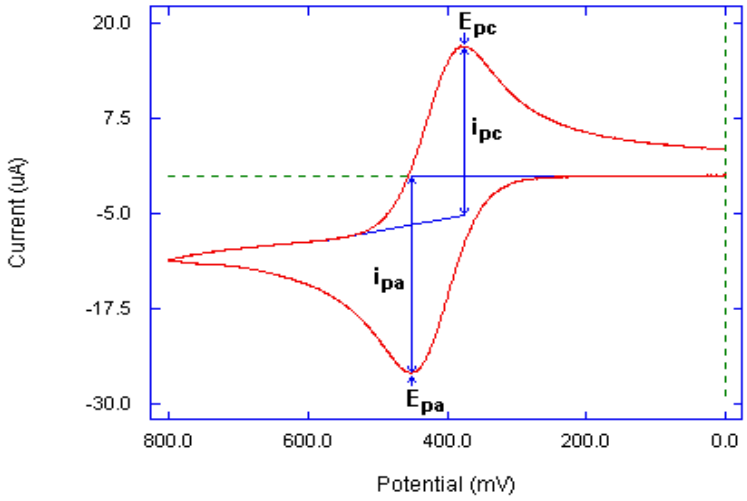

Figure 0.1: An i-E curve (voltammogram) demonstrating the most important parameters associated with cyclic voltammetry.

Source: ***http://www-bio.paisley.ac.uk/marco/Enzyme***

A potentiostat controls the potential applied at the electrode. A potentiostat is an instrument that allows the control of the potential between the working electrode (WE) and the reference electrode (RE), whereas the electric current flowing through the WE and the counter electrode (CE) is independently measured. Since the potential of the RE remains virtually constant during the experiments the potential control acts directly across the WE/electrolyte interface. The potentiostat used in this work was a BAS 100 B, BAS 50 W electrochemical workstation.

Driving the electrode to more negative potentials raises the electrode Fermi level; the energy of the electrons will eventually be high enough to allow them to occupy the vacant sites in the Lowest Unoccupied Molecular Orbitals (LUMO) of the electroactive material. This is marked by a flow of a reductive current as the electroactive species is reduced and a cathodic peak appears in the voltammogram. On the contrary, when the potential of the working electrode is made sufficiently positive, the energy of the electrons is lowered sequentially until eventually electrons flow from the Highest Occupied Molecular Orbitals (HOMO) of the electroactive species. An oxidative current

flows and an anodic peak is recorded in the voltammograms as the electroactive species is oxidized. For a multi-oxidation state electroactive species like polyaniline and its derivatives, several redox couples are recorded in the voltammogram and the critical potentials at which these limiting currents i_l (A) occurs are related to the standard electrode potentials E^0 (mV), for the specific chemical system. In practice the electrode kinetics, and therefore the appearance of the voltammetric peaks is closely intertwined to the system's mode of mass transfer in action. For a reversible system the rate of electron transfer is rapid and the only rate determining process would be the movement of flux to the surface of the electrode.

Figure 3.2 is an example of a cyclic voltammogram for protonic mineral acid doped polyaniline showing the potential regions for the various oxidation/reduction processes. Similar *i*-E curves are expected for strong acid-doped POMA and PDMA.

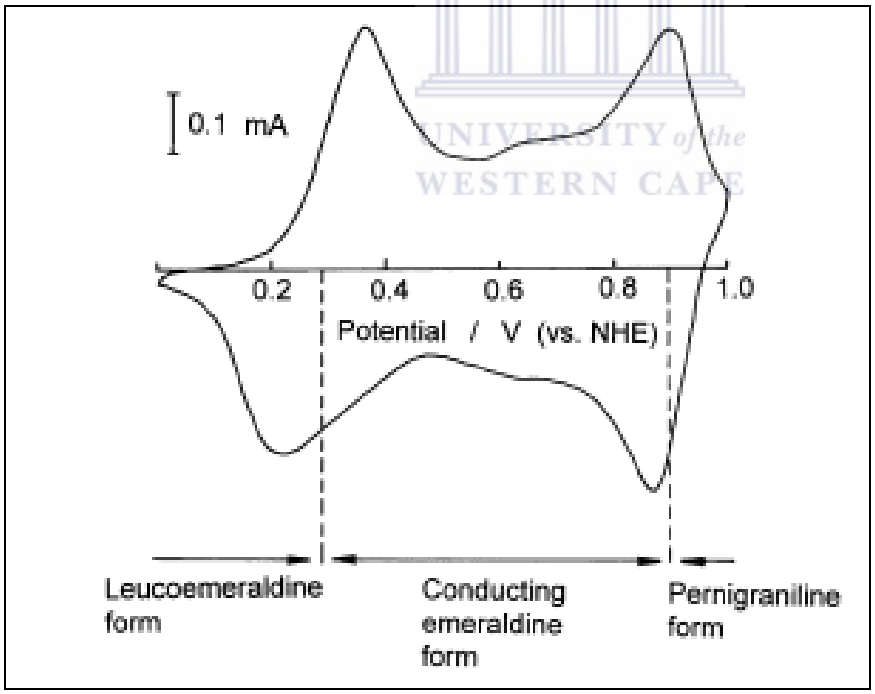

Figure 0.2: A typical cyclic voltammogram for polyaniline doped with a strong acid showing the potential regions for redox state inter-conversions.

Source: Malinauskas, (2001: 3957-3972)

3.3.1 Important parameters in Cyclic Voltammetry

In cyclic voltammetry, if a redox system remains in equilibrium throughout the potential sweep, then the redox process is reversible. It means the surface concentrations of the oxidized O, and reduced species R, maintain the values required by the Nernst equation. For such a system, the formal potential ($E^{0\prime}$) for the reversible couple is centered between the peak potentials for the anodic ($E_{p,a}$) and the cathodic($E_{p,c}$) processes.

- $(E^{0\prime}) = (E_{p,a} + E_{p,c}) / 2$ (3.3)

The number of electrons transferred (n) can be determined from the separation between the peak potentials:

- $\Delta E_p = E_{p,a} - E_{p,c} = 0.059 / n$ where ΔE_p is the peak separation between the anodic and cathodic peaks.
- The ratio of the cathodic peak current $I_{p,c}$ to that of anodic peak $I_{p,a}$ current is 'unity' at all scan rates.
- The peak current increases proportionally to the square root of the scan rate (and is independent of the scan rate) as governed by the Randles Sevcik equation.

$$I_p = 2.69 \times 10^5 n^{3/2} A C D^{½} \upsilon^{½} \quad (3.4)$$

where:

n = number of electrons transferred

A = the electrode area (cm^2)

C = concentration (mol cm^{-3})

D = Diffusion coefficient (cm^2s^{-1})

Often times, however, an electrochemical system may show departure from the above behaviour. Quasi-reversibility, or even irreversible behaviour, is a pointer that the heterogeneous rate constant k^0, for the redox couple is too small. It means the electron transfer kinetics is sluggish and cannot maintain the surface concentrations of the oxidized and reduced species as dictated by the Nernst equation. In fact reversibility

depends on the ratio of the heterogeneous rate constant (k^0) and the scan rate (υ) i.e. k^0/ υ (Monk, 2001: 17-24). For quasi-reversible systems this ratio is very small. At the same time the peak- to-peak separation for the redox couple ΔE_p is >>>59/*n* allowed for reversible systems. Luckily, by decreasing the scan rate υ of an electrochemical reaction, it is possible to convert a quasi-reversible system to a reversible one (Bard and Faulkner, 2001: 236-239). The rationale here is that a low scan rate would allow more time for the surface concentrations of the reaction species to adjust to new values as required on changing the potential thus satisfying the Nernstian equation requirements.

3.3.2 Characteristics of quasi-reversible systems

A cyclic voltammogram is useful in diagnosing quasi-reversibility or irreversibility from the shape of the i-E curve. For quasi-reversible systems for instance, the peak -to - peak separation ΔE_p is greater than the 59/*n* mV recommended for reversible systems. The cathodic and anodic peak currents differ in magnitude i.e. $I_{pc} / I_{pa} \neq 1$ and the peak current I_p increases unproportionally to the square root of the scan rate ($\upsilon^{1/2}$). It has been shown that most conducting polymers systems show reversibility at low scan rates but the behaviour transits to quasi-reversibility at higher scan rates. At these high scan rates therefore, the shapes of the quasi-reversible voltammograms for the organic conducting polymers are functions of the scan rate υ, the standard rate constant k^0, the transfer coefficient α, and the switch potential (E_λ) and Ψ (E) (a kinetic parameter). The effect of the switch potential on the shapes of quasi-reversible systems is easily eliminated by keeping the switch potential at least 90/*n* mV beyond the last cathodic peak (Bard and Faulkner, 2001: 242). It has also been shown that most quasi-reversible systems exhibit α values in the range $0.3 \leq \alpha \leq 0.7$. This way the observed waves are independent of the transfer coefficient α and depend only on the kinetic parameter Ψ (E). From well established ΔE_p / Ψ (E) tables established by Nicholson, the peak currents I_p and the heterogeneous rate constants for the quasi-reversible systems can be determined by use of the equations (Bard and Faulkner, 2001: 243);

$$i = F A D^{1/2} C_O^* f^{1/2} \upsilon^{1/2} \Psi(E) \qquad (3.5)$$

where;

F = the Farady

A = area of the electrode (cm^2)

D = diffusion coefficient (cm/s)

$f = F/RT$

Ψ = the kinetic facility dependent on $\Delta E_{p.}$

the heterogeneous rate constant for the quasi-reversible systems can then be obtained by use of the equation:

$$k^0 = \frac{\Psi(E).\,[D.\pi.\,\upsilon.\,n\,F/RT]^{1/2}}{(D_O/D_R)^{\alpha/2}} \qquad (3.6)$$

For $D_O = D_R = D$,

It has been established that the k^0 (cm/s) for quasi-reversible systems lie in the range; $0.3\upsilon^{1/2} \geq k^0 \geq 2 \times 10^{-5}\,\upsilon^{1/2}$

3.3.3 Estimating the surface concentration of a redox couple

The shapes and general appearance of cyclic voltammograms is significantly affected by the adsorption of one species or both. The location of the peak potential E_p relative to the formal potential $E^{0'}$ depends on the strength of the absorption. When O is strongly adsorbed, the wave is displaced towards negative potentials beyond the position of a reversible wave is expected to occur and vice versa (Bard and Faulkner, 2000: 592). Although the equations for solution species as discussed previously still hold, adsorption demands the choice of adsorption isotherms and therefore additional parameters thus complicating the situation (equation 3.7). Based on the applications of the linearized Langmuir adsorption isotherms, it has been shown that the current component in a cyclic voltammogram where either O or R or both are adsorbed is given by (Bard and Faulkner, 2001: 580-601):

$$i_p = \frac{n^2 F^2}{4RT} \upsilon A \Gamma^* \qquad (3.7)$$

where:

Γ^* (mol cm^{-2}) refers to the surface concentration of the adsorbed species and the other parameters have their usual meaning.

Under these circumstances, the peak current is proportional to the scan rate υ, and a Brown Anson plot (plot of peak current versus scan rate) is useful for the determination of the surface concentrations (Γ^*) of the adsorbed species. Another approach towards the determination of the surface concentration of the adsorption is based on the fact that the area under the oxidation/reduction wave ($nFA\ \Gamma^*$) is equivalent to the charge Q (coulombs) passed during oxidation/reduction (Bard and Faulkner, 2001: 580-601). Then the surface concentration for either the oxidized or reduced species is given by:

$$\Gamma^* = Q / n F A \qquad (3.8)$$

where Q is the charge in coulombs; other parameters have their usual meaning.

3.4 Differential pulse voltammetry (DPV)

Differential pulse voltammetry can be used in the identification of any species that appears on the surface of the electrode during a scan because each species generates an individual symmetric peak (Avril, 2001). It is generally a more sensitive potential compared to cyclic voltammetry and is often used as a complimentary tool. In DPV, the potential of the working electrode (WE) is scanned with a series of pulses with current measurements being measured before and at the end of the pulse. The difference between these current measurements for each pulse is automatically determined and plotted against base potential. The corresponding *i*-E curves display peak potentials proportional

to the concentration of the analyte in solution. The peak potential corresponds to the redox potential of the analyte.

3.5 Square wave voltammetry

Square voltammetry is a highly sensitive technique with detection limits as low as 10 nM. Its ability to eliminate background currents and speedy operation allows it for use in the study of many kinds of electrode kinetics. In square wave voltammetry, the excitation signal is a symmetrical square pulse of amplitude E superimposed on a staircase wave form (Fig. 3.4) of step height ΔE (Kounaves 1997: 720-721).The observed net current is the difference between the forward/reverse currents and corresponds to the analyte's redox potential. The magnitude of the peak current is proportional to the concentration of the electroactive species in solution.

3.6 Chemicals and reagents

3.6.1 Reagents for the Synthesis Procedures

Anthracene sulfonic acid (ASA) and naphthalene sulfonic acid (NSA) surfactant dopants were used for the preparation of the required composites. While the NSA was commercially available, the ASA dopant had to be synthesized in the laboratory. The required reagents used for the ASA preparation were: Anthracene 99 %, sodium chloride, sodium bicarbonate, and potassium bromide were of analytical grade and products of Sigma -Aldrich (Cape Town, SA). Fuming sulfuric acid was purchased from Aldrich, (Cape Town, SA)

3.6.1.1 Reagents for the preparation of the polymer composites, requirements for UV-Vis and FTIR characterization procedures

Napthalene sulfonic acid, 70%, and ammonium peroxydisulfate oxidant, $(NH_4)_2S_2O_8$ 98+ % were products of Aldrich, (Cape Town, SA) while anthracene sulfonic acid was prepared in-house as stated. The aniline 99.5%, Fluka, (Cape Town, SA), and O-

methoxyaniline 99+%, Sigma Aldrich (Cape Town, SA) monomers were doubly distilled under reduced pressure before use and stored in labeled Eppendorf vials at < 4°C when not in use. The 2,5-dimethoxyaniline monomer presented as black shiny beads was a product of Sigma Aldrich (Cape Town, SA), and was used as received. Hydrochloric acid (32%), diethylether and methanol (analytical grade quality) were purchased from Fluka, (Cape Town SA) and were used without any further purification. Dimethyl sulfoxide (DMSO, 99.6%), KBR, dimethyl formamide (DMF) and m-cresol were products of Sigma-Aldrich, (Cape Town, SA). Carbon tetrachloride (CCl_4), chloroform ($CHCl_3$), tetrahydrofuran (THF) and absolute ethanol were products of the Kimix Company, (Cape Town, South Africa). Ammonium hydroxide (25%) was obtained from Merck Company, (Cape Town, South Africa).

3.6.1.2 Reagents for the construction and characterization of biosensors and their pretreatment

Bovine serum albumin (BSA) and glutaraldehyde (50% w/v in water) were purchased from Fluka, (Cape Town, South Africa). The glutaraldehyde was diluted with distilled water to give a 2.5 % solution before use. The KBR salt was oven dried at 80 ºC for 2 h before use. AnalaR grade anhydrous disodium hydrogen phosphate and AnalaR grade potassium dihydrogen phosphate monohydrate were products of Aldrich, (Cape Town, South Africa). The anhydrous salts were oven-dried for 3 h at 110 ºC and cooled in desiccators before use for buffer preparation. Appropriate portions of 0.1 M solution of each salt separately prepared were mixed based on the Henderson-Hasselbalch relationship to yield phosphate buffer solutions with a final concentration of 0.1 M (pH 7.02 or pH 7.4) at conditions of room temperature and pressure. These solutions were utilized for biosensor measurements and were kept refrigerated whenever out of use to prevent growth of molds which could affect the pH. Hydrogen peroxide (30 %) was a product of Sigma-Aldrich, (Cape Town, South Africa) and was kept refrigerated at all times. A 0.01 M H_2O_2 peroxide stock solution was prepared freshly during each new biosensor measurements. Fresh preparation of H_2O_2 was necessary to ensure the same

concentration was used through out given that hydrogen peroxide quickly decomposes to water and oxygen.

Horseradish peroxidase (EC .1.11.1.7) type II, 200 units/ mg salt-free powder obtained from Sigma (CapeTown, South Africa) was used for the H_2O_2 biosensor preparation. Stock solutions were prepared by dissolving 0.2 or 0.4 mg of the enzyme in 1 mL phosphate buffer (pH 7.02) in epperndorf vials. The unconstituted enzyme was stored in the freezer when not in use. Fresh enzyme solutions were prepared for each new biosensor experiment.

Purified cytochrome P450 3A4 (EC. 1.14.14.1) and human recombinant isozyme containing >80 pmole cytochrome P450 /mg protein with a molecular weight between 45-60 kDa, were used as stated. The CYP3A4 was purchased from Sigma Adrich, (Cape Town, South Africa). A 14.4 μM L^{-1} enzyme stock solution was prepared for biosensor measurements. The erythromycin substrate (997μg/mg) was also a product of Sigma Aldrich and was presented in brown bottles to present chemical decomposition by light. The substrate was kept in the fridge when not in use.

The diazinon stock solution (8 μM, in acetone) was donated by Department of Agriculture (DoA), South African Agricultural Food, Quarantine & Inspection Services (SAAFQIS). The solution was used as received. Millipore Milli Q^{TM} water was used in all the biosensor experiments. Analytical grade argon gas was a product of the Afrox company, (Cape Town, South Africa). Glycerol (for molecular biology, 99%) was purchased from Sigma- Aldrich, (Cape Town, South Africa).

3.7 Instrumentation

All electrochemical measurements were carried out using either a BAS 50W or a BAS 100W electrochemical workstation from BioAnalytical Systems (BAS), (Lafayette, Illinois, USA) interfaced with a computer. The instruments were operated under the cyclic, square wave or differential pulse voltammetric modes. Sigma Plot 8.0 software

was used for all data analysis. All pH measurements were done using HANNA Instruments microprocessor pH meter which was calibrated regularly using Hanna buffers (pH 7.01, 4.01) to ensure accurate pH measurements. The UV-Vis absorbance experiments were performed with UV/Vis 920 Spectrometer GBC Scientific Instruments, (Australia) with the UV-Vis operational wavelength set between 200-900 nm. FTIR measurements were performed using Perkin Elmer Paragon 1000 PC FTIR, in the range 400 – 4000 cm^{-1} wave numbers. Scanning electron microscopy (SEM) was carried out using a Hitachi X-650 Scanning Electron Microanalyser with an operating voltage window of 5-40 kV.

3.8 Synthesis of Anthracene sulfonic acid (ASA) surfactant dopant

A three-necked distillation flask that had a separating funnel, a thermometer and a mechanical stirrer was used for the synthesis. 2 g of anthracene were heated through an open-air bath until it melted. To the molten anthracene, 3.73 g of 30 % fuming sulfuric acid were added and the mixture was stirred continuously at 160 ± 5 ° C. The resultant solution was quenched by pouring it into 20 mL ice-cold water. The resultant solution was partially neutralized by adding about 4 g $NaHCO_3$. The solution was then brought to boiling and saturated with NaCl. Recrystallization in 10 % NaCl yielded sodium anthracene sulfonate, a pale yellow crystalline and highly deliquescent salt. The salt was dried in an oven at 80° C. The properties of the salts are: yield 1.82 g (65 %).

3.8.1 Characterization of the synthesized anthracene sulfonic acid (ASA)

The resultant sodium anthracene sulfonate salt was subjected to FTIR characterization. About 0.01 g (1%) of sodium anthracene sulfonate salt was ground with 0.399 g (98%) of KBR using a mortar and pestle. The deliquescent KBR and the sodium anthracene sulfonate salts were previously oven dried for 2 h at 80 °C and allowed to cool in a dessicator. The ground mixture was then pelletized using a PYE UNICAM pelletizing instrument by applying 7-8 tons pressure. FTIR measurements were taken between 400 - 4000 wavenumbers. The existence of vibrational bands at 1040 cm^{-1}, 1020 cm^{-1} and 505

cm^{-1} associated with the $-SO_3H$ group were used as indicators to verify that the anthracene precursor material was successfully sulfonated to yield sodium anthracene sulfonate. Hydrolysis of the sodium anthracene sulfonate product yielded anthracene sulfonic acid. (1 M ASA, pH = 0.56).

3.9 Chemical synthesis of NSA and ASA-doped SPAH

The synthesis of SPAH was initially carried out at different monomer:dopant ratios. Eventually, the 1:0.5 ratio was chosen for all synthesis. The procedure for the preparation of the POMA and the PDMA ASA-doped polymers is similar to that ASA-doped PANi. Expect for POMA and PDMA, *o*-methoxyaniline or 2,5-dimethoxyaniline monomers are used in place of the aniline monomers respectively. A typical procedure using the 1:0.5 monomer to dopant ratio was as follows.

$2x10^{-3}$ mol of anthracene sulfonic acid and $4x10^{-3}$ mol aniline were dispersed in 20 mL distilled water under continuous magnetic stirring. The temperature of the mixture was slowly raised and held at between 50-60^{o}C for 20 min. to allow thorough mixing of the monomer with the dopant. The mixture was then immediately plunged into an ice-bath with the temperature held between 0-5 ^{o}C under continuous stirring. $4x10^{-3}$ mol of pre-cooled ammonium persulfate in 5 mL distilled water was added drop-wise to the reaction mixture. Vigorous stirring continued for the next 24 h during which the light yellow solution darkened to an emerald colour and later to dark green characteristic of doped PANi. The resultant colloidal suspension was allowed to stand for another 12 h. Vacuum filtration of the product was followed by thorough washing with distilled water, methanol and diethyl ether respectively. The polymer pastes were vacuum dried for 24 h prior to characterization. The polymer composites were placed in dry labeled storage vials and stored in a moisture free atmosphere awaiting characterization.

3.9.1 Synthesis of NSA-doped PANi, POMA and PDMA

The procedure followed for the synthesis of the NSA - doped PANi, POMA and PDMA composites was exactly the same as that described above for the ASA-doped composites except that the ASA dopant was replaced with NSA. Though several monomer to dopant ratios were used, eventually the 1:0.5 was found to produce the polymers with the desired characteristics.

3.10 Characterization procedures for the resultant ASA and NSA doped composites

3.10.1 Solubility test

The solubility of the resultant polymers in different laboratory reagents was tested. All the laboratory reagents used were of analytical grade. Exactly 10 mL of each of the following solvents was measured and placed in labeled stoppered vials; methanol, dimethyl sulfoxide (DMSO), dimethyl formamide (DMF), carbon tetrachloride (CCl_4), diethyl ether, chloroform ($CHCl_3$), tetrahydrofuran (THF) and m-cresol. To each of vials, 0.05 g of ASA-doped polyaniline was added. The mixture was stirred magnetically at room temperature for 5 minutes, and allowed to stand for a further 1 min. before the solubility determination. This procedure was repeated for all the other polymers composites in order to evaluate the effect of dopant and ring functionalization on the solubility of the resultant composites.

3.11 UV-Vis characterization procedures

0.001 g of each of the resultant polymer composites was carefully weighed out. The polymer was dissolved in 10 mL of DMSO to give blue/ or green solution depending on the composite. The choice of the DMSO solvent was because almost all the composites were soluble in it. UV-Vis measurements were recorded between 200-900 nm using a double beam 920 spectrometer GBC Scientific Instruments, (Australia) with the sample solutions placed in 4 cm^3 quartz cuvettes. The choice of the quartz cuvettes was because they are transparent both in the UV and the visible regions and therefore freely allowed

the passing of the optical light. Sample solutions were further diluted with DMSO when deemed necessary to give very dilute solutions. The DMSO solvent was reference and its absorption was automatically canceled out between the reference and sample beams.

It was also necessary to dedope some of the composites in order to verify the dopants effects on the observed spectra. The dedoping procedures were carried out as follows;

0.001 g of the weighed polymers composites were placed in a 2 cm^3 10 % $NH_3.H_2O$ for 12 h. The resultant polymers were dried under a dynamic vacuum for 24 h. The polymer composite was dissolved in 10 mL DMSO. Absorbance measurements for the dedoped polymers were carried out as described above. The spectra obtained were scrutinized and compared to verify the relationship between doping and existence of polaron/bipolaron bands.

3.12 FTIR characterisation procedures

0.012 g of each polymer composite and 0.399 g of the previous oven dried KBR were ground in a mortar using a pestle to give a homogeneous mixture. The mixture was then pelletized by application of 7 tons pressure. The resultant polymer / KBr pellets were scanned on a Perkin Elmer Paragon 1000 PC FTIR, in the range 400 – 4000 cm^{-1} wave numbers. Resultant spectra were scrutinized for bond displacement and existence of polaron bands - the signatures for conductivity. Dedoping procedure for FTIR was similar to that used for UV-Vis.

3.13 Scanning Electron Microscopy (SEM)

The morphological characterization of the ASA and NSA-doped polyanilines was carried out using a Hitachi X-650 scanning electron microscope with an operating voltage window of 5-40 kV. In order to prepare the samples for viewing, clearly labeled (on the underside) aluminium stubs were covered with conducting glue. The samples were then sparingly sprinkled on to the stubs. The sample containing stubs were held with a pair of

forceps and knocked on the sides to remove excess polymer leaving behind an evenly spread layer. The samples were then sprayed with a thin layer of gold under vacuum. Viewing was carried out at different magnifications to display the morphology of the composites both in the micro and nano- ranges. The resultant images were compared to show the morphological influence of the different dopants used.

3.14 Electrochemical procedures

3.14.1 Electrochemical characterisation of the chemically synthesized SPAH using the cyclic and square wave voltammetric techniques

Cyclic voltammetry (CV) was carried out in a 10 mL electrochemical cell except where stated otherwise. A typical diagram of an electrochemical cell is given in Figure 3.5. All potential measurements were made against a Ag/AgCl (3 M NaCl type) reference electrode. A 0.5 mm thickness platinum wire was used as counter electrode.

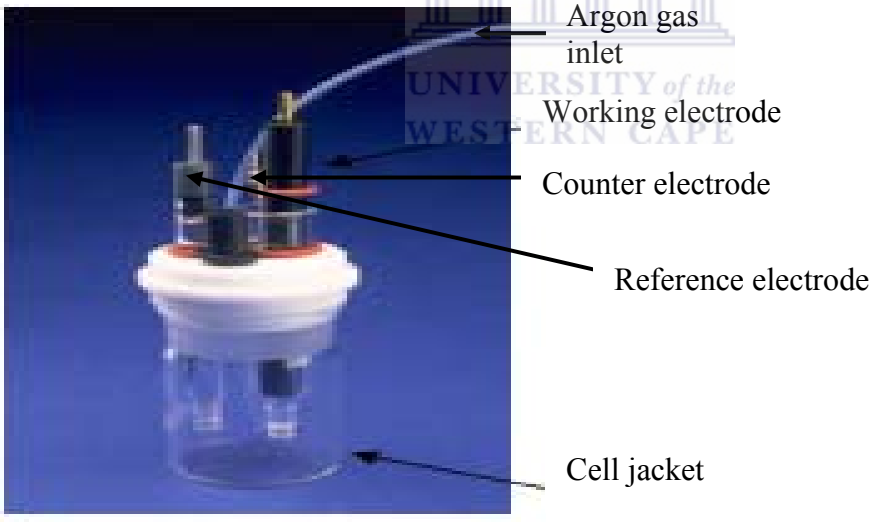

Figure 0.3: A typical electrochemical cell utilized in the project.

Prior to use, the various electrodes were pretreated as follows;

Reference electrode: The Ag/AgCl reference electrode was thoroughly rinsed in ultra pure Millipore Milli Q^{TM} water. It was always stored in 3 M NaCl solution when not in use.

Counter electrode: Firstly, the platinum wire counter electrode was acid treated by placing it in a 2 M HCl or H_2SO_4 solution in order to remove any soluble impurities. The counter electrode was then annealed on a flame until white hot after which it was allowed to cool. Annealing was important to get rid of any trace impurities which would have adsorbed on the electrode.

Working electrode: The working electrode was a platinum disc electrode with a diameter of $1.77x10^{-2}$ cm^2 purchased from Bioanalytical Systems Inc. (BAS). The following steps were followed to ensure strict electrode hygiene.

- To alumina pads Buehler (Illinois, USA) aligned on a glass substrate, alumina powder of 1μM, 0.3 μM and 0.05 μM particle sizes was placed.

- Slurries were made by addition of a sufficient amount of ultra pure Millipore Milli Q^{TM} water to the powder on each pad.

- Using circular motions, the surface of the working electrode was polished on each of the polishing pads from the largest to the smallest alumina particle sizes with rinsing using ultra pure Millipore Milli Q^{TM} water in between the polishing steps.

- The cleaned electrode was then placed in an ultrasonic bath containing ethanol. Ultrasonication was carried out for 10 min.

- A final rinsing of the electrode in Millipore Milli Q^{TM} water was followed by drying the electrode in a stream of argon gas.

The electrochemical experiments were carried out in a BAS C2 Farady cage. To the 10 mL electrochemical cell, 1 mL 1 M HCl was placed. The 0.05 g of PANi/ASA composite was added to the HCl solution to make a paste like solution. This solution was purged with analytical grade argon for 10 min prior to characterization in order to exclude di-

oxygen which could interfere with the observed electrochemistry. An argon blanket was maintained throughout the characterization experiments for the same reasons of excluding the atmospheric influence on the polymer electrochemistry. During characterization, the electrodes were placed in the cell and the cell contents subjected to 20 cycles of potential cycling between -400 mV and +1000 mV during which there was a steady and reproducible voltammogram and a thin film formed on the electrode. Multi-scan rate voltammograms were then recorded by sweeping the potential of the working electrode to and fro between -400 mV and +1000 mV at sweep rates between 5 – 100 mV/s. This potential window was found optimal towards producing well defined redox couples for nearly all the composites. The electrochemical characterization procedure was repeated for all the ASA and NSA doped polymer composites.

Characterization of the polymers using the square wave (SQW) technique was also carried out. This was necessary in order to verify whether the observed redox couples could solely be accrued to the polymer electrochemistry and not due to impurities. For this experiment, the same experimental setup as that used in the CV was employed. Oxidative square wave scan was done by cycling potential of the working electrode from an initial potential E_i = -400 to a final potential E_λ = +1000 mV. Reductive square wave scan was obtained on reversing the potential. Although many square wave parameters were tried out, those that gave best results were as far as the composite characterization were concerned: step height (4 mV), square wave amplitude (25 mV), frequency (5 Hz), samples per point (16), sensitivity 1 mA/V.

3.15 Procedure for the preparation of the SPAH composites through the electrosynthetic route

3.15.1 Electropolymerisation procedure

The polymerisation solution consisted of a 5 mL acid solution (1 M HCl) containing 100 mM aniline (or *o*-methoxyaniline, or 2,5- dimethoxyaniline) and 50 mM ASA, which was degassed for 15 min with analytical grade argon Afrox,(Cape Town, South Africa) and

an argon headspace maintained thereafter. The HCl solution was used as supporting electrolyte. The electrodes were pretreated as previously described. Films of PANi, POMA and PDMA were formed on the Pt disc working electrode by performing a 10-cycle cyclic voltammetry first at 5, 10, 20, 50, 100 mV/s. Finally a scan rate of 10 mV/s was chosen for SPAH deposition since at this scan rate the SPAH possessed reversible characteristics. An optimal potential window of between -200 to +1000 mV was used. The polymer-modified Pt electrode was removed from the polymerisation solution and rinsed thoroughly using Millipore Milli Q^{TM} water. The electrode was then placed in a cell containing a fresh 10 mL of argon degassed 1 M HCl for further characterization. For the electrodeposition of NSA - doped composites, the above experiment was repeated with the NSA dopant in place of ASA.

3.16 Multi-scan rate studies on the electrochemical behaviour of electrodeposited SPAH

3.16.1 Characterisation in HCl

The characterization of the ASA and NSA doped polyanilines was carried out by performing multi-scan rate cyclic voltammetry. The polymer modified electrode was placed in degassed 1 M HCl solution. The potential of the working electrode was then scanned to and fro between -200 to + 1000 mV potential limits and multi-scan rate voltammograms recorded at scan rates of 5 → 100 mV/s. This procedure was repeated for all the other electrodeposited ASA and NSA-doped composites.

3.16.2 Characterisation of the polymer composites in phosphate buffer

The characterisation of the polymer-modified electrodes in phosphate buffer was similar to that done in HCl. However, voltammograms were recorded at -1000 - +1000 potential limits. Measurements were carried out in phosphate buffer pH 7.02 and/or 7.4. Square wave measurements were carried out as previously described. It was deemed necessary to perform composite characterisation in phosphate buffer in order to verify their electroactivity and therefore validate their usefulness for biosensor construction.

3.17 Application of the polymers in the construction of Biosensors

3.17.1 Immobilization procedures for the chemically synthesized composites

Test enzymes employed for the biosensor construction in this project were; horseradish peroxidase, HRP (EC.1.11.1.7) and cytochrome P450 3A4 (EC. 1.14.14.1) human recombinant isoenzyme. Biosensors utilizing chemically synthesized polymers were prepared by the cross-linking method as follows:

The platinum disc electrode was pretreated as previously described (section 3.15). 0.2 mg of horseradish peroxidase (HRP E.C 1.11.1.7) type II, 200 units/ mg salt-free powder) was dissolved in 100 µL phosphate buffer (pH, 7.02 at 25 ºC). Separately, 3 mg of dry polymer composite was thoroughly mixed with 0.2 mg bovine serum albumin (BSA). The composite/BSA mixture was then added to the HRP solution with thorough stirring. Finally, 3 µL of 2.5 % (v/v) glutaraldehyde was quickly stirred into the composite/HRP/BSA mixture. To avoid hardening, a 3 µL aliquot of the mixture was quickly dropped on to the platinum micro-electrode using a discovery autoclave micro-pipette. The electrode was then covered with a clean dry 1000 mL beaker and allowed to dry for 2 h. The events surrounding the preparation of enzyme electrodes are summarized in Figure 3.6. Fabrication of the ASA- doped POMA and PDMA enzyme electrodes involved repeating the above procedure but using POMA or PDMA composites in place of the PANi. Similarly, enzyme electrodes based on NSA doped polyanilines were prepared in the same manner.

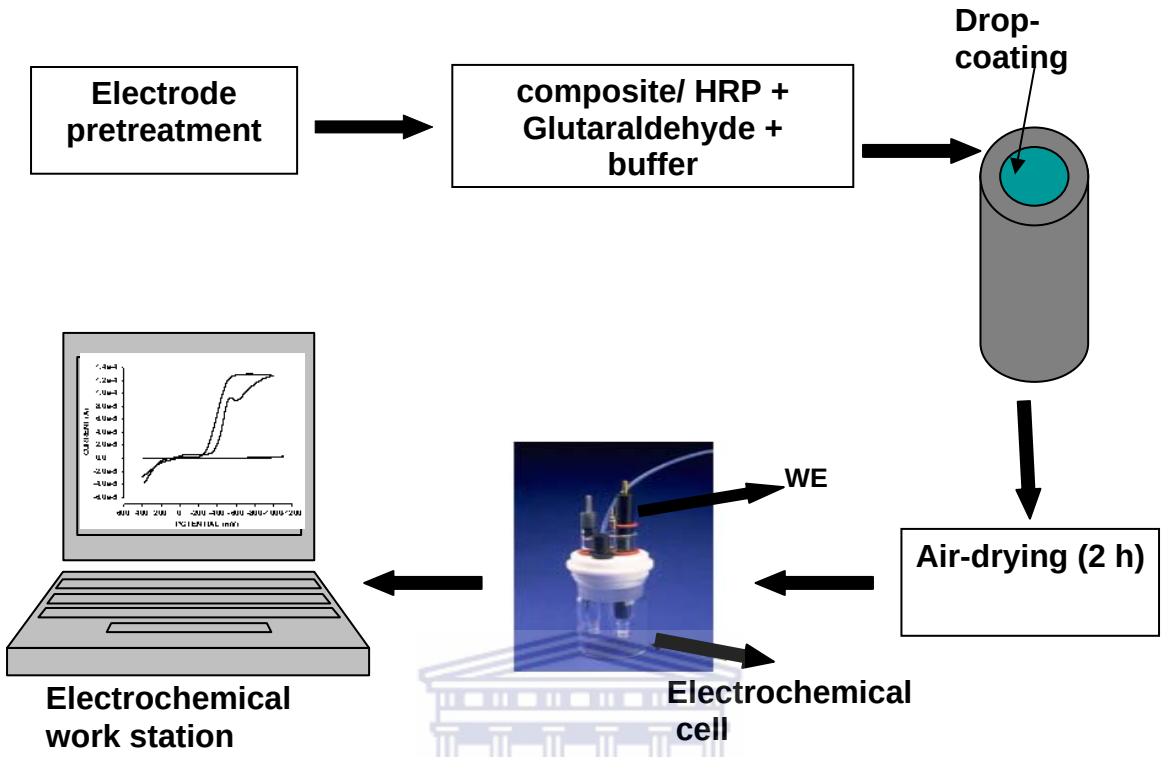

Figure 0.4: A scheme of the steps followed during the preparation of enzyme electrodes and ultimate biosensor application.

3.18 Immobilization procedures for the electrochemically synthesized composites

All experiments concerning use of enzymes were carried out in an air-conditioned atmosphere. This was necessary because enzymes are easily denatured in harsh conditions e.g. high temperatures, pH outside their physiological pH limits. The electrochemical procedure for enzyme entrapment was as follows:

The 10-voltammetric cycle polymer/dopant composite electrodeposited on the platinum electrode was thoroughly rinsed in phosphate buffer. This was followed by a cathodic polarization of the polymer electrode at -450 mV for 10 min in 10 mL degassed phosphate buffer (pH 7.02) under quiescent conditions. Cathodic polarization was achieved by setting the BAS system on the time-base mode. The enzyme immobilization was achieved by the oxidation of the polymer electrode in the presence of 50 µL HRP (4

mg mL^{-1}) for 20 min at a potential of +650 mV. During the oxidation, the bio-molecule was electrostatically doped onto the polymer film forming a giant complex. The enzyme electrode was lifted off the buffer solution and rinsed carefully with Millipore Milli Q^{TM} water to remove any loosely bound enzyme. The enzyme electrode was stored in buffer solution at -4 º C when not in use.

For the CYP 3A4 based biosensors, the enzyme stock solution was prepared to a final concentration of 14.4 μM L^{-1}. Phosphate buffer saline (0.1 M, pH 7.4, 100 mM KCl) in the presence of small amounts of glycerol was used to prepare the stock solution. The glycerol was used to maintain the polarity of the enzyme's active center for proper functioning. The immobilization procedure was similar to that used for HRP. The polymer electrode was first cathodically polarized at -450 mV in the presence of phosphate buffer saline (PBS). Anodic polarization was carried out using 50 μL CYP 3A4 (14.4 μM L^{-1}) by applying a positive potential (+ 650 mV). For all biosensor measurement purposes, the enzyme solutions were freshly prepared. This procedure was used for the preparation of all electrosynthetic based HRP and CYP enzyme/polymer modified electrodes.

3.19 Electrochemical measurements for biosensors based on direct analyte detection

3.19.1 Preparation of substrates

Hydrogen peroxide and erythromycin were directly determined using the biosensors. Hydrogen peroxide (30%) was constituted to give a stock solution of 0.01 M. 10 uL aliquots were drawn from the stock solution using a micropipette during each addition. The stock solution was prepared a fresh during each new biosensor construction. This was necessary because hydrogen decomposes easily in the atmosphere. The range of peroxide concentration studied was between 0-1.8 mM.

The erythromycin was constituted to give a final concentration of 500 μM in an ethanol / PBS mixture. Erythromycin readily dissolves in ethanol but is insoluble in water. The substrate was first dissolved in ca.1 mL absolute ethanol before topping up with phosphate buffer. 0.5 μL aliquots of erythromycin were added during biosensor measurements and the resultant steady state currents were recorded as above. The range of erythromycin studied was in the range 0.25 – 3.75 μM.

3.19.2 Actual Biosensor measurements

A similar procedure applied for biosensors fabricated through both the chemical and the electrochemical electrode modifying methods. Biosensor measurements were taken on a Bioanalytical System (BAS) CV-50W or 100W on the CV, DPV or the SQW modes. 1 mL phosphate buffer pH 7.02 (for HRP) or pH 7.4 (for CYP 3A4) was placed in the electrochemical cell. For the case of the CYP biosensors, 100 mM KCl was added to the phosphate buffer. The cell was purged with analytical grade argon for 10 min. Previously prepared enzyme electrodes were placed in the buffer solution in the presence of a Ag/AgCl reference and a platinum wire counter electrode. Cyclic, square wave, DPV voltammograms were recorded in the absence of substrate at suitable optimized parameters. 10 μL aliquots of 0.01 M H_2O_2 (for HRP) or 0.5 μL aliquots of 500 μM erythromycin (for CYP) were added sequentially. After each addition, the buffer solution was magnetically stirred and degassed sequentially each step taking two minutes. Steady state currents were recorded after each addition. For CYP 3A4, however, the buffer was not degassed after analyte addition. It was deemed fit not to degas the CYP enzyme system after analyte addition because the monooxygenase enzyme requires oxygen for its catalytic performance. Aliquots of substrates were added cumulatively and the resultant steady state (I_{ss}) currents as depicted by the recorded voltammetric waves were plotted on sigma plot software. Resultant data was used for the estimation of the various biosensor parameters.

3.19.3 Biosensors based on inhibition

A similar electrochemical cell as one described was used. These biosensors types were based on the ability of the HRP enzyme to be inhibited. Phosphate buffer (0.05 M, pH 7.02) was used. Reactions were conducted at room temperature and pressure. Cyclic and differential pulse voltammetric modes were used to study the biosensor reactivities. The initial enzyme activity was determined by adding small aliquots of 0.01 M H_2O_2 stock solution to the cell. After each addition the solution was magnetically stirred for two minutes, degassed (analytical grade, argon) for another two min and the resultant steady currents recorded. The maximum steady state current (I_{ss}) achieved correlated to the highest enzyme activity as per the experimental set-up.

To obtain the inhibition plot, the percentage inhibition method was followed. A freshly made biosensor was placed in fresh phosphate buffer. Biosensor responses were recorded in the absence and presence H_2O_2 (the aliquot of peroxide added was that giving the maximum steady state current). Small aliquots of diazinon (stock solution; 8 μM in acetone) were then added to the reaction cell cumulatively. The range of diazinon studied was between 0.88 - 4.0 μM. After each diazinon addition, the solution was stirred for 2 min., degassed for 5 min. Quiescent conditions were achieved by allowing the solution to stand for another 5 min. Steady state currents were recorded after each diazinon addition.

The decrease in the H_2O_2 reduction currents (signals) were used to construct the calibration curves for diazinon after correction for background current. The % inhibition was then calculated using the equation;

$$I\,(\%) = \frac{(I_{ss} - I_p) \times 100}{I_{ss}} \qquad (3.9)$$

where: I_{ss} was the maximum current obtained in the absence of inhibitor, and I_p is the current obtained in the presence of inhibitor. All the observed currents were corrected for the background current.

Chapter 4

Chemical synthesis and characterization of sulphonated polyanilines (SPAH)

4 Introduction

This chapter presents the synthesis and characterization results of the chemically synthesized anthracene sulphonic acid (ASA) and naphthalene sulphonic acid (NSA) doped polyanilines. Firstly, the characterization of the ASA dopant mainly using FTIR spectroscopy is discussed. An investigation as to the most appropriate monomer: dopant ratio that would produce both conductive and nanostructured composites then followed. This investigation was mainly based on PANi/NSA and UV-Vis spectroscopy was used. The relationship between doping and initial heating (temperature) of the dopant/monomer mixtures was also investigated investigated. Based on the findings of the above investigations, composites were prepared using the selected monomer: dopant ratio. The composites were then characterized using UV-Vis and FTIR techniques as spectroscopical signatures for composite conductivity. At the same time the FTIR technique was used to verify successful doping. An investigation of the solubility of the composites in common laboratory solvents based on the fact that surfactant doped composites should show improved organic solubility due to the presence of both polar and non-polar moieties within the polymer matrix is fathomed. The electrochemical behaviour of these composites in HCl and phosphate buffer (PB) studied through multi-scan rate experiments is then presented. Electrochemical studies were carried out to investigate whether the polymers were electroactive which is a prerequisite towards their application as mediators in the biosensors. Based on the multi-scan rate voltammograms, important composite kinetic parameters such as diffusion coefficients (D_e) and the heterogeneous rate constants (k^0) were estimated. The cyclic voltammetric data was also used to estimate the conductance of each of the composites. Improved conductivity with

respect to literature reported values of undoped polyanilines would indicate successful doping.

In this project, anthracene sulphonic acid (ASA) and naphthalene sulphonic acid (NSA) modulated composites for polyaniline and functionalized polyanilines were prepared (collectively referred as SPAH). They have been abbreviated as; PANi/ASA, POMA/ASA, PDMA/ASA, PANi/NSA, POMA/NSA and PDMA/NSA.

4.1 ASA characterisation results (FTIR)

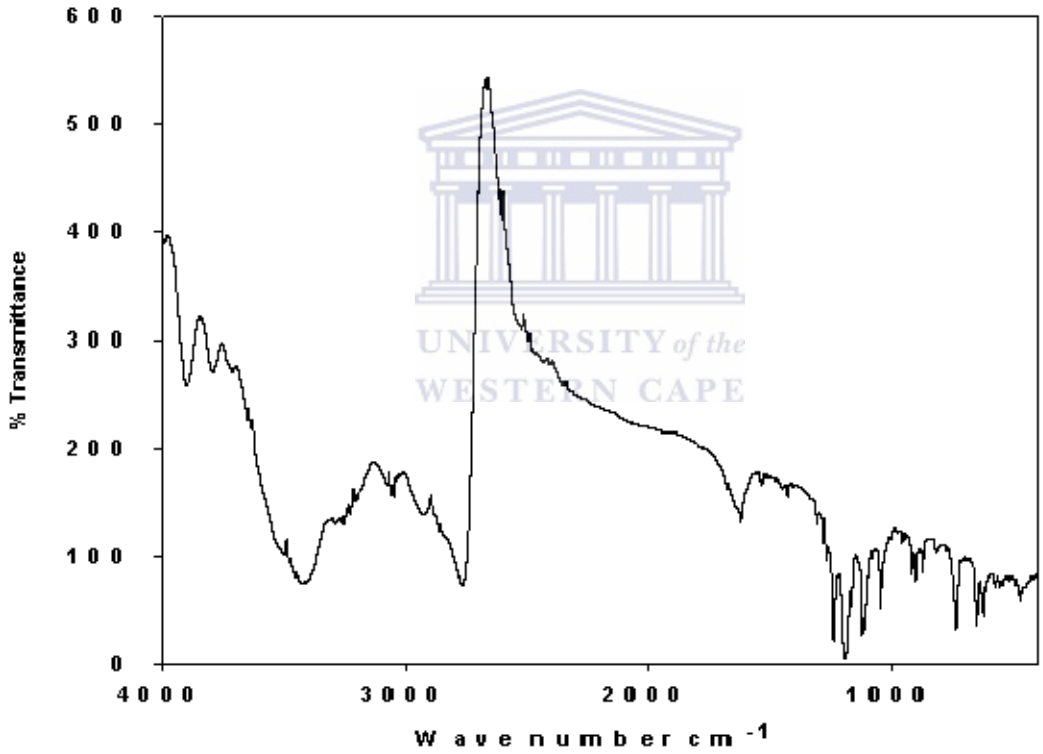

Figure 4.1: FTIR of anthracene sulfonic acid (ASA)

Figure 4.1 above presents FTIR spectra of the anthracene sulphonic acid dopant. Band assignment for the various absorption bands in the ASA spectrum were as follows; 3200-3400 cm^{-1} O-H *str* of the $–SO_3H$ functional group; 2800-3000 C-H *str* aromatic conjugation;1400-1600 C⎓C *str* of the aromatic rings; 1020, 1190, 620 bands associated with the SO_3H group; 730, 820 out of plane C-H def. of the aromatic rings;

(Kemp, 1987: 43-56). The presence of the above peaks especially at those related to the SO_3H group is indicative of successful sulphonation.

4.1.1 Characterization of the ASA dopant by cyclic voltammetry

Ideally one should expect the electrochemical behaviour of both the NSA and ASA dopants to be similar given that they have a similar aromatic trend and that they both contain a sulphonic group. The only difference between NSA and ASA is an extra benzene ring in the latter. Figure 4.2 (A and B) below shows that in the ASA CV, there is a redox couple at ca. 370 mV which is also reflected in the accompanying square wave voltammogram.

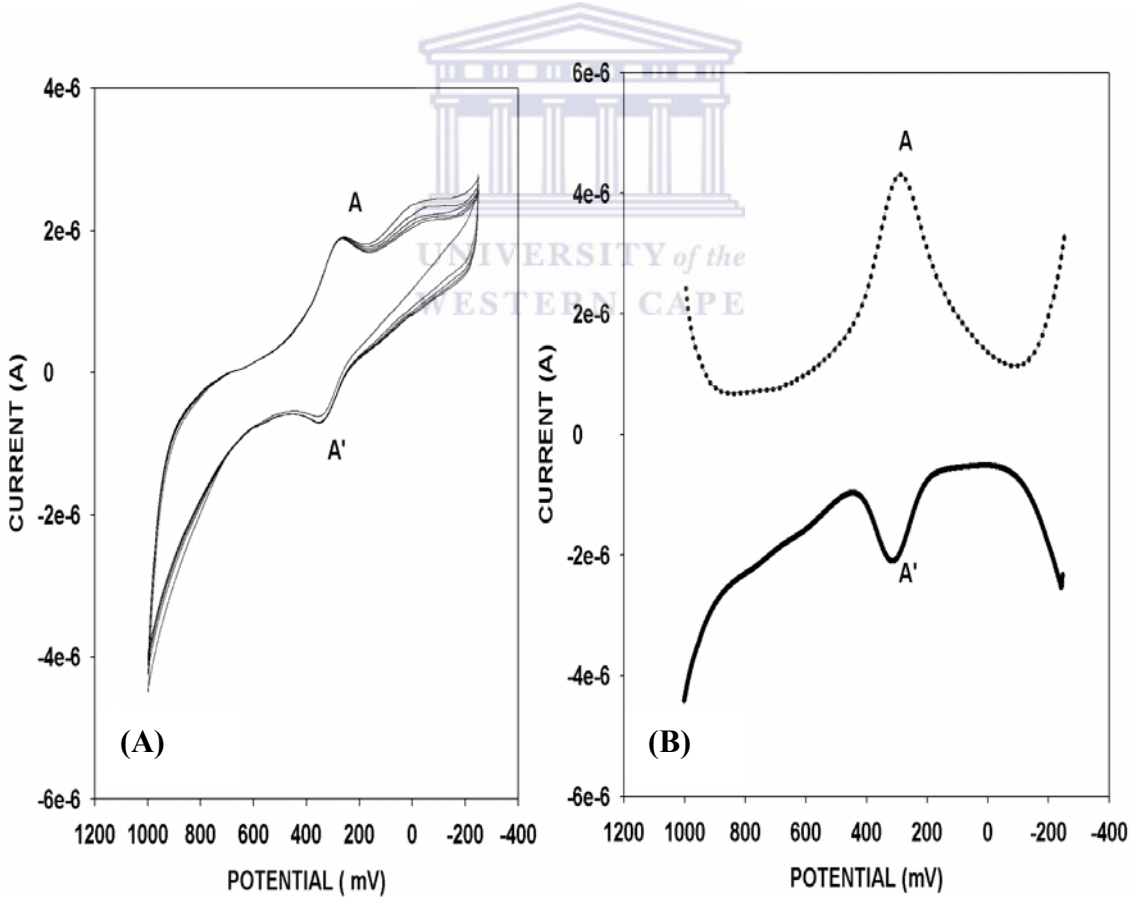

Figure 4.2: Cyclic and square wave voltammogram for anthracene sulphonic acid (ASA)

The figure also shows that the ASA dopant does not electropolymerize in the potential window used. For comparison purposes, commercially available naphthalene sulphonic acid (NSA) was also subjected to the same treatment. Figure 4.3 (A and B) shows that again only one redox couple appears in the CV and square wave voltammograms of NSA. The couple was observed at ca. 360 mV.

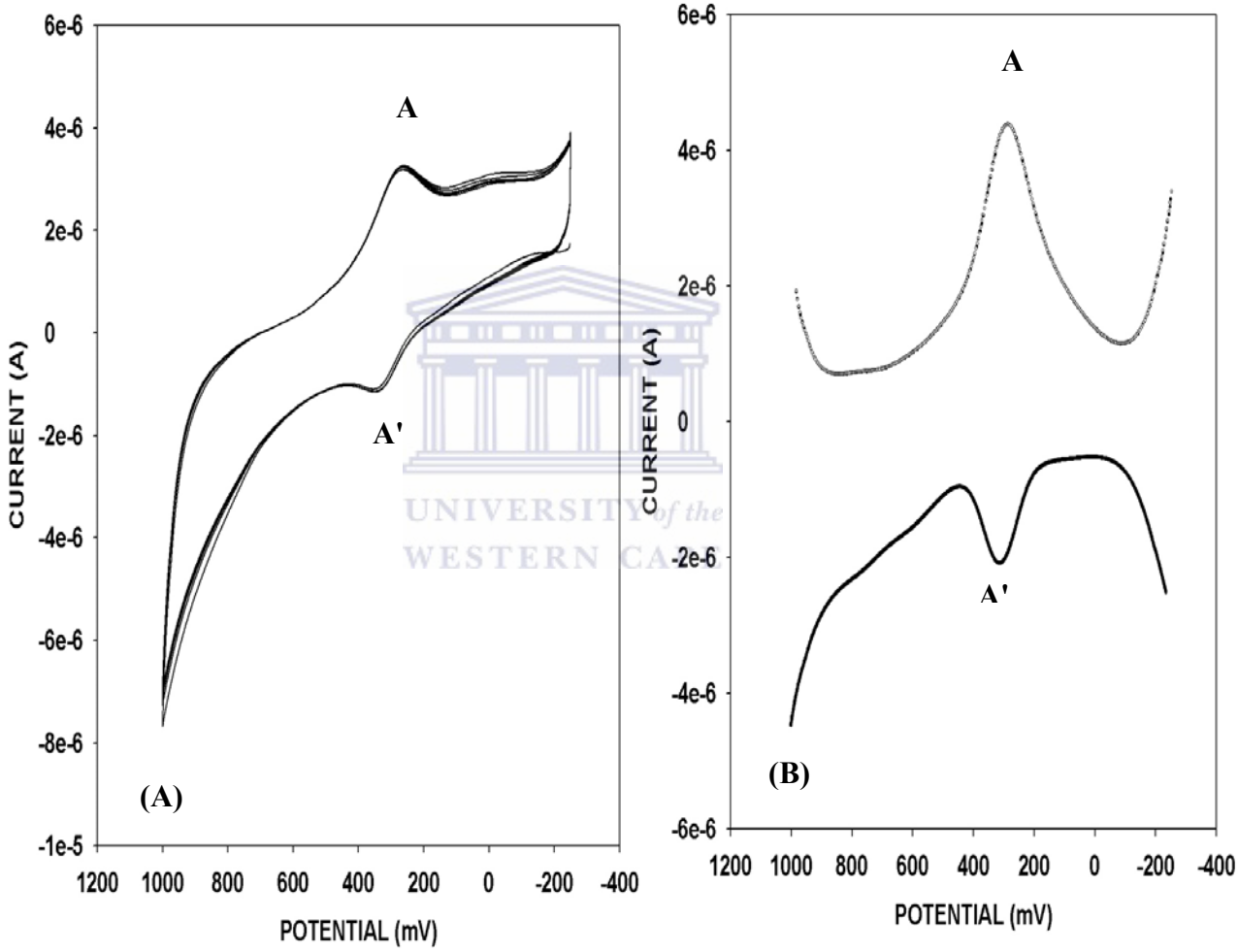

Figure 4.3: Cyclic and square wave voltammogram for naphthalene sulphonic acid (NSA).

It was also observed that like in the case of ASA, the NSA dopant did not electropolymerize considerably even after performing several cycles. This therefore could be taken as proof that indeed the ASA dopant had very similar characteristics to the naphthalene sulphonic dopant which was commercially available.

4.2 Solubility of SPAH

A major handicap towards large scale PANi applicability is related to its insolubility and intractability. One of the main purposes of the incorporation of sulphonated heteronuclear aromatic hydrocarbons into the PANi backbone is to improve its solubility. Another route has been to produce its derivatives. In view of this, the solubility of the SPAH was tested out for the various solvents. It was found out that both the NSA and ASA-based SPAH showed considerable improved solubility especially in polar organic solvents such as DMF and DMSO. However, it was found out that SPAH based on PANi derivatives was very soluble in these polar solvents and showed improved solubilities in tetrahydrofuran (THF) and chloroform where PANi non-sulphonated PANi is totally insoluble. The results are summarized in Table 4.1 below. Similar reports were obtained for substituted PANi (Nateghi et al., 2005: 11476-11483; Komsiyska et al., 2005: 88-95; Norris et al., 2000: 3237-3243).

Table 4.1: Solubility of SPAH in different solvents

Polymer/ Solvent	PANi/ASA	PANi/NSA	POMA/ASA	POMA/NSA	PDMA/ASA	PDMA/ASA
methanol	**ss**	**ss**	**ss**	**ss**	**ss**	**ss**
DMSO	**ss**	**ss**	**vs**	**vs**	**vs**	**vs**
DMF	**ss**	**ss**	**vs**	**vs**	**vs**	**vs**
Diethylether	**is**	**is**	**ss**	**ss**	**ss**	**ss**
chloroform	**is**	**is**	**ss**	**ss**	**ss**	**ss**
Tetrahydrofuran	**is**	**is**	**is**	**ss**	**ss**	**ss**

Key: is, insoluble; ss, slightly soluble; vs; very soluble.

4.3 Characterization of polymer nanocomposites using UV-Vis spectroscopy

The ultimate aim of this thesis was to apply the prepared polymer composites in the fabrication of biosensors. In biosensors, conducting polymer composites are expected to provide a suitable micro-environment for bio-molecule immobilization as well as to electromediate between the enzyme's redox center and the electrode. For the composites to occupy the above posts, it is demanded that they be both conductive and electroactive. In this respect, spectroscopical techniques come in handy.

The rationale behind the use of the UV-Vis spectroscopical technique as a spectroscopical signature for conductivity (MacDiarmid, 2001: 269-279) relies on the fact doped polymers are structurally modulated and their electronic spectra display additional absorption bands associated with the existence of polarons/bipolarons. The latter bands are delocalization charge defects in the polymer whose presence converts the polymer into an intrinsic conductor. It is now well known that the electronic spectra of undoped polyanilines (prestine) are basically made up of two absorption bands. A band at ca. 320 nm due to the π-π* transition of the benzoid rings and another at ca. 600 nm assigned to the π-π* of the quinonoid structures (Hino et al., 2006: 1327-1332). In addition to these bands, doped polyanilines are characterized by additional bands at ca. 420 and 800 nm associated with the polaron / bipolaron states in the polymer. The latter states are new electronic energy levels created within the polymer sub-gap energies during the polymer /dopants interactions.We aimed at exploring some of the factors that could affect the characteristics of the SPAH composites including the temperature and the monomer: dopant ratio.

4.3.1 Effect of Temperature on the composite conducting state

It was deemed important to evaluate the effect of temperature on polymer conductivity. In the study, PANi/NSA composites were prepared by exposing the monomer/dopant mixtures to different temperatures; 0-5 ^{o}C, room temperature, 50-60 ^{o}C for 20 min prior to polymerization. The monomer dopant ratio was first maintained at 0.3:1. Resultant

spectra were scrutinized for polaron bands as markers for conductivity. Figure 4.4 represents the UV-Vis spectra of NSA doped polyaniline (PANi/ASA) prepared at three different monomer /dopant ratios namely: 0.3:1 (i), 0.5:1 (ii), 1:1 (iii). During the preparation the various monomer/dopant mixtures were subjected to the above stated temperatures ranges within the first 20 min prior to the addition of the ammonium peroxydisulfate polymerization initiator.

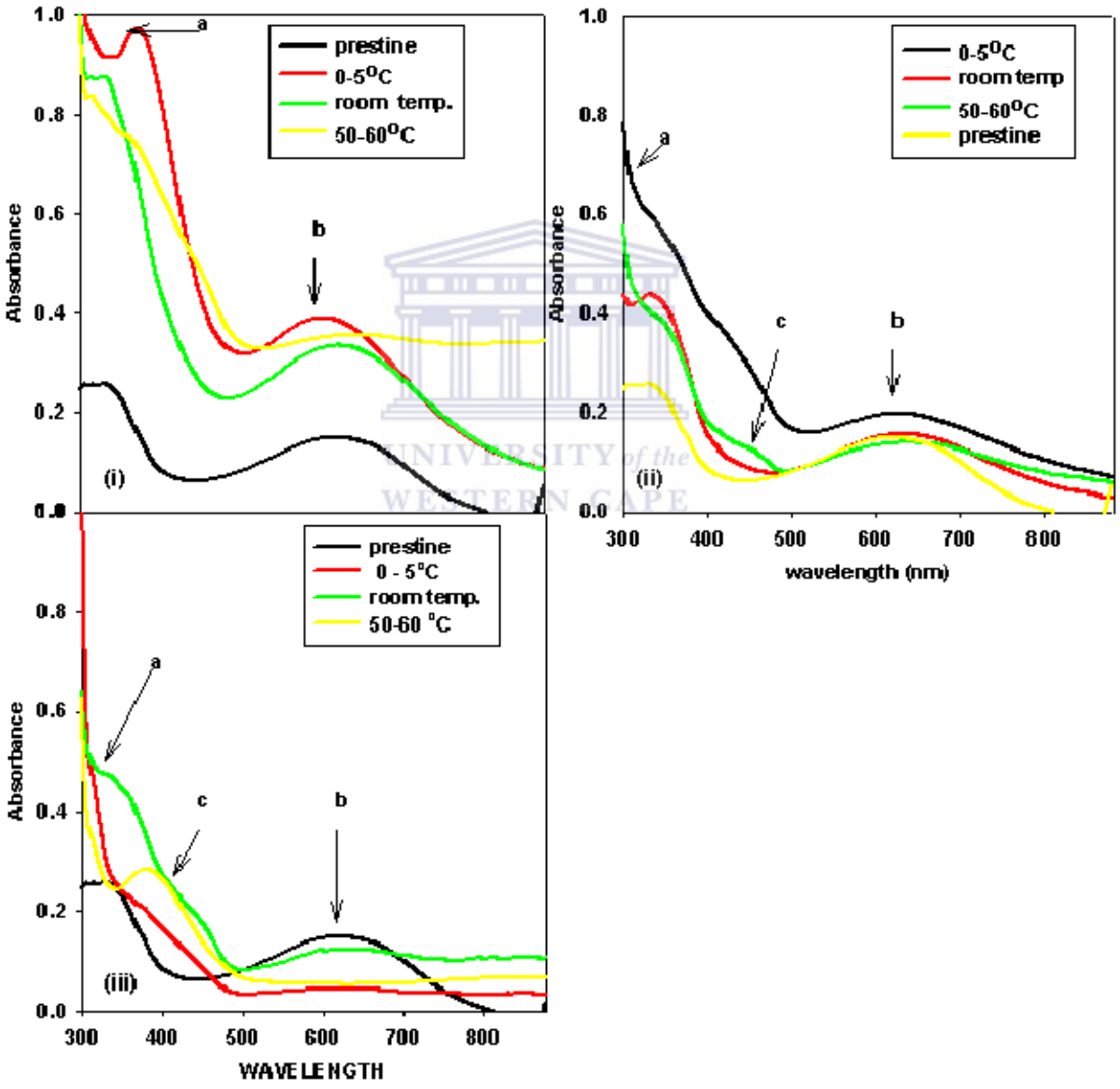

Figure 4.4: Effect of temperature on the UV-Vis behaviour of the polymer composites prepared at different monomer to dopant ratios and temperatures; (i) (0-5 ºC), (ii) room temperature; (iii) 50-60 ºC

The results obtained are summarized in Table 4.2 below. In accordance to this table, at 0-5 ^{o}C and room temperature the spectra of the composites prepared at 0.3:1 ratio (graph i) consisted of the two characteristic bands similar to those of undoped (prestine) PANi – band (a) between 300-350 nm is the π-π* due to the benzoid ring. Band (b) at ca. 600 nm is due to the π-π* due to the quinoid ring. The absence of polaron bands (c) at these temperatures indicated the polymers were non conductive. However for the 0.3:1 composite that was subject to a 20 min. interlude of heating prior to polymerization, besides the traditional π-π* band due to benzoid structures, the band at 600 nm translates into a free carrier tail characteristic of completely doped PANi .

Table 4.2: Summary of the absorption bands observed when the polymer composites were prepared at different monomer ratios and temperature

Temp / **Mon/Dop. ratio**	**0-5 ^{o}C**	**Room Temp.**	**50 – 60 ^{o}C**
0.3:1	**300-350(π-π*,benzonoid)** **600 nm π-π*, quinoid**	**320 nm(π-π*,benzoid)** **600 nm π-π*, quinoid**	**< 300 nm(π-π*,benzoid)** **600 nm absent** **Free carrier tail**
0.5:1	**“**	**300-320 nm(π-π*, benz.)** **600 nm (π-π*, quinod)**	**300-350 nm(π-π*,benzoid)** **420 nm (polaron band)** **600 nm (diminished)**
1:1	**Ca. 300 nm (π-π*, benz.)** **Free carrier tail**	**320 nm(π-π*, benz.)** **600 nm-diminished** **Free carrier tail**	**300 nm (π-π*, benzoid)** **600 nm absent** **400-420 nm –polaron** **Free carrier tail**

This free-carrier tail has been observed in other polyaniline studies (Kim et al: 2001: 297-304; Palys and Celuch, 2006: 4115-4124) and is assigned to the delocalization of electrons in the polaron band. The authors explain that this electron delocalization is promoted by a ‘straightening-out’ of the polymer chain as its coil structure becomes expanded with a reduction in the π defects caused by the ring twisting (Kim et al: 2001: 297-304).

On raising the doping level to 0.5:1 and pretreating the monomer/dopant mixtures to various temperatures (Table 4.2), again no significant signs of conductivity were seen at 0-5 ^{o}C and at room temperature (graph ii). However, the presence of an additional band at 420 nm (polaron band, (c)) when the composites at 0.5:1 were preheated indicated the composites were conductive. An interesting feature however is observed for the PANi/NSA composites prepared at a 1:1 monomer/dopant ratio at all temperatures. Polaron bands were observed in all the cases (Table 2, Fig. 4.4, (iii)) except in dedoped PANi. Even so, a careful observation of the resultant spectra (Fig. 4.4 (iii)) still shows a small hub for the quinonoid π-π* structures in the 0.3:1 and 0.5:1 prepared PANi/NSA composites. This can be taken as indication to show the importance of initial heat treatment of the monomer/dopant mixtures. From the above observations, it can be concluded that preheating of the monomer/dopant mixtures prior to polymerization was important in order to obtain conductive composites. It is proposed that higher temperatures increased the kinetic energies of the reactants (monomer/dopant) leading to a higher degree of monomer/dopant interactions with improved doping (conductivity).

4.3.2 Effect of the doping state on the conducting state of the prepared composites

Figure 4.5 below exhibits the spectra of PANi/NSA composites prepared at different monomer dopant ratios but at the same temperature (room temperature). According to this figure complete doping was only achieved for composites prepared at the 1:1 monomer to dopant ratio (green curve). Although a slight indication of polaron bands is evident from the 0.5:1 ratio, the existence of the band at 600 nm is indicative of incomplete doping. It means therefore complete doping could be achieved at any temperature so long as the monomer to dopant ratio was maintained at 1:1 or higher. Increase in conductivity (as depicted by formation of polaron bands) with increasing doping level can be explained similarly to the temperature effect above. At higher monomer/dopant levels, the increased concentration of reactants accelerates the interaction between the various molecules with the consequential increased conductivity.

Elsewhere, increase in conductivity with increase in doping level has been reported (Hopkins et al., 2004: 474-480; Wei et al., 2002: 917-921).

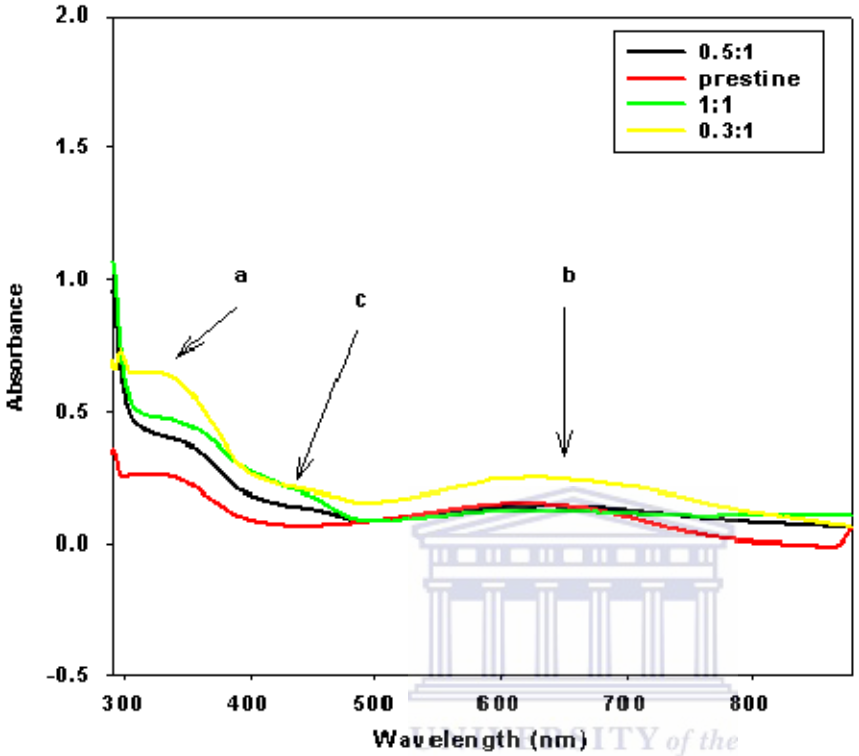

Figure 4.5: Doping level effect on the conductivity characteristics of the resultant composites. Data based on PANi/NSA composite prepared at room temperature

Following the above observations therefore, the 0.5:1 and the 1:1 ratio with initial heat pretreatment were thought to be ideal for production of conductive polymer composites. However, as will be explained later based on the SEM analysis, the 0.5:1 ratio was chosen for preparation of all other polymer composites.

4.3.3 Characteristics of ASA /NSA- doped polyanilines prepared at a 0.5:1 monomer to dopant ratio.

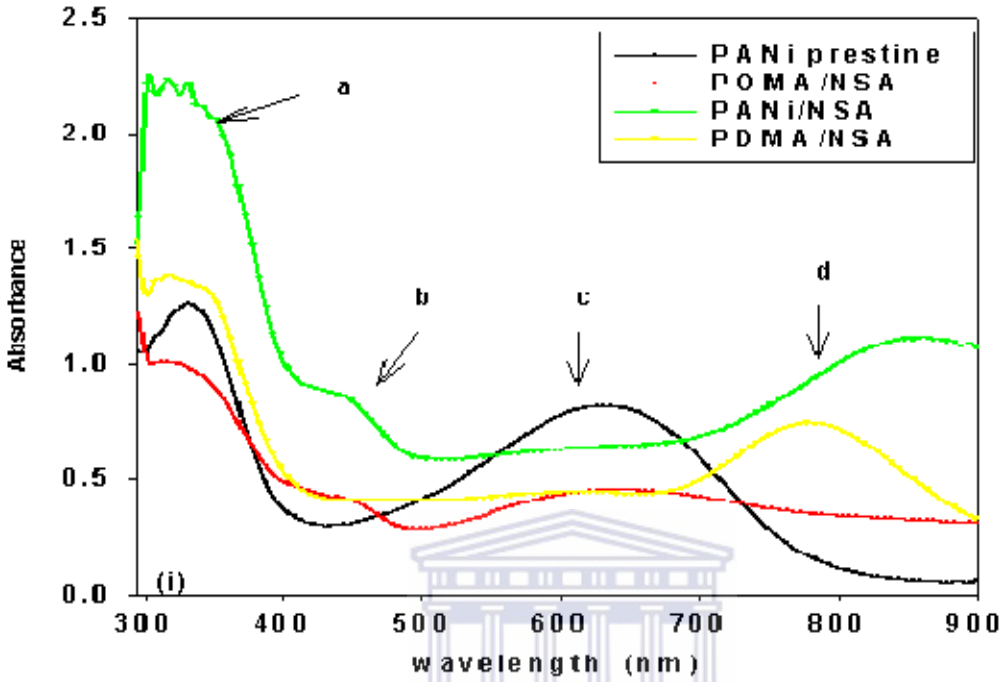

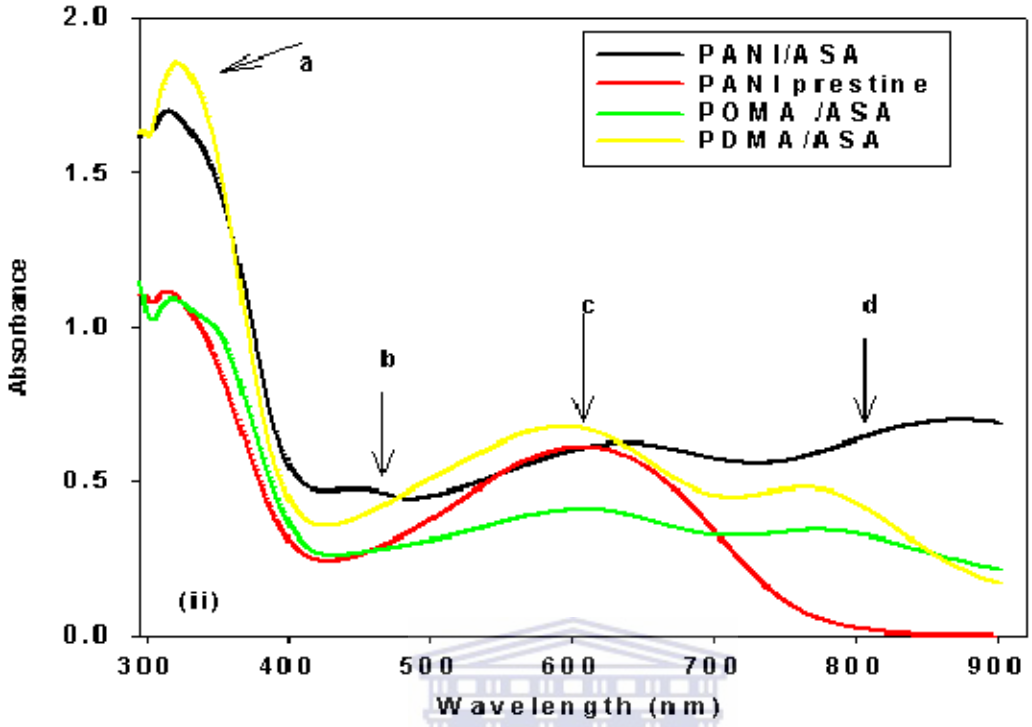

Figure 4.6: UV-Vis results for the NSA (i) and ASA (ii) doped polyanilines prepared at 0.5:1 monomer to dopant ratios.

A comparison between the UV-Vis spectra of the NSA in Figure 4.6 (i) and ASA (ii) composites shows basically the same trend. In both case dedoped PANi gave rise to the two characteristic bands: benzene ring π-π* (ca. 320 nm) and quinine ring π-π* (ca. 600 nm). Beside these bands, for both NSA and ASA doped PANi, polaron bands were observed at 420 nm and at 850 nm. The complete semblance of the two spectra suggests that polaron formation is not dependent on dopant type. While a polaron band at 420 nm was observed for POMA/NSA that of POMA/ASA was negligible. However, the reverse was true for the second polaron band which was observed at ca. 800 nm for POMA/ASA but 'straightened out' in the case of POMA/NSA to form a free carrier tail. This could suggest that the conformations of the two composites could be different. For the PDMA-based composites, only one polaron band was observed at ca. 780 nm for both dopants.

4.4 SEM Analysis

The anthracene and naphthalene sulfonic acids used in these work are surfactant dopants. The morphological modulation of the composites due to the use of these surfactants was studied using scanning electron microscopy (SEM). Composites subjected to SEM analysis were prepared using 0.5: 1 and 1:1 monomer/dopant ratios. Figure 4.7 and 4.8 represent the SEM micrographs obtained for the various NSA and ASA doped polymers.

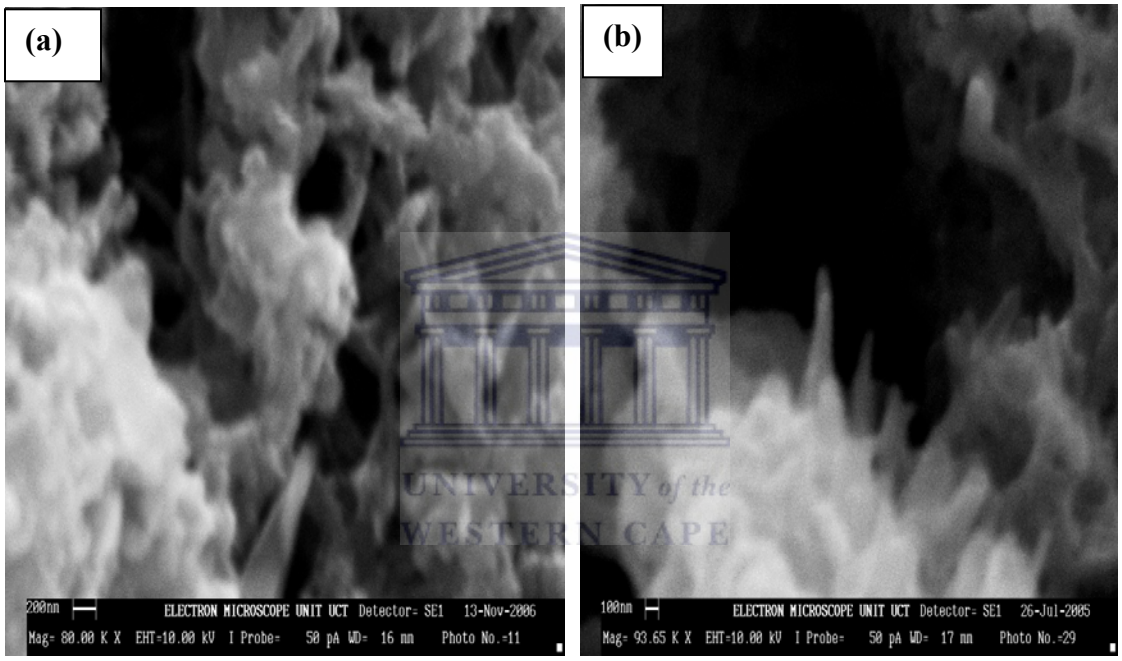

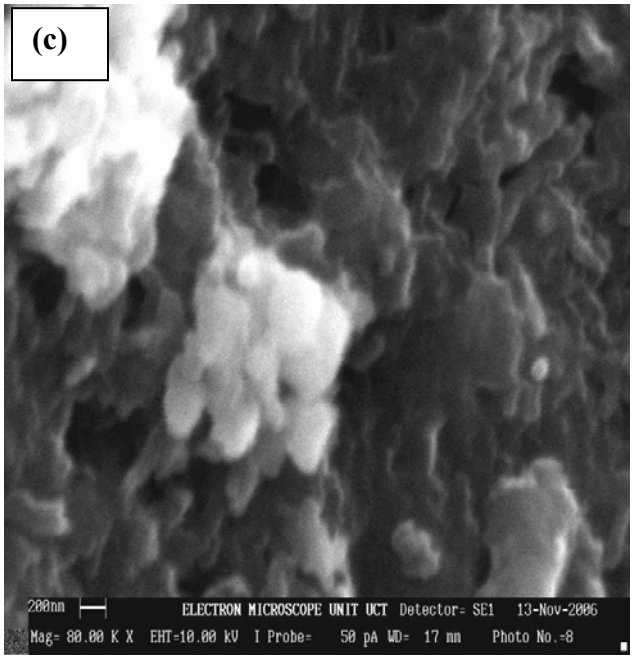

Figure 4.7: SEM micrographs for ASA doped polyaniline (a), poly-o-methoxyaniline (b) and poly 2,5-dimethoxyaniline (PDMA) prepared at 0.5:1 monomer/dopant ratio.

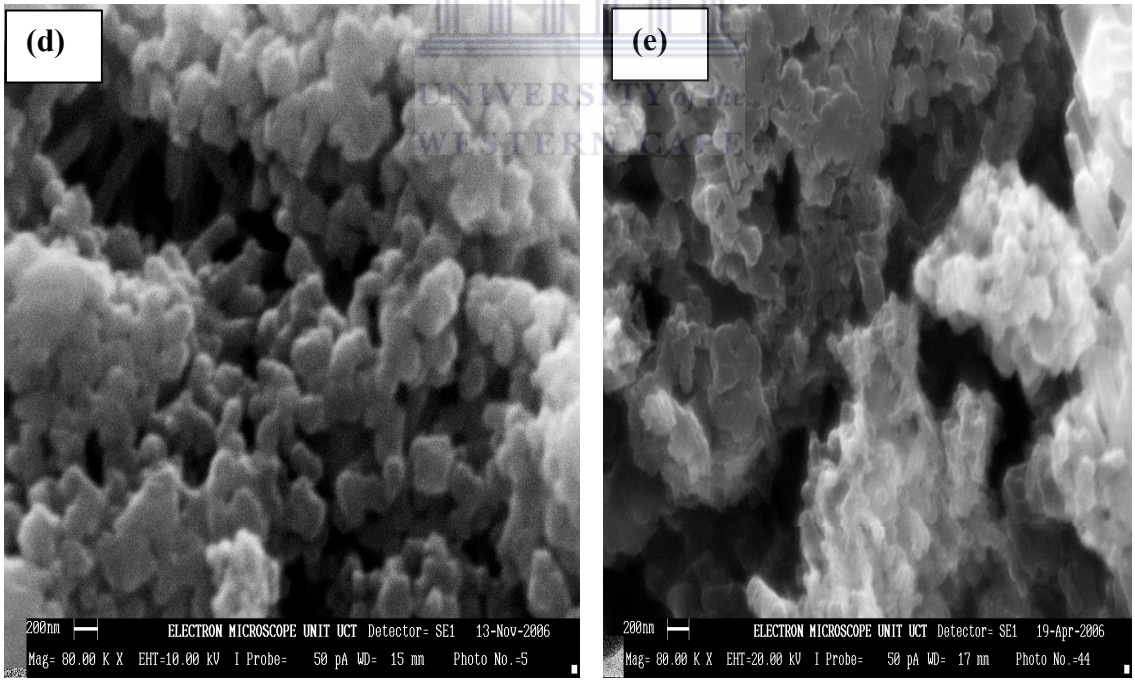

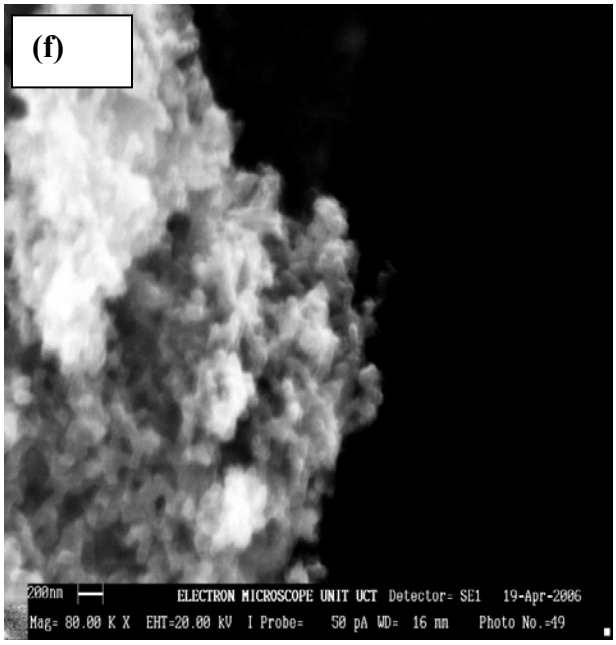

Figure 4.8: SEM micrographs for NSA doped polyaniline (d), POMA (e) and PDMA (f) showing the resultant microstructure , (0.5:1 monomer/dopant ratio).

Although it was quite difficult to coin a particular morphology to each of the synthesized composites, nevertheless general statements can be made. Based on the results in figure 4.7, it appeared the ASA dopant tended to modulate the various polymers into nanofibrils. The diameters of the fibrils were < 200 nm for the ASA doped PANi and POMA composites. For the PDMA/ASA, fibrillar morphology is intermingled with high degree of agglomerations. Such agglomerations are also evident for the PANi and POMA/ASA composites and as Huang and Kaner (2006: 3915-3917) points out is a characteristic of composites prepared through convectional methods. According to the two authors, the inability to suppress polymer overgrowth in the convectional methods leads to appearance of irregularly-shaped agglomerates. On the other hand, particle agglomeration can be attributed to existence of intermolecular interactions (e.g. hydrogen bonding) (Raposo and Oliviera, 2002: 6866-6874). This was possible in our case because all the composites were hygroscopic. The fibrous morphology has been reported for several polyaniline based composites (Xinyu et al., 2004: 2360-2361; Xing et al., 2006: 2303-2313).

The NSA doped polyanilines on other hand tended to form fibrillar/rod like morphology at the 0.5:1 monomer to dopant ratio (Fig. 4.8). For PANi/ NSA a small density of well defined rodular fibrils with diameter sizes in the range 100-200 nm were seen. In POMA/NSA a cluster of similar structures with well rounded ends indicated they are solid in nature. Surprisingly, PDMA/NSA mainly produced short nanofibrillar like clusters with diameter sizes well below 200 nm. In all the cases, irregularly shaped agglomerated particles were seen.

A comparison of the SEM micrographs of the polymer composites produced at 0.5:1 and 1:1 monomer to dopant ratios revealed that the tendency to form a network of nanofibrillar for both the ASA and NSA -doped composites respectively decreased with increase in the monomer dopant level. Composites prepared at 1:1 ratio exhibited mainly granular morphology (appendix A) and was actually thought to represent dopant units or micelles. Granulated PANi morphology has been reported (Goel et al., 2007: 71-76).

A comparison between the ASA and NSA doped composites there was a higher tendency to form a higher density of nanofibrillar network for ASA composites. It is accepted that the dopant structure can greatly affect the molecular structure, morphology and physical properties of a conducting polymers (Zhang et al., 2005: 1373-1379). A mixture of nanofibrils/rods mixed with granular morphology was more evident for the NSA doped polymers. It could imply that ASA was a better structure directing material probably due to its longer hydrocarbon chains compared to NSA. Granulated morphology was observed for the composites at 1:1 ratio.

The fibrillar morphology has been described as been molecular one - dimensional structures with ability to act as molecular wires (Wei et al., 2002: 917-921). Since fibrillar morphology was a product of the 0.5:1 monomer to dopant ratios, composites applied in biosensor fabrication were synthesized at this ratio. It was believed the nanofibrils would perfectly molecularly wire the immobilized enzymes to the electrode.

4.5 Characterization of the polymer nanocomposites using FTIR spectroscopy

The characterization of conducting polymers by IR spectroscopy has been used extensively to depict the conducting state of a polymer as well as to predict successful doping (Patil et al., 2004: 57-63; Cataldo and Maltese, 2002: 1791-1803). Doped polyanilines exist in the emeraldine salt forms which are essentially delocalized polysemiquinone radical cations whose stability is maintained by the presence of dopant anions. In this project the $C_{10}H_7SO_3^-$ and $C_{14}H_9SO_3^-$ dopant anions played the stabilizing role. An example of how this stabilization can take place is given in Figure 4.9.

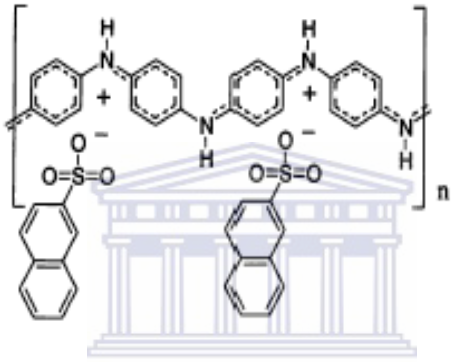

Figure 4.9: Stabilization of the polyemeraldine salt of PANi (PES) by the naphthalene sulfonate anion, $C_{10}H_7SO_3^-$.

The degree of electron delocalization in the polysemiquinone forms of the doped polyanilines manifests itself in the form of an 'electronic like band' at ca. 1100 cm^{-1} associated with polarons (Patil et al., 2004: 57-63). Figure 4.10 (i) and (ii) represents the FTIR spectra of the ASA and NSA doped polyanilines. The striking semblance between the PANi and the substituted polyanilines spectra basically proves the existence of the same basic unit.

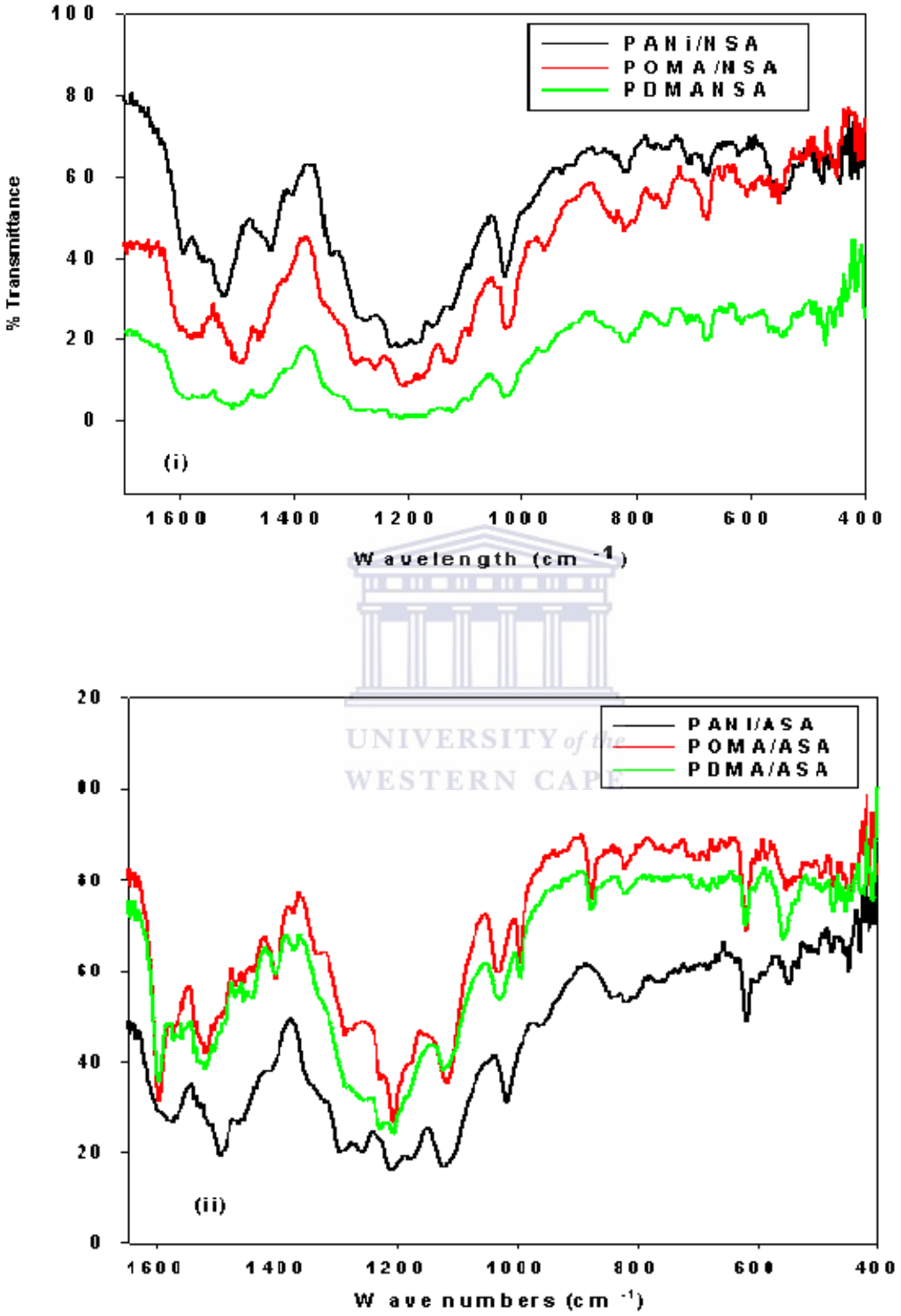

Figure 4.10: The FTIR spectra of the NSA (i) and ASA (ii) doped polyanilines.

It has been shown that most vibrational bands of significance in doped polyanilines occur between 400-1600 cm^{-1} (Goel et al., 2007: 71-76). Outside this range, other important bands include the N-H stretching vibrations as well as the C-H stretching vibrations due to the alkyl and aromatic groups. The N-H stretching vibrations for the ASA and NSA doped polyanilines occurred in the range 3200-3400 cm^{-1} (full spectra displayed in appendix A). These bands form a broad -valley like depression with a broad tail ending on the lower frequency side indicating the protonation of the N-H groups which are involved in H-bonds of various strengths (Widera et al., 1998: 265-272). The presence of hydrogen bonds may indicate the polymer is hygroscopic. The pair of weak bands at ca. 2900 cm^{-1} PANi and 2800 (alkyl stretching) observed in the ASA doped polymers (Cataldo and Maltese, 2002: 1791-1803) are not obvious for the NSA doped composites.

For the NSA doped polyanilines the C=C stretching vibrations in the quinonoid units were observed at 1600, 1580 and 1590 cm^{-1} for the PANi, POMA and PDMA composites respectively. In undoped PANi, the C=C stretching vibrations have been found to occur at 1610 cm^{-1} (Cataldo and Maltese, 2002: 1791-1803). It appears that a shift in the quinoimine band occurs in the NSA doped polyanilines and is associated with successful protonation or doping. For the ASA doped polyanilines the C=C bands due to the quinonoid units occurred at 1580, 1600, 1600 cm^{-1} for PANi, POMA, PDMA respectively and appearance of band shift as discussed is proof of doping. Likewise the C=C stretching vibrations due to the benzene units were observed at 1550, 1520, 1530 cm^{-1} for the NSA doped polyanilines as compared to 1490,1510, 1500 cm^{-1} for the ASA doped polyanilines. The observed bands are in close agreement with those reported in literature (Zhang and Wan, 2002, 83-89; Li and Mu, 2005: 143-149; Feng-Jiin et al., 2007, in press). Comparatively, for all the composites the intensity of the quinoimine band was always less than the benzoid one which could mean incomplete doping. This was expected, however, given the fact that the composites were prepared from a 0.5:1 monomer to dopant ratio as previously discussed.

The relatively strong bands at ca. 1400 cm^{-1} for the NSA doped polyanilines and ca. 1400-1450 cm^{-1} in the ASA doped polyanilines are assigned to the C-N stretching

vibrations in the quinonoid imine units. The bands appearing in the range1250-1300 cm^{-1} and 1270-1300 cm^{-1} in the the spectra of the NSA and ASA doped polyanilines respectively were assigned to the C-H stretching of the aromatic conjugation (Zhang et al., 2005: 1373-1379). The bands at ca. 1175, 1050 cm^{-1} for PANi/NSA; 1170, 1030 cm^{-1} for POMA/NSA, and 1170, 1030 cm^{-1} for PDMA/NSA: were assigned to the asymmetric and symmetric stretching modes of the $–SO_2$-OH group (Cataldo and Maltese, 2002: 1791-1803). For ASA-doped polyanilines the above bands were observed at 1170-1020 cm^{-1} for PANi at 1200, 1030 cm^{-1} for POMA and at 1200, 1030 cm^{-1} for PDMA. For all the composites the bands observed at ca. 605 cm^{-1} were assigned to bending modes of the sulfonic group. The presence of these sulfonic group related vibrations was a sign of successful doping. The electronic like bands associated with existence of polarons within the polymer units were observed at 1150, 1130, 1120 cm^{-1} for the NSA doped polyanilines and at 1120, 1110, 1110 cm^{-1} for the ASA doped composites. The bands between 970-980 cm^{-1} in all the composites were assigned to the C-H out of plane deformations of the aromatic rings. The appearance of bands ca. 690, 760, 810 cm^{-1} is indicative of the presence of para and ortho-substitution (Kemp, 1987: 44-56). Since the amine group occupies position 1 in the aromatic rings it can safely be assumed that polymer formation takes place through a head to tail coupling of the generated radical cations during polymerization.

4.6 Electrochemical Characterisation of the ASA/NSA doped composites

A prerequisite towards the use of the anthracene and naphthalene sulphonic acid doped-polyanilines in biosensor construction is that they should be electroactive. Molecules for which a redox potential can be measured are referred to as electrochemically active (electroactive) (Monk, 2001: 17-24). Electroactive molecules can be oxidized (ox) or reduced (red) and therefore have the ability to pass on an electron(s) from one species to another. Figure 4.11 (a) and (b) illustrates the role played by electron mediators (e.g. conducting polymers) in an amperometric biosensor.

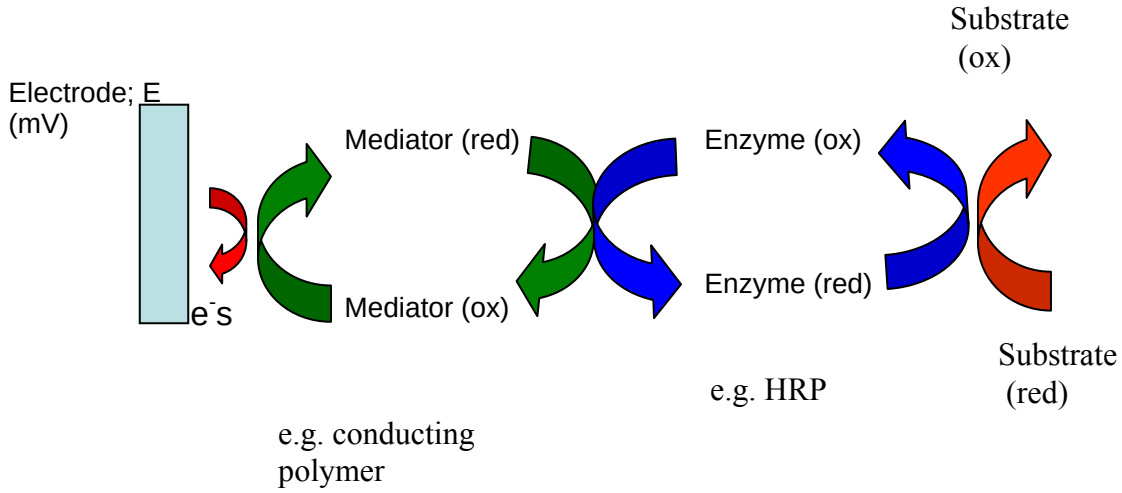

(a)

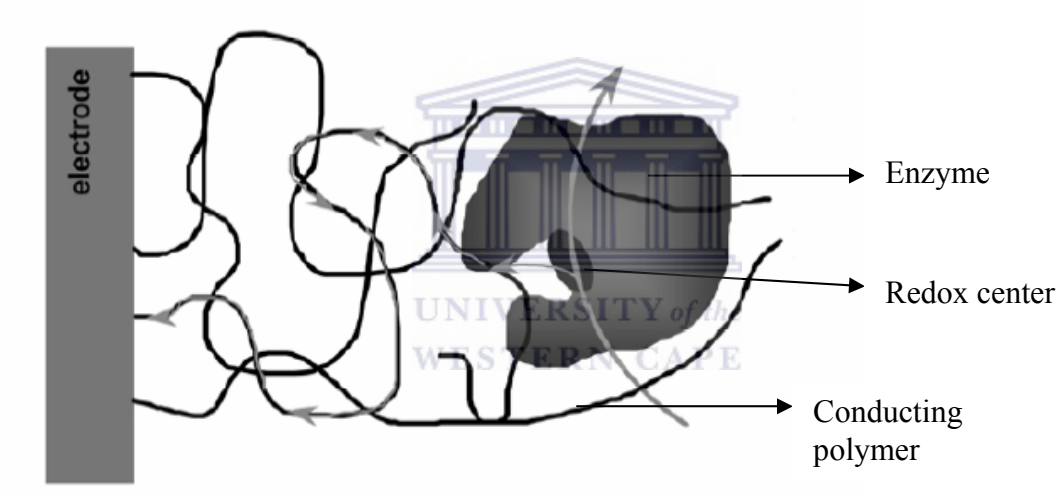

(b)

Figure 4.11: The role played by electron mediators e.g. conducting polymers in the performance of an amperometric biosensor.

In an amperometric biosensor the conducting polymer provides a link between the deep buried enzyme redox center and the electrode. Conducting polymers can only fulfill this role if they are electroactive. In order to verify the nature of the chemically synthesized products, a multi-scan rate study at an optimized potential window was performed. Figures 4.12-4.17 depict the multi-scan rate cyclic and square wave voltammetric responses of the composites obtained in 1 M HCl as the swamping electrolyte.

According to these Figures, all the prepared composites gave rise to either two or three well formed redox waves indicating their electroactive nature. It has been shown that polyaniline-based systems have the ability to undergo more than one oxidation or reduction and therefore have multi-redox potentials. Accordingly, it is now known that polyaniline-based systems can exist in three oxidation states, the most reduced polyleucoemeraldine form (PLE); the protonated polyemeraldine form (polyemeraldine salt-PES), and the fully oxidized polypernigraniline form (PPN) (MacDiarmid, 2001: 2581-2590; Lindfors and Ivaska , 2002: 43-52).

Figure 4.12 and 4.13 depict the electrochemical behaviour of ASA and NSA doped polyaniline respectively. While the PANi/ASA composite exhibited two major redox couples, three redox couples were observed in the PANi/NSA CV and SQW waves.

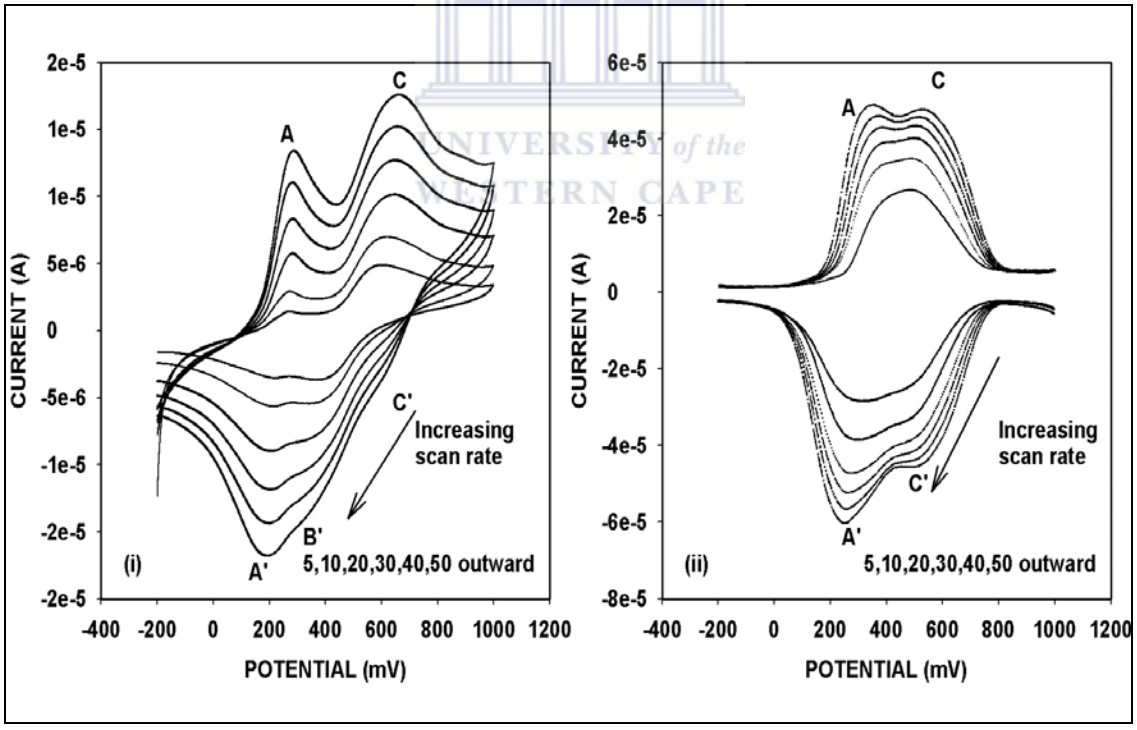

Figure 4.12: Cyclic (i) and square wave (ii) voltammetric responses of PANi/ASA at scan rates 5-50 mV/s; sensitivity 100 µA/V;-200 → +1000 mV/s potential window.

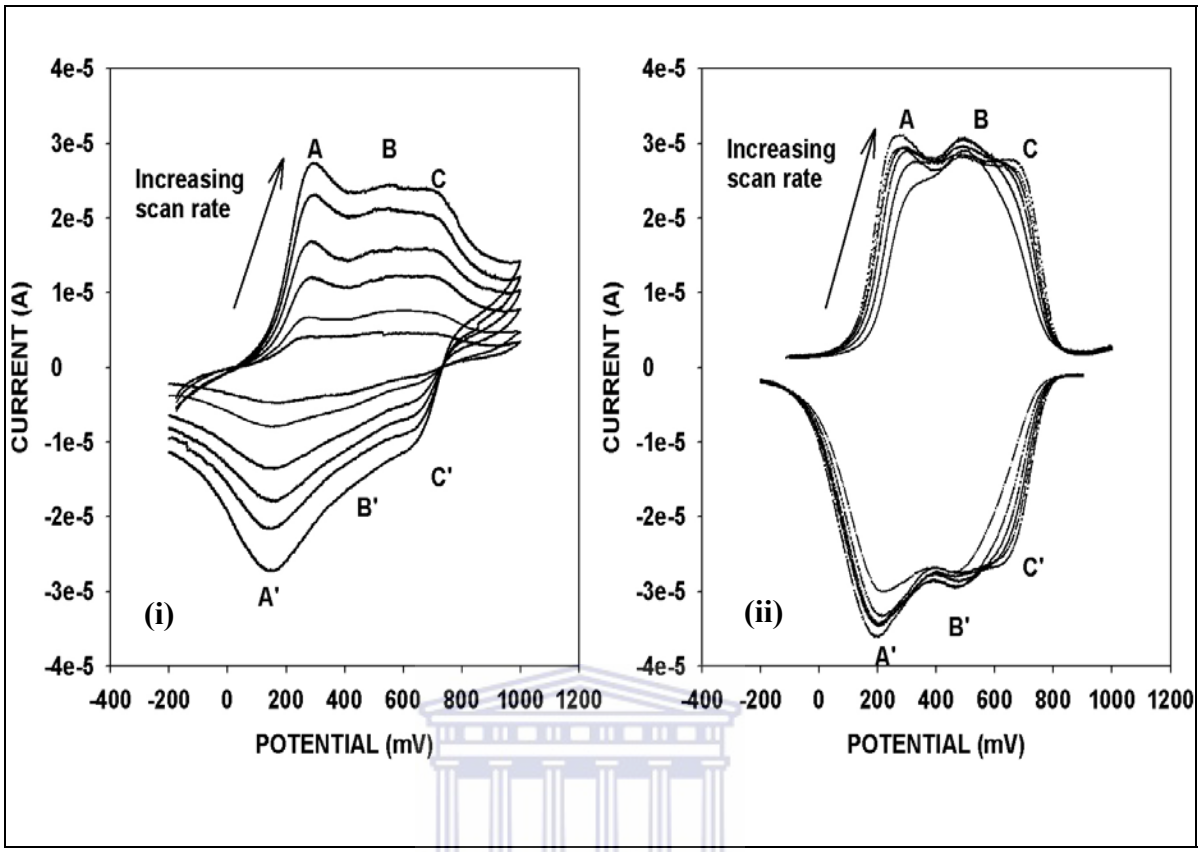

Figure 4.13: Cyclic (i) and square wave (ii) voltammetric responses of PANi/NSA at scan rates 5-50 mV/s; sensitivity 100 µA/V;-200 → +1000 mV/s potential window.

In the voltammograms, redox couple A/A' at a formal potential $E^{0'}$ (mV) 241± 11 PANi/ASA; 217 ± 8 PANi/NSA represents the polyleucoemeraldine (A)/polyemeraldine salt transition. Peaks C/C' at a formal potential $E^{0'}$ (mV), 582 ± 10 PANi/ASA; 629 ± 22 PANi/NSA, is the polyemeraldine/polypenigraniline transition (Moulton et al., 2004: 402-406; Lindfors and Ivaska, 2002: 43-52). In addition a middle redox wave (B/B') at ca. 400 mV seen in both the CV and SQW voltammograms of PANi/NSA can be attributed to the oxidation/reduction of dimers and oligomers entrapped within the polymer matrix (Widera et al., 1997: 29-37). In PANi /ASA CV, only the reductive peak of this middle couple is seen. It is well known that the oxidative polymerization of aniline and aniline related monomers is a chain reaction whose chain termination step involves the coupling of the radical cations to forms dimers, oligomers and finally the polymer (Prévost et al., 1999: 1229-1236; Malinauskas, 2001: 75-83). There is a possibility of dimmer or oligomer entanglement with the polymer leading to the detection of the latter

in the CV and SQW voltammograms. The middle peak/couple has otherwise been assigned to the degradation products of over-oxidized polyaniline (Yue et al., 1991:2665-2671) or to the quinone/hydroquinone by-products (Huang et al., 2006: 2756-2764: Sivakumar and Saraswathi 2003: 381-390). Similarly, this middle couple has been attributed to defects in the linear structure of the polymer (Valter et al., 2002: 1535-1541).

Figures 4.14 and 4.15 are the cyclic and square wave responses of ASA and NSA doped poly-*o*-methoxyaniline.

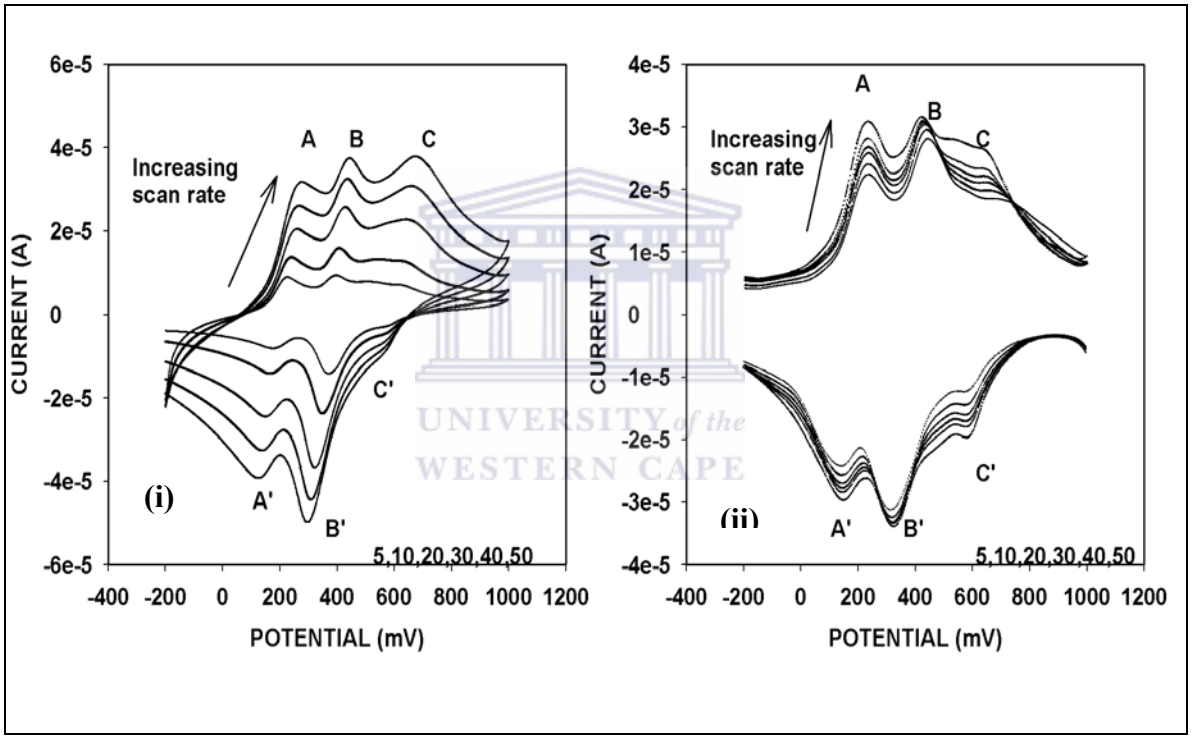

Figure 4.14: Cyclic (i) and square wave (ii) voltammetric responses of POMA/NSA at scan rates 5-50 mV/s; sensitivity 100 µA/V;-200→+1000 mV/s potential window.

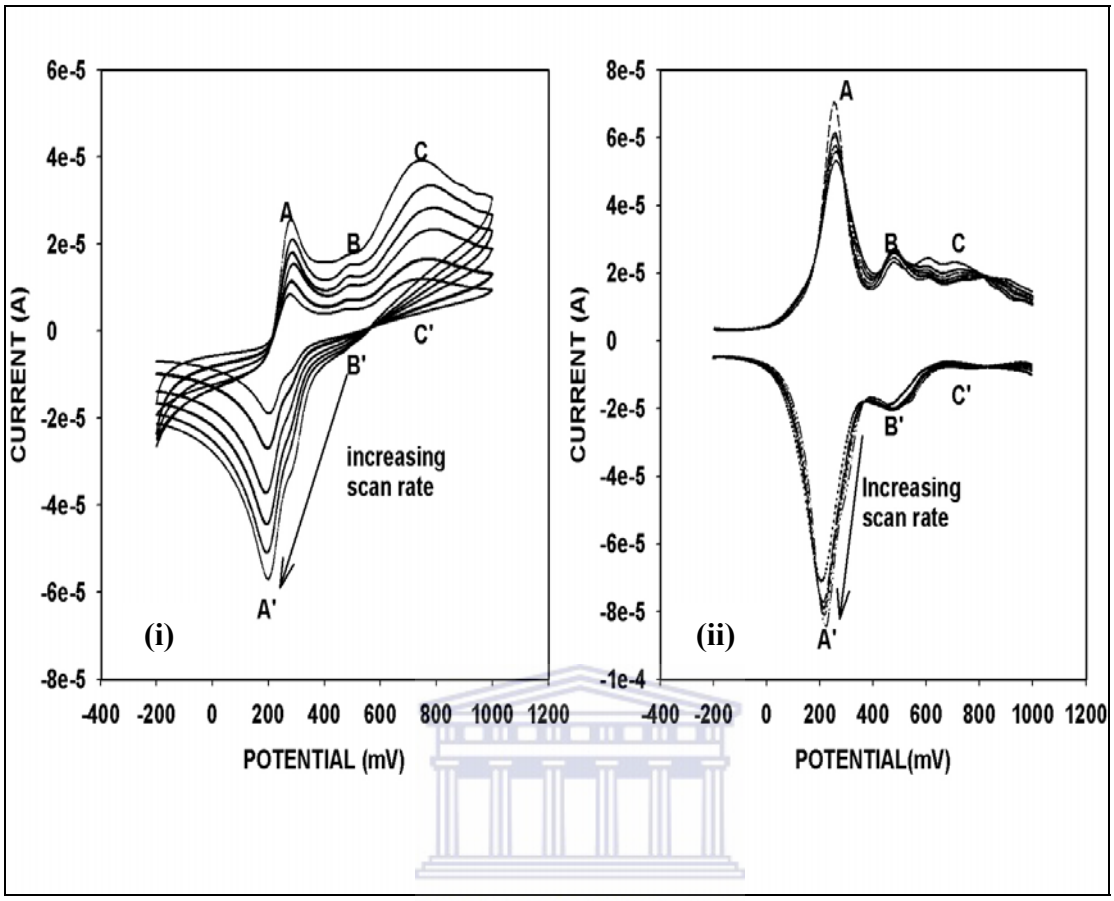

Figure 4.15: Cyclic (i) and square wave (ii) voltammetric responses of POMA/ASA at scan rates 5-50 mV/s; sensitivity 100 µA/V;-200 → +1000 mV/s potential window.

In both NSA and ASA doped poly-*o*-methoxyaniline composites, three redox couples were observed as is evident from both the CV and SQW results. In the POMA/NSA voltammograms, peaks A/A' appeared at 203 ± 12; C/C' 611± 9 and were assigned as previously discussed. The reversible middle couple due to oligomers or over-oxidation of poly-*o*-methoxyaniline appeared at a formal potential ca. 387± 15 mV. A similar trend was observed in POMA/ASA with the redox couple for peaks A/A', B/B' and C/C' been observed at 237 ± 9, 422 ± 11, 567 ± 9 respectively and were similarly assigned. These formal potentials ($E^{0'}$, mV) observed for the ASA and NSA doped POMA agree closely with those reported in literature POMA (Mazur and Krysińska, 2002: 7093-7101). In the POMA composites the enhancement of the middle couple as compared to that of either ASA or NSA doped PANi could indicate polymer instability with respect to PANi or the

fact that polymerization of derivatised polyaniline could be yielding more oligomers/dimers in comparison to that of unsubstituted PANi. The tendency towards dimerization or infact to form shorter polymer chains has been reported for substituted PANi (Tran and Kaner, 2006: 3915-3917). The presence of substituents on the benzene rings affects the stereochemistry of the polymers thus limiting the number of monomer units that can chain up.

Figures 4.16 and 4.17 depict the electrochemical behaviour of the doped poly-2,5-dimethoxyaniline polymers. In PDMA/ASA (Fig. 4.16), the redox couple A/A' represented the polyleucoemeraldine/polyemeraldine salt transition occurred at ca. 230 ± 8 mV. That of the polyemeraldine salt /polypernigraniline transition (C/C') was seen at 600 ± 12 mV. In PDMA/NSA peaks A/A' and C/C' were observed at 240 ± 20, and 632 ± 31 mV. For both ASA and NSA doped PDMA, the peaks B/B' due to over-oxidation did not appear or could have merged with the redox couple A/A'. Besides the previously observed redox couples in PANi and POMA composites, additional peaks assigned here as D/D' (at ca. 100 mV) and E (ca. 800 mV) to distinguish them from the above the fundamental peaks characteristic of doped polyanilines are observed. However, these peaks (in some cases) are not very evident on the CVs but their existence is verified by the more sensitive technique-square wave voltammetry. On comparing the cyclic voltammograms (CV) of the ASA and NSA doped PDMA (poly-2,5-dimethoxyaniline) with CVs (Fig. 4.18 ‘a’ and ‘b’) for the pure dopants (solutions in distilled water) on the same electrode suggested that these new peaks could have emanated from the dopant themselves. According to Malinauskas (1999: 75-83), conducting polymers when doped with large polyanions such as ASA and NSA cannot expel them into solution. Instead they form hybrid composites bearing both the anion and the polymer characteristics. In other words, the appearance of dopant peaks in the CVs and SQW of the doped PDMA could be used as proof that indeed the composites are a kind of hybrid material, a general indication of successful doping. However it was not immediately clear as to why dopants peaks were not so vividly clear in the other composites.

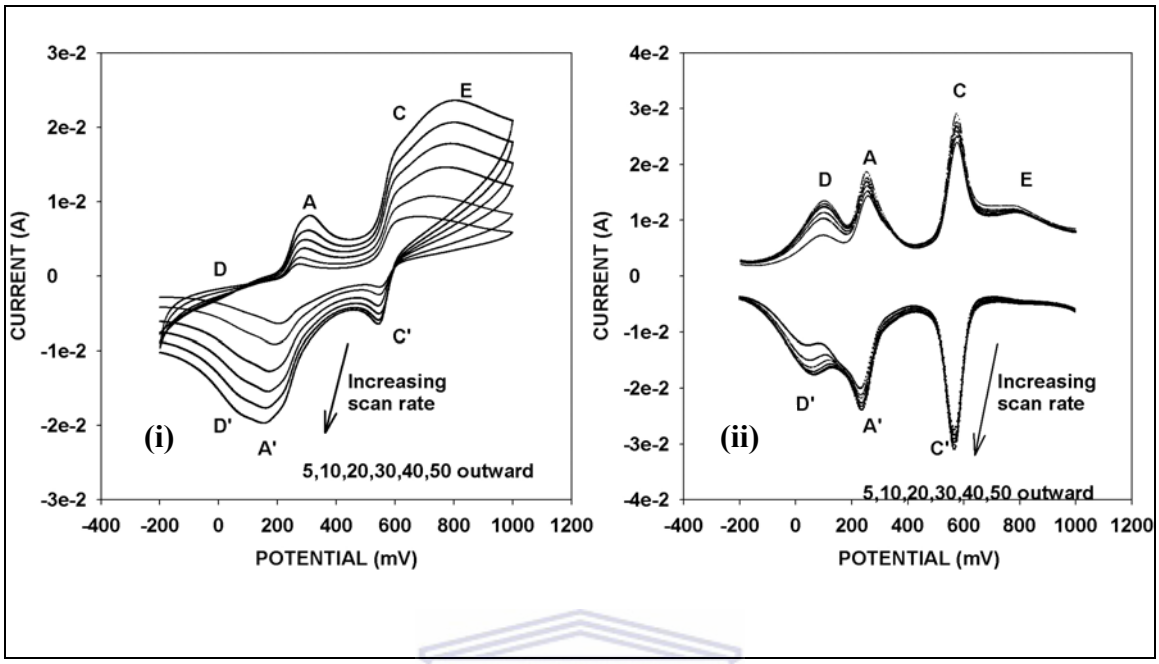

Figure 4.16: Cyclic (i) and square wave (ii) voltammetric responses of PDMA/ASA at scan rates 5-50 mV/s; sensitivity 100 µA/V;-200 → +1000 mV/s potential window.

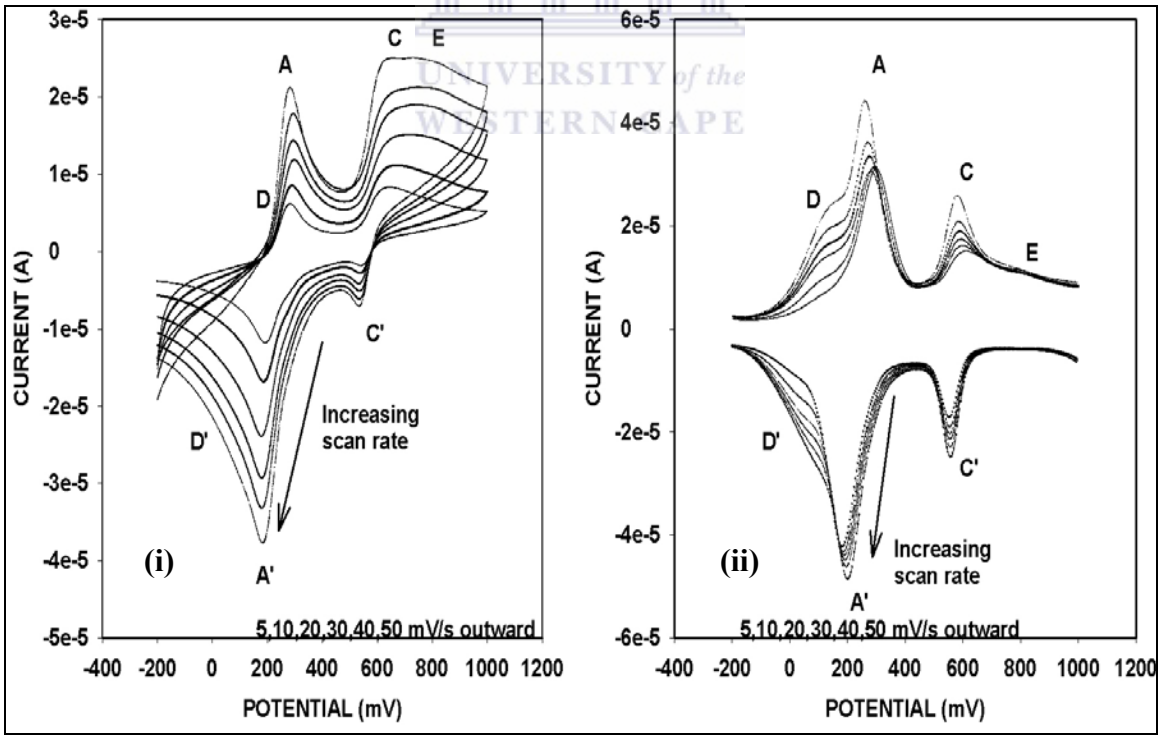

Figure 4.17: Cyclic (i) and square wave (ii) voltammetric responses of PDMA/NSA at scan rates 5-50 mV/s; sensitivity 100 µA/V; -200→+1000 mV/s potential window.

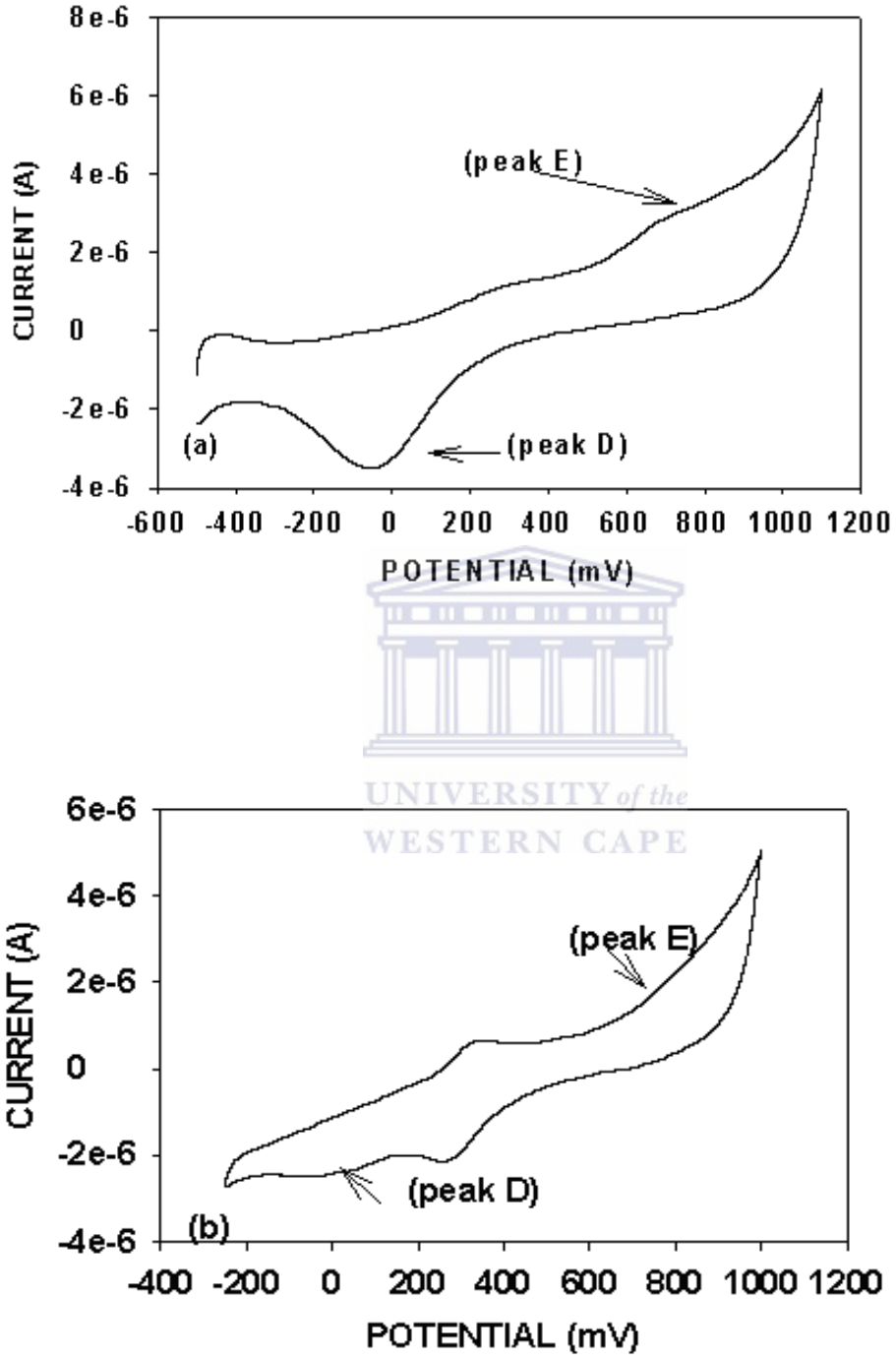

Figure 4.18: Cyclic voltammograms of ASA (a) and NSA (b) acid in distilled water on a platinum electrode showing the presence of peaks at ca. 100 and 800 mV.

4.7 Kinetic parameters: Diffusion coefficients and heterogeneous rate constants

4.7.1 Surface concentration (Γ* mol cm^{-2})

During the electrochemical characterization of the polymer composites in HCl, it was found out for all the polymers, a thin green layer of polymer adhered at the surface of the electrode as the potential was scanned. This layer was assumed to be the 'active layer' and was used to estimate the surface concentration Γ* (mol cm^{-2}) of each of the polymers. According to the Anson model, therefore, the area under either the reductive or oxidative wave corrected for any background current (Bard and Faulkner, 2001: 591), represents the charge required for the full reduction/oxidation of the layer and is related to the surface concentration in the manner;

$$\Gamma^* = Q/nFA \qquad (3.8)$$

where Q (C) is the charge required for the full oxidation/reduction of the layer and other constants have their usual meaning.

It is already established that polyaniline and its related polymers exists in three allowed oxidation states. Of these forms, the polyemeraldine salt (PES) form which is a delocalized semiquinone radical cation is the most conductive (MacDiarmid, 2001: 269-279; Albuquerque et al., 2004: 1-10). It has also been shown that during the functioning of amperometric biosensors it is this form of PANi that accepts the electron from the electrode and passes to the enzyme. During amperometric detection, the catalytic enzymatic reaction is coupled to the oxidation/reduction reactions of the PES form of PANi. The PES peak, (peak A) in all the voltammograms is therefore the most important and all the surface concentrations were calculated with respect to this peak. Accordingly, the charge Q (μC) under the PES wave (peak A) were; 15.17 PANi/NSA; 18.32

PANi/ASA; 33.08 POMA/NSA; 6.88 POMA/ASA; 31.98 PDMA/NSA; 17.25 PDMA/ASA. Correspondingly, the estimated surface concentrations Γ* (mol cm^{-2}) for all the polymers were; 1.0 x 10^{-8} PANi/NSA; 8.9 x10^{-9} PANi/ASA; 1.9 x10^{-8} POMA/NSA; 4.0 x 10^{-9} POMA/ASA; 1.1 x 10 $^{-8}$ PDMA/NSA; 1.0 x 10 $^{-8}$ PDMA/ASA. Comparatively, it appears the surface concentration of NSA doped polyanilines were higher than those of the corresponding ASA composite. This observation was attributed to the bulkiness of the ASA dopant which could have contributed to the slow formation of the 'active layer'. The Γ* (mol cm^{-2}) obtained agree with those reported by Mathebe et al. (2004: 115-120) and Iwuoha et al. (1997: 749-761). It means the polymer composites exhibited surface concentration characteristics close to those of electropolymerized polyanilines.

4.7.2 Diffusion coefficient (D_e cm^2/s)

The diffusion coefficient of a polymer refers to the rate at which the electrons hop along the polymer units. The magnitude of the D_e can be useful to determine the suitability of a polymer as electron shuttling mediators in biosensor construction. Low D_e (probably less than 10^{-12}), would indicate that polymer cannot serve as an effective mediator. Based on the peak to peak separation (ΔE_p values) for the PES couple (A/A') either the Randles- (equation 3.4) or the Nicholson and Shain (equation 3.5) methods were used for the estimation of D_e. The Randles-Sevćik equation applies for reversible systems where $\Delta E_p \leq 59$ mV. However, for systems that deviate from reversibility i.e. $\Delta E_p > 59$ mV, the Nicholson and Shain equation (equation 3.5) was applied. In the latter case, the kinetic parameter Ψ, is dependent on peak-to-peak separation, ΔE_p. In this work, Ψ values were adopted from the Ψ values chart in Bard and Faulkner (2001: 243). For all the calculations the moles of electrons n was taken as one (Orata and Okong'o, 2000: 211-216).

The PANi/NSA system was found to exhibit near reversibility characteristics with the ΔE_p values been 51 ± 10 and an anodic to cathodic peak current ratio, $|I_{pa} / I_{pc}|$ of 0.92 ± 0.083. The near 'unity' $|I_{pa} / I_{pc}|$ ratio indicates the surface concentrations of both the reduced and oxidized forms of PANi/NSA (redox couple A/A'), obeyed the Nernst

equation. However, the rest of the composites with respect to redox couple A/A' were found to deviate form reversibility with ΔE_p been greater than 59 mV. The ΔE_p mV for the rest of the composites were found to be: 85 ± 20 PANi/ ASA; 77 ± 23 POMA/NSA; 88 ± 17 POMA/ASA; 77 ± 25 PDMA/NSA; 85 ± 15 PDMA/ASA. However, it was found that nearly all the systems were reversible at low scan rates (e.g. 5 mV/s) but transited to quasi-reversibility with scan rate increase. The $|I_{pa} / I_{pc}|$ for the systems were found to be; 0.74 ± 0.07 PANi/ASA; 0.876 ± 0.11 POMA/NSA; 0.5 ± 0.05 POMA/ASA; 0.45 ± 0.03 PDMA/NSA; 0.5 ± 0.06 PDMA/ASA. The deviation of this anodic to cathodic peak to peak current ratio from unity was indicative of quasi-reversibility.

A close examination of the cyclic voltammograms presented in Figures 4.12-4.17 revealed that in all the voltammograms except in PANi/NSA, peak 'A'' shifted cathodically with scan rate. The observed shifts (mV) were: 205 ± 10 PANi/ASA; 178 ± 22 POMA/NSA; 144 ± 25 POMA/ASA; 195 ± 10 PDMA/NSA; 182 ± 8 PDMA/ASA. In PANi /NSA an anodic shift of 278 ± 15 mV in peak 'A' was observed. The shifting of these peaks with scan rates were indicative of an electron hopping process occurring along the benzene rings (Mathebe et al., 2004: 115-120) and that the reaction kinetics were diffusion controlled. Figures 4.19-4.21 represent the plots of peak currents (I_p, A) of these peaks versus the square root of the scan rate υ (V/s). The slopes of these peaks were employed to estimate the D_e (cm^2) using the above stated equations. The slopes obtained were; 2.84e-4 (r^2=0.99) for PANi/NSA; 5.26e-4 (r^2 =0.99) PANi/ASA; 2.32e-4 (r^2 =0.99) for POMA/NSA; 8.68e-5 (r^2 =0.99) for POMA/ASA; 2.44e-4 (r^2 =0.99) for PDMA/NSA; 1.7e-4 (r^2 =0.99) PDMA/ASA.

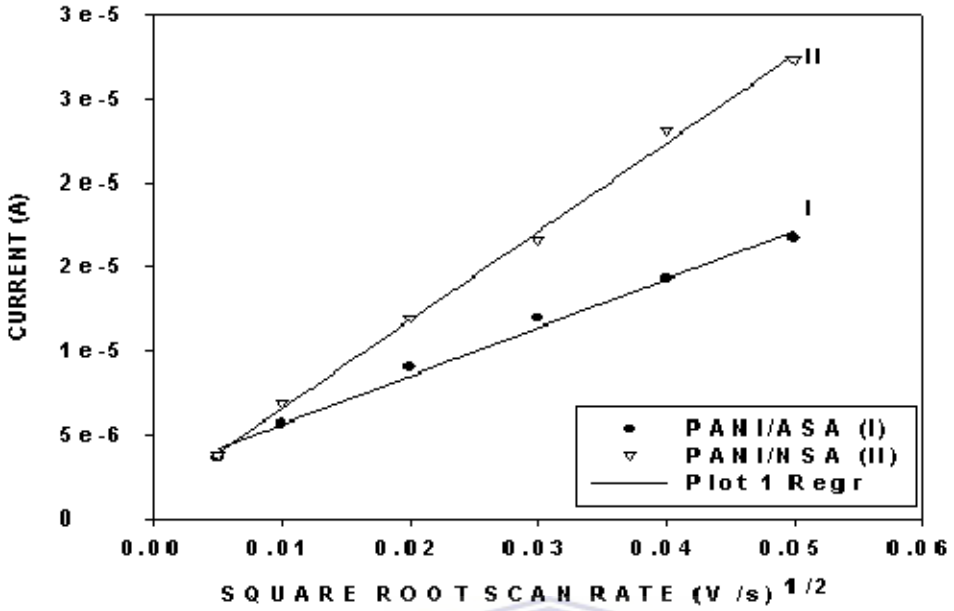

Figure 4.19: Plot of peak current variation with square root of scan rate for PANi/ASA (curve 1) and PANi/NSA (curve II).

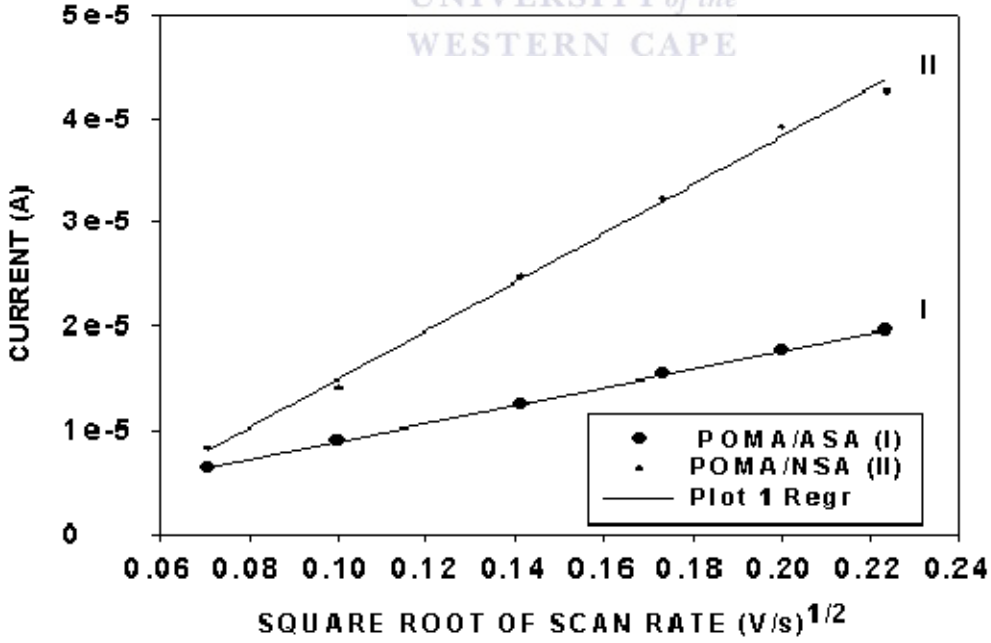

Figure 4.20: Plot of peak current variation with square root of scan rate for POMA/ASA (curve 1) and POMA/NSA (curve II).

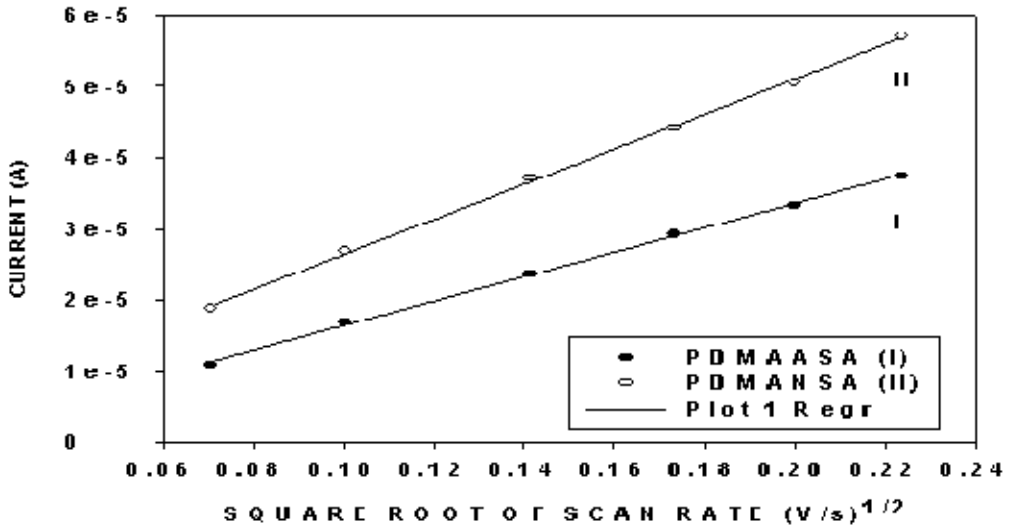

Figure 4.21: Plot of peak current variation with square root of scan rate for PDMA/ASA (curve 1) and PDMA/NSA (curve II).

In turn, the D_e (cm/s) values estimated were; 8.9 x 10 $^{-6}$ PANi/NSA; 2.4 x 10^{-6} PANi/ASA; 2.1 x 10^{-6} POMA/NSA; 4.0 x 10^{-6} POMA/ASA; 1.6 x 10^{-6} PDMA/NSA; 2.2 x 10^{-6} PDMA/ASA. The estimated D_e values follow the trend PANi > POMA > PDMA when compared according to the dopant type of course with a few anomalies. This trend was as expected because the rate of electron hopping is known to be affected by the inter-chain distances. For POMA and PDMA the methoxy group substituents may cause steric hindrance that would impede the movement of electrons along the polymer chain. The D_e values obtained here are slightly higher than those reported by Mathebe et al. (2004:115-120) for polyaniline systems. However, it is important to note that the different dopants used, e.g. polyvinyl sulfonate, could have contributed to this difference due to their larger molecular masses. Also these D_e values are slightly higher than those reported for carbon nanotube/polyanisidine complexes and the difference is similarly explained (Valter et al., 2002: 1535-1541). The high D_e values realized for both the NSA and ASA composites means that the composites are suitable for electromediation but preference would first be given to polyaniline that had the highest diffusion coefficient values.

4.7.3 Heterogenous rate constants (k^0 cm/s)

The heterogeneous rate constant of a system is a measure of the kinetic facility of that process. Low k^0 values on a scale where 10^{-12} is too small predict the process proceeds to a very small extent. On the other hand large k^0 values of ca. 10 cm/s predict a situation where the electron transfer reactions are very fast as is characteristic of simple ionic species in solution (Bard and Faulkner, 2001: 96-98). In this work the estimated k^0 values lay in the range 1.7 x 10^{-2} – 6.2 x 10^{-4} which implies the rate of electron transfer between the composites and the electrode were relatively fast gauged on the above scale (all results are summarized in Table 4.3). In fact these values lay in the $0.3\ \upsilon^{1/2} \geq k^0 \geq 2 \times 10^{-5}$ cm/s predicted for quasi-reversible systems (Bard and Faulkner, 2001: 239). The estimated k^0 values realized for the ASA and NSA doped polyanilines compared well with those reported in literature for PANi /Pt and PANi/PEDOT systems which exhibited k^0 values in the range 0.049-5.4 x 10^{-3} and 15-45.3 x 10^{-3} cm^2/s respectively (Pauliukaite et al., 2004: 159; Akinyeye et al., 2006: 2441-2450).

4.8 Conductance of the generated composites

Conductivity may be considered as the ability of a substance to conduct electricity (current, electrons). For application in amperometric biosensors, the polymer composites are thus required to be conductive. So far various methods have been employed towards determining the conductivity of the polymer composites. Normally, the two or four point probe or the conductivity meter has been used in the determination of conductivity (Jayanty et al., 2003: 7265-7270; Narayan et al., 2006: 3665-3672). It is also possible to estimate the conductance of conducting polymers based on cyclic voltammetric data (Iwuoha et al., 2006: 453-458) based on the equation;

$$\text{Conductance (S/cm)} = \Delta I_v / \Delta E_v \qquad (4.0)$$

where ΔI_v (A) is the current difference between two voltammetric data points taken at different scan rates and ΔE_v is the potential difference between the two points. In this case, $\Delta I_v = I_{50\ mV/s} - I_{5\ mV/s}$. Similarly, $\Delta E_v = E_{50\ mV/s} - E_{5mV/s}$. Using the above equation

which is actually a derivation of the classical Ohm relationship, the conductances of the various composites were estimated to be in the range (0.27 – 7.3) x 10^{-3} as is summarized in Table 3 below. In general the conductances obtained here predicted successful doping the values were several orders of magnitude above those reported for undoped PANi. It has been shown that undoped polyanilines usually have conductivities as low as 10^{-9} (Stejskal and Gilbert, 2002: 857-867). With some anomalies, the conductances of the ASA doped polyaniline and poly-*o*-methoxyanilines were lower than that for corresponding NSA counterparts. Again the trend could be attributed to steric hindrance. However, contrary to what was expected, the conductivity values for both PDMA/ASA and PDMA/NSA were relatively high and infact higher than that of NSA doped polyaniline. Similar observations are reported (Palys et al., 2000: 111-119; Huang et al., 2005: 300-307). In general, however, the conductances obtained here were lower than those reported for PANi/PVA and PANi/DBSA systems whose conductivity values were one order of magnitude higher (Stejskal et al., 2003: 1353-1358; Jayanty et al., 2003: 7265-7270).

Table 4.3: Summary of the estimated kinetic parameters for the chemically synthesized NSA and ASA composites. In the ΔEp (mV) column, the values for the first (A/A') and third redox couples (C/C') are presented.

Polymer	Ip_a/Ip_c	ΔE_p (mV)	$E^{0'}$ (mV)	Γ* (mol cm^{-2})	D_e (cm^2/s)	k^0 (cm/s)	Conductance (S/cm)
PANi/ NSA	0.92 ± 0.08	51± 10 23± 12	217± 8 629± 22	8.9×10^{-9}	8.9×10^{-6}	1.8×10^{-2}	1.38×10^{-3}
PANi/ ASA	0.74 ± 0.07	85 ±20 53± 12	241±11 582 ± 10	1.0×10^{-8}	2.4×10^{-6}	4.8×10^{-4}	0.27×10^{-3}
POMA/ NSA	0.87± 0.10	77±23 88±15	203±3 611 ±9	1.9×10^{-8}	1.1×10^{-6}	1.3×10^{-4}	1.50×10^{-3}
POMA/ ASA	0.50 ± 0.05	88± 17 53±5	237± 9 567±7	4.0×10^{-9}	4.0×10^{-6}	6.2×10^{-4}	0.78×10^{-3}
PDMA/ NSA	0.45 ± 0.03	77±25	240±2	1.1×10^{-8}	1.6×10^{-6}	1.5×10^{-4}	2.9×10^{-3}
PDMA/ ASA	0.50 ± 0.05	85±15	237 620±10	5.9×10^{-8}	2.2×10^{-6}	2.1×10^{-4}	7.3×10^{-3}

4.9 Characteristics of the chemically synthesized composites in phosphate buffer

This study presents the stages towards production of amperometric biosensors intended for future use in vivo measurements. In view of this, the electrochemical behaviour of the polymer composites in phosphate buffer (PB) was investigated to simulate bodily enzymatic conditions. Although many pH values were tried out for the characterization of the chemically synthesized composites, it was found out the best results were displayed at pH 7.02 (0.1 M). However, according to literature results, polyaniline especially in its undoped form is known to show hysterisis undergoing rapid deprotonation with loss of electroactivity (Grennan et al., 2006: 1591-1600; Iwuoha et al., 1997: 749-761). The authors, however, generally agree that doped polyaniline especially of SPAH type, is quite stable and undergoes no deprotonation. This was the case observed for both the ASA/NSA doped composites which were found to be stable the applied conditions. Figure 4.22 are representative results of a multi-scan rate study performed in phosphate buffer (PB, pH 7.02) and shows that the composites were electroactive. For almost all the composites, two peaks were observed during the cathodic scan. Reductive square wave voltammetric data indicated that the two peaks lay at or close to peak potentials, 0 and -250 mV. The latter peak was assigned to the PES form of polyaniline whose reduction (by receiving an electron from the electrode) in amperometric biosensors is coupled to the enzymatic catalytic reaction. The peak can be used to monitor the catalytic reduction of the substrate of interest.

It means the use of the stabilization surfactant dopants helped to maintain electric neutrality and composites stability at this pH. These properties emanated from the fact that the bulky dopants (NSA/ASA) anions could not be exchanged with simple H^+ as known to be the case with undoped PANi (Malinauskas, 1999: 75-83). However, there was a need to investigate the effect of changing the supporting electrolyte from HCl to phosphate buffer on the rate of electron hopping along the polymer chains and the heterogeneous rate constants. The evaluation of the two parameters was critical towards determination of polymer use for electron shuttling in the biosensors.

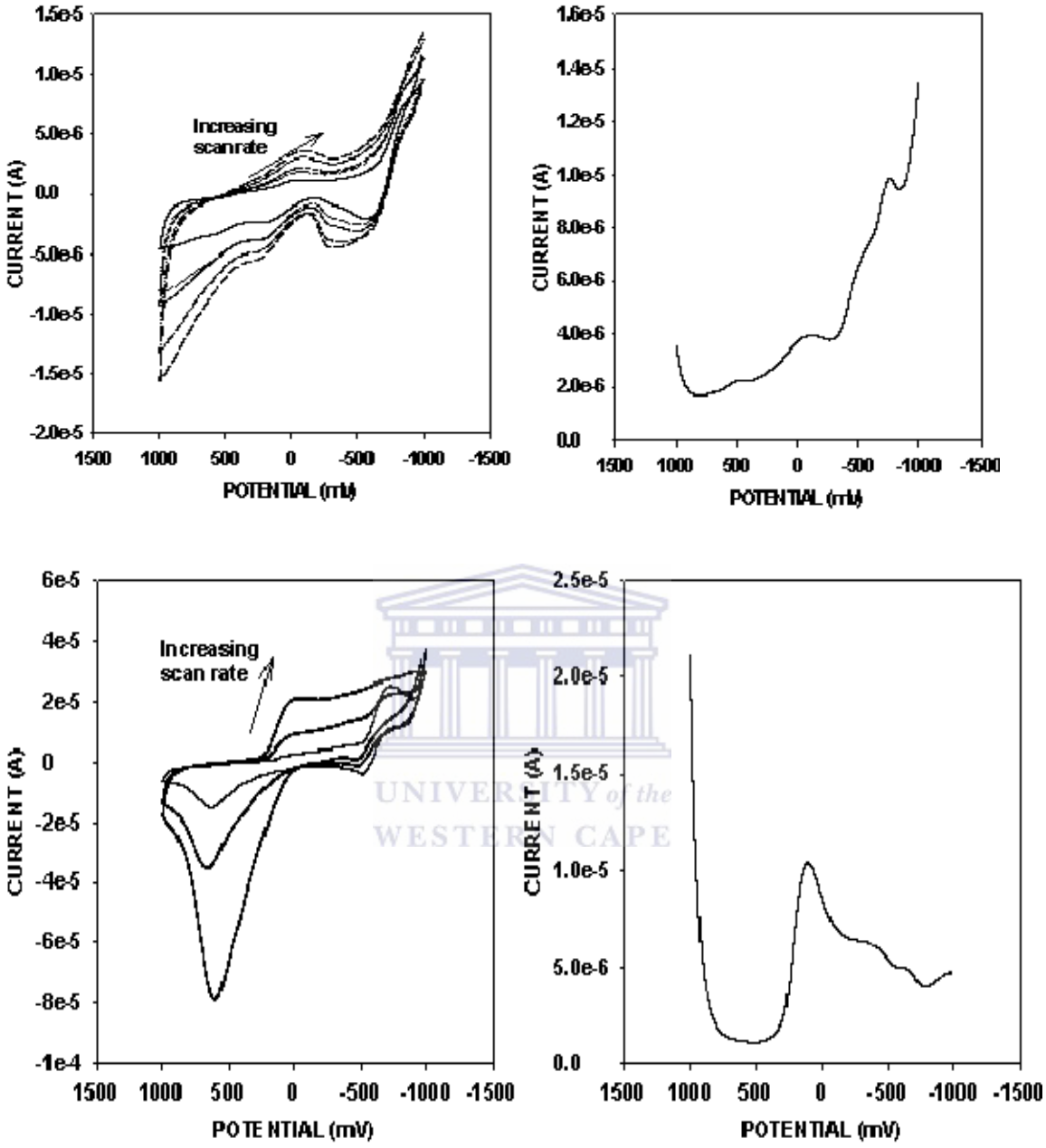

Figure 4.22: Representative cyclic and square wave voltammograms for PANi/NSA (above) and POMA/ASA (below) taken in phosphate buffer pH 7.02.

The estimated D_e values of the composites in phosphate buffer lay in the range 10^{-10} - 10^{-9} cm^2/s which indicates the rate of electron hopping was relatively slowed down in phosphate buffer probably because the medium is not as conductive as that of HCl. The heterogeneous rate constants had magnitudes of 10^{-5} cm/s which again depicted slower

electron transfer exchange rates. However, the addition of KCl to the buffer electrolyte greatly boosted its conductivity with resultant kinetic parameters being comparable to those observed in HCl. Furthermore, the addition of KCl would not affect any intended applications since the KCl is a component in bodily fluids.

4.7 Conclusion

The successful chemical synthesis of ASA and NSA doped polyaniline composites has been presented. UV-Vis and FTIR characterization showed the composites were conductive and doped. Scanning electron microscopy micrographs showed a tendency to form fibrillar morphology at lower monomer to dopant ratios but formation of granulated PANi at higher ratios. The polymer composites mainly displayed two types of electrochemistry. The PANi/NSA composites displayed reversibility with the rest displaying typical quasi-reversible characteristics as was confirmed by estimated range of values for the heterogeneous rate constants. The composites were electroactive with main redox couples centered around 200 and 600 mV. Additional peaks were associated with the degradation products of over-oxidized polyanilines, or to the incorporation of dimmers/oligomers within the polymer matrix. Evidence for formation of polymer/surfactant hybrid complexes was observed in both ASA and NSA-doped PDMA composites. This was taken as proof for successful doping and at the same time as evidence that the new materials bore both polymer and surfactant characteristics. The calculated diffusion coefficient values for the composites in the range (1.1 – 8.9) x 10^{-6} in HCl were in agreement with those reported for polyaniline systems and were indicative of the composites suitability for application in mediation roles. There was a considerable decrease on the electrode kinetics of the composites on changing from a more conductive medium (HCl) to a less conductive one (PB). Finally, the polymers displayed good electroactivity even in phosphate buffer around neutral pH indicating the dopants had enabled the polymers to achieve electroneutrality.

Chapter 5

Electrosynthesis and characterisation of sulphonated polyanilines

5 Introduction

This chapter discusses the electrodeposition of SPAH mainly using potentiodynamic techniques (cyclic voltammetry) followed by an electrochemical study of the behaviour of the resultant polymers in acidic and buffer solutions. The electrodynamics of the electrodeposition processes and the kinetic behaviour in the two solutions are interrogated through the Randels-Sevćik and Anson models. The classical Ohms relation was employed to evaluate the conductivity characteristics of the SPAH films and values compared with those of closely related polymers based on the four point probe method.

5.1 Electrosynthesis of SPAH

For all the sulphonated polyanilines prepared in this study, the potential sweep techniques were used for the electrodeposition. The various SPAH prepared included those of anthracene and naphthalene sulphonic acid doped PANi and its derivatives. They have been abbreviated as; PANi/NSA, POMA/NSA, PDMA/NSA, PANi/ASA, POMA/ASA, and PDMA/ASA. All potentials were measured against an Ag/AgCl electrode.

5.2 Optimization of scan rate for electrosynthesis

It is known that the characteristics of the resultant polymer are greatly dependent on the synthesis conditions. The supporting electrolyte, reagent concentration, applied potential, type of solvent and the pH of polymerisation bath are factors that have been found to influence the characteristics of the resultant PANi (Widera et al., 1998: 265-272). In view of this, the electrodeposition of SPAH was carefully designed to keep the synthetic conditions as similar as possible. For all the electrodeposition processes the same

concentration of supporting electrolyte (1 M HCl) and a dopant to monomer ratio of 0.5:1 was maintained. The same electropolymerisation potential window was used for all the electrodeposition processes. Although different potential windows were tried out, the window of -200 → +1000 mV was found to be the best for the production of highly electroactive SPAH as depicted through the well defined redox processes. For all the electrodeposition processes, the pH of the polymerisation baths was maintained between 0.5 - 1. In order to obtain the best scan rate for producing visible, green coloured, compact PANi with reversibility characteristics, the polymerisation of the polyanilines was carried out at different scan rates 5, 10, 20, 50 and 100 mV/s (Fig. 5.1). The different films obtained were eye-inspected for colour and homogeneity but reversibility was evaluated based on the peak-to-peak separations for the third redox couple (C/C') in the consequent graphs (Figures 5.2 - 5.4).

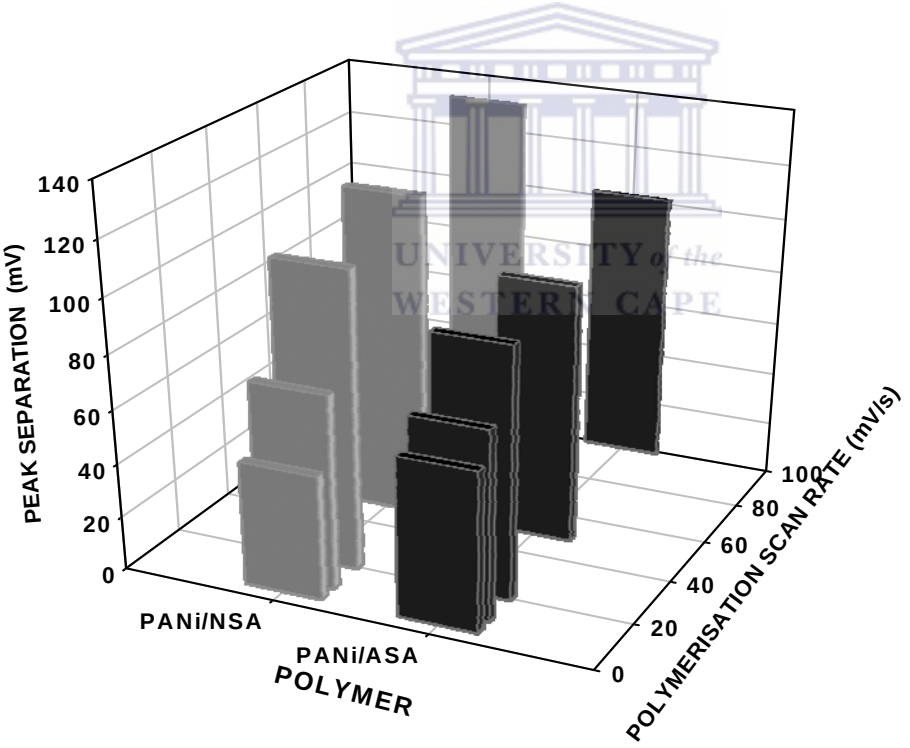

Figure 0.1: Evaluation of polymer reversibility based peak-to-peak separation with variation in the polymerisation scan rate.

Figure 5.1 shows that the peak-to-peak (ΔE_p, mV) separations for the ASA and NSA doped PANi increased with scan rates. At scan rates of below 20 mV/s, ΔE_p values were

less or close to 59/*n* (mV), associated with a reversible system. The polyanilines have been identified as one electron systems (Orata et al., 2000:211-216). However, as the polymerisation scan rate increased, ΔE_p, (mV) also increased to about 100 and 130 mV for the PANi/ASA and the PANi/NSA films respectively. It means the PANi systems exhibited Nernstian characteristics at low scan rates but deviated to quasi-reversibility as the scan rates increased. Furthermore, although the films obtained at high scan rates were very scanty, those prepared at especially 5 and 10 mV/s were green, visible homogeneous, compact films. Slow scan rate allowed for more time for the movement of flux to the electrode leading to deposition of more polymers at low scan rates. Analysis of the ΔE_p values as depicted by the third redox couple indicated at the low scan rates of 5 and 10 mV/s, the values were close to 59/*n* mV, indicating reversibility. Reversibility demands that the electron transfer kinetics be fast enough to maintain the surface concentrations of the oxidized and reduced species as dictated by the Nernst equation (Bard and Faulkner, 2001:161). Low scan rates allow for the surface concentrations of the reduced /oxidized forms of the polymer to adjust as per the potential change thus obeying the Nernst equation. Similar trends were realized for the POMA and PDMA systems doped with both NSA and ASA. A scan rate of 10 mV/s was chosen for all the electrodeposition processes.

5.3 Electrosynthesis of SPAH

Figures 5.2 – 5.4 (graphs **i**, **iii**, **v**, **vii**, **ix**, **xi**) present the cyclic voltammograms (CV) for the electrodeposition of the various sulphonated polyanilines. The graphs have been coded as; PANi/ASA (**i)**, PANi/NSA **(iii)**, POMA/ASA **(v)**, POMA/NSA (**vii)**, PDMA/ASA **(ix)**, PDMA/NSA **(xi**). In all the electrodeposition CVs three redox couples were observed indicating that the SPAH was electroactive in nature. In addition, the peak currents (I_p) increased with the cycle number which was evidence for the continual electrodeposition of SPAH at the working electrode. Since electrodeposition occurred on previously deposited layers as the cycling continued, it means the SPAH was conductive providing electrical communication between new polymer layers and the electrode.

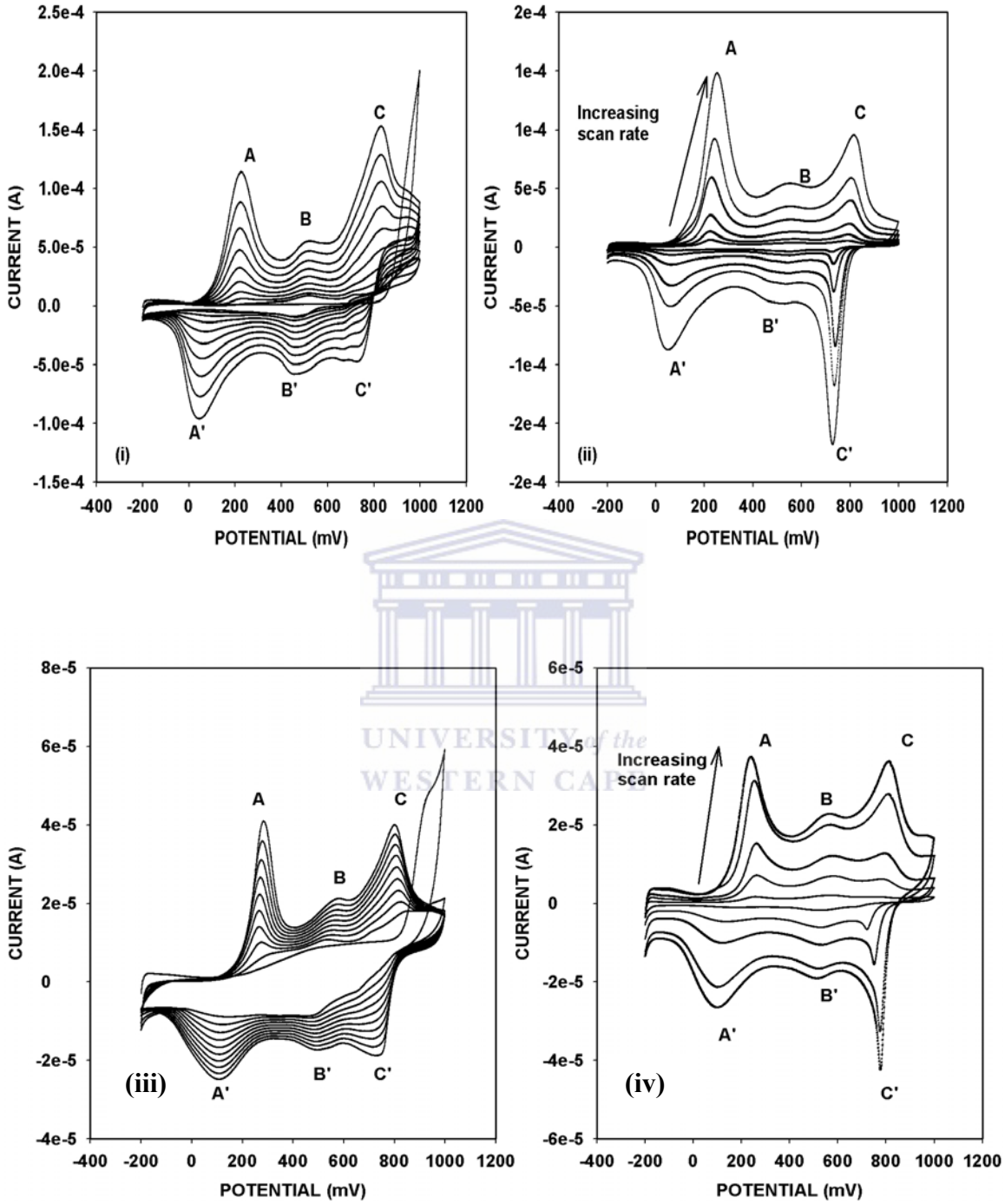

Figure 0.2: Cyclic voltammograms for the electrodeposition of PANi/ASA (i), PANi/NSA (iii).

Synthesis conditions were; -200 → +1000 mV potential window, 10 cycles on a platinum disc electrode at a scan rate of 10 mV/s. Figures (ii) and (iv) are multi-scan CVs for PANi/ASA and PANi/NSA respectively in 1 M HCl at same window.

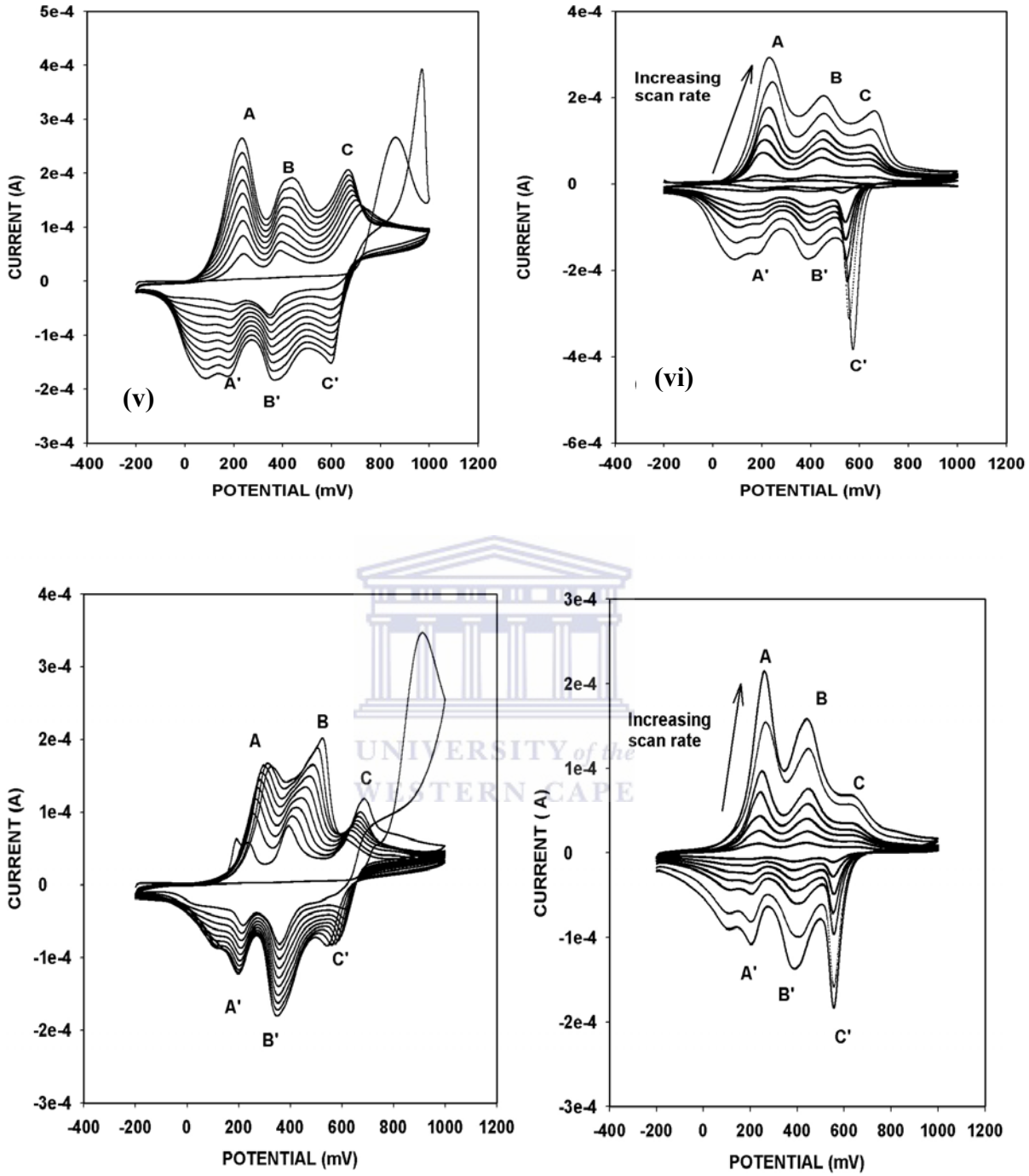

Figure 0.3: Cyclic voltammograms for the electrodeposition of POMA/ASA (v), POMA/NSA (vii).

Synthesis conditions were; -200 → +1000 mV potential window, 10 cycles on a platinum disc electrode at a scan rate of 10 mV/s. Multi-scan rate voltammograms for POMA/ASA (vi), POMA/NSA (viii) in 1 M HCl at same window.

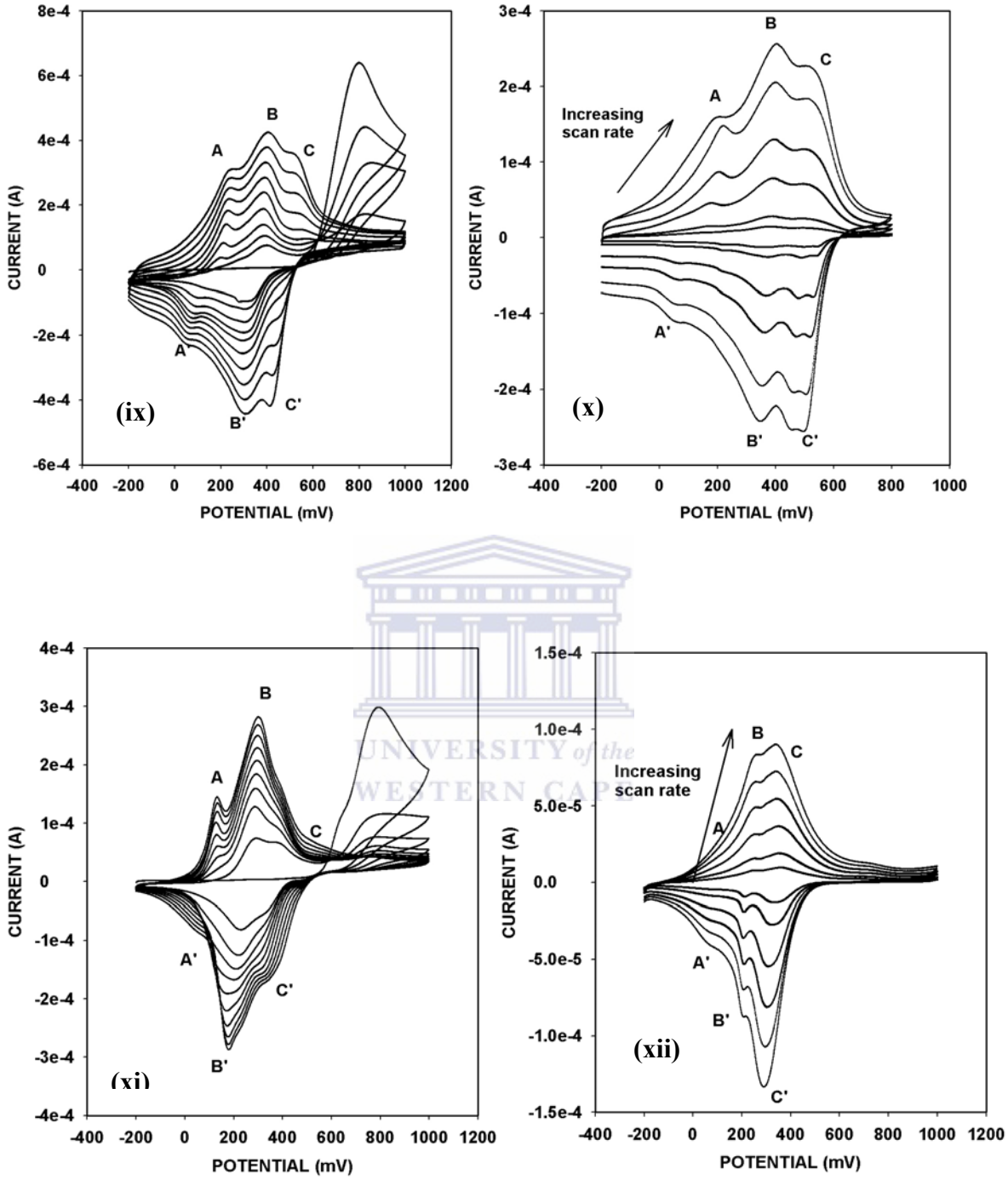

***Figure 0.4: Cyclic voltammograms for the electrodeposition of PDMA/ASA (ix), PDMA/NSA (xi*).**

Synthesis conditions were; -200 → +1000 mV potential window, 10 cycles on a platinum disc electrode at a scan rate of 10 mV/s. Figures (x) and (xii) are multi-scan rate CVs for PDMA/ASA, and PDMA/NSA respectively for in 1 M HCl at same window.

5.3.1 Peaks A/A'

According to MacDiarmid et al. (2001:269-279) the first redox couple A/A' in the electrodeposition graphs (**i**, **iii**, **v**, **vii**, **ix**, **xi)** represents the polyleucoemeraldine/polymeraldine salt (PLE/PES) transition. The formal potentials ($E^{0'}$, mV) for the various SPAH for this redox couple were estimated to be; 135 for PANi/ASA; 185 for PANi/NSA; 203 for POMA/ASA; 215 for POMA/NSA; 200 for PDMA/ASA. For PDMA/NSA peak 'A' occurs at 134 mV but the corresponding peak 'A'' merges with the middle couple making it difficult to identify.

Thus, with a few anomalies, it was observed that the oxidation of the (polyleucoemeraldine) PLE form of SPAH to the (polyemeraldine salt) PES form, occurred at lower formal potentials for PANi as compared to the substituted polyanilines. For instance the oxidation of the PLE form of PANi/ASA occurred at an $E^{0'}$ value of 135 mV compared to 200 and 203 mV for POMA/ASA and PDMA/ASA respectively. In other words, the formal potentials for the PLE/PES transition in substituted PANi is shifted to higher potentials compared to that of parent polyaniline. A similar trend was observed for alkyl substituted polyanilines and was attributed to an increase in torsional angle between the phenyl rings of the polymer due to the presence of relatively bulky alkyl substituents in the polymer chain (Lindfors and Ivaska, 2002: 65-74). According to the authors such an increase in torsional angle leads to a decrease in the degree of orbital overlap between the π-electrons in the phenyl rings and lone pair of nitrogen atoms (the immine nitrogen on the polymer chain) causing a decrease in conjugation length with a consequential increase in the oxidation potential (Wei et al., 1989: 495-499; Lindfors and Ivaska, 2002: 43-52; Barbero et al., 1991:437-443).

Elsewhere, in agreement with this observation, Yue et al. (1991: 2665-2671) ascribed this shift to positive potentials in the case of substituted polyanilines to the subsequent ring twisting due to bulkier substituents with a consequential reduction in chain conjugation. Such reduction in conjugation length resulted in the reduced stability of the polyleucoemeraldine radical cation formed in the first anodic process because the

methoxy groups within the substituted PANi matrix caused steric hindrance forcing the adjacent phenyl rings in the polymer chains to twist from a coplanar arrangement with a decreased stability of this redox couple. As a result the oxidation of PLE form of substituted PANi takes place at higher potentials.

5.3.2 Peaks B/B'

The middle couple B/B' in all the electrodeposition voltammograms occurred at formal potentials between 300-500 mV and has been assigned differently by different authors. It is due to degradation products of over-oxidized PANi (Wei et al., 1989: 495-499), reactions in the polymer side chains (Komsiyska et al., 2005: 88-95) or to the redox reactions of the degradation products hydroquinone to quinone (Huang et al., 2006: 2756-2764). Elsewhere, Widera et al. (1997: 29-37) assigned this second couple to the incorporation of linear or cyclic dimers within the polymer matrix whereas Valter et al. (2002: 1535-1541) assigned it to the defects in the linear structure of the polymer. It has been shown that at potentials ≥ 1000 mV PANi systems may undergo some degradation and that substituted polyanilines easily undergo dimerisation. For all the electrodeposited SPAH, this middle couple was assigned in line with the explanation of Wei et al. and Widera et al..

A close observation of the electrodeposition voltammograms reveals that this middle couple is higher for POMA and PDMA compared to that due to PANi in almost all the electrodeposition CVs. The area under a redox wave is essentially an integration of the overall charge (Q, mC) passed during the peak formation. It was found out that the charge (Q, mC) realized for both PANi and substituted PANi based on peaks B/B' were different. For instance, the charge (mC) recorded for the oxidation peak ‘B’ was 0.073 for POMA/ASA, 0.1632 for PDMA/ASA, and 0.0094 for PANi/ASA. Thus the area under this peak ‘B’ was 12.8% and 58% higher in POMA/ASA and PDMA/ASA respectively than that recorded for PANi/ASA. Since this middle-couple formation is often associated with dimer formation as Widera et al. (1997: 29-37) explains, the above observations

indicated that substituted polyanilines had a tendency to undergo dimerisation than the parent PANi.

It has been found out that the initial polymerisation of substituted PANi is relatively fast compared to that of the parent PANi at initial electrodeposition cycles. Palys et al. (2000: 111-119) observed that for instance the deposition of PDMA occurred very fast with a polymer layer appearing on the electrode by the first cycle. According to the last authors, such polymer formation was due to dimerisation in substituted PANi. However, as cycling continues the tendency to dimerisation for substituted PANi hampers the polymerisation rate thus reversing the trend as is evident form the electrodeposition CVs especially those of POMA/NSA (**vii**) and PDMA/NSA (**xi**). This is because once the dimers are formed they diffuse away from the surface of the electrode, leading to diminished polymer growth (Lindfors and Ivaska, 2002: 43-52; Kilmartin and Wright, 1999: 145-156).

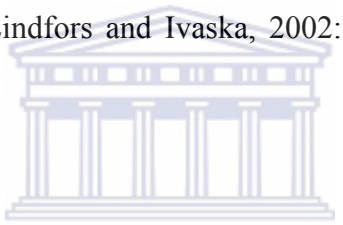

5.3.3 Peaks C/C'

The third redox couple C/C' represents the polyemeraldine salt /polypernigraniline PES/PPN transition. This couple was observed at $E^{0'}$, mV of 779 for PANi/ASA, 771 for PANi/NSA, 590 for POMA/ASA, 583 for POMA/NSA, 476 for PDMA/ASA, and 402 for PDMA/NSA. A comparison of these formal potentials reveals that the oxidation of the polyemeraldine salt to the polypernigraniline form (PPN) of PANi (third redox couple) occurs at higher potentials in either PANi/NSA or PANi/ASA compared to the corresponding substituted polyanilines. A similar behaviour was observed for alkyl substituted polyanilines (Wei et al., 1989: 495-499; Lindfors and Ivaska, 2002: 43-52) and was attributed to the electron donating effect of the alkyl groups that stabilized the PPN forms of alkyl substituted polyanilines leading to its oxidation at lower potentials. Given the methoxy substituents in POMA and PDMA can also express similar inductive effects, a similar reason is assumed here.

5.4 Nucleation signals for the electrodeposition of SPAH

In order to understand the mechanisms involved during the electrodeposition of SPAH, a scrutiny of the first electrodeposition cycle was done. In all the voltammograms, a nucleation loop signal associated with the formation of radical cationic species emanating from monomer oxidation was observed. Barriós et al. (2006: 128-135) have demonstrated that polymer formation at a working electrode involves the nucleation (indicated by the nucleation loop) and the polymer growth stages.

Figure 5.5 is a mapping of the first electrodeposition cycle of the ASA doped polyanilines. For PANi, the first anodic sweep exhibits a maximum current at ca. 950 mV. On potential reversal, the aniline oxidation current remains positive until about 650 mV (Fig. 5.5) which indicates an increasing electrode surface area (Norris et al., 2000: 3237-3243).

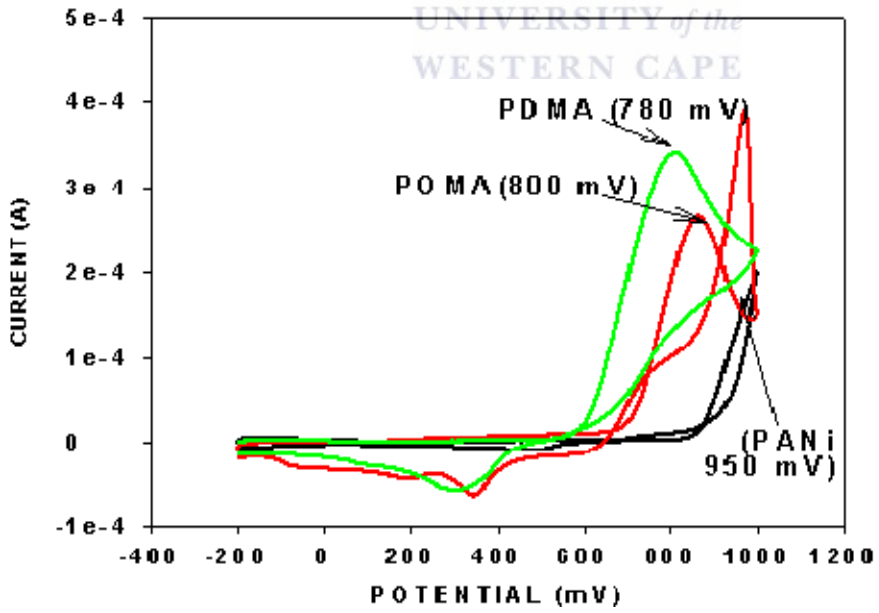

Figure 0.5: Mapping of the first electrodeposition cycle to show onset of monomer oxidation for PANi/POMA/PDMA /ASA.

Two more reduction peaks appear on the cathodic sweep. With consequent scan, rapid growth of well formed redox couples at a considerably lower potential of ca. 700 mV is observed (electrodeposition graphs **(i)** and **(iii)**). For instance, prior to nucleation the current observed for the PLE peak 'A' was close to 0.000 mA. After nucleation, this peak increased from 0.009 mA in the second cycle to 0.048 mA by the 10 cycle for PANi/ASA. The dramatic 18.7% current increase between the 1st and 10th voltammetric cycle indicates the autocatalytic effect of the nucleating species on the subsequent polymer deposition. A similar trend was observed for PANi/NSA.

In POMA/ASA monomer oxidation onsets at ca. 800 mV, with two cathodic peaks at 200 and 400 mV appearing on the reverse scan. Consequent polymer deposition occurs at much lower potentials the maximum being 500-600 mV (graphs **v, vii**). In PDMA/ASA, monomer oxidation onsets at ca.780 mV, followed by the formation of a very broad peak at ca.300 mV in the reverse scan. Rapid growth was observed during the subsequent cycles distinguishing between the nucleation and polymer growth stages (graphs **ix, xi**).

5.5 Multi-scan rate study of the electrochemical behaviour of SPAH

The electrochemical behaviour of SPAH electrodeposited on a platinum disc electrode was studied in 1 M HCl between -200 - +1000 mV potential limits (graphs **ii, iv, vi, viii, x, xii** in figures 5.2-5.4). An Ag/AgCl (3 M NaCl) reference and a platinum wire counter electrode were used. The CVs obtained closely resemble those reported for the various polyanilines (Barriós et al., 2006: 128-135; Viva et al., 1999: 180-189; Palys et al., 2000: 111-119). In all the voltammograms, three redox couples identified similarly to the previous discussion were observed (see Section 5.3).

During the multi-scan rate study, potential cycling was carried out at scan rates of between 5-100 mV/s. The formal potentials for the various SPAH during the multi-scan rate study closely agreed with those reported for the same processes during the electrodeposition but cathodic or anodic potential shifts were observed with increase in

scan number. The formal potentials (mV) observed for the PLE/PES transition were; 144±14 for PANi/ASA (**ii**); 185±10 for PANi/NSA (**iv**); 183±20 for POMA/ASA(**vi**); 215±6 for POMA/NSA (**viii**); 160± 4 for PDMA/ASA (**x**); 235±12 for PDMA/NSA (**xii**). The formal potentials (mV) realized for the third redox process similarly identified as the PES/PPN transition as in the electrodeposition CVs were; 766±4 for PANi/ASA (**ii**); 771±18 for PANi/NSA (**iv**); 590±6 for POMA/ASA (**vi**); 583±5 for POMA/NSA (**viii**); 476±12 for PDMA/ASA (**x**); 376±12 for PDMA/NSA (**xii**). The fact that the polymers were solely tethered to the electrode unlike during electrodeposition where both solution and immobilized species were involved meant that the only mode of electrical communication was through the diffusion of electrons along the polymer chain which could lead to a time lag of the electron exchange processes at the interface leading to peak shifting and spreading.

A comparison of the formal potentials of this PES/PPN transition reveals that the formal potentials for the PDMA polymers were lower in all cases compared to the other polymers. This phenomenon has been associated with the extra stabilization of the double methoxy groups on the PDMA ring and also on the ensuing steric hindrance associated with these groups causing a reduction in orbital overlap and a decrease in conjugation, with consequences of lowered oxidation potential.

A closer study of the cyclic voltammograms revealed in almost all multi-scan rate voltammograms, the peak separation between the PLE/PES transition was often >100 mV. However, on a closer scrutiny, it can be seen that the PES peak (A') is actually a combination of two closely stationed peaks. This is especially evident on the POMA CVs (graphs **vi** and **viii**) but is also the case for the other polymers e.g. PANi/NSA (Fig.5.6) and could be supportive of the polyaniline inter-conversion mechanism proposed by Lindfors and Ivaska, (2002: 65-74) (Fig. 2.3). It is proposed that the PLE/PES transition is actually a two stage process involving first the conversion of the PLE form to the polyemeraldine base form followed by Protonation of the latter to the PES form. Alternatively, there exists an equilibrium between the polyemeraldine base and the

polyemeraldine salt forms (Fig. 2.3) marked by the movement of protons into and out of the polymer chain.

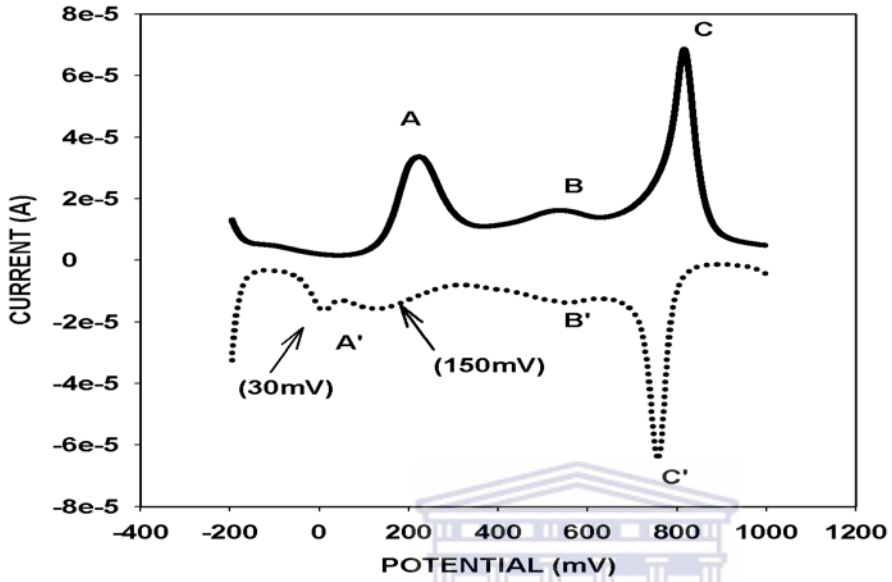

Figure 0.6: Oxidative (upper) and reductive (lower) square wave voltammetric scans for PANi/NSA at 100 mV/s scan rate in 1 M HCl supporting electrolyte between -200 - +1000 mV.

5.5.1 Kinetic behaviour of the electrodeposited SPAH in acidic medium

The ultimate goal of the synthesis of SPAH was to access their possible applications in biosensor construction as effective electron transfer mediators. A study of the electrodynamics of the deposition processes and the behaviour of SPAH in both acidic and neutral solutions was a prerequisite towards evaluating the utility of the SPAH as electromediators in biosensors. Under normal physiological circumstances, the HRP and CYP based biosensors will reduce substrates by the transfer of reducing equivalents resulting in the enzyme oxidation (Iwuoha et al., 1997: 749-761, Iwuoha and Smyth 2003: 237-244). Natural electron donors, e.g. NADPH, then regenerate the oxidized enzymes to their resting states and the cycle continues. In HRP or CYP-based biosensors, the transfer of reducing equivalents to the substrates leaves the enzymes in their oxidized

forms. Electron supply from a cathodically polarized electrode regenerates the enzyme to their resting state for more substrate reduction.

Electron mediators have been used extensively to provide the link between the enzyme redox center and the electrode without which there would be no meaningful electrical relays. It has been shown that the acceptance of reducing equivalents by the PES (A') form of PANi leads to its reduction to the PLE (A) form (Iwuoha et al., 1997: 749-761). The transfer of reducing equivalents from the PLE form of PANi to the oxidized enzyme regenerates the enzyme to its resting state. That is, in biosensor construction, the PLE/PES (A/A') transition plays the key electromediation role. In view of this, the consequentially discussed electron processes are solely based on this redox couple.

Based on the multi-scan rate voltammograms for the various SPAH (Figures 5.2-5.4, graphs **ii, iv, vi, viii, x, xii**), it was noticed that peak (A') did not vary much with scan rate. The peak shifts (mV) recorded for this peak was: 64±4 for PANi/ASA (**ii**), 108±11 for PANI/NSA (**iv**), 143 ±10 for POMA/ASA (**vi**); 204±5 for POMA/NSA (**viii**); 102±4 for PDMA/ASA (**x**); 202±10 for PDMA/NSA (**xii**). This minimal potential shifting with scan rate is characteristics of a surface bound species (Mathebe et al., 2004: 115-120) and is described by the Anson model (Bard and Faulkner, 2001: 592). Under such circumstances the area under the reduction/oxidation peak is an integration of the overall charge passed during its formation and is governed by the equation:

$$\Gamma^* = Q / nFA \qquad (3.8)$$

where Γ^* is the PES (peak A') surface concentration (mol cm^{-2}), n is the moles of reducing equivalents passed, F (C mol $^{-1}$) is the Farady constant and A (cm^2) is the electrode area.

The overall charge (Q, mC) obtained for the PES peak for the various SPAH and the corresponding surface concentrations are collected in Table 5.1. Based on the Anson model, the surface concentrations (Γ^*, mol cm^{-2}) obtained for the various SPAH were;

5.2 x 10^{-8} PANi/ASA; 5.9 x 10^{-9} for PANi/NSA; 1.7 x 10^{-8} for POMA/ASA; 1.9 x10^{-8} for POMA/NSA; 9.8 x 10^{-9} for PDMA/ASA; 1.3 x 10^{-8} for PDMA/NSA. These surface concentrations agree with those reported in literature for similar PANi systems (Mathebe et al., 2004: 115-120; Brahim et al., 2003: 123-137). While it was not immediately clear as to why the surface concentration of PANi/NSA was relatively low compared to the other SPAH, the trend that emerged was; PANi > POMA > PDMA. Given the presence of methoxy group substituents in the *o*-MA and DMA monomers, the diffusion of flux to the electrode is bound to be slower for the two leading to the lower concentrations.

It was also found that the PLE peak, 'A' in almost all the multi-scan rate voltammograms shifted either cathodically or anodically depending on the polymer. For instance, there were 29 and 22 mV cathodic potential shifts for the PLE peak in POMA/ASA and PDMA/NSA respectively. Similar, albeit smaller, potential shifts were observed for the other SPAH and depicted diffusion controlled kinetics associated with an electron hopping process along the polymer chains. According to Mathebe et al. (2004: 115-120), such an electron hopping processes is likely to occur along the benzene units on the polymer chains. Under such circumstances, the Randels-Sevćik model (equation 3.4) or the Nicholson and Shain relation (equation 3.5) could give a viable estimate of the rate at which the electrons are hopping along the benzene units. This electron hopping rate (D_e, cm^2/s) estimate is a useful indicator of the suitability of a polymer for use in electromediation on a scale where D_e values of 10^{-12} cm^2/s are relatively too low for effective electrical communication. Figure 5.7 is a Randels-Sevćik plot (plot of square root of scan rate versus peak currents) for the various SPAH based on the PLE peaks ('A').

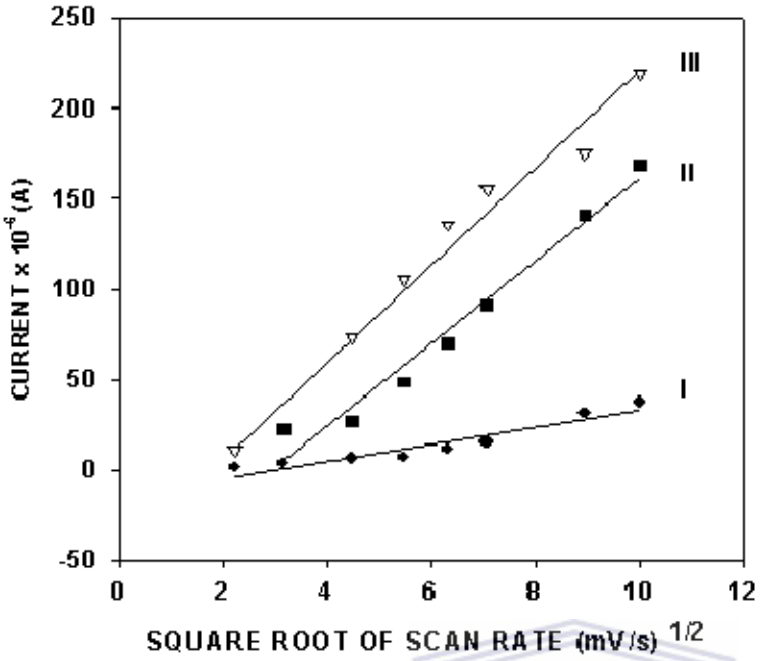

Figure 0.7: A typical Randles- Sevćik plot showing the peak current (peak A) dependence on square root of scan rate. PANi/NSA (I), PDMA/NSA (II) and POMA/NSA (III).

The slopes obtained from the plots were; 17.5 (r^2=0.91) for PANi/NSA; 4.7 (r^2=0.93) for PANi/ASA; 26.8 (r^2=0.98) for POMA/NSA; 26.8 (r^2=0.93) for POMA/ASA; 17.5 (r^2=0.97) for PDMA/NSA; 22.87(r^2=0.98) for PDMA/ASA. The slightly higher deviation from linearity for some plots was interpreted to indicate quasi-reversibility. This was further implied by the increasing peak-to- peak separations and the deviation of the ratio of the cathodic to anodic peak currents from 'unity'. For instance the $|I_{pc} / I_{pa}|$ obtained from the various systems were; 1.86±0.13 for PANi/ASA; 0.736±0.12 for PANi/NSA; 0.601±0.09 for POMA/ASA; 0.55±0.06 for POMA/NSA; 0.76±0.19 for POMA/ASA; 1.03±0.04 for PDMA/ASA.

These findings imply the fact that, despite using a low scan rate for polymer deposition (in order to obtain a polymer with reversibility characteristics), the actual behaviour of the electrodeposited polymer is dependent on the media of characterisation and the potential sweep rate. This explains why the PANi systems display reversibility at low

scan rates and deviate from reversibility as the scan rate increases. For instance, for the POMA/ASA and PDMA/NSA systems, ΔE_p (mV) were 60 and 57 respectively at 5 mV/s. Thus based on the results on the 5 mV/s the Randels-Sevćik equation was used to estimate the diffusion coefficients (D_e cm^2/s) for the various systems. The D_e values obtained lay in the range 2.6 - 6.4 x 10^{-6} cm^2/s and are reported in Table 5.1. In general the diffusion coefficients obtained for the PANi systems (all redox states) are higher than D_e of 6.5 x 10^{-8} cm^2/s reported for PANi-polyvinylsulfonate systems (Iwuoha et al., 1997: 749-761). The D_e of 1.78- 0.75 x 10^{-8} cm^2/s obtained for doped –POMA (Raposo and Oliviera, 2002: 6866-6874) are also lower than those obtained here for the POMA and PDMA systems. Invariably, one should expect the D_e for the PANi systems to be higher than those of the substituted PANi. This trend did not emerge but could imply the existence of dimers and/or oligomers of substituted PANi at the electrode. The latter have shorter polymer chains and thus the diffusion of electrons and the electron exchange at the interface could be faster.

Similarly, the rate of electron exchange at the interface were estimated by use of equation 3.6 as explained in (Section 3.3.2). The estimated k^0 (cm/s), values for the PLE/PES transition in all the polyanilines lay in the range 2.6 x 10^{-4} - 6.16 x 10^{-3} cm/s. The standard rate values obtained here depict moderately fast kinetics on a scale where 10 cm/s values suggest fast electrode kinetics (characteristic of freely diffusing ionic species) and 10^{-12} (cm/s) being too sluggish (Bard and Faulkner, 2001: 87-102). It means for the PLE/PES transitions, the SPAH can attain equilibrium on a short time scale and that only small activation overpotential is needed to drive the electrode process as long as the sweep rate is kept low.

5.5.2 Conductances of electrodeposited SPAH

Based on the previous discussion, it has been shown that the PLE/PES peaks are the most important for biosensor applications. In view of this, the conductance of the various electrodeposited SPAH was estimated based on this peak by use of the classical Ohms

relation as described in section 4.5.4. The conductances realized for the various SPAH were in the range 0.085 – 3.47 x 10^{-2} S/cm.

Table 0.1: A summary of the kinetic parameter values for the SPAH systems

Polymer	I_{pc}/I_{pa} ratio at 5 mV/s	Charge(Q, mC) under peak A (PES)	Surface concentration Γ*(mol cm^{-2})	Diffusion coeff. (D_e, cm^2/s)	rate const.k^0 cm/s)	Conduct -ance (S/cm)
PANi/ASA	1.22	0.089	5.2 x10^{-8}	1.72 x10^{-6}	2.60 x10^{-4}	1.08 x10^{-2}
PANi/NSA	1.04	0.010	5.9x10^{-9}	2.28 x10^{-6}	2.94 x10^{-4}	0.085 x10^{-2}
POMA/ASA	0.75	0.029	1.7 x10^{-8}	1.34 x10^{-6}	2.86 x10^{-3}	1.10 x10^{-2}
POMA/NSA	0.68	0.032	1.9 x10^{-8}	1.39 x10^{-6}	2.91 x10^{-3}	0.98 x10^{-2}
PDMA/ASA	0.80	0.011	9.8 x10^{-8}	6.41 x10^{-6}	6.61 x10^{-3}	0.90 x10^{-2}
PDMA/NSA	1.03	0.024	1.3 x10^{-8}	4.20 x10^{-6}	3.92 x10^{-3}	3.47 x10^{-2}

As observed in the diffusion coefficient values, the highest conductance obtained was that of PDMA/NSA. Ideally, it is expected that the conductances for unsubstituted PANi should actually be higher than that of substituted PANi. The bulkier methoxy groups in the latter would cause steric hindrance and an increased inter-chain distance with the consequences of lowered frequency of electron hopping between the polymer units leading to lower conductivities. However, other authors have reported the same phenomenon (D' Aprano et al., 1993: 145-158; Palys et al., 2000: 111-119). According to the latter authors, PDMA forms more regular materials that exhibit high conjugation length and conductivity despite the presence of substituents. Elsewhere, Huang et al. (2002: 155-163), has reported that PDMA has conductivity characteristics similar to that of PANi meaning that other factors other than steric hindrance come into play. In general the conductance of all SPAH was generally high except in the case of PANi/NSA whose conductivity was an order of magnitude lower. The SPAH conductivity estimates compare well with those reported for PANi-CSA (Zhang and Wan, 2005: 24-31), PANi-

PSSA-FA and PANi-FA systems (Iwuoha et al., 2006: 453-458) and are infact several orders of magnitude higher than those reported for halogenated PANi (Ay§egül et al., 2004: 41-48).

5.6 Behaviour of SPAH in neutral medium

It is well known that enzymes are pH sensitive and operate best around their physiological pH. The physiological pHs for the HRP and CYP enzymes have been reported to be 6.7-7.2 and 7.2-7.5 respectively. In view of this a multi-scan rate study was performed in phosphate buffer. Figures 5.8-5.9 represent some cyclic and square wave voltammograms of some of the SPAH. In all the CVs, well formed redox waves are observed indicating that the SPAH were still electroactive even in neutral and/or slightly basic media. Ideally, undoped polyaniline is pH sensitive and looses electroactivity beyond pH 4. It means the incorporation of sulphonic groups into the SPAH matrices stabilized the polymers thus allowing them to maintain electroactivity even at neutral pH. This is because the bulky sulphonic groups cannot easily diffuse out of the polymer matrices once incorporated.

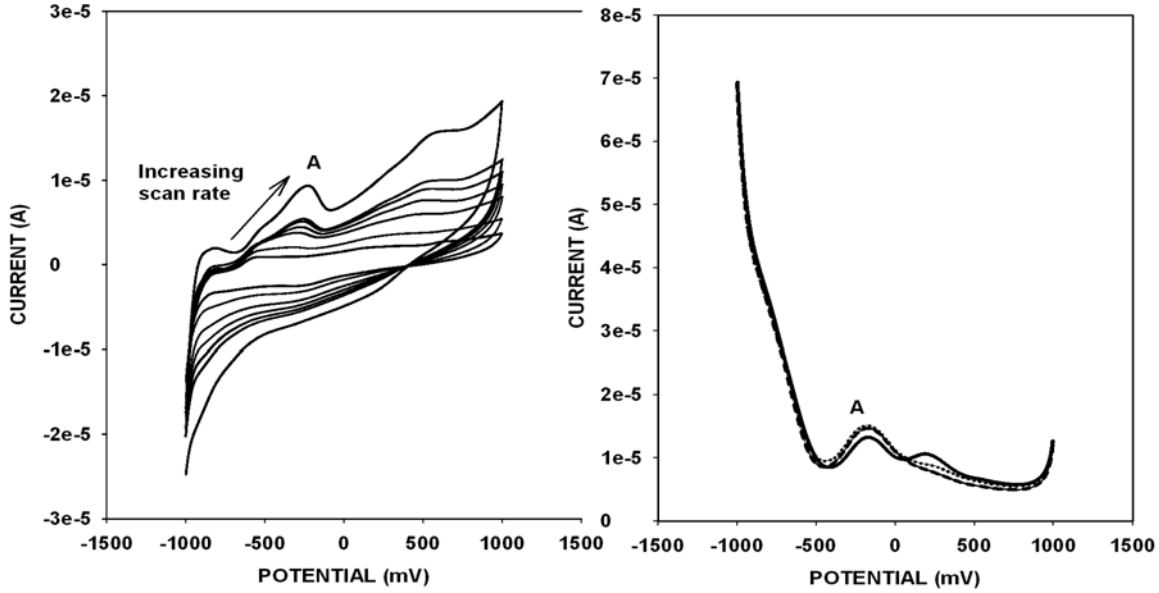

Figure 0.8: Cyclic and square wave voltammetric responses of POMA/ASA in phosphate buffer pH 7.02 at -1000 → + 1000 potential limits.

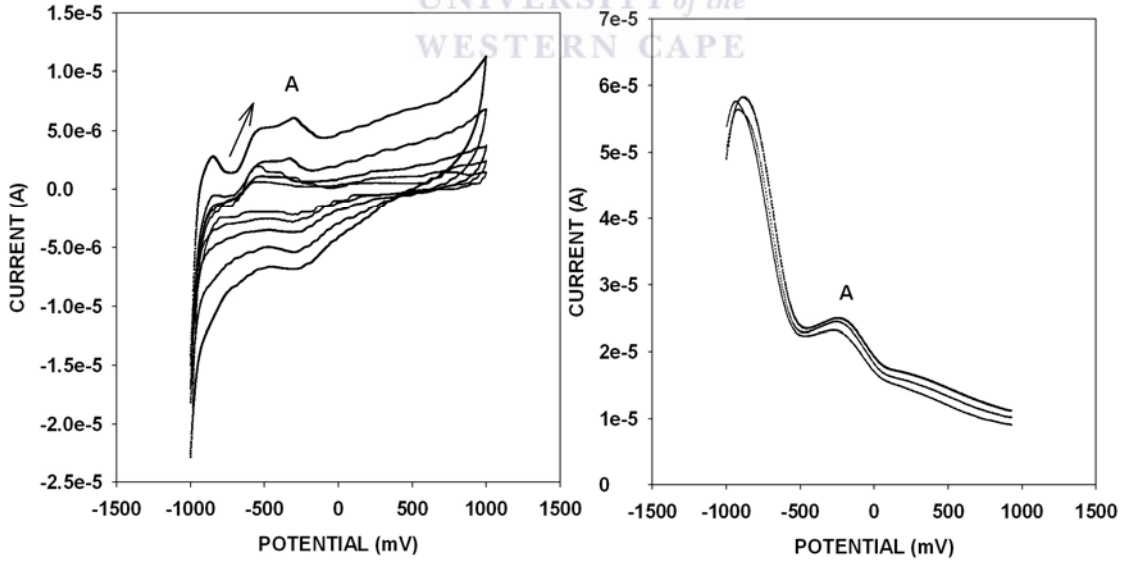

Figure 0.9: Cyclic and square wave voltammetric responses of PANi/NSA in phosphate buffer pH 7.02 at -1000 →+ 1000 potential limits.

Thus the successful doping of SPAH is expressed by the fact that the polymers maintained their electroactivity even at a pH 7.2 unlike HCl doped PANi that rapidly undergoes deprotonation as the pH rises above 4. However, in all the CVs, the PLE peak (peak A) was very distinct but slightly shifted to lower potentials. The conductivities realized for the SPAH in buffer lay in the range 1.4 x 10^{-4} in PANi/NSA to 3.5 x 10^{-3} PANi/ASA. At the same time the diffusion coefficients for the SPAH in buffer was slightly lower in buffer at most being an order of magnitude lower than that of the corresponding polymer in HCl. Nevertheless, the ability of the SPAH to maintain electroactivity and conductivity in neutral media means it can play as effective electron transfer mediators for the construction of biosensors.

5.7 Conclusion

This chapter was aimed at the study of the electrodeposition and electrodynamics of SPAH. It was found that SPAH electrodeposited on a platinum electrode was both electroactive and conductive in both acidic and neutral media showing well formed redox couples. The relatively high diffusion coefficients for the electrogenerated SPAH both in the range 2.6 - 6.4 x 10^{-6} cm^2/s in 1 M HCl and in the magnitude of 10^{-7} cm^2/s in PBS are similar to those reported in literature for similar systems. They imply the suitability of SPAH for electromediation purposes. Again the conductivities of SPAH in the range 0.085 – 3.47 x 10^{-2} S/cm in HCl and 1.4 x 10^{-4} - 3.5 x 10^{-3} in PBS indicates the doping of the polymers with the NSA and ASA dopants stabilized the polymers as expected. It was however noticed that the PDMA form of SPAH would fall off from the electrode after standing in the buffer solution for sometime thus indicating its inability to form stable biosensors.

Chapter 6

Some biosensor applications of sulphonated polyanilines

6 Introduction

After synthesis and exploration of the electrodynamics of SPAH a piloting study was performed on some of the SPAH to verify their applicability as effective electron transfer mediators in the construction of biosensors. Both chemically and electrochemically synthesized SPAH was considered. This chapter therefore, presents results obtained for various types of SPAH using different substrates. The enzymes that were utilized for the sensor construction were mainly horseradish peroxidase (EC.1.11.1.7) type II, 200 units/ mg salt-free powder and the purified human recombinant isozyme cytochrome $P450_{3A4}$ (EC. 1.14.14.1). The substrates employed were hydrogen peroxide, erythromycin and diazinon (inhibitor) and were of high purity.

Having established that the SPAH was both electroactive and conductive in acidic and neutral media, the next task was to determine its electrochemical behaviour in the presence of macromolecules such as enzyme. To accomplish this, the SPAH was co-immobilized with either HRP/or CYP enzyme in the presence or absence of a respective substrate. Either electrostatic doping or drop-coating techniques were used to attach the macromolecule. Figure 6.1 represents the square wave voltammetric results of NSA doped PANi and POMA recorded in phosphate buffer pH 7.02 between -1000 to +1000 mV potential window. The sensitivity was 100 μA/V and potential measured against an Ag/AgCl reference electrode.

Figures 6.1 (**i**) and (**ii**) depict the electrochemical behaviour PANi/NSA and POMA/NSA in phosphate buffer. Only the reductive waves are shown because CYP or HRP catalysed reactions are essentially reductive in nature. All HRP experiments were conducted under anaerobic conditions. In both voltammograms, two cathodic peaks at ca. 189 mV and -

200 mV are observed. Two other smaller hubs were observed at ca. -616 mV and -729 mV all showing the electroactive nature of both PANi and POMA.

On attaching the enzyme, (Fig. 6.1 **ii** and **iv**) the dominant peaks joined up into one peak at ca. -250 mV which is a -71 mV cathodic shift. In addition the relatively smaller peaks shifted to ca. -800 mV. The existence of well formed reductive peaks even after enzyme immobilization was an indication that the PANi or POMA/enzyme complex allowed effective electrical communication between the electrode and the electrode and the enzyme's Fe^{3+} prosthetic group. However, a slight decrease in current was observed upon the immobilization of the biomolecule. For instance, prior to immobilization the peak currents (I_p, μA) for the peak at -189 mV in PANi and POMA were 7.0 and 5.1 respectively. But after immobilization, the currents decreased by one order of magnitude in each case. The decrease of peak current with enzyme immobilization could be associated with the additional diffusional barrier involved due to the addition of the enzyme layer (Adeyoju et al., 1995: 57-64).

On substrate addition, there was a huge current increase of about 5.70 x 10^{-4} A at 1.8 mM concentration of H_2O_2 at ca. -670 mV. Meanwhile, this potential at maximum current shifted persistently to a maximum potential of -800 mV. It was found that despite the original PANi or POMA prominent peak been at -250 mV, upon substrate binding the potential constantly drifted towards more negative potentials. Such a potential shift was reported by Pravda et al. (1995: 127-138) and the shifting towards lower potentials was indicative of an enzyme controlled catalytic reduction of the peroxide. This is so because enzymes provide new reaction pathways with lowered activation energies explaining the decreasing potential on substrate binding.

Figure 6.2 and 6.3 are cyclic voltammograms of the PANi/NSA and POMA/NSA response to 0 and 1.8 mM H_2O_2. The substrate stock concentration was 0.01 M. The CVs show that the current flow at 0 mM substrate concentration is minimal. However upon adding 1.8 mM H_2O_2 a dominating cathodic current is observed.

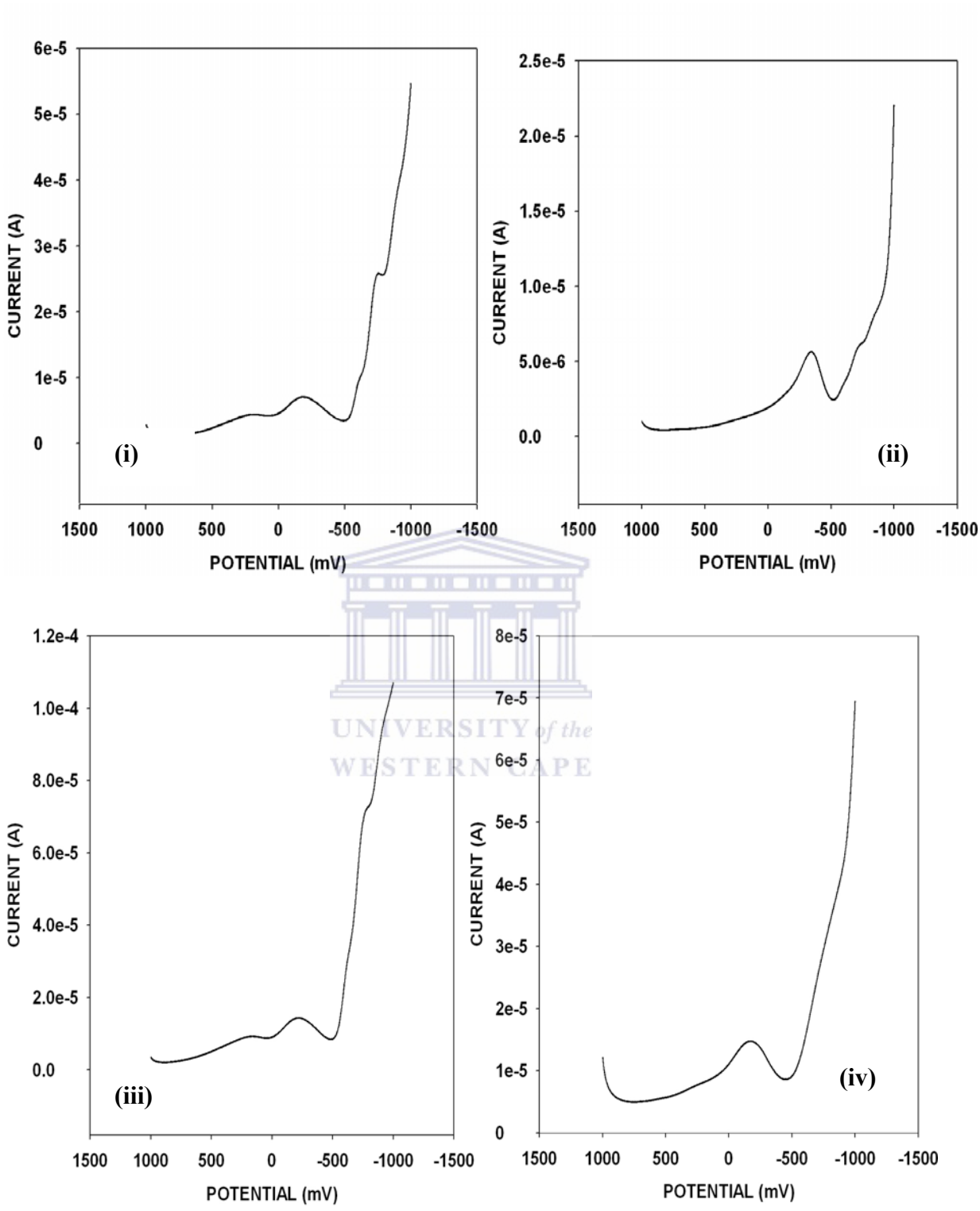

Figure 6.1: Square wave voltammetric responses of PANi (i) and POMA(ii)before enzyme dopingand (iii) and (iv) after enzyme doping.

The reverse anodic peaks in the CVs is either diminished or completely absent which is indicative of an electron transfer reaction coupled to a catalytic process.

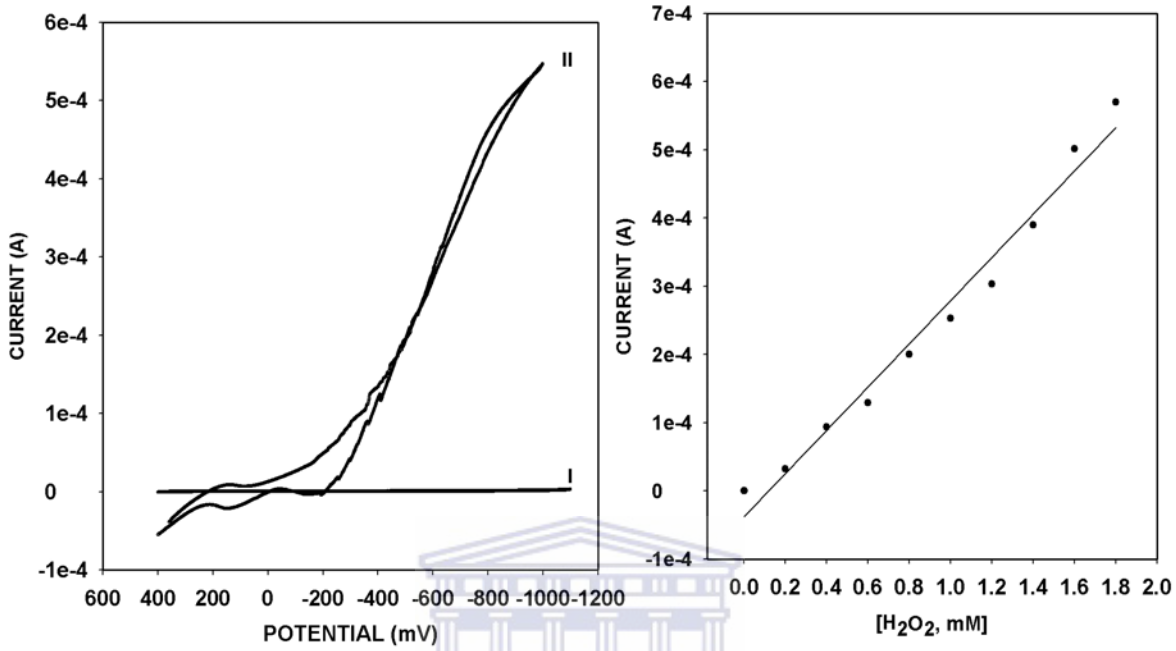

Figure 6.2: Cyclic voltammetric biosensor responses of the PANI/NSA/HRP biosensor 0 and 1.8 mM H_2O_2 concentrations. Calibration curve for the PANi/HRP biosensor response to different concentrations of H_2O_2.

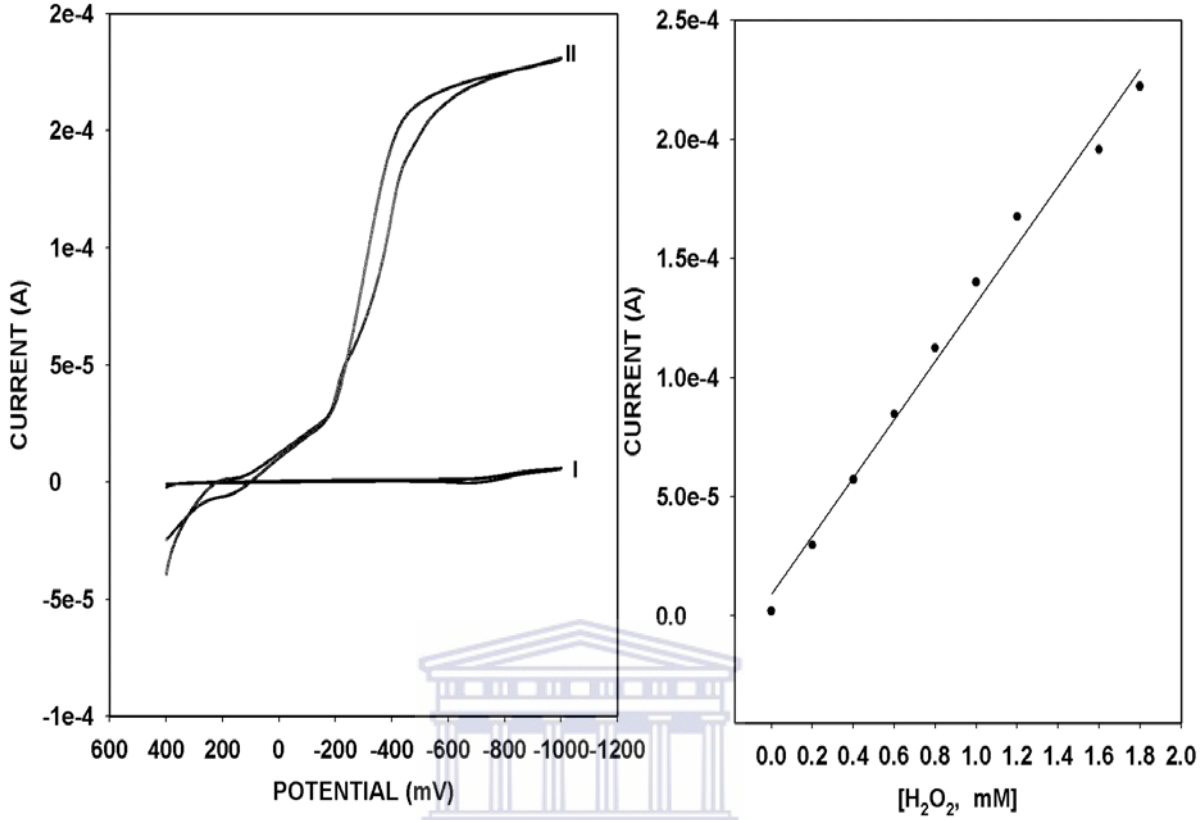

Figure 6.3: Cyclic voltammetric biosensor responses of the POMA/NSA/HRP biosensor 0 and 1.8 mM H_2O_2 concentrations. Calibration curve for the PANi/HRP biosensor response to different concentrations of H_2O_2 .

It means the oxidation/reduction processes of the PLE/PES SPAH forms can effectively communicate with the oxidized-HRP redox center leading to its regeneration. The catalytic reduction of hydrogen peroxide begins when the peroxide (substrate) accepts two electrons from the HRP/ferric prosthetic group which through a series of steps culminates into the reduction of H_2O_2 into di-oxygen and water.

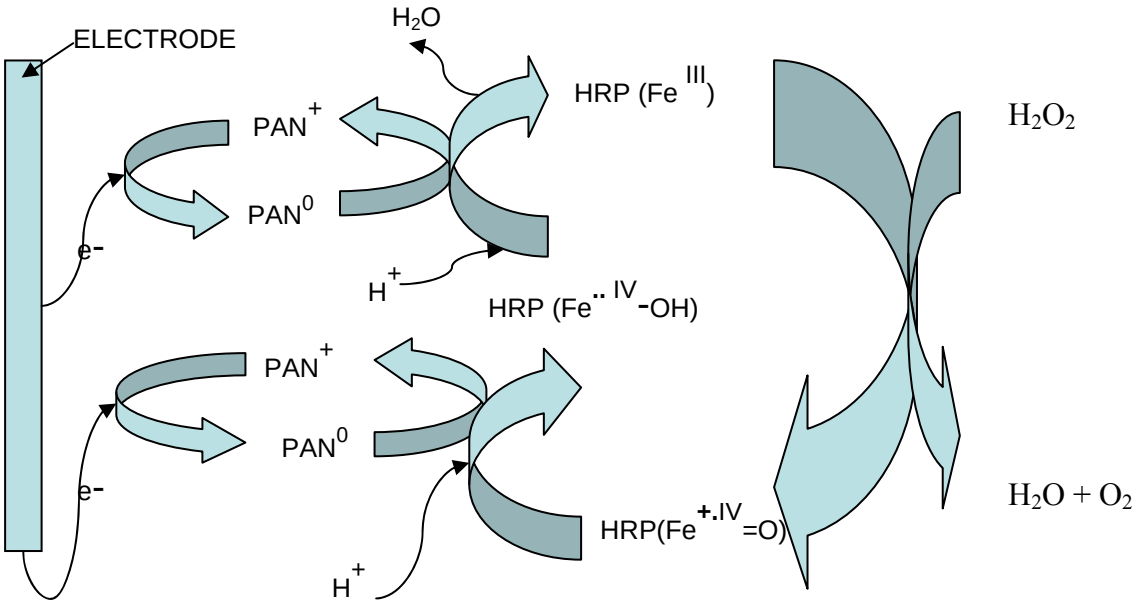

Figure 6.4: A scheme showing the catalytic reduction of hydrogen peroxide.

Figure 6.4 above shows the role played by the SPAH in the whole H_2O_2 reduction scheme presented as $PANi^+$ (PES) and $PANi^0$ (PLE). The HRP/Fe^{3+}- resting enzyme is converted to the unstable oxyferryl state HRP ($Fe^{\cdot+IV}$=O) intermediate, HRP-I, two oxidation equivalents above the resting state, the second positive charge been a porphyrin π-cation radical. In the presence of donor molecules, the unstable oxyferryl complex HRP-I accepts an electron converting to a more stable complex the hydroxyferryl complex (HRP ($Fe^{\cdot\cdot IV}$=OH), HRP-II, one oxidation equivalent above the resting state. Another electron accepted from the donor molecule regenerates the enzyme for further catalysis. The flow of electrons (catalytic current) is equal in magnitude to the concentration of the substrate (peroxide) in solution. This scheme agrees well with those reported in literature (Iwuoha et al., 1997: 53-75; Setti et al., 2007: in press). In the immobilized state, the electron shuttling role between the ferric/HRP redox center and the electrode is played by the electromediators e.g. SPAH synthesized in this study.

During the electro-mediation role, the electroactive SPAH (in the PES form) accepts an electron from the electrode and is converted to the reduced PLE (PAN^0) form. The PLE form of SPAH will then pass on the electron to the oxidized enzyme leading to its reduction to the ferric resting state. Meanwhile the PLE form of SPAH reconverts back to the PES form (PAN^+) and the cycle is repeated. The overall equation for the reduction of hydrogen peroxide is governed by the equation:

$$H_2O_2 + 2e^- \rightleftharpoons H_2O + O_2$$

In accordance to Figures 6.2/6.3 above the PANi/NSA/HRP and the POMA/NSA/HRP biosensors did not obey typical Michaelis-Menten kinetics. Instead, a linear relationship extending to a maximum current value (A) of 5.70×10^{-4} and 2.5×10^{-4} was realized for the PANi and POMA-based electrochemically prepared biosensors respectively. The estimated linear range (in the range of 0-1.8 mM H_2O_2 concentration used) for the PANi/NSA biosensor was 0.0012- 1.8 mM H_2O_2. That of the POMA/NSA biosensor was 0.00813-1.8 mM H_2O_2. This linear range obtained here is higher than the 0.01- 0.1 mM range obtained for a H_2O_2 biosensor based on poly-2-methylaniline-5-sulphonic acid (PMAS) (Orawan et al., 2005: 183-188). The slope of the calibration curve represents the biosensor sensitivity. The slope of the calibration curve and therefore the sensitivity of the sensor was 317.2 and 138.1 μA/mM H_2O_2 respectively where r^2 = 0.978 PANi/NSA/HRP and 0.990 POMA/NSA/HRP. The limits of detection (LOD) for both the PANi and POMA biosensors were estimated to be 1.197×10^{-3} mM and 8.13×10^{-3} mM respectively at an estimated signal to noise (S/N) ratio of 3.

6.1 Fabrication of a H_2O_2 biosensor based on ASA -doped PANi and POMA

In this biosensor format, chemically as-synthesized PANi/POMA was constituted in a suitable solvent and then mixed with a predetermined amount of the horseradish peroxidase enzyme thus tuning the sensor for hydrogen peroxide (H_2O_2) sensing. The preformed polymers/enzyme mixture could either be drop-dry, dip –dry or spin –coated on the 0.0177 cm^2-diameter- platinum disc working electrode and tethered to the

electrode by use of a cross-linker. Amongst the various coating techniques, the drop-coating followed by drying method gave rise to a stable enzyme/polymer layer and was predominantly used.

Prior to modification, the platinum electrode surface was cleaned by polishing with aqueous slurries of 0.3, 0.1 and 0.05 μm alumina. Rinsing was done after each polishing step. The electrode was then sonicated in distilled water for 10 min. and dried under an argon headspace. The enzyme solution was prepared by dissolving 0.2 mg HRP in 100 μL, 0.05 M phosphate buffer, pH 7.0. To the HRP solution, 3 mg of PANi/ASA powder, 0.2 mg bovine serum albumin (BSA) was thoroughly mixed. 0.9 μL, glutaraldehyde (2.5 %) was stirred into the above mixture and a 3 μL aliquot drop-coated on to the platinum electrode surface (0.0177 cm^2) and allowed to dry in the air for 2 hr. The electrocatalytic behaviour of the PANi/ASA/HRP biosensor was studied using Bioanalytical System (BAS) CV-50W on the potentiodynamic mode. CVs were recorded (at 5 mV/s in a potential range of 400→800 mV) with and without H_2O_2, in phosphate buffer 7.0, using platinum counter and a Ag/AgCl (3 M NaCl) reference electrode.

Figure 6.5 depicts the CVs of the ASA-doped HRP modified polymer electrodes with no H_2O_2, in the presence of 0 mM and 1.8 mM H_2O_2, under anaerobic conditions.

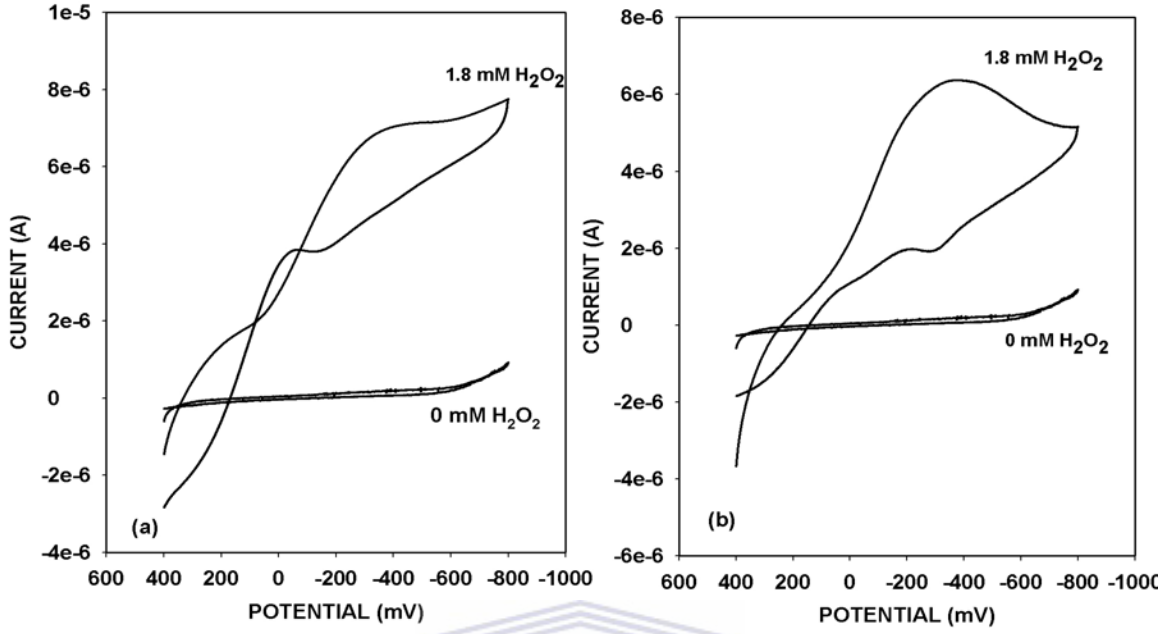

Figure 6.5: Anthracene sulfonic acid doped PANi (a) and POMA (b) horseradish peroxidase biosensor response to 0 and 1.8 mM H_2O_2.

The voltammograms depict the catalytic currents resulting from the coupling of the electro-oxidation of the ASA –doped polyanilines to the catalytic reduction of hydrogen peroxide. The currents produced at any particular potential depend on the concentration of hydrogen peroxide present in the solution. That is, the ASA- doped polyanilines are functioning as electron-transfer mediators between the platinum electrode and the HRP biomolecule. Clearly after the addition of a small amount of H_2O_2, there is an enhancement of the cathodic peak at around -300 mV. The increase in the current of the peak at -300 mV demonstrated an effective electrocatalytic reduction of H_2O_2 on the platinum electrode. The on going sensor results were based on the assumptions that the HRP redox catalytic sites were non-diffusional. It was also assumed that the polymer-ASA-HRP sensors were thin homogeneous films in which the H_2O_2 reduction charge is propagated along the polymer chain by fast electron reactions involving the reduced and oxidized forms of the polymers (Iwuoha et al., 1997: 749-761). This way, for a substrate limited kinetic case, the expression for the steady state current (*I*), simplifies to the electrochemical Michaelis-Menten equation (Iwuoha et al., 1997: 749-761) given by;

$$I = I_{max}\,[H_2O_2] / \; ([H_2O_2] + K_M^{app}) \qquad (6.1)$$

where I is the observed catalytic current, I_{max} is the steady state current for the biosensor, and $[H_2O_2]$ is the bulk solution concentration of hydrogen peroxide. Equation 6.1 is a modification of the equation 2.1. Figures 6.6 and 6.7 represent the calibration curves for the various sensors response to different concentration of H_2O_2 as fitted into the Michaelis – Menten paradigm.

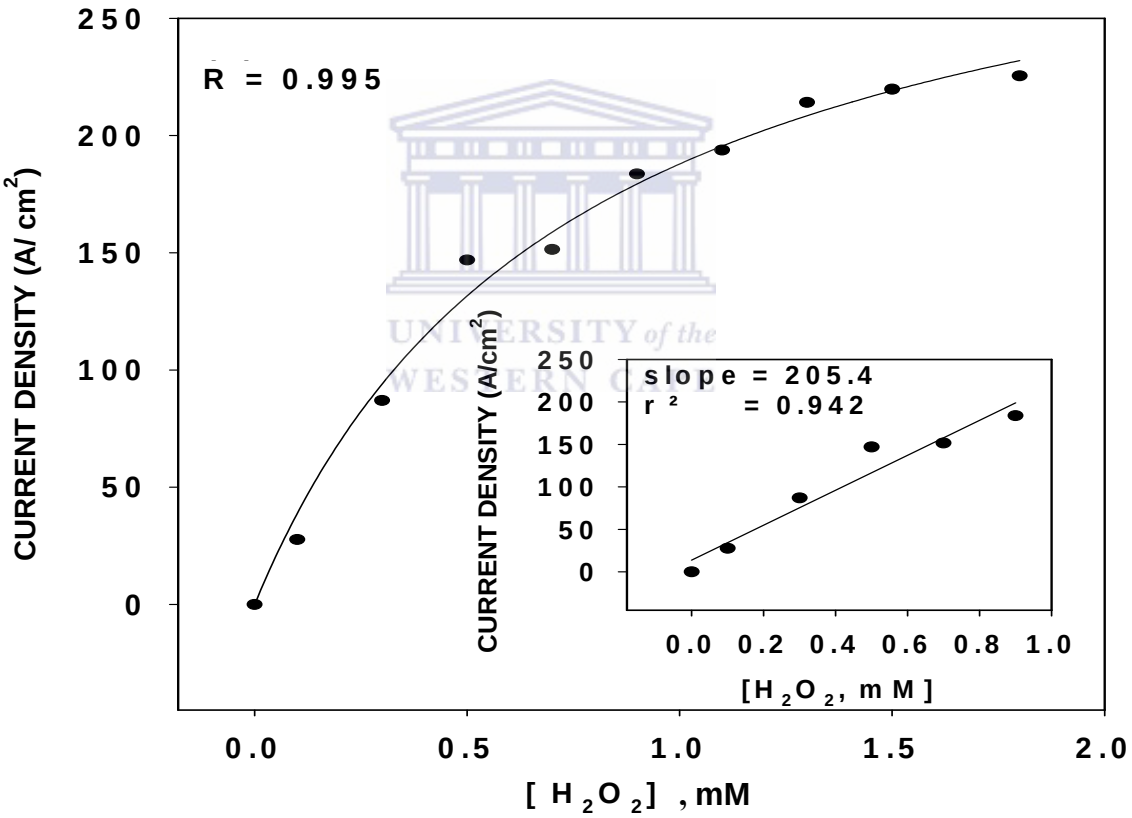

Figure 6.6: Calibration curve for the PANi/HRP biosensor response to different concentrations of H_2O_2. Inset analytical linear range of the biosensor.

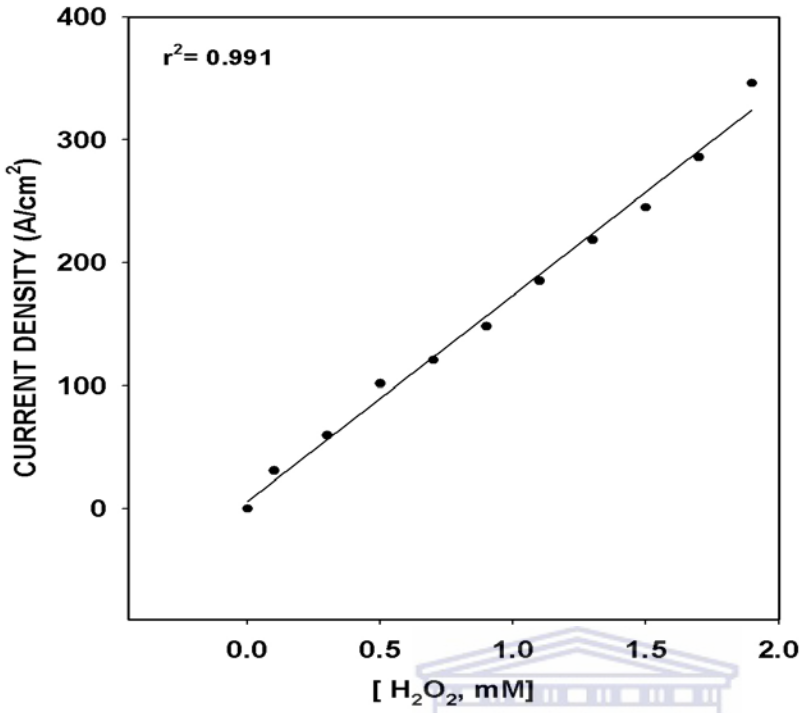

Figure 6.6: Calibration curve for the POMA/HRP biosensor response to different concentrations of H_2O_2.

The estimated linear range for the PANi and POMA based biosensors were 0.01 – 1.0 mM and 0.01- 1.8 mM H_2O_2 respectively. The linear ranges obtained were higher than the 0.01- 0.1 mM range obtained for a H_2O_2 based on poly-2-methylaniline -5- sulfonic acid (PMAS) (Orawan et al., 2005: 183-188). The slope ($=I_{max} / K_M^{app}$) of the calibration curves were used to estimate the sensitivities of the two biosensors. The estimated sensitivities (μA /cm^2/ mM) were; 205.4 PANi; 167.4 POMA. These sensitivity values indicated that the PANi/HRP biosensor was 1.3 times more sensitive than the POMA based one. The difference could be associated with the ability of charge propagation along the polymer chain. Previous findings (earlier sections) indicate slower electron propagation along the POMA backbone due to increased inter-chain distance related to the bulky methoxy substituents. The estimated K_M^{app} values for the PANi and POMA sensors were 0.4 and 0.7 mM respectively. These values represented the hydrogen peroxide concentration at which the sensors reaction kinetics changed from being first order to zero order (Pravda et al., 1995: 127-138; Adeyoju et al., 1995: 57-64). Also, the maximum current density I_{max}, values obtained for the biosensors were 220 μA/ cm^2

PANi; 300 μA/ cm^2 POMA. The values represent the current densities generated by the hydrogen peroxide concentration that brings about the switch in kinetic order. Thus the K_M^{app} gives an indication of the enzyme- substrate system. The higher K_M^{app} for the POMA-ASA based sensor therefore showed that the rate of decomposition of the HRP/H_2O_2 complex was higher than the rate of formation implying for the case of POMA, the enzyme-substrate complex formation was the rate determining step. The lower K_M^{app} for PANi-HRP complex on the other hand was indicative of complex stability. It means the saturation of the enzyme active site occured fast in the latter case thus leading to a higher sensor response. Low K_M^{app} value for PANi meant a higher sensitivity and the ability of the sensor to detect low substrate concentrations. The limit of detection (LOD), for the PANi and POMA biosensors were relatively low and were calculated to be 2.0 x 10^{-6} and 4.4 x 10^{-6} M respectively at an estimated signal to noise (S/N) ratio of 3.

6.2 Detection of diazinon

The simplified model representing in general most enzymatic reactions is;

$$E + S \rightleftharpoons ES \rightleftharpoons E + P$$

The model postulates that enzymatic reactions proceed through the formation of an enzyme (E) – substrate (S) complex (ES] with a rate constant k_1 (Stryer, 2000: 104-128). The fate of the ES complex is such that it can dissociate back to E and S with a rate constant k_2 or proceed to form a product P with a rate constant k_3. The success of enzymatic catalysis is greatly dependent on the specificity of the enzyme towards its substrate. Such specificity is possible because enzymes contain hydrophobic clefts or crevices (active sites) that allow only the binding of the specific ligand or substrate. However, inhibitors may reversibly or irreversibly block these enzymatic active centers with a decreased catalytic signal. The basis of amperometric inhibition based biosensors involves the measurement of the enzymatic catalytic activity before and after exposure to

the inhibitor. The resultant catalytic current de-attenuation correlates directly to the concentration of the inhibitor in solution (Ciucu et al., 2003: 303-310).

The horseradish peroxidase enzyme predominantly known to catalyze the reduction of peroxides amongst other substrates is easily inhibited by organic sulfur containing compounds (Adeyoju et al., 1995: 57-64). It is little wonder then that diazinon ($C_{12}H_{21}N_2O_3PS$), an organophosphate pesticide (OP) was chosen for the inhibition studies. Figure 6.8 represents the behaviour of the Pt/PANi/HRP biosensor on exposure to 0, 1.8 mM H_2O_2 in the presence of 2.5 μM diazinon.

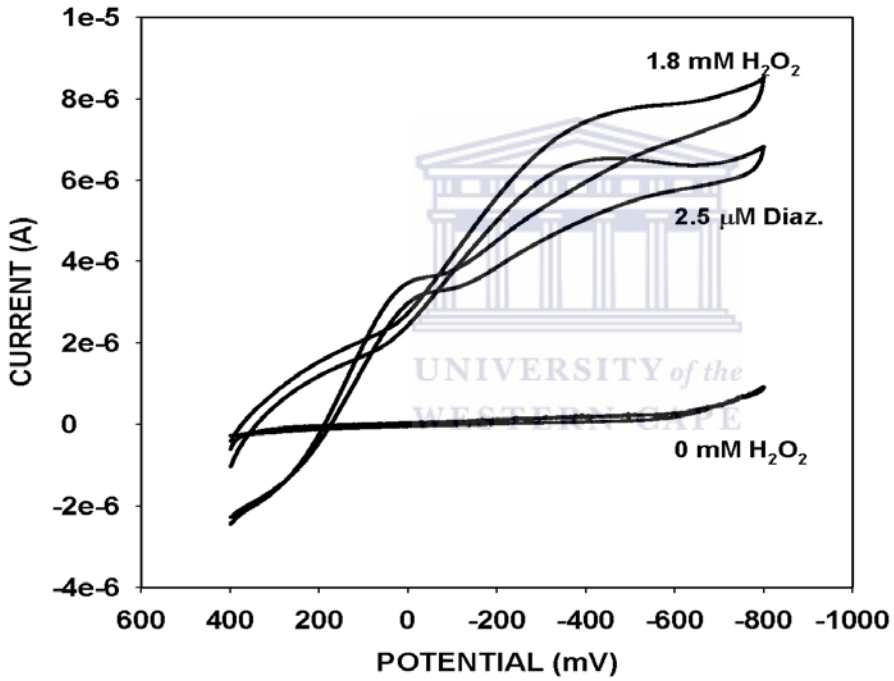

Figure 6.7: Cyclic voltammograms depicting biosensor reactivities at 0, 1.8 mM H_2O_2 and in presence of 2.5 μM diazinon. Data shown for the polyaniline based biosensor only.

Results show that the catalytic current decreased by a factor of 2 μA in the presence of the inhibitor. Similar trends were realized for the Pt/POMA/HRP biosensor (data not shown). The resultant current de-attenuations were expressed as % inhibition using equation 3.9. The resultant inhibition plots (Figure 6.8) indicate that only partial inhibition was achieved for the two biosensors values being; 41 % for PANi/HRP; 62 % for POMA/HRP. Slopes of these inhibition plots expressed as % inhibition /decade

yielded the biosensor sensitivities to the inhibitor. Values of -30.8 and –107.4 were obtained for the PANi and POMA-based biosensors respectively.

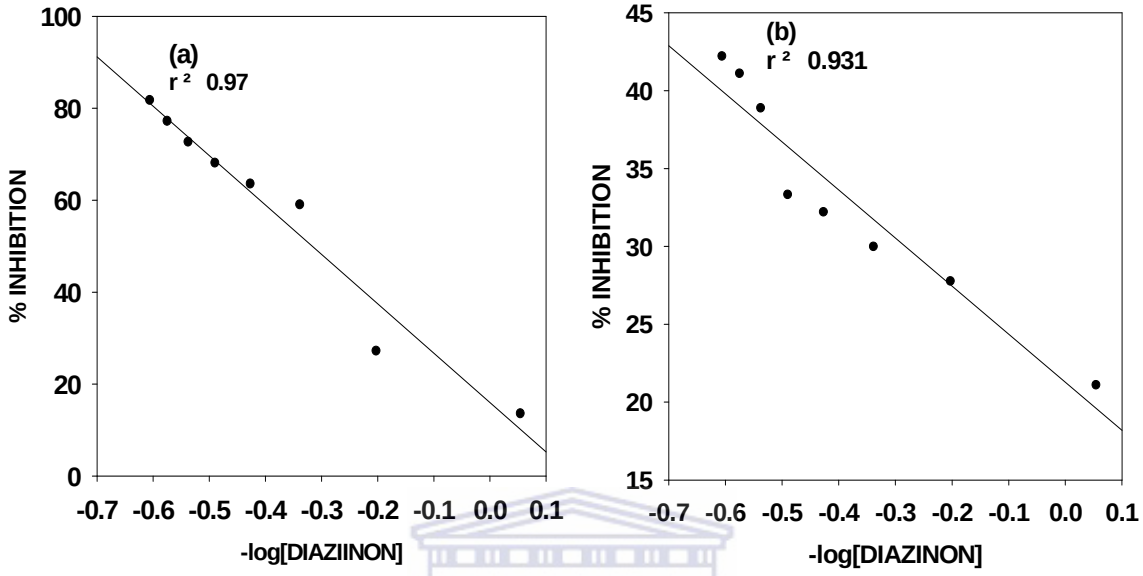

Figure 6.8: Plots of % inhibition versus –log [Diazinon]. Concentrations of diazinon inhibitor studied were in the range 0.88- 4.0 µM. Plot (a) PANi and (b) POMA.

The results suggest the POMA-based biosensor was more sensitive to diazinon agreeing with the % inhibition results. The concentration of diazinon at the x-intercept of the inhibition curve represents the theoretical detection limit of the sensor (Pritchard et al., 2004: 765-772). Based on the linear equations y =-30.8x +21.2 (r^2=0.97) and y = -107x+15.9 (r^2= 0.93) the detection limits for the PANi and POMA based biosensors worked 0.20 and 0.71 µM respectively.

A second method employed in the construction of inhibition biosensors was through incubation techniques. By determining the catalytic activity of the two biosensors before and after incubation with 1.8 µM diazinon (for 20 min) (Fig. 6.10, **II**) and comparing it with that in the absence of inhibitor (**I**) Lineweaver-Burk plots were constructed to establish the nature of the inhibition. According to Fig. 6.10 (plot based on POMA

results), diazinon inhibits HRP non-competitively. Under such circumstances, the maximal catalytic current in the presence of a noncompetitive inhibitor I^1_{max} is given by;

$$I^1_{max} = I_{max} \text{ (no inhibitor)} / 1 + ([I] / K_i) \quad (6.2)$$

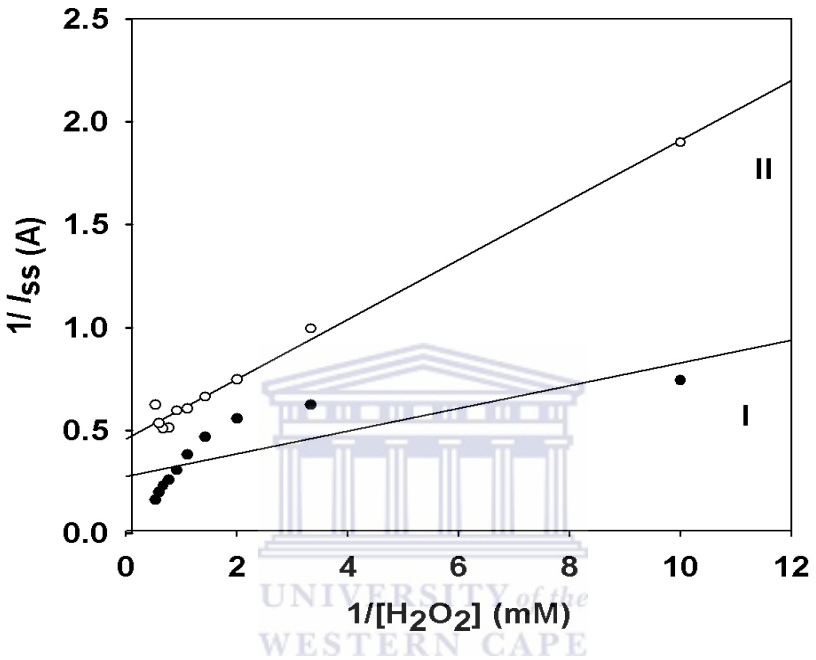

Figure 6.9: Lineweaver-Burk plot based on poly-o-methoxyaniline (POMA) data.

where [I] is the concentration of the inhibitor and K_i is the inhibition constant. Based on results on the calibration and inhibition plots, the inhibition constants for the two biosensors were estimated. For POMA, the assumption made was that the observed catalytic current at 1.8 mM H_2O_2 was close to the value of I_{max}. The computed inhibition constants (K_i) were 1.8 and 1.0 for the PANi and the POMA based biosensors respectively. A higher (K_i) value for the latter biosensor could indicate a greater affinity for diazinon for the POMA/HRP system, leading to better sensor sensitivity.

6.3 Amperometric responses for the CYP 3A4/PANi/ASA electrode.

Cytochrome P450 3A4 is the major enzyme involved in the phase-1-biotransformation of xenobiotics. Cytochrome P450 3A4 is known to catalyse the N-demethylation of erythromycin, an antibiotic normally used to treat respiratory tract infections (Wang et al., 1997: 25). Under normal physiological conditions, the demethylation reaction of CYP 3A4 follows the monooxygenation pathway in which NADPH acts as the source of the two electrons that drive the reaction (Iwuoha et al., 2004: 37) as shown in the below. Erythromycin contains two terminal methyl groups. It means that 4 electrons are needed for the complete demethylation process demanding a repeat of the scheme below.

$$NADPH + O_2 + R\text{-}N(CH_3)_2 \rightarrow NADP^+ + HCHO + RNHCH_3 \quad .....(i)$$

$$NADPH + O_2 + R\text{-}NHCH_3 \rightarrow NADP^+ + HCHO + RNH_2 \quad ……(ii)$$

In the construction of the CYP 3A4 –based amperometric biosensor for erythromycin, the electrons for the monooxygenation were supplied by applying the appropriate potential through the Pt/PANi-ASA system. Figure 6.11 shows the Pt-PANi/ (14.4 µmol/L^{-1} solution) bioelectrode response in 1 mL phosphate buffer saline (0.1 M, pH 7.4, 100 mM KCl) with or without erythromycin.

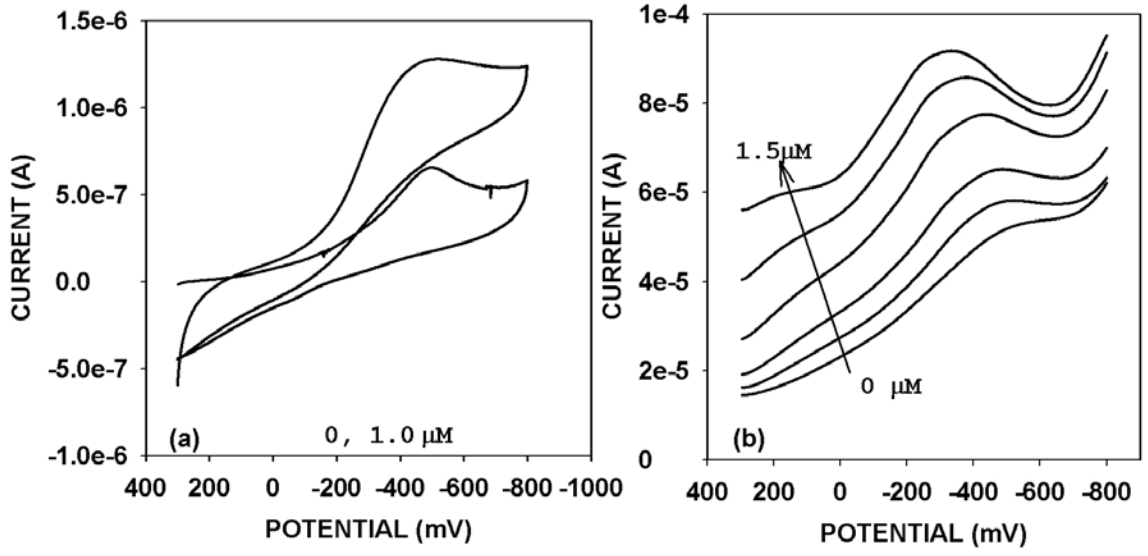

Figure 6.10: Cyclic voltammetric and differential pulse responses of PANi/ASA Platinum/14.4 µmolL-1 CYP 450 3A4 bioelectrode for erythromycin. Scan rate was 5 mV/s vs Ag/AgCl at 20°C.

The cyclic voltammetric responses of the PANi/ASA CYP 3A4 bioelectrode to different concentrations of erythromycin show one cathodic peak, (E_{pc} = -538 mV). The cathodic peak current increased as the concentration of the erythromycin substrate increased. Differential pulse voltammetric responses (Fig. 6.11 'b') of the PANi/ASA CYP electrode to different concentrations of erythromycin (0 – 3.75 μM) indicate there was a 286 mV potential shift towards more positive values. This indicated the presence of a catalytic reduction process coupled to an electrode transfer reaction at the electrode. This was also confirmed by the increase in cathodic current I_{pc} as the concentration of erythromycin increased up to 3.75 μmol/L^{-1} erythromycin. A possible reaction scheme for the sensor-based N, N-demethylation of erythromycin is summarized in Fig. 6.12.

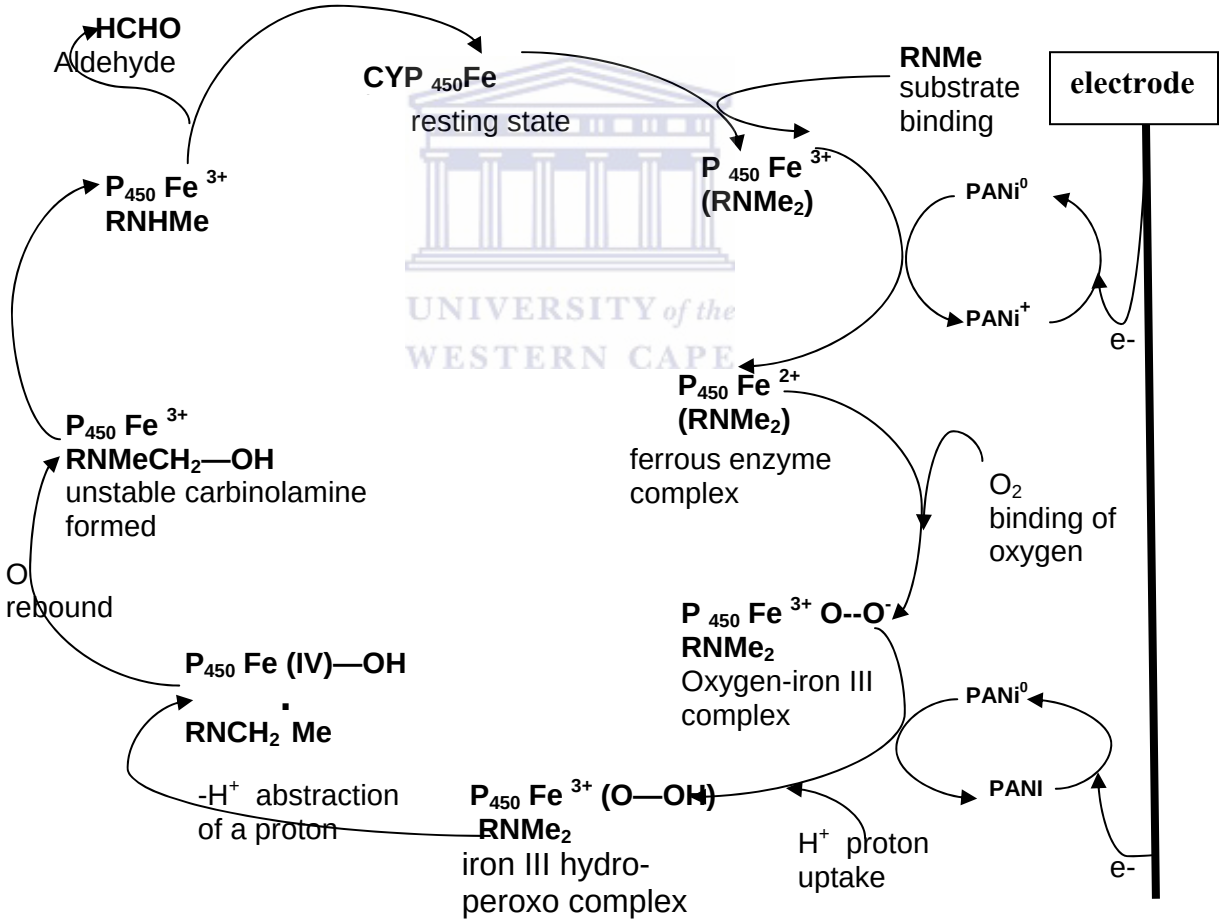

Figure 6.11: Proposed scheme for the N, N-demethylation of erythromycin on a platinum/PANi/ASA, CYP 3A4 biosensor. Erythromycin consists of two N-CH_3 groups therefore the above cycle is repeated for complete demethylation.

Under anaerobic conditions the reduction of the ferric redox state in CYP 3A4

$$P_{450}\,Fe^{3+} + e^- \rightleftharpoons P_{450}\,Fe^{2+} \quad E^{0'} = -538 \text{ mV}$$

is coupled to the PANi $^{0/+}$ oxidation /reduction as shown below:

$$PANi^+ + e^- \rightleftharpoons PANi^0$$

The DPV results (Fig. 6.11 'b') shows that the binding of erythromycin reduces the formal potential for the P450$Fe^{3+/2+}$ by 286 mV at a substrate concentration of 3.75 μM/L

$$P_{450}\,Fe^{3+}(RNMe_2) + e^- \rightleftharpoons P_{450}\,Fe^{2+}(RNMe_2) \quad E^{0'} = -352 \text{ mV}$$

It has been shown that in this ferrous form (P_{450} Fe^{2+} ($RNMe_2$), the enzyme is an extremely efficient reducing agent and combines with molecular oxygen to form a relatively stable oxygen-iron III complex, (P_{450} $Fe^{3+}O\text{-}O^-$) (Meunier et al., 2004: 3947-3980). For the ongoing sensor, the phosphate buffer solution was not degassed after the addition of the substrate thus providing the oxygen necessary for this step. The acceptance of a second electron of this oxygen-iron III complex from the electrode through the PANi mediator, coupled with an uptake of a proton from the solvent, produces an iron III hydroperoxo compound ($P_{450}Fe^{3+}OOH$) with an extremely high affinity for protons. It quickly abstracts a proton from one of the methyl groups in the erythromycin accompanied by a loss of a water molecule to form an iron IV hydroxo intermediate (P_{450}FeIV-OH). Through an oxygen rebound process, an unstable carbinolamine (Meunier et al., 2004: 3947-3980; Guengerich et al., 1996: 27321-27329, Miwa et al., 1983: 14445-14449) is formed and finally breaks down to HCHO and $RNHCH_3$. The cycle is then repeated for the complete demethylation of erythromycin.

The intergrity of the PANi/CYP3A4 biosensor was evaluated through calculation of several biosensor parameters. Data points were fitted into the Michaelis-Menten equation

to obtain a calibration curve (Fig. 6.13). The apparent $K'M_{app}$ of the sensor for erythromycin was 0.8 ± 0.1 µmol L^{-1}. The maximum current density I_{max} had a value of (2.21 ± 0.03) x10^{-3} µA cm^{-2} for the bioelectrode. The linear range of the biosensor has an upper limit of approximately 1.3 µM (r^2 = 0.971).

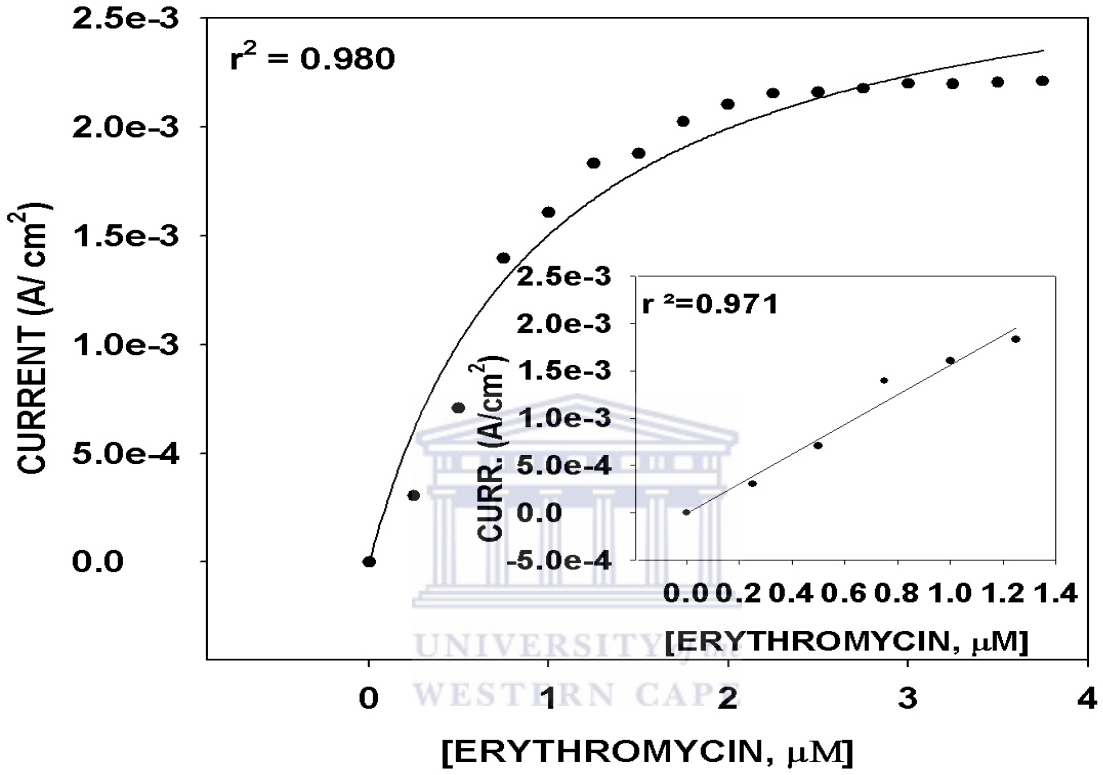

Figure 6.12: Calibration curve for the polyaniline/Cytochrome P450 3A4 biosensor responses to different concentrations of 500 µM erythromycin. Inset: dynamic linear range of the sensor.

The sensitivity of the biosensor representing the slope of the calibration graph was 1.57 x 10 $^{-3}$µA cm^{-2} $(µM)^{-1}$. The PANi CYP 3A4 bioelectrode had a detection limit equal to 7.58 x 10^{-2} µM.

6.4 Conclusion

This chapter has demonstrated the fact that sulphonated polyanilines can act as effective electron transfer mediators in biosensor construction. Although this is only a preliminary study, the ability of the SPAH to house macromolecules of different sizes and geometry is advantageous. It means SPAH can act as immobilization hosts to different types of biomolecules thus forming a focal point towards the fabrication of a variety of sensors for different analytical purposes. This is achievable because SPAH consists of a flexible backbone that can easily be modified as need be. Furthermore, the ability of SPAH to maintain conductivity and electroactivity even at neutral pH is promising towards the production of sensors that are not prone to 'hysteresis' with pH change.

Chapter 7

Conclusions and recommendations

7 Objectives of the study

The ultimate aim of the study was to synthesize sulphonated polyanilines (SPAH), study their electrodynamics and evaluate their possible application for sensor technology as effective electron transfer mediators. This was to be carried out by use of self-assembled nanostructured polyaniline (PANi), poly-*o*-methoxyaniline (POMA) and/or poly-2,5-dimethoxyaniline (PDMA). Preparation of the polyaniline and functionalized polyaniline was carried out in the presence of sulphonated polynuclear aromatic hydrocarbons (anthracene sulfonic acid (ASA) and naphthalene sulfonic acids (NSA) playing the dual role of surfactant and dopant. In some cases, the preparation of some precursor materials such as anthracene sulphonic acid (ASA) was necessary since they were commercially unavailable.

The characteristics of the SPAH was interrogated through spectroscopic (UV-Vis, FTIR) and microscopic (SEM) as well as electrochemical techniques. The behaviour of the SPAH- polyanilines was studied both under acidic and neutral medium (phosphate buffer) in order to assess their suitability as electrode modifying matrices for biosensors. Finally, some CYP 3A4 or HRP SPAH biosensors were constructed and biosensor reactivities modeled to the Michaelis-Menten kinetics paradigm where applicable.

7.1 Summary of results

Results showed that both chemically as-synthesized and electrodeposited PANi were conductive and electroactive. Two or three redox couples identified as the polyleucoemeraldine/polyemeraldine salt transition (PLE/PES) and the polymeraldine salt/polypernigraniline transition (PES/PPN) were identified in acidic electrolytic medium. Both chemically/electrosynthesized SPAH retained its electrochemical

behaviour even at neutral pH, which was evidence for the incorporation of the sulphonic acids into the polymer matrices. The comparison of the SPAH behaviour with that of mineral acid doped PANi (in literature), suggested that the grafting of sulphonic groups within the polymer backbones improved their stability, maintained their conductivity even at neutral pH and reduced pH related hysteresis. The study has been shown that the incorporation of indiffusible bulky sulphonic into PANi matrix can produce conductive SPAH at neutral pH, which is usually the physiological pH for most enzymes. The study has also shown for the fist time that indeed the conversion of the first redox couple in the polyaniline (PLE/PES) is actually a two-stage process. It involves first the conversion of the PLE to the polyemeraldine base form followed by protonation to PES.

The electrodynamics of the SPAH as studied under acidic/neutral medium revealed the SPAH systems exhibited near Nerstnian behaviour at low potential sweep rates but deviated to quasi-reversibility at higher scan rates prompting the use of low scan rates for biosensor measurements as expected. The diffusion coefficient values (cm^2/s) of (1.1-8.9) x 10^{-6} and (1.34-6.41) x 10^{-6} for the chemically and electrochemically synthesized SPAH was moderately fast and was interpreted to mean that the SPAH could act as an effective electron mediator for biosensor applications. This was compounded by the moderately fast heterogeneous rate constants which were in the range 1.3-6.2 x10^{-4} cm^2/s and 2.60 x 10^{-4} - 6.61 x 10^{-3} for the chemically assynthesized and electrodeposited polymers respectively.

UV-Vis spectroscopy showed the existence of polaron bands at ca. 420 and ca.800 nm for the chemically synthesized SPAH as the presence of an electronic like band at ca. 1100 cm^{-1} for the various SPAH was indicative that the SPAH was conductive. The shifting of the quinoimine bands for the benzene and quinoid units in the FTIR of chemically synthesized SPAH to lower wavenumbers was indicative of successful doping. Though UV-Vis and FTIR studies were not conducted for the electrochemically synthesized SPAH, the fact that polymer growth was observed marked by the increasing peak currents with scan rates (I_p, A) was indicative of their conducting nature. Scanning electron microscopy gave rise to SPAH of different morphology. The monomer: dopant

ratio, and initial heat pre-treatment were found to influence the morphology of the resultant SPAH. Granulated SPAH was predominant at 1:1 monomer dopant ratio while as low monomer to dopant ratio e.g. 0.3:1 yielded nanofibrillar morphology. The monomer dopant ratio of 1:0.5 produced both fibrillar and doped PANi. Thus spectroscopic studies suggested that both chemically and electrochemically synthesized SPAH was conductive. Through the classical Ohms relation, the conductivities of the various SPAH was estimated to be between 0.27-7.8 $x10^{-3}$ S/cm and (0.085-3.47) x 10^{-2} S/cm for the chemically and electrodeposited SPAH respectively. It was therefore concluded that both the chemically and electrosynthesized SPAH could be used for electromediation purposes in biosensor construction where the SPAH is expected to provide an electronic link between the biomolecule redox center and the electrode.

Indeed results of some of the various SPAH for biosensor applications were of good sensitivities. Preliminary results for the application of chemically synthesized PANi/POMA ASA-doped SPAH cross-linked to the electrode through the use of glutaraldehyde were good. The resultant biosensors exhibited high sensitivities ($\mu A/cm^2$ mM^{-1}) of 205.4 PANi and 167 POMA to H_2O_2. A 1.8 mM H_2O_2 concentration provided the optimal enzyme activity with I_{max} (μA) values of 220 and 300 for PANi and POMA respectively. Inhibition studies were achieved by exposure of the biosensor to between 0.88-4 μM diazinon in the presence of optimal H_2O_2 concentration. The resultant signal de-attenuations expressed as % inhibition were 44 % PANi and 81 % POMA. It means the POMA sensor was more sensitive to diazinon. The Limits of detection estimated for the two sensors were 0.4 and 0.71 μM for PANi and POMA respectively.

Similarly application of the PANi/ASA based SPAH in the construction of a CYP3A4 sensor for erythromycin was successful. The resultant biosensors displayed typical Michaelis-Menten behaviour. The apparent Michaelis-Menten constant obtained was 0.80 ± 0.1 μM L^{-1} for the erythromycin biosensor. The maximum current density I_{max} had a value of (2.21 ± 0.03) $x10^{-3}$ μA cm^{-2} for the bioelectrode. The linear range of the biosensor exhibited an upper limit of approximately 1.3 μM (r^2 = 0.971). The sensitivity

for the erythromycin sensor was 1.57 x 10^{-3} A cm^{-2} $mM^{-1}$and detection limit was found to be 7.58 x 10^{-2} μM.

The ongoing results indicate that it was possible to employ various SPAH for electromediation purposes for the construction of biosensors for the various analytes.

7.2 Recommendations

One of the major problems hampering PANi application in large scale processes has been its insolubility, infusibility and intractability. It is thus suggested that the incorporation of sulphonic groups could provide a solution to this problem.

It has been verified that, both anthracene sulphonic acid and naphthalene sulphonic acid doped SPAH are electroconductive and can serve as effective electromediators in biosensor construction. This was a pilot study. A more detailed study with optimization of all the parameters involved would be beneficial towards a prototype biosensor for the various analytes. The biosensors for instance could be applied to other pesticides and CYP catalyzed drugs etc.

One of the major problems encountered during the characterization of either ASA/ NSA doped PDMA in neutral medium was that the polymer would fall off or chip away during sensor work despite the use of a cross-linker e.g. for the chemically synthesized product applications. It is recommended that, a suitable cross-linker be sought that would not interfere with the polymer electrochemistry but at the same time tether the polymer to the electrode.

More processible SPAH was prepared and thus the problem of insolubility of SPAH can be overcome by use of sulphonated polyanilines. The SPAH have great potential as electromediators in construction of biosensors for different analytes. Such biosensors would be useful for health, environmental monitoring as well as in quality control.

This study utilized electrochemical and UV-Vis and FTIR spectroscopies to elucidate the electroconductive nature of the chemically synthesized SPAH. It is however, further suggested that the nature and identity of chemically synthesized SPAH could be further characterized by other techniques including nuclear magnetic resonance spectroscopy (NMR), gel permeation chromatography, mass spectrometry and XPS.

References

Adeyoju O., Iwuoha E. I., Smyth M. R., (1995). Reactivities of amperometric organic phase peroxidase-modified electrodes in the presence and absence of thiourea and ethelenethiourea as inhibitors. *Analytica Chimica Acta* 305: 57-64.

Adeyoju O., Iwuoha E. I., Smyth M. R., (1994). Amperometric determination of butanone peroxide and hydroxylation via direct electron transfer at a horseradish peroxidase modified platinum electrode. *Analytical process*, 31: 177-179.

Adhikari B., Majumdar S., (2004), Polymers in sensor applications. *Progress in Polymer Science,* 29: 699-766.

Aizawa, M., Wang L., Shinohara H., Ikariyama Y., (1990). Enzymatic synthesis of polyaniline film using copper-containing oxido-reductase: bilirubin oxidase. *Journal of Biotechnology*, 14: 301-309.

Akinyeye R., Michira I., Sekota M., Al-ahmed A., Baker P., Iwuoha E., (2006). Electrochemical interrogation and sensor Applications of nanostructured polypyrolles. *Electroanalysis*, 18: 2441-2450.

Amine A., Mohammadi H., Bourais I., Palleschi G. (2006). Enzyme inhibition-based biosensors for food safety and environmental monitoring. *Biosensor and Bioelectronics*, 21: 1405-1423.

Anand J., Palaniappan S., Sathyanarayana D. N. (1998). Conducting polyaniline blends and composites. *Progress in Polymer Science*, 23: 993-1018.

Athawale A. A., Kulkarni M. V., Chabukswar V. V. (2002). Studies on chemically synthesized soluble acrylic acid doped polyanilines. *Materials Chemistry and Physics*, 73: 106-110.

Avril R. W-D., (2001). Monosubstituted squarate ligands and their transition metal and lanthanide complexes: Structural and electrochemical studies. PhD Thesis submitted at the chemistry department, Faculty of Agriculture and Natural Sciences, St. Augustine, University of West Indies.

Ay§egül G., Bekir S., and Muzaffer T. (2004). Synthesis and characterization of conducting substituted polyanilines. *Synthetic Metals*, 142: 41-48.

Babero C., Salovagione H. J., Acevedo D. F., Grumelli D. E., Gray F., Planes G. A., Morales G. M., Miras M. C. (2004). Novel synthetic methods to produce functionalized conducting polymers I. Polyanilines. *Electrochimica Acta*, 49: 3671-3686.

Bańka E. and Łużny W., (1999). Structural properties of polyaniline protonated with camphorsulphonic acid, *Synthetic Metals*, 715-716.

Barbero C., Miras M. C., Haas O. and Kötz R., (1991). Alteration of the ion exchange mechanism of an electroactive polymer by manipulation of the active site: Probe beam deflection and quartz crystal microbalance study of poly(aniline) and poly(N-methylaniline) *Journal of Electroanalytical Chemistry*, 310: 437-443.

Bard A. J. and Faulkner L. R. (2001). Electrochemical methods, fundamentals and application, 2nd Edition, Wiley & Sons, US, pp 1, 23-35, 87-102, 161, 240 -250, 580-601.

Barra G. M. O., Jacques L. B., Oréfice R.L, Carneéno J. R.G. (2004). Processing, characterization and properties of conducting polyaniline sulfonated (SEB) block copolymers. *European Polymer Journal*, 40: 2017-2023.

Barriós E. M., Mujica G. A., Velasquez C. L., Martinez Y., (2006). Studies of the presence of dicarboxylic acids in the electrochemical synthesis of poly(aniline): case polyitaconic acid. *Journal of electroanalytical chemistry*, 586: 128-135.

Bartlett P. N. and Cooper J., (1996). Application of electroactive Polymers in Biochemistry and Bioelectronics, In: *Electroactive Polymer electrochemistry, Part 2 , Methods and Applications,* Michael E.G. Lyons, Plenum Press, NewYork, USA, chapter 9, pg 233-269.

Bartlett P. N., Whitaker R G. (1988). Strategy of the development of amperometric enzyme electrodes. *Biosensors* : 3: 359-379.

Bejan D., and Duca A. (1998), Voltammetry of aniline with different electrodes and electrolytes, *Croatica Chemica Acta*, 71: 745-756.

Benard M. C., Hugot-Le G. (2006). Quantitative characterization of polyaniline films using Raman spectroscopy II. Effects of self-doping in sulphonated polyaniline. *Electrochimica Acta*, 52: 728-735.

Bernard M. C., Goff A.H., Joiret S., Arkout H., saïdani B. (2005). Influence of the nature of substituents on charge mechanisms in substituted polyanilines (SPANi, POMA) studied by Raman and optical spectroscopies. Electrochimica Acta, 50: 1615

Bernhardt R. (2006). Cytochrome P450 as versatile biocatalysts; *Journal of Biotechnology*, 124: 128-145.

Bistolas N., Christenson A., Ruzgas T., Jung C., Scheller F. W., Wollenberger U. (2004). Spectroelectrochemistry of cytochrome P450cam. *Biochemical and Biophysical Research Communications,* 314: 810-816

Bistolas N., Wollenberger U., Jung C., Scheller F. W., (2005). Cytochrome P450 Biosensors –a Review . *Biosensors and Bioelectronics*, 20: 2408-2423.

Boopathy S., Karnes H. T. (2002). Determination of (3S)-3-hydroxyquinidine for metabolism screening experiments using direct injection capillary electrophoresis and laser-induced fluorescence detection. *Biomedical Chromatography*, 16: 1-6.

Brahim S., Wilson A. M., Narinesingh, Iwuoha E., Guiseppi-Elie A. (2003). Chemical and biological sensors based on electrochemical detection using conducting electroactive polymers. *Microchimica Acta*, 143: 123-137.

Brett C. M. A and Brett A. M. O. (2005). Electrochemistry, principles, methods and applications. Oxford Science Publications, oxford University Press, pp 137-142.

Cai L-T., Yao S-B., Zhou S-M. (1997). Surfactant effects on polyaniline film. *Synthetic Metals*, 88: 209-212.

Carlos S., Horacio J. S., Arius-Pardilla J., Emilla M. (2007). Tuning the electroactivity of conductive polymer at physiological pH. *Electrochimica Acta*, 52: 2978-2986.

Carrilo J. A., Dahl M L., Svensson J O., Rodriguez I., Bertillson L. (1996). Disposition of fluvoxamine in humans as determined by the polymorphic CYP 2D6 and also by the CYP1A2 activity. *Clinical Pharmacology therapeutics*, 60: 183-190.

Cataldo F. and Maltese P. (2002). Synthesis of Alkyl and N-Alkyl-Substituted Polyanilines. A Study on their Spectral Properties and Thermal Stability. *European Polymer Journal*, 38: 1791-1803.

Cataldo F., Maltese P., (2002). Synthesis of Alkyl and N-Alkyl-Substituted Polyaniline. A study on their Spectral Properties and Thermal Stability. European Polymer Journal 38: 1971-1803.

Chandrakanthi R. L. N., Careem M.A., (2002). Preparation and Characterisation of CDS and Cu_2S nanoparticle/polyaniline Composite Films. *Thin Solid Films*, 471: 51-56.

Chaplin M. (2004). *What are Biosensors* ?
Hyperlink: http:/www.Isbu.ac.uk/biology/enzetech/biosensors.html

Chauret V., Dobbs B., Lackman R. L., Batiman K., Nicole-Griffith D. A., Stresser D. M., Ackermann J. M., Turner J. D., Miller V. P., Crespi C. L. (2001). The use of 3-[2-(N-N-Diethyl-N-Methylammonium)Ethyl}-7-methoxy-4-methylcoumarin (AMMC) as specific CYP2D6 probe in human liver microsomes. *Drug Metabolism and Disposition*, 29: 1196-1200.

Chen Y-H., Wu J-Y., Chung Y-C. (2006). Preparation of polyaniline modified electrodes containing sulphonated polyelectrolytes using leyer-by-layer techniques. *Biosensor and Bioelectronics,* 22: 489-494.

Cho M. S., Park S. Y., Hwang J. Y., Choi H. J. (2004). Synthesis and electrochemical properties of polymer composites with nanoparticles, *Material Science and Engineering* C24: 15-18.

Choi B. C., Chung I. J., Chun J. H., Ko J. M., (1999). Electrochemical characterization of dodecylbenzene sulphonic acid-doped polyaniline in aqueous solutions. *Synthetic Metals*, 99: 253-256.

Ciucu A. A., Negulescu Carmela, Baldwin R. P., (2003). Detection of pesticides using an amperometric biosensor based on ferophthalocyanine chemically modified carbon paste electrode and immobilized bienzymatic system. *Biosensor and Bioelectronics* 18: 303-310.

Cornelison D.M., Dillingham T. R., Bullock E., Benally N.T., Townsend S.W., (1995). In-situ scanning tunneling microscopy on vapour deposited polyaniline thin films. *Surface Science*, 343: 87-94.

Cosnier S. (1999). Biomolecule immobilization on electrode surfaces by entrapment or attachment to electrochemically polymerized films: A review. *Biosensor and Bioelectronics*, 14: 443-456.

Cruz G. J., Morales J., Castillo-Ortega M. M., Olayo R., (1997). Synthesis of polyaniline films by plasma polymerisation. *Synthetic Metals*, 88: 213-218.

Dalen P., Dahl M. L., Eichelbaum M., Bertilsson L., Wilkinson G R. (1999). Disposition of debrisoquine in caucasians with different CYP2D6 genotypes including those with multigenes.*Pharmacogenetics*, 9: 697-706.

D'Aprano G., Leclerc M., Zotti G. (1993). Steric and electronic effects in methyl and methoxy substituted polyanilines. *Journal of Electroanalytical Chemistry*, 35: 145-158.

De Albuquerque J. E., Mattoso L.H.C., Faria R.M., Masters J.G., MacDiarmid A.G.. (2004). Studies of the Interconversion of Polyaniline Oxidation States by Optical Absorption Absorption Spectroscopy. Synthetic Metals 146: 1-10.

Delvaux M., Duchet Jannick, Stavaux P-Y., Legras R., Demoustier-Champagne S. (2000). Chemical and Electrochemical Synthesis of Polyaniline micro-and nano-tubules. *J. Synthetic Metals*, 113: 275-280.

Dixit V., Misra S. K. C., Sharma B. S. (2005). Carbon monoxide sensitivity of vacuum deposited polyaniline memiconducting thin films. *Sensors and Actuators B*, 104: 90-93.

Dorne J. L. C. M, Walton K., Kenwick A. G. (2003). Human Variability in CYP3A4 metabolism and CYP3A4 related uncertainty factor for risk assessment. *Food and Chemical Toxicology*, 41: 201-224.

Durcharme J., Abdullah S., Wanner I W. (1996). Dextromethorphan as an in vivo probe for the simultaneous determination of CYP2D6 and CYP3A4 activity. *J. Chromatography B, Biomedical Applications*, 29: 113-128.

Erdem A., Pabuccuoglu A., Meric B., Kerman K., Ozsoz M. (2000). Electrochemical biosensors based on horseradish peroxidase for the determination of oxidizable drugs. *Turkey Journal of Medical Science*, 30: 349-354.

Erdem E., Karakişla M., Saçak M., (2004), The chemical synthesis of conductive polyaniline doped with dicarboxylic acid. *European Polymer Journal* 40: 785-791.

Extonet, Extension Toxicology Network, pesticide information profiles (1996), Hyperlink: http://extonet.orst.edu/pips/diazinon.htm

Falcou A., Duchêne A., Hourquebie P., Marsacq D., Balland-Longeau A. (2005). A new chemical polymerization process for substituted anilines. Application to the synthesis of poly(*N*-alkylanilines) and poly(*o*-alkylanilines) and comparison of their respective properties. *Synthetic Metals,* 149: 115-122.

Faulkner C. M., Cox H. L., Williamson J. C. (2005). Unique aspects of antimicrobial use in older adults. *Clinical Infectious Diseases*, 40: 997-1004.

Feng X (2005). Applications of Oxidoreductases: Recent advances Review. Staff Scientist, *Novozymes Inc.* , 1445, Drew Avenue, Davis, CA 95616.

Feng-J., Li-M. H., Ten-C. W., Gopalan A., Ju-S. H., (2007). Intrfacial Synthesis of Platinum Loaded Polyaniline Nanowires in Polystyrene Sulfonic Acid. *Material Letters*, in press.doi9.10.1016/jmatlet.2007.02.030

Fernandes K. F., Lima C. S., Lopes F. M., Collins C. H., (2005). Hydrogen Peroxide Detection System Consisting Of Chemically Immobilized Peroxidase Spectrometer. *Process Biochemistry*, 40: 3441-3445.

Fernandes M. R., Garcia J. R., Schultz M. S., Nart F. C. (2005). Polaron and Bipolaron Transitions in Doped Poly(p-phenylene Vinylene films). *Thin Solid Films*, 474: 279-284.

Fleming B. D., Tian Y., Bell S. G., Wong L-L., Urlacher V., Allen H., Hill O. (2003). Properties of cytochrome P450BM3 measured by direct methods. *European J. Biochemistry*, 270: 4082-4088.

Gandhi R., and Snedeker S. M. (1999). Critical Evaluation of Diazinon's Breast Cancer Risk, Cornel University Program on Breast Cancer and Environmental Risk Factors in NewYork State (BCERF), *Critical Evaluation* ,10: 1-27

Gavryshin V. and Žukauskas, 2002. Functional combinations in solid States. Hyperlink: http://www.mtmi.vu.it/vg/

Geng Y H., Sun Z C., Li J., Jing X. B., Wang X. H., Wang F. S. (1999). Water Soluble Polyaniline and its Blend Films Prepared by Aqueous Solution Casting. *Polymer*, 40: 5723-5727.

Genies E. M., Tsintavis C., (1995). Redox mechanism and electrochemical behaviour of polyaniline deposits. *Journal of electroanalytical Chemistry*, 195: 109-128.

Gerald M., Aubey A., Malhotra B. D. (2002). Application of conducting polymers to biosensors. *Biosensor and Bioelectronics*, 17: 345-359.

Gillman K at http:/www.psychotropical.com/1_cyp_introduction.html

Goel S., Gupta A., Sign K. P., Mehrotra R., Kandpal H. C. (2007). Optical studies of polyaniline nanostructures. *Material Science and Engineering A*, 443: 71-76.

Gök A., Sari B., Talu M., (2004) Synthesis and Characterisation of Conducting Substituted Polyanilines. *Synthetic Metals* 142: 41-48.

Gospodinova N., Terlemezyan L., (1998). Conducting Polymers Prepared by Oxidative Polymerization: Polyaniline. *Progress in Polymer Science*, 8: 1443-1484.

Grennan K., Killard A. J., Hanson C. J., Cafolla A. A., Smyth M. R. (2006). Optimisation and Characterisation of Biosensors based on Polyaniline. *Talanta*, 68: 1591-1600.

Guengerich F. P., Yun C-H., Macdonald T. L. (1996). Evidence for a 1-Electron Oxidation Mechanism in N-Dealkylation of N, N-Diakylanilines by Cytochrome P450 2B1. *The Journal of Biological Chemistry*, 271: 27321-27329.

Guerra E. M., Brunello C. A., Graeff C. F. O, Oliviera H. P., (2002). Synthesis, Characterisation, and conductivity Studies of Poly-o-methoxyaniline Intercalated into V_2O_5 Xerogel. *Journal of Solid State Chemistry*, 168: 134-139.

Guo Y., Gudalupe A. R. (1997). Direct electrochemistry of horseradish peroxidase adsorbed on glassy carbon electrode from organic solutions, *Chemical communications* 15: 1437-1438.

Han D., Chu Y., Liu Y., Lu Z. (2005). Reversed micelle polymerization: a new route for the synthesis of DBSA-polyaniline nanoparticles. *Colloids and surfaces A: Physicochemistry and Engineering aspects,* 259: 179-187.

Han D., Chu Y., Yang L., Zongxian L. (2005). Reversed micelle polymerization: anew route for the synthesis of DBSA-polyaniline nanoparticles. *Colloids and Surfaces A: Physicochem. Engineering Aspects*, 259: 179-187.

Han M. G., Cho S. K., Oh S. G., Im S. S. (2002). Preparation and characterization of polyaniline nanoparticles synthesized from DBSA micellar solution. *Synthetic Metals,* 126: 53-60.

Hara M. (2000). Application of P450s for biosensing: Combination of Biotechnology and electrochemistry, *Material Science and Engineering C*, 12: 103-109.

Hino T., Namiki T., Kuramoto N. (2006). Synthesis and characterization of novel conducting composites of polyaniline prepared in the presence of sodium dodecyl sulfate and several water soluble polymers. *Synthetic Metals,* 156: 1327-1332.

Honeychurch M. J., Hill H. A. O., Wong L-L. (1999). The thermodynamics and kinetics of electron transfer in the cytochrome P450cam enzyme system. *FEBs Letters*, 451: 351-353.

Hopkins A. R., Lipeles R. A., Kao W. H., (2004), Electrically conducting polyaniline microtube blend. *Thin Solid Films*.447-448: 474-480.

http://extonet.orst.edu/pips/diazinon.htm

http://www.unige.ch/LaBPV/Publications/silaghi/Dumistrecu.html

Hu X., Tang K., Liu S-G, Zhang Y-Y., Zou G-L., (2005). Hemoglobin-biocatalysts synthesis of a conducting polyaniline. *Reactive and Functional Polymers*, 65: 239-248.

Huang L-M., Wen T-C., Gopalan A. (2003). Synthesis and characterisation of soluble poly(aniline-co-2,5-dimethoxyaniline). *Material Letters*, 57: 1765-1774.

Huang J., Wan M. (1998). Temperature and pressure dependence of conductivity of polyaniline by insitu doping polymerization in the presence of organic functional acids as dopants. *Solid State Communications*, 108: 255-259.

Huang J. (2006). Syntheses and Applications of Conducting Polymer Polyaniline Nanofibres. *Pure and Applied Chemistry,* 78: 15-27.

Huang J., Kaner R. B. (2006). The intrinsic nanofibrillar morphology of polyaniline. *Chemical communication*s, 367-376.

Huang Li-M., Wen T-C., Gopalan A., (2005). Electron and junction properties of poly(2,5-dimethoxyaniline)-polyethylene oxide blend/metal Schottky Diodes. *Thin solid Films*, 473: 300-307.

Huang Li-Ming, Wen T-C., Gopalan A., Ren F. (2003). Structural influence on the electrochromic properties of methoxy substituted polyaniline /aluminum schottky barrier diodes. *J. Material Science and Engineering* B,104: 88-95.

Huang L-M., Wen T-C., Gopalan A., (2002) .In situ UV-Visible Spectroelectrochemical studies on electrochemical behaviour of poly(2,5-dimethoxy aniline). *Synthetic Metals*, 130: 155-163.

Huang L-M., Chen C-H., Wen T-C, Gopalan A., (2006). Effects of secondary dopants on electrochemical and spectroelectrochemical properties of polyaniline. *Electrochimica Acta* , 51: 2756-2764.

Huang L-M, Wen T-C, Gopalan A. (2002). In situ UV–visible spectroelectrochemical studies on electrochromic behavior of poly(2,5-dimethoxy aniline). *Synthetic Metals*, 130: 155-163.

Hyperlink: http:/www.Isbu.ac.uk/biology/enzetech/biosensors.html .

Hyperlink: http://www-bio.paisley.ac.uk/marco/enzyme

Innis P. C., Norris I. D., Maguire L. A. P. K, Wallace G. G. (1998). Formation of chiral polyaniline colloids codoped with (+) or (-)- 10-camphor sulphonic acid with polystyrene sulphonated. *Macromolecules*, 31: 6521-6528.

Iwuoha E. I., Mavundla S. E., Somerset V. S., Petrik L. F., Klink M. J., Sekota M., Baker P. (2006). Electrochemical and spectroscopical properties of flyash-polyaniline matrix nanorods composites. *Microchimica Acta*, 155: 453-458.

Iwuoha E. I. and Smyth M., (1996). Polymer-based amperometric biosensors, In: *Electroactive Polymer electrochemistry, Part 2 , Methods and Applications,* Michael E.G. Lyons, Plenum Press, NewYork, USA, chapter 11, pg 297-328.

Iwuoha E. I., Saenz de Villaverde D., Garcia N. P., Smyth M. R., Pingarron J. M. (1997). Reactivities of organic phase biosensors. 2. The amperometric Behaviour of horseradish peroxidase immobilised on a platinum electrode modified with an electrosynthetic polyaniline film. *Biosensor and Bioelectronics*, 12: 749-761.

Iwuoha E. I., Wilson A., Howel, Mathebe N. G. R., Montane-Jaime K., Narinesingh D., Guiseppi-Elie A., *Analytical letters*, **2004**, 37, 5, 000-000.

Iwuoha E. I., Shiba J., Zhang Z., Smyth M. R., Fuhr U., de Montellano P. R. O. (1998). Drug metabolism biosensors: electrochemical reactivities of cytochrome P450 cam immobilized in synthetic vesicular systems. *Journal of Pharmaceutical and Biomedical Analysis*, 17: 1101-1110.

Iwuoha E. I., Wison A., Howel M., Mathebe N. G. R., Montane-Jaime K., Narinesingh D., Guissipie-Elie A. (2004). Cytochrome $P450_{2D6}$ (CYP 2D6) bioeletrode for fluoxetine. *Analytical Letters*, 37: 929-941.

Iwuoha E. I., Smyth M. R., (2003). Reactivities of organic phase biosensors: 6> Square-wave and differential pulse studies of genetically engineered cytochrome $P450_{cam}$(CYP101) bioelectrodes in selected solvents. *Biosensors and Bioelectronics,* 18: 237-244.

Iwuoha E. I., Smyth M. R., Lyons M. E. G., (1997). Organic phase enzyme electrodes: kinetics and analytical applications 12: 53-75.

J. Yue, Z.H. Wang, K. R. Cromack, A. J. Epstein and A. G. MacDiarmid, (1991). Effect of sulphonic acid group on polyaniline backbone. *J. American Chemical Society*, 113: 2665-2671.

Jayanty S., Prasad G. K., Sreedhar B., Radhakrishnana T. P. (2003). Polyelectrolyte templated polyaniline-film morphology and conductivity. *Polymer*, 44: 7265-7270.

Jiang H., Geng H., Xiabin J. L., Wang J. F. (1997). Organic acid doped polyaniline derivatives. *Synthetic Metals*, 84: 125-126.

Jin Z., Su Y. X., Duan Y., (2001). A novel method for polyaniline synthesis with immobilized horseradish peroxidase enzyme. *Synthetic Metals*, 122: 237-242.

Jing X., Wang Y., Wu D., Qiang J., (2007). Sonochemical synthesis of polyaniline nanofibres. *Ultrasonic Sonochemistry*, 14: 75-80.

Joseph S., Rusling J. F., Lvov Y. M., Friedberg T., Fuhr U. (2003). An amperometric biosensor with human CYP3A4 as a novel drug screening tool. *Biomedical Pharmacology*, 65: 1817-1826.

Jr Santos J.R., Malmonge J.A., Conceiçao S., Motheo A.J., Mascarenhas Y.P., Mattoso L. H. C., (1995). Characteristics of polyaniline electropolymrizsa in camphor sulphonic acid. *Synthetic Metals*, 69: 141-142.

Kan J., Pan X., Chen C. (2004). Polyaniline uricase biosensor prepared with template. *Biosensor and Bioelectronics*, 19: 1635-1640.

Karakişla M., Saçak M., (2002). The chemical synthesis of conductive polyaniline by use of benzoyl peroxide. *Journal of Molecular Science Pure and Applied Chemistry*, 39: 1349-1359.

Katoh M., Nakajima M., Yamazaki H., Yokoi T. (2001). Inhibitory effects of CYP3A4 substrates and their metabolites on P-glucoprotein-mediated transport. *European Journal of Pharmaceutical Sciences*, 12: 505-513.

Kaushik M., Mike J. W., Andy D., Mike S. S., (2005), Polymerization of aniline by auric acid: Formation of gold decorated polyaniline nanorods. *Molecular Rapid Communications*, 26: 232-235.

Kemp W., (1987). Organic Spectroscopy. 2nd Edition, ELBS/Macmillan, Hong Kong pp 44-56.

Kenworthy K. E., Bloomer J. C., Clarke S. E., Houston J. B. (1999). CYP3A4 drug interactions:correlation of 10 in vitro probe substrates. *Journal of Clinical Pharmacology*, 48: 716-727.

Killard A. J, Smyth M. R., Micheli L., Palleshi G. (2000). Rapid antibody biosensor assays for environmental analysis. *Biochemical Society Transcations*, 28: 81-84.

Kilmartin P. A., Wright G. A., (1999). Photoelectrochemistry and spectroscopy of substituted polyanilines. *Synthetic Metals*, 104: 145-156.

Kim B-J., Oh S-G., Han M-G., Im S-S., (2001), Synthesis and characterization of polyaniline nanoparticles in SDS micellar solutions; *Synthetic Metals*, 122: 297-304.

Kim J., Kwon S., Ihm D. (2007). Synthesis and characterization of organic soluble polyaniline prepared by one step emulsion polymerization. *Current Applied Physics,* 7: 205-210.

Kirchheiner J., Seeringer A. (2007). Clinical implications of pharmacogenetics of cytochrome P450 drug metabolizing enzymes. *Biochimica et Biophysica Acta*, 1770: 489-494.

Kocherginsky N. M., Wang Z. (2006). Redox reactions of polyaniline films doped with d, *l*-camphor sulfonic acid. *Reactive and Functional Polymers*, 66: 1384-1393.

Kohut-Svelko N., Reynaud S., François J. (2005). Synthesis and characterization of polyaniline prepared in the presence of nonionic surfactants in an aqueous dispersion. *Synthetic Metals*, 150: 107-114.

Komsiyska L., Tsacheva Ts., Tsakova V. (2005). Electrochemical formation and Copper Modification of Poly-*o*-methoxyaniline. *Thin Solid Films*, 493: 88-95.

Kounaves S. P. Voltammetric Techniques, In: Handbook of Instrumental Techniques for Analytical Chemistry, Settle F. A, Upper Saddle River, NJ: Prentice Hall, PTR, 1997, chp 37: 720-721.

Lazarou J. (1998). Incidence of adverse drug reactions in hospitalized patients, a meta-analysis of prospective studies. JAMA 279: 1200-1205.

Li C., Mu S., (2005). The Electrochemical Activity of Sulfuric Acid Ring Substituted Polyaniline in the wide Range of pH. *Synthetic Metals*, 149: 143-149.

Li J., Tan S. N., Ge H. (1996). Silica sol-gel immobilized amperometric biosensor for hydrogen peroxide. *Analytica Chimica Acta,* 335: 137-145.

Lindfors T., and Ivaska A. (2002). Potentiometric and UV-vis characterisation of N-substituted Polyaniline, *J. of Electroanalytical Chemistry*, 535: 65-74.

Lindfors T., and Ivaska A. (2002). pH sensitivity of polyaniline and its substituted derivatives. *Journal of electroanalytical Chemistry*, 531: 43-52.

Lindfors T., Ivaska A. (2002). Potentiometric and UV-Vis characterisation of N-substituted polyanilines. *Journal of electroanalytical chemistry*, 535: 65-74.

Long Y., Chen Z., Wang N., Zhang Z., Wan M. (2003). Resistivity study of polyaniline doped with protonic acids. *Physica B*, 325: 208-213.

Lukachova L. V., Shkerin E. A., Puganova E.A., Karyakina E. E., Kiseleva S.G., Orlov A. V., Karpacheva G. P., Karyakin A. A., (2003). Electroactivity of chemically synthesized polyaniline in neutral and alkaline aqueous solutions. Role of self-doping and external doping. *J. electroanalytical chemistry*, 544: 59-63.

Ma Y., Li N., Yang C., Yang X. (2005). One step synthesis of water-soluble gold nanoparticles/polyaniline composite and its application in glucose sensing. *Colloids and Surfaces A: Physico-Chemical and Engineering Aspects*, 269: 1-6.

MacDiarmid A. G. (2001). "Synthetic Metals": A Novel Role of Organic Polymers (Nobel Lecture)**. *Angewadte Chemie International Edition*, 40: 2581-2590.

MacDiarmid A. G., (2001). 'Synthetic Metals': A novel role for organic polymers. *Current Applied Physics,* 1: 269-279.

Maceij M., Magdalen T., Barbara P., Krystyna J. (2003). Template synthesis of polyaniline and poly (2-methoxyaniline) nanotubes: comparison of the formation mechanisms. *J. Electrochemistry Communications*, 5: 403-407.

Malhotra B. D., Chaubey A., Singh S. P. (2006). Prospects of conducting polymers in biosensors, *Analytica Chimica Acta*, 578: 59-74.

Malinauskas A., Malinauskiené J., Ramnavičius A. (2005). Conducting polymer-based nanostructurized materials: Electrochemical Aspects. *Nanotechnology*, 16: R51-R62

Malinauskas A. (1999). Electrocatalysis at conducting polymers. *Synthetic Metals*, 107: 75-83.

Malinauskas A. (2001), Chemical deposition of conducting polymers. *Polymer*, 42: 3957-3972.

Malinauskas A., Holze R. (1998). Cyclic UV-Vis spectrovoltammetry of polyaniline *Synthetic Metals*, 97: 31-36.

Márquez A. G. C., Rodríguez L. M. T., Rojas A. M. (2007). Synthesis of fully and partially sulphonated polyanilines derived from ortanilic acid: An electrochemical and electrogravimetric study. *Electrochimica Acta*, in press.

Material Safety Data Sheet - MSDS- (2000). Hydrogen Peroxide 30-50%. Data Prepared by Fisher Scientific Company; 1 Reagent Lane, Fair Lawn, NJ, 07410. http://avogadro.chem.iastate.edu/MSDS/H2O2_30pct.htm

Mathai C. J., Saravanan S., Jayalekshni S., Ventikachalam S., Anatharaman M.R., (2003). Conduction mechanism in plasma polymerized aniline thin films, *Material Letters*, 57: 2253-2257.

Mathebe N. G. R., Aoife M., Iwuoha E. I. (2004). Electrochemistry and scanning electron microscopy of polyaniline/peroxidase-based biosensor, *Talanta*, 64: 115-120.

Mazur M., Michota-Kamińska A., Bukowska J., (2006), Surface-catalysed growth of poly(2-methoxyaniline) on gold. *Electrochimica Acta*, doi: 10.1016/j.electacta 2006.10.043

Mazur M., Krysiński P., (2002). Covalently immobilized 1,4-phenylenediamine on 11-mercaptoundecanoic acid-coated gold: effect on surface –confined monomers on the chemical in situ, deposition of polyaniline and its derivatives. *Langmuir* 17: 7093-7101.

Meunier B., P.de Visser S., Shaik S., (2004). Mechanism of oxidation reactions Catalysed by cytochrome P450 Enzymes. *Chem Reviews*, 104: 3947-3980.

Michaelson J. C., McEnvoy A. J. (1994), Interfacial polymerisation of aniline. Journal of American Chemical Society, *Chemical Communications*, 79-80. DOI:10.1039/C39940000079.

Mirmohseni A., Wallace G. G, (2003). Preparation and characterisation of processable elecroactive polyaniline- polyvinyl alcohol composite. *Polymer*, 44: 3523-3526.

Miwa G. T., Walsh J. S., Kedderis G. L., Hollenberg P.F. (1983). The use of intramolecular isotope effects to distinguish between deprotonation and hydrogen atom abstraction mechanisms in cytochrome P450 and peroxidase catalysed N-demethylation reactions. *J. Biological Chemistry*, 258: 14445-14449.

Mogharrab N., Hedayatolla G. (2005). Anthraquinone 2-carboxylic acid as an electron shuttling mediator and attached electron relay on horseradish peroxidase. *Electrochemical Communications*, 7: 466-471.

Monk P. M. S., (2001). Fundamentals of electroanalytical chemistry. Wiley & Sons, NY, USA, pp 17-24.

Morrin A., Ngamna O., Killard A. J., Moulton S. E., Smyth M. L., Wallace G. G. (2005). An amperometric enzyme biosensor fabricated from polyaniline nanoparticles. *Electroanalysis*, 17: 423-430

Moulton S. E., Innis P. C., Maguire L.A. P. K., Ngamna O., Wallace G. G. (2004). Polymerization and characterization of conducting polyaniline nanopartical dispersions. *Current Applied Physics*, 4: 402-406.

Murugesan R., Subramanian E. (2003). Effect of organic dopants on the electrodeposition and characteristics of polyaniline under the varying influence of H_2SO_4 and $HClO_4$ electrolyte media. *Material Chemistry and Physics*, 80: 731-739.

Narayan H., Alemu A. H., Iwuoha E., (2006). Synthesis, Characterisation and Conductivity Measurements of Polyaniline and Polyaniline/flyash composites; the Royal Society of Chemistry; 203: 3665-3672.

Nascimental G. M, Constantino V. R. L., Lander R., Temperini M. L. A. (2006). Spectroscopic characterization of polyaniline formed in the presence of montomorilonite clay. *Polymer*, 47: 6131-6139.

Nateghi M. R., Zahedi M., Mosslemin M. H., Hachemian S., Behzad S., Minnai A., (2005). Autoacceleration/degradation of Electrochemical Polymerisation of Substituted Polyanilines. *Polymer*, 46: 11476-11483.

Nekrasov A.A., Ivanov V.F., Gribkova O.L., Vannikov A. V., (1996). Electrochemical and chemical synthesis of polyaniline on the surface of vacuum deposited polyaniline films. J. *of Electroanalytical Chemistry*, 412:133-137.

Ngamna O, Morrin A., Moulton S. E., Killard A. J., Smyth M.R., Wallace G. G.,. (2005). An HRP Based Biosensor using Sulfonated Polyaniline .*Synthetic Metals*, 153: 185-188.

Njuguna J., Pielichowski K. (2004). Recent Developments in Polyurethane –Based Conducting Composites. *J. Material Science*, 39: 4081-4094.

Norris I. D., Kane- Maguire L. A. P., Wallace G. G. (2000). Electrochemical Synthesis and chiroptical Properties of optically Active Poly-*o*- methoxy aniline. *Macromolecules*, 33: 3237-3243.

Norris I. D., Kane- Maguire L. A. P., Wallace G. G. (2000). Electrochemical synthesis and chiroptical properties of optically active poly-*o*- methoxy aniline. *Macromolecules*, 33: 3237-3243.

Oh S-G. and Im S-S. (2002). Electroconductive polymer nanoparticles preparation and characterisation of PANi and PEDOT nanoparticles . *Current Applied Physics* 2: 273-277.

Orata D. and Okong'o E., (2000). Allen-Hickling Equation as Applied to the Quasi-Reversible Polyaniline Redox System. *Reactive and Functional Polymers,* 45: 211-216.

Orawan N., Aoife M., Moulton S.E., Killard A. J., Smyth A. J., Wallace G. G. (2005). An HRP based biosensor using sulphonated polyaniline. *Synthetic metals*. 155: 185-188.

Österholm J.-E., Cao Y., Klavetter., Smith P. (1993). Emulsion polymerization of aniline. *Synthetic Metals*, 55: 1034-1039.

Palaniappan S., Amarnath C. A., (2006). A novel polyaniline maleic acid-dodecylhydrogensulphate salt: Soluble polyaniline powder. *Reactive and Functional Polymers,* 66: 1741-1748.

Palys B., Kudelski A., Stankiewwicz, Jackowska K., (2000), Influence of anions on formation and electroactivity of poly-2,5-dimethoxyaniline. *Synthetic Metals*, 108: 111-119.

Palys B. and Celuch P. (2006). Redox transformations of polyaniline nanotubes cyclic voltammetry, infrared and optical absorption studies. *Electrochimica Acta*, 51: 4115-4124.

Palys B., Celuch P., (2006). Redox transformations of Polyaniline Nanotubes: Cyclic Voltammetry, Infrared and Optical Absorption Studies. *Electrochimica Acta,* 51: 4115-4124.

Pant R. P., Dhawan S. K., Katana N. D., Suri D.K. (2002). Investigations of Ferrofluid-Conducting Polymer composites and its Applications. *Journal of Magnetism and Magnetic Materials*, 16-19.

Park T-M., Iwuoha E.I., Smyth R. M. (1997). Development of a Sol-gel Enzyme Inhibition –Based on Amperometric Biosensor for Cyanide. *Eletroanalysis*, 9: 1120-1123.

Paternolli C., Antonini M., Ghisellini P., Nicolini C. (2004). Recombinant cytochrome P450 Immobilization for biosensor applications. *Langmuir,* 20: 11706-11712.

Patil S., Mahajan J. R., More M. A., Patil P.P. (1999). Electrochemical synthesis of poly(*o*-methoxyaniline) thin films: effects of post treatment. *Material Chemistry and Physics,* 58: 31-36.

Patil V., Sainkar S. R., Patil P. P. (2004). Growth of Poly(2,5-Dimethoxyaniline) Coatings on Low Carbon Steel. *Synthetic Metals*, 140: 57-63.

Pauliukite R., Brett C. M. A., Monkman A. P., (2004). Polyaniline Fibres as Electrodes. Eletrochemical Characterization in Acid Solutions. *Electrochimica Acta*, 50: 159-167.

Plank R. V., Dinardo N. J., Vogs J.M., (1997). Chemical and electronic properties of vapour –deposited polyaniline films on metal substrates. *Synthetic Metals*, 89: 1-9.

Pravda M., Jungar C. M., Iwuoha E., Smyth M. R., Vytras Karel., Ivaska A. (1995). Evaluation of amperometric glucose biosensors based on co-immobilization of glucose oxidase with an osmium redox polymer in electrochemically generated polyphenol films. *Analytica Chimica Acta*, 304: 127-138.

Prévost V., Petit A., Pla F., (1999). Studies on Chemical Oxidative Copolymerisation of Aniline and O-alkoxysulfonated anilines. II Mechanistic Approach and Monomer Reactivity Rates. *European Polymer Journal*, 35: 1229-1236.

Prokeš J. and Stejskal J., (2004), Polyaniline prepared in the presence of various acids.2.Thermal stability and conductivity. *Polymer degradation and Stability* 86: 187-197.

Ptirchard J., Law K., Vakurov A., Millner P., Higson S.P.J., (2004). Sonochemically fabricated enzyme microelectrode arrays for the environmental monitoring of pesticides, *Biosensor Bioelectronics*, 20: 765-772

Pud A., Ogurstov N., Korzhenko A., Shapoval G. (2003). Some aspects of preparation methods and properties of polyaniline blends and composites with organic polymers. *J. Progress in Polymer Science,* 28: 1701-1753.

Rahmanifar M. S., Mousavi M. F., Shamsipur M., Riahi S. (2006). A study of the influence of anionic surfactants on electrochemical degradation of polyaniline. *Polymer degradation and stability*, 91: 3463-3468).

Rao S. P., Subrahmanya S., Sathyanarayana D. N. (2002). Inverse emulsion polymerization a new route for the synthesis of conducting polyaniline. *Synthetic Metals*, 128: 311-316.

Raposo M., Oliviera O. N., (2002). Adsorption of poly-*o*-methoxyaniline in Layer-by-Layer films. *Langmuir*, 18: 6866-6874.

Reipa V., Mayhew M. P., Vilker V. L. (1997). A new direct electrode-driven P450 cycle for biocatalysis. *Journal of Biochemistry*, 94: 13554-13558.

Roković M. K., Duíc Lj. (2006). Electrochemical synthesis of poly(ortho-ethoxyaniline) from phosphoric and sulphuric acid solutions. *Electrochimica Acta*, 51: 6045-6050.

Romach M. K., Otton S. V., Somer G., Tyndale R. F., Sellers E. M. (2000). Cytochrome P450, 2D6 and treatment of codeine dependence. J. *Clinical PsychoPharmacology*, 20: 43-45.

Rumbau V., Pamposo J. A., Alduncin J. A., Grande H., Mecerreyes D., Ochoteco E., (2007). A new biofunctional template for the enzymatic synthesis of conducting polyaniline. *Enzyme and Microbial Technology*, 40: 1412-1421.

Salomi B. S. B., Mitra C. K. (2007). Electrochemical studies on horseradish peroxidase covalently coupled with redox dyes. *Biosensors and bioelectronics*, 22: 1825-1829.

Sandra R. M., Domingo H-V., Artur J. M., (2004). Characteristics of polyaniline synthesized in phosphate buffer solution. *European Polymer Journal,* 40: 2033-2041.

Sandra R. M., Domingo H-V. Artur J. M., (2003). Corrosion protection of stainless steel by polyaniline electrosynthesized from phosphate buffer solutions. *Progress in Organic Coatings*, 48:28-33.

Sangodkar H., Sukeerthi S., Srinivasa R. S., LaL R., Contractor A. Q. (1996). A biosensor array based on polyaniline. *J. American Chemical Society*, 68: 779-783.

Santos J. R., Malmonge J. A., Conceição S., Motheo A. J., Mascarenhas Y. P., Mattoso L. H. C. (1995). Characteristics of polyaniline electropolymerized in camphor sulphonic acid. *Synthetic Metals*, 69: 141-142.

Sathiyanarayanan S., Azim S. S., Venkatachari G. (2007). Preparation of polyaniline-TiO_2 composite and its comparative corrosion protection performance with polyaniline. *Synthetic Metals*, in press.

Segal E., Tchoudakov R., Narkis M., Siegmann A., Wei Y. (2005). Polystyrene /polyaniline Nanoblends for Sensing Aliphatic Alcohols. *Sensors and Actuators B*, 104: 140-150.

Setti L., Fraloeni-Morgera A., Mencarelli I., Filippini A., Ballarin B., Biase M. D., (2007). An HRP-based amperometric biosensor fabricated by thermal inkjet-printing. *Sensors and actuators B*, in press.

Shaw J., Marin D. (2002**)** *History & coating Applications of conductive polymers, Report for Chemistry***,** pp 446.

Shiba J., Rusling J. F., Lvov Y. M., Friedberg T., Fuhr U., (2003). An Amperometric Biosensor with human CYP3A4 as a Novel Drug Screening Tool. *Biochemical Pharmacology*, 65: 1817-1826.

Shilpa T., Mukesh D., Yakhmi J. V. (2001). Redox behaviour of polyaniline as influenced by aromatic sulphonated anions: cyclic voltammetry and molecular modeling, 125: 401-413.

Shou M., Grogan J., Mancenicz J. A., Kransz K. W., Gonzalez F. J., Gelboin H. V., Korzekwa K. R. (1994). Activation of CYP 3A4: Evidence for the simultaneous binding of two substrates in a cytochrome P450 active site. *Biochemistry*, 33: 6450-6455.

Shumyansteva V. V., Bulko T. V., Samenkova N. F., Kuznetsova G. P., Usanov S. A., Schultze H., Bachmann T. T., Schmid R. D., Archakov A. I. (2006). A new format of electrodes for the electrochemical reduction of cytochrome P450. *J. Inorganic Biochemistry*, 100: 1353-1357.

Shumyantseva V. V., Bulko T. V., Usanov A. A., Schmid R. D., Nicolini C., Archakov A I. (2001). Construction and characterization of biolectrocatalytic sensors based on cytochrome P450. *Journal of Inorganic Biochemistry*, 87: 185-190.

Shumyantseva V. V., Bulko T. V., Archakov A. I., (2005). Electrochemical Reduction of Cytochrome P450 as an Approach to the construction of Biosensors and Bioreactors. *J of Inorganic Biochemistry*, 99: 1051-1063.

Sivakumar M., Gedankan A., (2005). A sonochemical method for the synthesis of polyaniline and Au-polyaniline composites using H_2O_2 for enhancing rate and yield, *Synthetic Metals*, 148: 301-306.

Sivakumar R., Saraswathi R. (2003). Redox polyaniline properties of poly-N-methylaniline. *Synthetic Metals*, 138: 381-390.

Siwei L., Kaizheng Z., Yi Z., Jiarui X., (2006). Cyclic polyaniline nanostructures from aqueous/Organic interfacial polymerization induced by polyacrylic acid. *Polymer* 47: 7680-7683.

Slanar O., Porkona P., Cerna O., Buzkova H., Pechandova K., Perlik F. (2006). Polymorphism of CYP2D6 in the Czech population. Eurpoean Journal of Pain, Vol.10 (supp S1), 5th EFIC congress, Free presentations.

Sofiane B., Didier H., Laurent L. P.(2006). Syntheis and characterization of composite Hg-polyaniline powder material. *Electrochimica Acta*, 52: 62-67.

Song Y., Wang L., Ren C., Zhu G., Li Z. (2006). A Novel hydrogen peroxide sensor based on horse radish peroxidase immobilized in DNA films on a gold electrode. *Sensors and Actuators,* B 114: 1001-1006.

Sproule B. A., Otton S. V., Cheung S. W., Zhong X. H., Romach M. K., Sellers E. M. (1997). CYP 2D6 inhibition in patients treated with setraline. *Journal of Clinical Psychopharmacology*, 17: 102-106.

Stejskal J., Omastova M., Fedorova S., Prokes J., Tichova M., (2003). Polyaniline and polypyrolle prepared in the presence of surfactant; a comparative conductivity study. *Polymer,* 44: 1353-1358.

Stejskal J., Sapurina I., Trchova M., Konushenko E. N., Holler P. (2006). The genesis of polyaniline nanotubes. *Polymer*, 47: 8253-8262.

Stejskal J., and Gilbert R G., (2002). Polyaniline. Preparation of a conducting polymer. *International Journal of Pure and Applied Chemistry,* 74: 857-867.

Storrier G. D., Colbran S. B., Hibbert D. B., (1994). Chemical and electrochemical synthesis and characterization of poly-(2,5-dimethoxyaniline) PDMA: a novel, soluble, conducting polymer. *Synthetic Metals,* 62: 179-186.

Stryer L., (2000), Biochemistry, fourth edition, Freeman publisher, chapter 6, pp104-128

Tang H., Kitani A., Yamashita T., Ito S. (1998). Highly sulphonated polyaniline electrochemically synthesized by polymerizing aniline-2,5-disulphonic acid and copolymerizing it with aniline. *Synthetic Metals*, 96: 43-48.

Tang Z., Liu S., Wang Z., Dong S., Wang E. (2000). Electroachemical synthesis of polyaniline nanoparticles. *Electrochemistry Communications* 2: 32-35.

Thévenot D. R., Toth K., Durst R.A., Wilson G. S. (2001). Electrochemical biosensors: recommended definitions and classification. *Biosensor and Bioelectronics*, 16: 121-131.

Thummel K., Wilkinson G. R. (1998). In vitro and in vivo drug interactions involving human CYP3A: annual reviews. *Pharmacological Toxicology*, 1998: 389-430.

Tran D. H., Kaner R.B., (2006). A general synthetic route to nanofibres of polyaniline derivatives. The Royal Society of Chemistry, *Chemical Communications*, 3915-3917.

Triotsky V. I., Berzina T. S., Fontana M. P. (2002). Langmuir- Blodgett Assemblies with Patterned Conductive Polyaniline Layers. *Material Science and Engineering:C*, 22: 239-244.

Vakurov A.,. Simpson C. E., Daly L., Gibson T. D., Millner P. A. (2004). Acetylcholine esterase-based Biosensor Electrodes for Organophosphates Pesticide Detection. I. Modification of Carbon surface for Immobilization of Acetylcholine esterase, *Biosensors and Bioelectronics* 20: 1118-1125.

Valter B., Ram M.K., Nicolini C., (2002). Synthesis of multiwalled carbon nanotubes and Poly(*o*-anisidine) nanocomposite material: fabrication and characterization of its Langmuir-Schaefer films. *Langmuir,* 18:1535-1541.

Varela H., Maranhão S. L. de A., Mello R. M. Q., Ticianelli E. A., Torresi R M. (2001). Comparisons of charge compensation process in aqueous media of polyaniline and self-doped polyanilines. *J. Synthetic Metals*, 122: 321-327.

Viva F. A., Andrade E. M., Molina F. V., Florit . M. I (1999). Electropolymerization of 2-MethoxyAniline. electrochemical and spectroscopical product characterization. *Journal of Electroanalytical Chemistry*, 471: 180-189.

Walsky R L., Obach R. S. (2004). Validated assays for human cytochrome P450 activities. *Drug metabolism and disposition*, 32: 647-660.

Wang R.W., Newton D. J., Scheri T. D., Lu A. Y. H. (1997). Human cytochrome P450 3A4-catalysed testosterone 6β-hydroxylation and erythromycin N-demethylation. *Drug Metabolism and Disposition*, 25: 502-507.

Wei D., Lindfors T., Kvarnström C., Kronberg L., Sjöholm R., Ivaska A. (2005). Electrosynthesis and characterization of poly(*N*-methylaniline) in Organic Solvents. *J of Electroanalytical Chemistry*, 575: 19-26.

Wei Y., Hariharan R., Patel A. S. (1990). Chemical and electrochemical copolymerization of aniline with alkyl ring-bubstituted anilines. Macromolecules, 23: 758-764.

Wei Z., Zhang Z., Wan N., (2002). Formation mechanism of self-Asembled polyaniline micro/nanotubes. *Langmuir*, 18: 917-921.

Wei, Y., Focke, W. W., Wnek, G. E., Ray, A., MacDiarmid, A. G. (1989). Synthesis and electrochemistry of akyl-ring-substituted polyanilines. *J. Physical Chemistry* 93: 95-499.

Wessling B. (1998). Dispersion as the link between basic research and commercial applications of conductive polymers (polyaniline). *Synthetic Metals,* 93: 143-154.

Widera J., Palys B., Bukowska J., Jackowska K. (1998). Effects of anions on the electrosynthesis, electroactivity and molecular structure of poly-(*o*-methoxyaniline). *Synthetic Metals*, 94: 265-272.

Widera J., Skompska M., Jackowska K. (2001). The influence of anions on formation, electroactivity, stability and morphology of poly(*o*-methoxyaniline) films-EQEM studies. *Electrochimica Acta*, 46: 4125-4131.

Widera J., Grochala W., Jackoska K., Buckowska J., (1997). Electrooxidation of *o*-methoxyaniline as studied by electrochemical and SERs Method. *Synthetic Metals*, 89: 29-37.

Wong L. S., Vilker V. L., Yap W. T., Reipa V. (1995). Characterization of mercaptoethylamine-modified gold electrode surfaces and analyses of direct electron transfer to putidaredoxin. *Langmuir*, 11: 4818-4222.

www.medicinenet.com/erythromycin/article.htm

Xing S., Zhao C., Jing S., Wang Z., (2006). Mophorlogy and conductivity of polyaniline nanofibres prepared by 'seeding' polymerization, *Polymer* 47: 2305-2313.

Xinyu Z., Roch C-Y-K, Anil J., Sanjeev K. M., 2004: Nanofibres of polyaniline synthesized by interfacial polymerization. *Synthetic Metals*, 145: 23-29.

Xinyu Z., Sanjeer K. M., (2004), Polyaniline Nanofibres: Chemical Synthesis Using Surfactants. *The Royal Society of Chemistry*, *Chemistry Communications*, 2360-2361.

Xu Y., Peng W., Liu X., Li G. (2004). A new film for the fabrication of an unmediated H_2O_2 biosensor. *Biosensor and Bioelectronics*, 20: 533-537.

Yang S. M., Chen K. H., Yang Y. F. (2005). Synthesis of polyaniline nanotubes in the channels of anodic alumina membranes. *Synthetic Metals*, 152: 65-68.

Yang Y., Yang M., Wang H., Jiang J., Shen G., Yu R., (2004). An Amperometric peroxidase inhibition biosensors based on a cystemine self-assembled monolayer for the determination of sulfides. *Sensors and Actuators B*., 2004: 102: 162-168.

Yano J. K., Wester M. R., Schoch G. A., Griffin K. J., Stout C. D., Johnson E. F. (2004). The structure of human microsomal cytochrome P450 3A4. determined by X-ray crystallography to 2.05 A˚ resolution. *Journal of Biological Chemistry*, 279: 38091-38094.

Yue J., Epstein A. J., Zhong Z., Gallaghar P.K. (1991). Thermal stabilities of polyaniline. *Synthetic Metals* 41: 765-768.

Yue J., Wang Z. H., Cromack K. R., Epstein A. J., MacDiarmid A.G., (1991). Effect of sulfonic acid group on polyaniline backbone. *J. American Chemical Society*, 113: 2665-2671.

Zaharis G. A., Shi H H., Bent S. F., (2006). Characterization of polyconjugated thin films synthesized by hot-wire chemical deposition of aniline. *Thin Solid Films*, 501: 341-345.

Zhang L., Wan M. (2005). Chiral polyaniline nanotubes via self-assembly process. *Thin Solid Films*, 477: 24-31.

Zhang L., Wan M. (2002). Synthesis and characterization of self-assembled polyaniline nanotubes doped with D-10-camphor sulphonic acid. *Nanotechnology*, 13: 750-755.

Zhang D., Wang Y. (2006). Synthesis and applications of one-dimensional nano-structured polyaniline; an overview. *Material Science and Engineering B*, 134: 9-19.

Zhang L., Dong S. (2004). The electrocatalytic oxidation of ascorbic acid on polyaniline synthesized in the presence of camphor sulphonic acid. *J of electroanalytical chemistry*, 568: 189-194.

Zhang Z., Wei Z., Zhang L., Wan M. (2005). Polyaniline nanotubes and their dendrites doped with different naphthalene sulfonic acids. *Acta Materialia*, 53: 1373-1379.

Zhang Z., Wan M. (2002). Composite films of nanostructured polyaniline with poly(vinyl alcohol). *Synthetic Metals*, 128: 83-89.

Zhang Z., Nasaar A-E. F., Lu Z., Schenkman J. B., Rusling J. F. (1997). Direct electron injection from electrodes to cytochrome P450 cam in biomembrane-like film. *Journal of American Chemical Society, Farady Transcations,* 93: 1769-1774.

Zhang Z., Wei Z., Zhang L., Wan M. (2005). Polyaniline nanotubes and their dendrites doped with different naphthalene sulfonic acids. *Acta Materialia*, 53: 1373-1379.

Zhang Z., Wan M., (2002). Composite films of nanostructured polyaniline polyvinylalcohol. *Synthetic Metals*, 128: 83-89.

Zheng L Z., Xiong L., Liu C., Jin L. (2006). Electrochemical synthesis of novel sulphonated polyaniline and its electrochemical properties. *European Polymer Journal*, 42: 2328-2333.

Zou Y., Sun L-X., Xu F. (2007). Biosensor based on polyaniline-prussian Blue/multiwalled carbon nanotube hybrid composites. *Biosensors and Bioelectronics*, 22: 2669-2674.

Appendix A

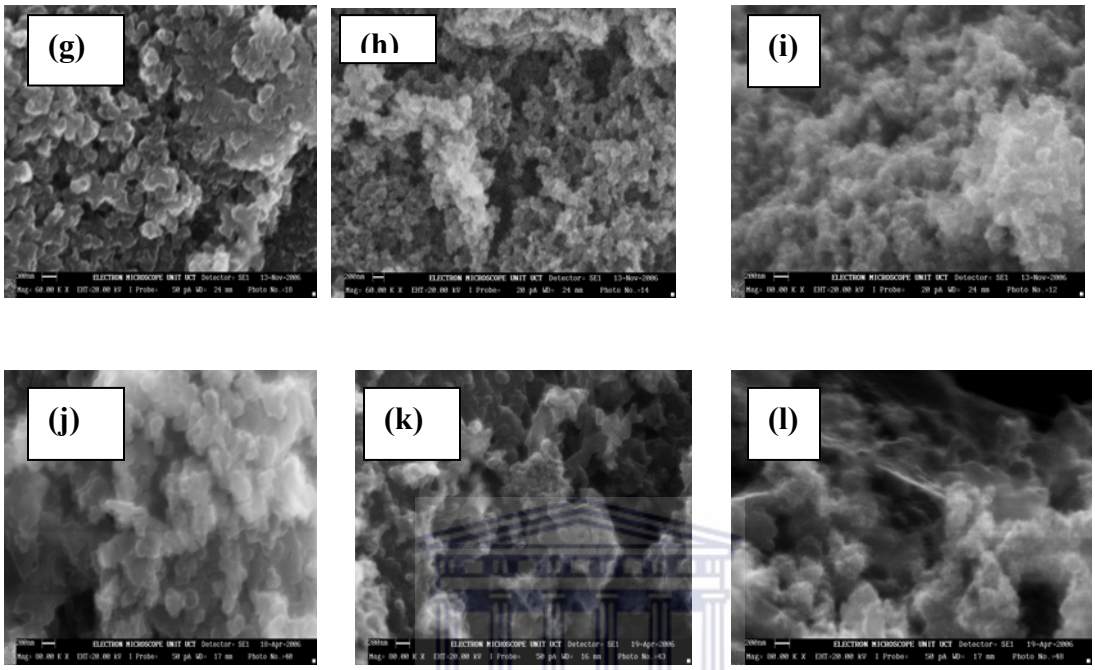

SEM micrographs PANi /ASA (g), POMA/ASA (h) and PDMA/ASA (i) PANi/NSA (j), POMA/NSA (k) and PDMA/NSA (l). composites prepared at 1:1 monomer to dopant ratio

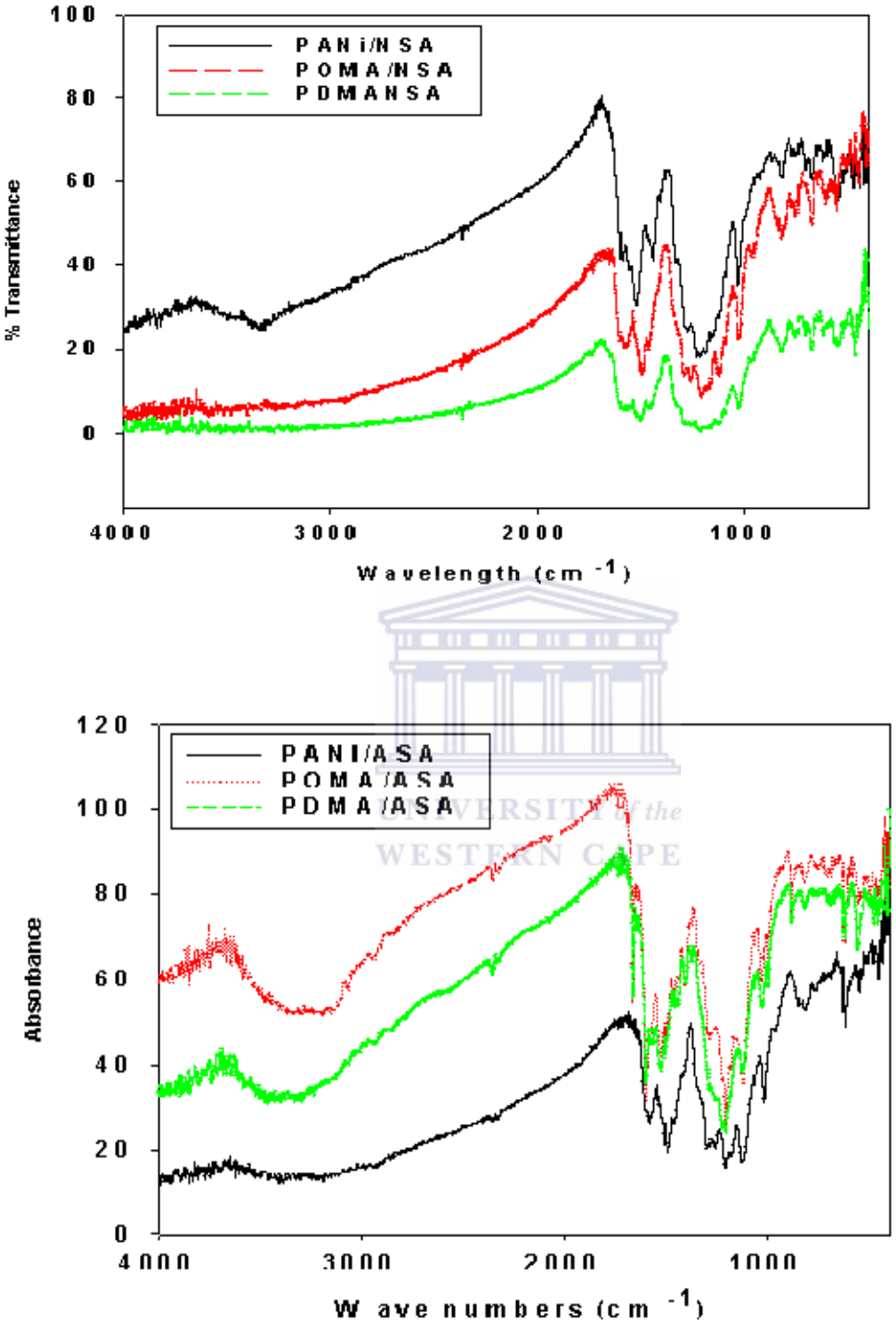

Full spectra for the NSA and ASA doped composites showing the N-H stretches.